

**CLIMATE AND ANTHROPOGENIC FOOTPRINTS IMPLICATIONS
ON THE SURFACE AND GROUNDWATER DYNAMICS ON THE
SOUTHERN SLOPES OF MOUNT KILIMANJARO, TANZANIA**

Mateso Said

**A Thesis Submitted in Fulfillment of the Requirements for the Degree of Doctor of
Philosophy in Hydrology and Water Resources Engineering of the Nelson Mandela
African Institution of Science and Technology**

Arusha, Tanzania

October, 2021

ABSTRACT

Climate and land use/cover changes impact water resources all over the world. This study aimed at developing a conceptual understanding and management of the impacts of present and future climate change and human activities on surface and groundwater resources on the Kikafu-Weruweru-Karanga (KWK) watershed. The methodology includes simulation of the present and prediction of the future hydrological fluxes and streamflow prediction under changing climate and land use/cover. Calibration and validation of the hydrological model, Soil and Water Assessment Tool (SWAT) showed satisfactory performance (Nash-Sutcliffe Efficiency (NSE)) > 0.50). A total of 22 parameters were used, and Curve number for soil moisture condition II, Baseflow alpha-factor, and average slope steepness were the most sensitive parameters. Future climate data for two Representative Concentration Pathway (RCPs) from Regional Atmospheric Climate Model -22T and Climate Limited Area Modeling 4 models were used. Land use/cover (LULC) maps were generated by classifying time-series (1996, 2006, and 2018) satellite images, selected spatial metrics were used to predict the LULC changes for the next decade using 2018 as a base year. Furthermore, the implications of selected staple crops production over the next decade was predicted. Simulated LULC shows expansion in built-up (by 32.55% and agriculture (by 39.52%) areas from 2018 to 2030, and the forest area is projected to shrink by 6.37%. However, the results suggest that farm size plays a minor role in increasing crop production. Expansion in cultivation land and built-up area attributed to the changes in water yield, surface runoff, evapotranspiration (ET), and groundwater flow. Rock-water interaction chiefly controls the groundwater quality in the presence of HCO_3 enrichment and mixed CaNaHCO_3 water types. The $\delta^2\text{H}$ and $\delta^{18}\text{O}$ values confirmed that recycled water is the primary recharge means, and glacier melts on Mt. Kilimanjaro sustains downstream water availability during the dry season. Furthermore, temperatures were projected to increase by $0.2^\circ\text{C}/\text{year}$, and a decrease in precipitation was projected up to 2100 in both highland and lowland areas. The findings suggested the need to intensify the production per unit area rather than expanding the farm size. Also, improving the vegetation cover on the hillside and abandoned land area could help to reduce the direct surface runoff, and floods recurring in the area. The findings of this study are useful to facilitate sustainable water resources management in the watershed and other watersheds with or without modification.

DECLARATION

I, Mateso Said, do hereby declare to the Senate of The Nelson Mandela African Institution of Science and Technology that this Thesis titled “*Climate and Anthropogenic Footprints Implications on the Surface and Groundwater Dynamics on the Southern Slopes of Mount Kilimanjaro, Tanzania*” is my own original work and that it has neither been submitted nor being concurrently submitted for degree award in any other institution.

Mateso Said

Name and Signature of the Candidate

Date

The above declaration is confirmed by:

Dr. Hans Charles Komakech

Name and Signature of Supervisor 1

Date

Dr. Ibrahimu Chikira Mjemah

Name and Signature of Supervisor 2

Date

COPYRIGHT

This thesis is copyright material protected under the Berne Convention, the Copyright Act of 1999 and other international and national enactments, in that behalf, on intellectual property. It must not be reproduced by any means, in full or in part, except for short extracts in fair dealing; for researcher private study, critical scholarly review or discourse with an acknowledgement, without the written permission of the office of Deputy Vice-Chancellor for Academics, Research and Innovations, on behalf of both the author and The Nelson Mandela African Institution of Science and Technology.

CERTIFICATION

The undersigned certify that they have read and hereby recommend for examination by the Nelson Mandela African Institution of Science and Technology a thesis titled “*Climate and Anthropogenic Footprints Implications on the Surface and Groundwater Dynamics on the Southern Slopes of Mount Kilimanjaro, Tanzania*” in fulfilment of the requirements for the Degree of Doctor of Philosophy in Hydrology and Water Resources Engineering at Nelson Mandela African Institution of Science and Technology, Arusha Tanzania.

Dr. Hans Charles Komakech

Name and Signature of Supervisor 1

Date

Dr. Ibrahimu Chikira Mjemah

Name and Signature of Supervisor 2

Date

ACKNOWLEDGEMENTS

I am grateful to Almighty God, the creator of the universe and all living and non-living things, for giving me good health, strength and understanding to accomplish this work. I recognize the significant contribution of my supervisors Dr. Hans Charles Komakech and Dr. Ibrahimu Chikira Mjemah. I owe a considerable debt of gratitude to their enthusiastic encouragement, patience, motivation, wisdom, understanding, useful critiques, invaluable guidance, and continuous supervision during my study.

I acknowledge the Dean School of Materials, Energy, Water and Environmental Sciences (MEWES) Prof. Revocatus Lazaro Machunda, Head of the Department of Water and Environmental Sciences (WESE), Dr. Mwemezi Rwiza and all MEWES staff for their encouragement to this successful ending. I extend my sincere appreciation to the late Prof. Alfred Nzibavuga Nyarubakula Muzuka, who sadly passed away in the middle of this work. His love and commitments have left a mark in my life, and I pray that his soul rests in eternal peace.

I would also like to express my gratitude to the African Development Bank (AfDB) through grant number 2100155032816, hosted at The Nelson Mandela African Institution of Science and Technology, Arusha, Tanzania, for granting a scholarship to pursue my PhD. I also acknowledge the academic secondment to the Indian Institute of Technology-Delhi (IIT Delhi), the program organized and financed by the world bank through the Centre of Excellence in Water Infrastructure and Sustainable Energy Futures (WISE-FUTURES). I also owe appreciation to the National Institute of Hydrology (NIH) in Roorkee, India, for assistance in analysing stable isotopes of water ($\delta^{18}\text{O}$ and δD).

My heartfelt appreciation goes to Dr. Canute Benedict Hyandye and Mr. Kassim Ramadhani Mussa for the continued support in modelling works and data analysis algorithms. Furthermore, I would like to offer my special thanks to Dr Surdith Kumar of the National Institute of Hydrology (NIH), India. For the acceptance in the analysis of stable isotopes of water ($\delta^{18}\text{O}$ and δD). Prof. Dr. Chahar B. R. of the Civil engineering department at the Indian Institute of Technology-Delhi for assistance in placement at the Water resources Simulation Laboratory. My laboratory mates at the Water resources simulation laboratory at the Indian Institute of Technology, Dr. Alemayehu Shawul, Mr. Fatimata Dialo, Mr. Kassim Ramadhani Mussa, and Mr. Noel, for motivating me towards the completion of my modelling work.

I would like to express my appreciation to MEWES laboratory scientist; Mis. Teresia Kimario and Mr. Wilson Mahene for their technical support and help during my laboratory work. I also acknowledge Mr. Masumbuko Msongo of Ngurdoto defluoridation research station and Mr. Mesia Lufingo of the Rufiji basin water quality laboratory (Iringa) for analysis of some of the parameters in water samples.

It is my honour to express my cordial thanks to my beloved daughters and close friends Glory and Grace for their patience during my absence; your love has always been a motivating factor towards completing this work. Special thanks go to Mis. Jane Emmanuel, who spent years taking care of my daughters with excessive love all the time I was absent from home. I extend my sincere thanks to my mother, Namkunda Mrindoko and my father Mborouk Mhema, my brothers and my sisters for providing a loving environment that allowed me to pursue my studies to this level.

DEDICATION

This work is dedicated to: Namkunda Mrindoko, my mama, my family, my lovely wife Rufina Fredrick and our children Glory Grace, and Gideon.

TABLE OF CONTENTS

ABSTRACT	i
DECLARATION.....	ii
COPYRIGHT	iii
CERTIFICATION	iv
ACKNOWLEDGEMENT	v
DEDICATION	vii
TABLE OF CONTENTS	viii
LIST OF TABLES	xiii
LIST OF FIGURES	xv
LIST OF APPENDICES	xix
LIST OF ABBREVIATIONS AND SYMBOLS.....	xx
CHAPTER ONE.....	1
INTRODUCTION	1
1.1 Background of the Study	1
1.2 Statement of the Problem.....	11
1.3 Rationale of the Study.....	13
1.4 Objectives of the Study	14
1.4.1 General Objective	14
1.4.2 Specific Objectives	14
1.5 Research Questions	14
1.6 Significance of the Study	17
1.6.1 Overall Significance	17
1.6.2 Scientific Contribution	17
1.7 Delineation of the Study	19
CHAPTER TWO.....	20

LITERATURE REVIEW	20
2.1 Introduction.....	20
2.2 Land use Change on Mount Kilimanjaro Slopes	22
2.1.1 Land Use and Hydrology of Kilimanjaro	22
2.3 Groundwater-Surface Water Interaction.....	24
2.4 Land Use and Crop Production on Mount Kilimanjaro Slopes	26
2.5 Changes in Forest Land and Agricultural Land Conversion.....	26
2.6 Land Use/Cover Changes Detection.....	27
2.7 Climate Change and its Impacts.....	28
2.7.1 Climate Change and Hydrology on the Southern Slopes of Kilimanjaro	28
2.7.2 Mount Kilimanjaro Glacier as an Indicator of Climate Change.....	30
2.7.3 Climate and land Use/Cover Changes and Implication on Food Production along Kilimanjaro Slopes	33
2.7.4 Climate Change and its Implications on River Discharge.....	35
2.8 Climate and Land Use Change and Implications on Water-Food-Energy (WFE nexus).....	38
2.9 Motivation.....	42
2.10 Evaluation of the Impacts of Climate and Land Use Changes on Water Resources ..	43
2.10.1 The Hydrologic Simulator.....	43
2.10.2 Partial Least Squares Regression Analysis.....	45
2.10.3 Historical and Future Climate Change Simulation.....	46
CHAPTER THREE	49
MATERIALS AND METHODS	49
3.1 The Study Area Characteristics.....	49
3.1.1 Background Characteristics.....	49
3.1.2 Rainfall and Temperatures	49
3.1.3 Geology and Soils.....	52

3.1.4	Hydrogeological Setting.....	53
3.1.5	Population and Economic Activities	53
3.2	Assessment of the Historical and Future Land Use/Cover Dynamics on Mt. Kilimanjaro Slopes.....	56
3.2.1	Data Acquisition and Image Pre-Processing	56
3.2.2	Image Classification and Accuracy Assessment	58
3.2.3	Data Preparation and Future Land-Use and Land-Cover Projection.....	61
3.3	To assess the Impacts of the Present and Future Land Use/Cover Changes on the Water Budget of Mount Kilimanjaro Slopes	67
3.3.1	Input Data Collection and Processing	68
3.3.2	Model Set-up and Parameterization	72
3.3.3	Calibration and Validation of the Soil and Water Assessment Tool Model ..	72
3.3.4	Streamflow Validation.....	74
3.3.5	Model Application for Scenarios Simulation	74
3.4	To Assess the Impact of Past, Present, and Future Climate Changes on the Water Budget (Surface and Groundwater) of the Mount Kilimanjaro Slopes	75
3.4.1	Climate Data from the Coordinated Regional Climate Downscaling Experiment (CORDEX) Regional Climate Models	75
3.4.2	Bias Correction.....	78
3.4.3	Linear Scaling for Precipitation.....	78
3.4.4	Linear Scaling for Temperature.....	79
3.4.5	Trend Analysis.....	80
3.4.6	Assessment of the Impacts of Climate Change on the Hydrology of Kikafu, Weruweru and Karanga Watershed.....	82
3.5	To Assess the Impacts of the Present and Future Land-Use Changes on Water Quality on the Slopes of Mount Kilimanjaro.....	83
3.5.1	Sample Collection	83

3.5.2	Samples Analysis.....	84
3.5.3	Groundwater Quality for Irrigation Assessment	86
3.5.4	Data Analysis.....	89
CHAPTER FOUR		91
RESULTS AND DISCUSSION.....		91
4.1	Current and Future Land Use/Cover Changes and the Association to Food Production	91
4.1.1	Assessment of Classification Accuracy and Generation of Land-Cover Maps	91
4.1.2	Patterns of Land Use/Cover Changes.....	92
4.1.3	Projection and Validation of Land Use/Cover Change on the Slopes of Kilimanjaro.....	94
4.1.4	The Transition Matrix of Land Use/Cover Change on the Slopes of Kilimanjaro	98
4.1.5	Projected Land Use/ Cover Changes on the Slopes of Kilimanjaro.....	100
4.1.6	Food Production and Expansion in Agricultural Land.....	105
4.2	The Impacts of the Present and Future Land Use/Cover Changes on the Water Budget	108
4.2.1	Sensitivity Analysis	108
4.2.2	Model Parameters, Calibration and Validation	110
4.2.3	The Impact of Land Cover Changes on the Hydrology of the Kikafu, Weruweru and Karanga Watershed.....	113
4.2.4	The Variations of Individual Land Cover Changes on Water Balance Components.....	117
4.2.5	Hydrological impacts of individual land cover changes on the selected water balance components.....	120
4.3	The Impacts of the Present and Future Land-Use Changes on Water Quality	125
4.3.1	The General Insight from Water Samples and Physical Parameters.....	129

4.3.2	Water Classification and Hydrogeochemical Facies.....	130
4.3.3	Hierarchical Cluster Analysis of Water Sources	131
4.3.4	Origin of Groundwater Sources and Mechanism Controlling Geochemistry.....	133
4.3.5	Isotopic Analysis	135
4.3.6	Multivariate Statistical Method	138
4.3.7	Potential Variations of pH with Fluoride, Depth and Dissolved Oxygen	144
4.3.8	Water Quality Suitability for Potable Uses	147
4.3.9	Suitability of Water quality for Irrigation Application.....	151
4.4	Impacts of Past, Present, and Future Climate Changes on the Water Budget (Surface and Groundwater) of the Mount Kilimanjaro Slopes.....	159
4.4.1	Impacts of Climate Change on Precipitation.....	159
4.4.2	Impacts of Climate Change on Temperature.....	167
4.4.3	Expected Future Hydrology of the Watershed	175
4.4.4	The Impacts of Climate Change on Water Balance Components	180
4.4.5	The Projected Hydrology and its Implication in Water-Food-Energy (WFE nexus)	183
CHAPTER FIVE		185
CONCLUSION AND RECOMMENDATIONS		185
5.1	Conclusion	185
5.2	Recommendations.....	187
REFERENCES		191
APPENDICES		245
RESEARCH OUTPUTS		252

LIST OF TABLES

Table 1:	Glacier and ice cover retreat in the Mount Kilimanjaro	32
Table 2:	Characteristics of the data used	58
Table 3:	Land use/cover classes and their description.....	59
Table 4:	The criteria used in the preparation of suitability maps	62
Table 5:	Description of data types and sources	70
Table 6:	Coordinated regional climate downscaling experiment regional climate modelling used in the study	77
Table 7:	Daily weather data used in the study area	78
Table 8:	Accuracy assessment results of the classified images	91
Table 9:	Losses/gains in land use/cover areas (km ²)	92
Table 10:	Components of agreement/disagreement between the observed and simulated Land-use and land-cover maps of 2018.....	95
Table 11:	Probability transitional matrix of land-use and land-cover of 1993 and 2006 for simulation of land-use and land-cover of the year 2018	99
Table 12:	Land-use and land-cover change matrix between 2018 and 2030 (km ²)	102
Table 13:	Parameters sensitive to streamflow, their default range, fitted value during calibration and final values used	112
Table 14:	Model performance statistics for the calibration and validation periods.....	113
Table 15:	Area land-use change, annual basin values (mm) for different consecutive years in the study area (Note: Rocky surface and Glacier ice were not used in this analysis)	115
Table 16:	Results of the partial least squares regression model of the hydrological components in the Kikafu, Weruweru and Karanga watershed	119
Table 17:	Variable importance for the projection values and partial least squares regression model weights for independent variables in the Kikafu, Weruweru and Karanga watershed	120

Table 18: Correlation matrix for the land cover variables and selected hydrologic components.....	124
Table 19: Analytical results	126
Table 20: Descriptive statistics water quality with drinking guideline	129
Table 21: Pearson correlation matrix for studied samples.....	139
Table 22: Principal component loadings of analyzed data	140
Table 23: Indices used to evaluate water samples for irrigation suitability.....	153
Table 24: Average annual basin values as simulated by soil and water assessment tool model fed with climate data from regional atmospheric climate model 22T- Irish Centre for High-End Computing for two scenarios representative concentration pathway 4.5 and representative concentration pathway 8.5	177
Table 25: Average annual basin values as simulated by soil and water assessment tool model fed with climate data from climate limited area modeling 4-CNRM for two scenarios, representative concentration pathway 4.5 and representative concentration pathway 8.5	179
Table 26: Mean annual basin values as simulated by soil and water assessment tool model fed with climate data from regional climate model ensemble average for two scenarios representative concentration pathway 4.5 and representative concentration pathway 8.5	181

LIST OF FIGURES

Figure 1:	The conceptual framework of data, activities, steps and processes used in this study	16
Figure 2:	The study area, weather and gauging stations (a), features and elevation (b), and annual rainfall distribution (c).....	51
Figure 3:	Geology (d), Soils (e) and Slope (f) maps of the study area	55
Figure 4:	Image classification and accuracy assessment workflow	60
Figure 5:	A summary of the procedures used to simulate land-use and land-cover map of the year 2030	65
Figure 6:	Land use/cover classes suitability maps for Built-up area (a), Agricultural land (b), Water (c), Forest (d), Barrenland (e), Grassland (f), Wetland (g), Shrubland (h), Rocky surface (i), Glacier ice (j)	66
Figure 7:	Slope and soil maps.....	71
Figure 8:	Land use map for the year 2006	71
Figure 9:	Conceptual diagram for application of soil and water assessment tool model in assessing impacts of land cover on the hydrology of Kikafu, Weruweru and Karanga watershed	75
Figure 10:	Summary of the methods applied in determining the impacts of land use on water quality.....	84
Figure 11:	Observed (left) and simulated (Right) land-use and land-cover maps for 2018.....	95
Figure 12:	Classified land use/cover image maps for the year 1993 (a), 2006 (b) and 2018 (c)	97
Figure 13:	Simulated land-use and land-cover map of the year 2030	103
Figure 14:	Total food production in five districts along the study area and the land use change trend	106
Figure 15:	Results of parameter sensitivity analysis (P-value and t-stat).....	109
Figure 16:	Comparison between the simulated and observed monthly discharge of Kikafu, Weruweru and Karanga watershed	111

Figure 17:	Piper diagram for the chemical composition of surface and groundwater sources	131
Figure 18:	Dendrogram showing a spatial relationship among data collection sites.....	132
Figure 19:	Gibbs plot for (a) Cations and (b) Anions.....	133
Figure 20:	Durov plot for surface and groundwater samples	134
Figure 21:	Schoeller plot of the water samples	135
Figure 22:	Observational plot of $\delta^2\text{H}$ and $\delta^{18}\text{O}$ for rivers, shallow well and deep wells with global and local meteoric water lines	136
Figure 23:	Variation in surface water, shallow water and deep water sources for Weru River (a) Water quality contaminants, (b) Stable isotopes	141
Figure 24:	Variation in surface water, shallow water and deep water sources for Karanga River (a) Water quality contaminants, (b) Stable isotopes	142
Figure 25:	Chadha's classification for the hydrogeochemical process delineation of (left) Upper area, and (right) Lower area, water quality	143
Figure 26:	Binary plots of (a) $\text{Ca}^{2+}+\text{Mg}^{2+}$ vs $\text{HCO}_3^-+\text{SO}_4^{2-}$, (b) $\text{Mg}^{2+}/\text{Mg}^{2+}+\text{Ca}^{2+}$	143
Figure 27:	Plot of Na/Cl vs electrical conductivity	144
Figure 28:	Fluoride (F^-) variation with pH in the upper and lower parts of the study area	145
Figure 29:	Variation of dissolved oxygen with groundwater sources depth	146
Figure 30:	Surface and groundwater variation of temperature and dissolved oxygen ...	147
Figure 31:	Nitrate and Cl concentration for lowland and upland areas	151
Figure 32:	Classification of river water in terms of the degree of suitability for irrigation: electrical conductivity versus sodium adsorption ratio (Richards 1954)	153
Figure 33:	Spatial distribution of the indices used to assess irrigation suitability.....	158
Figure 34:	Historical regional atmospheric climate model 22T model for annual rainfall in different weather stations in the Kikafu, Weruweru and Karanga watershed.....	160

Figure 35:	Regional atmospheric climate model 22T model annual rainfall projections under representative concentration pathway 4.5 in the different weather station	161
Figure 36:	Regional atmospheric climate model 22T annual rainfall projections under representative concentration pathway 8.5 in the different weather station ...	162
Figure 37:	Climate limited area modeling 4 historical rainfall in lowlands and highland.....	163
Figure 38:	Climate limited area modeling 4 future rainfall projections under representative concentration pathway 4.5	164
Figure 39:	Climate limited area modeling 4 future rainfall projections under representative concentration pathway 8.5	165
Figure 40:	Historical minimum temperature projections for the different weather stations in the Kikafu, Weruweru and Karanga watershed	167
Figure 41:	Minimum temperature projections for different weather stations under representative concentration pathway 4.5	168
Figure 42:	Minimum temperature projections for different weather stations under representative concentration pathway 8.5	169
Figure 43:	Historical maximum temperature projections for the different weather stations in the Kikafu, Weruweru and Karanga watershed	169
Figure 44:	Maximum temperature projections for different weather stations under representative concentration pathway 4.5	170
Figure 45:	Maximum temperature projections for different weather stations at Kikafu, Weruweru and Karanga watershed under representative concentration pathway 8.5.....	171
Figure 46:	Historical average minimum temperature for climate limited area modeling 4 model.....	171
Figure 47:	Historical average maximum temperature for climate limited area modeling 4 model.....	172
Figure 48:	Future average maximum temperature for climate limited area modeling 4 model under representative concentration pathway 4.5	173

Figure 49:	Future average minimum temperature for climate limited area modeling 4 model under representative concentration pathway 4.5	173
Figure 50:	Future average maximum temperature for climate limited area modeling 4 model under representative concentration pathway 8.5	174
Figure 51:	Future average minimum temperature for climate limited area modeling 4 model under representative concentration pathway 8.5	174

LIST OF APPENDICES

Appendix 1:	Historical and scenario simulation for October-November-December (OND) and March-April-May (MAM) for regional atmospheric climate mode 22T under representative concentration pathways 4.5 and 8.5.....	245
Appendix 2:	Historical and scenario simulation for October-November-December and March-April-May for climate limited area modeling 4 under representative concentration pathways 4.5 and 8.5.	248
Appendix 3:	Geological map and sampling locations for surface and extended groundwater.....	251

LIST OF ABBREVIATIONS AND SYMBOLS

δ	Sigma
‰	Per-mille
AAS	Atomic Absorption Spectrophotometer
AGR	Agricultural Land
AHP	Analytical Hierarchy Process
ALPHA_BF.gw	Baseflow Alpha Factor (Days)
BAR	Bare Land
BIO_INIT.mgt	Initial Dry Weight Biomass (kg/ha)
BU	Built-up Area
Ca	Calcium
CA–Markov	Cellular Automata (CA) and the Markov Chain
CANMX.hru	Maximum Canopy Storage (mm H ₂ O)
CCLM4	Climate Limited Area Modeling
CEP	Country Environmental Profile
CFSR	Climate Forecast System Reanalysis
CH_K2.rte	Effective Hydraulic Conductivity in Main Channel Alluvium (mm/h)
CH_k2.rte	Effective Hydraulic Conductivity in Main Channel Alluvium (mm/h)
CH_N1.sub	Manning’s ‘n’ Value for the Tributary Channels
CH_W2.rte	Average Width of Main Channel at Top of Bank (m)
CLM	Climate Limited-Area Modelling
CMhyd	Climate Model for Hydrological Modeling Software
CN2.mgt	Initial SCS Runoff Curve Number for Moisture Condition II
CNRM	CNRM-CERFACS-CNRM-CM5
CO ₃	Carbonate
CORDEX	Coordinated Regional Climate Downscaling Experiment
DEM	Digital Elevation Model
DO	Dissolved Oxygen
dS	Decisiemens

EC	Electrical Conductivity
EPCO.hru	Plant Uptake Compensation Factor
ERA-Interim	European Centre for Medium-Range Weather Forecasts Interim Re-Analysis
ESCO.bsn	Soil Evaporation Compensation Factor
ESP	Exchangeable Sodium Per cent
ET	Evapotranspiration
FAO	Food and Agriculture Organization
FOR	Forest
GCM	General Circulation Model
GIS	Geographical Information System
GITEC	German Engineering Consultancy Company
GLI	Glacier Ice
GMWL	Global Meteoric Water Line
GNIP	Global Network for Isotopes Precipitation
GRA	Grassland
GW_DELAY.gw	Groundwater Delay (Days)
GW_REVAP.gw	Groundwater “Revap” Coefficient
GWQ	Groundwater Flow
GWQMN.gw	Threshold Depth of Water in the Shallow Aquifer for Return Flow to Occur (mm H ₂ O)
H ₀	Null Hypothesis
H ₁	Alternative Hyporhesis
HCO ₃	Bicarbonate
HDPE	High-Density Polyethylene
HRU_SLP.hru	Average Slope Steepness (m/m)
ICHEC	Irish Centre for High-End Computing
IDRISI software	Integrated Geographic Information System and Remote Sensing
IOD	Indian Ocean Dipole
IPCC	Intergovernmental Panel on Climate Change
ITCZ	Inter-Tropical Convergence Zone
IUCN	International Union for Conservation of Nature

K	Potassium
KMO	Kaiser-Meyer-Olkin
KNMI	Royal Netherlands Meteorological Institute
KWK	Kikafu, Weruweru and Karanga
LAI_INIT.mgt	Initial Leaf area index
LAM	Limited Area Models
LatQ	Lateral Flow
LMWL	Local Meteoric Water Line
LMWL	Local meteoric Water Line
LULC	Land Use/Land Cover
LULCC	Land-Use and Land-Cover Change
m.a.m.s.l	Metres Above Mean Sea Level
MAM	March-May
MAR	Magnesium Adsorption Ratio
MCE	Multi-Criteria Evaluation
MD	Monotonically Decreasing
meq/L	Milliequivalents
Mg	Magnesium
MH	Magnesium Hazard
MI	Monotonically Increasing
Mm	millimetres
NCEP	National Centres for Environmental Prediction
NO ₃	Nitrate
NSE	Nash and Sutcliffe simulation Efficiency
NSE	Nash-Sutcliffe Efficiency
OA-ICOS	Off-axis Integrated Cavity Output Spectroscopy
OLI	Operation Land Imager
OND	October-November-December
OV_N.hru	Manning's "n" Value for Overland Flow
PAST	Paleontological Statistics
PBIAS	Per cent Bias
PBWO	Pangani Basin Water Office

PCA	Principal Component Analysis
PHU_PLT.mgt	Total Number of Heat Units or Growing Degree Days Needed to Bring Plant to Maturity
PLAPS	Lapse Rate of Precipitation
PLSR	Partial Least Squares Regression
QGIS	Quantum Geographical Information System
RACMO	Regional Atmospheric Climate Model
RCHRG_DP.gw	Deep Aquifer Percolation Fraction
RCM	Regional Climate Model
RCP	Representative Concentration Pathway
RCs	Regression Coefficients
REVAPMN.gw	Threshold Depth of Water in the Shallow Aquifer for "Revap" to Occur (mm H ₂ O)
RMSE	Root Mean Square Error
RMSECV	Cross-Validated Root Mean Squared Error
ROS	Rocky Surface
RSR	Observations Standard Deviation Ratio
SHB	Shrubland
SLSUBBSN.hru	Average Slope Length (m)
SOL_AW().sol	Available Water Capacity of the Soil Layer
SOL_K().sol	Saturated Soil Hydraulic Conductivity (mm/h)
SRTM	Shuttle Radar Topography Mission
SurfQ	Surface Flow
SURLAG.bsn	Surface Runoff Lag Time (days)
SWAT	Soil and Water Assessment Tool
SWAT-CUP	SWAT Model Calibration and Uncertainty Procedure
TDS	Total Dissolved Solids
TLAPS	Lapse Rate of Temperature
TMA	Meteorological Authority
TPC	Tanganyika Planting Company
TZS	Tanzania Standards
UNDP	United Nations Development Programme

URT	United republic of Tanzania
USGS	United States Geological Survey
VIP	Variable Importance for the Projection
VSMOW	Vienna Standard Mean Ocean Water
WAT	Water
WatQ	Water Yield
WET	Wetland
WHO	World Health Organization
WLC	Weighted Linear Combination
μS	Microsiemens

CHAPTER ONE

INTRODUCTION

1.1 Background of the Study

Land and water are the highly essential natural resources of the earth that sustain human development, ecosystem functioning, and economic progression of a country (Uniyal *et al.*, 2015). However, the continuous rise of human development has led to the remarkable transformation of many catchments worldwide both in terms of land use patterns and climate (Shi *et al.*, 2013a). In most areas of the world, land use and climate changes have adversely impacted watershed hydrology (Dwarakish & Ganasri, 2015; Zhang *et al.*, 2016). These impacts are expected to increase worldwide in the future due to ongoing anthropogenic activities and global warming (Fischer, 2013). Population growth, which implies increased water needs, is likely to increase pressure on water resources which may deepen many countries around the world into water scarcity (Miralles *et al.*, 2017).

Changes in the hydrological system have increased uncertainty in the future demand and availability of water in many parts of the world (Middelkoop *et al.*, 2001). Projections from the fifth report of the Intergovernmental Panel for Climate (IPCC) show the major impacts in water availability and supply in rural areas worldwide; leading to reduction in renewable surface and groundwater resources in most dry subtropical regions (Intergovernmental Panel on Climate Change [IPCC], 2014d). The reduction in surface and groundwater availability intensifying the unsustainability in water supply in rural areas around Africa (MacDonald *et al.*, 2009b). Understanding the complicated and dynamic land surface and its interacting components is needed to make accurate projections of the future water balance (Feyen & Vazquez, 2011). The combined rapid land use/ cover and climate changes are envisaged to increase hydrologic impacts (Chen & Yu, 2013). Impacts of changes have driven the changes in research focus in hydrology resulting into quantitative assessments of the impact of climate and land use/cover changes on water resource (Yin *et al.*, 2017).

The temperature in Africa has increased by more than 0.5°C during the last 50 to 100 years (Gan *et al.*, 2016; IPCC, 2014d; Niang *et al.*, 2014). Also, temperatures are reported to have increased by 1–2°C from 1970 to 2004 (IPCC, 2014a). Moreover, a similar trend is projected by the end of 2025 (Mitchell, 2013). Furthermore, the maximum and minimum temperatures have shown increasing trends during the last decades (Adhikari *et al.*, 2015; Mengistu *et al.*,

2014; Niang *et al.*, 2014). The increase in temperature is accompanied by a steady decline in precipitation in some parts of the African region (Lyon & DeWitt, 2012; Mekasha *et al.*, 2014), but the observed long-term precipitation trends are not significant (Mengistu *et al.*, 2014).

Changes in climate have the potential to intensify the existing pressures to human security, including the pressure on food, health, and economic insecurity in most African countries (Pachauri *et al.*, 2014b). Topographical location, proximity to the equator and socioeconomic attributes in East Africa (EA) make the regions among the most vulnerable to the current temperature variations attracting several studies with broader consequences (Omambia *et al.*, 2017). Currently, significant evidence of climate change includes frequent droughts and increase in drylands areas which affects water and food availability for humans, livestock, and wildlife (Munishi *et al.*, 2015; Omambia *et al.*, 2017). For instance, the fast retreats of glaciers on Mount Kilimanjaro, and Mount Kenya, and changes in the rainfall patterns in the East Africa region have been reported as evidence of climate change impacts (Adhikari *et al.*, 2015). Studies show that there might be impacts on the hydrological system that are of limited knowledge (Mckenzie *et al.*, 2010).

Climate assessments studies named Tanzania among countries prone to extreme weather events, ranging from droughts to floods (Pachauri *et al.*, 2014b). The rise in temperature, for example, results in an increase in evapotranspiration, changes in timing, consistency, and intensity of rains, as well as duration and incidences of floods and droughts (Oguge *et al.*, 2011). The impacts of climate change could be noted in variations in surface water discharges, quality and groundwater table fluctuations (Mckenzie *et al.*, 2010). As a result, water managers have shifted their focus to developing groundwater systems for domestic uses and agricultural production (Kumar, 2016). Although the natural groundwater recharge solely depends on precipitation patterns (Shah, 2009), observations in Tanzania have shown variations in yields of boreholes due to increases in climate variability (Kashaigili, 2010).

Access to water is a critical input into the national economy in Tanzania. Water supports agricultural sector, the major employer (employing more than 80% of the workforce) and source of revenue, less than 30% of national GDP (Epaphra & Mwakalasya, 2017), and about 55% of foreign exchange incomes (United Republic of Tanzania [URT], 2010a, b). However, water availability is strained by the increasing water needs and ongoing impacts of climate change that is responsible for repeated droughts and drying up of surface water sources

(Rwebugisa, 2008; Salama, 1979; Taylor *et al.*, 2012b). Reduced surface water access for cropping has led to a rapid increase in food prices and increased groundwater pressure (Taylor *et al.*, 2013).

Climate and rapid urbanization were named as major causes for nearly all urban centres failing to meet domestic water demands (URT, 2010 a, b). Nationally, water scarcity has also been associated with conflicts, including tribal, ecological and sectarian conflicts involving farmers, livestock keepers and wildlife (Shemsanga *et al.*, 2010). Farming, livestock keeping, and hydroelectric production need a lot of water to run, which leads to increased water demand and disputes among water users in the region (Andersson *et al.*, 2006; Burton & Chiza, 1997; Tagseth, 2010). As a result, climate change would have an effect on a wide range of community members, from households to plantation agriculture. Thus, there is a pressing need to address future resilience.

Initial runoff forecasts in Tanzania's northeastern rivers indicate both temporal and spatial monthly variations. The discharge along Pangani and Kikuletwa rivers are expected to decrease by around 6% and 9% annually, respectively (Agrawala *et al.*, 2003). However, different trend was reported where the precipitation levels along the Pangani River are expected to increase by 16 to 18% (by the 2050s), resulting in a 10% increase in runoff despite lower peak flows (Kishiwa *et al.*, 2018). This mismatch in runoff estimation highlights the need for high-resolution impact studies on the southern slopes of Kilimanjaro to determine the extent of the impact and possible water supply scenarios.

Kilimanjaro region is often reported as an early indicator of climate change impacts and adverse land use changes (Mckenzie *et al.*, 2010). The current climate variability and anthropogenic activities have negative surface and groundwater quality and quantity implications (Kashaigili, 2010; MacDonald *et al.*, 2009b; Mckenzie *et al.*, 2010). Initiatives to address climate change impacts over Kilimanjaro are reported to have started late in 18th century, the major focus of the researchers has been on glacier retreat as a result of climate change (Kaser, 1999; Kaser *et al.*, 2004; Mölg *et al.*, 2008; Mölg *et al.*, 2009; Thompson, 2000; Thompson *et al.*, 2002), and forest cover changes impacts on glacier retreat (Agrawala *et al.*, 2003; Hemp, 2005). Climate variability is reported to have caused drought that has affected regional life forms, agriculture and vegetation (Mölg *et al.*, 2009). Mckenzie *et al.* (2010) warns that climate change impacts on the Kilimanjaro hydrological system is still not

well understood. Therefore, there is a need to study the impacts of present and future climate change on the surface and groundwater hydrology of the Kilimanjaro.

Agriculture is the main water extracting activity in the Pangani basin (Lalika *et al.*, 2015), with small to large-scale rice, sugar cane irrigated plantations along Kahe plains being among the major water users. However, Pangani is reported to be a water-stressed basin with the available renewable water supply below 1200 m³ per person per year, and also that the water use efficiency of most irrigation systems is <15% (Pangani Basin Water Office [PBWO] & International Union for Conservation of Nature [IUCN], 2010).

Occurring in tandem with increased climate variable is land use change on the Kilimanjaro (Chiwa, 2012; Palamuleni *et al.*, 2011). Mount Kilimanjaro is a unique social and ecologic ecosystem which harbors natural vegetation, home gardens, agroforest trees and savannah in the lowlands. Previous studies in the study area show increased forest degradation on the southern slopes from 1606 ha to 5170 ha between 1973 and 2000 (Mbonile, 2005), also, cultivated land increased from 54% (in 1973) to 63% in 2000 on the southern and eastern slopes (Misana *et al.*, 2012). Studies further show that closed and open forests decreased by 56% and 64%, respectively (Munishi *et al.*, 2009). The loss of more than 41 km² of the forest between 1952 and 1982 (Yanda & Shishira, 2001). Further, riverine vegetation decreased by 53% (Munishi *et al.*, 2009). These reflect the replacement of the perennial vegetation with seasonal crops; thus, triggering the need to establish past which will help to establish the future Land use/cover trend on the southern slopes of Mount Kilimanjaro.

Conversion of other Land use/land cover (LULC) types to agricultural land is a continuous phenomenon. Studies show the conversion by 53 km² of combined shrub, grassland and sparse vegetation to maize and vegetable cultivation from 1987 to 2005 in Kahe plains (German engineering consultancy company [GITEC], 2011). Further, about 49.97 km² (32.8%) of shrubs and bushland were converted to agriculture and other uses from 1961 to 2000 years in the Kirua Vunjo division (Soini, 2005b). Furthermore, 39.5% of bushland was converted to agriculture between 1973 and 2000 years (Mbonile *et al.*, 2003). However, none of the previous studies established the relationship between increase in Agricultural land and food production. Therefore, these land conversions prompt the need to establish a link between an increase in agricultural land and food production.

Studies show that land use/cover change has the potential to impact the regional climate over Kilimanjaro, but the magnitude and exact nature of the impact is not well documented (Fairman *et al.*, 2011; Mölg *et al.*, 2008). The Regional Atmospheric Modelling system simulations show that deforestation at lower elevations of Kilimanjaro contributes to the decrease in cloud occurrence frequency at all elevations on the mountain (Fairman *et al.*, 2011). However, the results were based on one dry season month and did not include information for wet seasons. Therefore, there is a need to include climate change impacts in water resources management (Kumar, 2016).

Mount Kilimanjaro has long served as a water tower, supplying rivers and springs to the communities that surround its slopes. On Mt. Kilimanjaro's southern slope, there are about 1800 kilometres of irrigation canals that supply about 200 million cubic meters of water for agriculture and domestic use (Mckenzie *et al.*, 2010). Furthermore, there are few perennial rivers source from the mountain slopes at an elevation of 3939 m.a.m.s.l (Mwende, 2009); however, the forest belt in the Kilimanjaro national park and the irrigation belt under the forest (1100 – 1640 m.a.m.s.l) contributes about 71-94% of the recharge to the Kahe basin (GITEC, 2011). This means that the future of irrigated agriculture and domestic water supply in the Kahe basin's lowlands is solely dependent on the sustainability of Mount Kilimanjaro.

Changes in land use/cover resulting from increased anthropogenic activities influence surface and groundwater quality. There is a growing pressure on the surface and shallow groundwater quality reported across Africa (MacDonald *et al.*, 2009b). For example, poor agronomic practices especially in the management of fertilizers and pesticides are named as major cause of increased nitrate levels in the groundwater system in Moshi Tanzania (Mckenzie *et al.*, 2010). Land use/cover changes is estimated to contribute to 60% of present soil erosion and siltation (Yang *et al.*, 2003). There is a need to understand the impact of anthropogenic activities, climate impacts and their interactions on water resources (Fairman *et al.*, 2011; Leterme & Mallants, 2011).

In practice, land cover changes affect the surface water balance of an area, thus impacting evapotranspiration, initial surface runoff, and groundwater flow (Fohrer *et al.*, 2001; Foley *et al.*, 2005). Apart from impacting water resources and hydrologic water balance, land use/cover (LULC) changes can directly affects local communities, the biota, and possible water management plans (Abe *et al.*, 2018; Dos Santos *et al.*, 2018). The spatial distribution patterns of land-use/cover can substantially impact runoff and sediment transport processes

at different dimensions (Defersha & Melesse, 2012; Fu *et al.*, 2009). It has both local, regional and global occurrence and is reported to continue in the future (Foley *et al.*, 2005). Changes in land use/cover is potentially of large impacts on water resources; thus, It is important to understand the possible effects of LC changes in the runoff variability and possible measures (Shawul *et al.*, 2019).

Most places in East Africa have experienced a conversion of natural forests to settlements, urban centres, farmlands, and grazing lands at varying dimensions (Maitima *et al.*, 2009; Smith *et al.*, 2016). The conversion of natural forests to settlements creates a need for a balance between food production and minimization of the negative environmental impacts on other ecosystem services such as quality and quantity of water (Mustard *et al.*, 2012). Although food production requires a sustainable water supply, land use/cover changes resulting from the expansion in agriculture affect water resources. These changes affect food production in the long run (Guzha *et al.*, 2018). Thus, it is essential to manage land use/cover changes at a catchment scale (Bradford *et al.*, 2001). However, quantifying its impacts is challenging (Stonestrom *et al.*, 2009).

Mount Kilimanjaro slopes are typical landscapes with the highest recorded land cover dynamics, and their consequences on water resources, food and energy production have been reported in previous studies (Said *et al.*, 2019). Changes in land cover in most of the areas surrounding Mt. Kilimanjaro slopes have the potential to impact water resources (Chiwa, 2012; Mbonile *et al.*, 2003; Misana *et al.*, 2012; Mmbaga *et al.*, 2017; Ngugi *et al.*, 2015; Soini, 2005b). These changes trigger the need to understand land cover change trajectories and surface-groundwater interaction among the critical requirements in water management practices in the area. Surface-groundwater interaction affects water management and water rights changes, nutrients loading from aquifers to streams, and in-stream flow requirements for aquatic species at a watershed scale (Bailey *et al.*, 2016). The knowledge regarding land use/cover changes in relation to water balance components on the slopes of Mt. Kilimanjaro is of utmost importance due to limited information with regards to groundwater flow (Mckenzie *et al.*, 2010).

Land degradation and land cover changes have contributed to the decline in surface water resources around Mt. Kilimanjaro (Ngugi *et al.*, 2015). Human activities are reported as the main contributor to the rapid land cover changes around the same area. The activities include encroachment due to logging, agricultural expansion and settlements, which in turn have

created significant changes in the land cover (Shishira & Yanda, 2018). Indeed, the increased anthropogenic activities are mainly driven by the fast-growing population, strengthening the pressure on the available water resources on a day to day basis (Gao *et al.*, 2017). Other drivers include socio-economic development and pressure on land for expansion in agriculture (Lambin *et al.*, 2003).

Anthropogenic activities such as those leading to extensive land cover changes and climate change are among the main drivers for changes in hydrological processes of the watershed (Briones *et al.*, 2016; Neupane & Kumar, 2015; Zhou *et al.*, 2017). Anthropogenic modification of land use/cover is a topmost determinant of environmental changes at spatial and temporal scales (Gashaw *et al.*, 2018; Karimi *et al.*, 2018). It is a principal determining factor of global environmental changes with severe impacts on human livelihoods (Olson *et al.*, 2008), and that the current rates are higher than ever recorded (Baldus *et al.*, 2003).

Many studies have also shown that land use/cover changes influence the hydrology of watersheds (Kashaigili & Majaliwa, 2013; Kitalika *et al.*, 2018; Marhaento *et al.*, 2018). Thus, evaluation of the impact of the Land cover (LC) and climate changes on water resource availability is an important challenge for the current hydrological science (Yin *et al.*, 2017; Zhang *et al.*, 2017). Further, there is a growing need for a scientific community to balance human needs and environmental sustainability (Foley *et al.*, 2005). Thus, understanding the environmental impacts of land use/cover changes is a fundamental part of sustainable land planning and development (Memarian *et al.*, 2014).

Some of the proposed strategies to curb the expansion of agriculture due to demand for food to suffice the expanding population on the slopes of Mount Kilimanjaro include the improvement of the land tenure security and introduction of modern land and water conservation measures. These strategies aimed at increasing per capital production and discourage opening up of more land for agriculture (Ngugi *et al.*, 2015). Shrinking in the forest area along the mountain landscapes has also been reported in several studies (Agrawala *et al.*, 2003; Mbonile, 2005). However, the quantitative estimates of water losses due to deforestation in the Pangani basin are scanty or missing (Shaghude, 2006). Hence, it is essential to understand the effect of land management practices at the basin and subbasins scale; these practices increase the impact of hydrologic variability on the society and ecosystem (Shawul *et al.*, 2019).

The main objective of this study is to develop a set of methodologies for integrated surface and groundwater management to maximize the net benefit for domestic, agriculture, and industrial production systems. These methodologies include remote sensing (RS) and geographical information system (GIS) that was adopted to assess the historical and future land use/cover dynamics. Also, a methodology for assessing hydrological fluxes and specifically stream flow pattern prediction at the outlets under changing land use as well as future climate change context. Furthermore, a methodology was developed for ground and surface water quality analysis to judge the qualitative aspect of surface and groundwater for domestic, industrial and agricultural production. Finally, a methodology was adopted to assess historical and prediction of the future climate changes; the results were integrated with hydrological fluxes and food and hydropower production.

Climate change and land use/cover changes are connected through the hydrologic cycle. The relationship between climate, land use, and hydrology of a particular area appears both intuitive and complex (Schulze, 2000). Since climate change, water supply conditions, and land use/cover changes all affect one another, understanding the effect of climate change on the water cycle necessitates a multifaceted study of its dynamic and nonlinear interrelated processes (Xia *et al.*, 2017). Many possible impacts on the hydrological system are anticipated as a result of ongoing local and global changes in the climate system of Kilimanjaro (Mckenzie *et al.*, 2010).

Climate change phenomena are deemed to affect the livelihood of people and afflict ecosystem services production globally. Climate change has the potential to intensify the existing pressures on humans by afflicting food, health, and economic security in most African countries (Pachauri *et al.*, 2014a). According to climate assessments, Tanzania is among the countries prone to extreme events, including droughts and floods (Pachauri *et al.*, 2014a). The impacts of climate change can be noted in surface water discharges, quality and groundwater table fluctuations (Mckenzie *et al.*, 2010). Studies show variations in yields of boreholes due to an increase in climate variabilities (Kashaigili, 2010). Thus, in order to design a mitigation option, there is a need to better understand the extent of the impact, trends and future implication.

For domestic and agricultural needs, the local population on the slopes of Mt. Kilimanjaro depend solely on streams and springs (Mckenzie *et al.*, 2010). Smallholder farmers and conventional agropastoralists, however, dominate about 85% of arable land; the former

primarily rely on rainfed agriculture (Lein, 2004). Weather and climate changes on Mt. Kilimanjaro would have an effect on regional water supply availability and ecological sustainability (Fairman *et al.*, 2011). This shift affects water and water use, which is related to social, economic, political, and historical ties and processes in Kilimanjaro and the Pangani River (Lein, 2004). This requires the need for developing a conceptual understanding of the overall availability and predictability of water resources (Rowhani *et al.*, 2011).

Uncertainty in agriculture production depends on the stochastic nature of rainfall; frequent droughts and floods occur in the study area. Farmers in the lowlands areas are highly dependable to groundwater resources for their irrigation needs. Changes in surface water and groundwater level can be attributed to changes in discharge and recharge rate under projected precipitation and areal potential evapotranspiration.

There are only a few research studies that have quantified the hydrological responses to future predicted climate conditions (Adhikari *et al.*, 2017). However, in many parts of the country, the scarcity of high-quality data remains a major concern. This makes it difficult to comprehend the observed changes and improve the efficiency of hydrological models around the world (Kundzewicz *et al.*, 2009). Runoff reconstruction, for example, is hindered by data availability and data quality (Gedney *et al.*, 2006; Peel & McMahon, 2006). Thus, there is a need to conduct high-resolution studies deemed to generate good quality hydrological data for future water balance under changing climate and land use.

A modelling approach is typically used to assess the impacts of land use/cover change on the water balance in a catchment. Models can be used to evaluate the historical and future implications of land use/cover changes on the hydrology of a catchment (Huisman *et al.*, 2009). The hydrologic model, Soil and Water Assessment Tool (SWAT) is a continuous-time, physically based, spatially distributed watershed model used to simulate runoff, sediment and agricultural chemical yield in the watershed scale. The SWAT can be used to model the physical processes associated with water flow, sediment transport, crop growth, nutrient cycling (Shi *et al.*, 2013a). The Calibration Uncertainty Program for SWAT (SWAT-CUP) enables automatic calibration of the model. Other models such as SWAT+ could be used in this study, however, the automatic calibration procedure (SWAT+ CUP) was not released during conceptualization and conduction of this work. Further, this study assesses the impacts of epistemic uncertainty on the streamflow pattern using a hydrological model. Impacts of climate on a watershed were quantified, and future climate projections (CCLM4

and RACMO) in terms of precipitation and temperature as per IPCC fifth assessment report and the corresponding two concentration pathways (RCP) were used.

Meeting regional water needs will depend on the way water resources are understood and managed (Hamza, 1993; MacDonald *et al.*, 2009a). Access to enough and quality water for various uses requires a thorough understanding of available water and protection from pollution while carefully balancing abstraction of surface water and groundwater (Taylor *et al.*, 2012a; Taylor *et al.*, 2012b). Thus, water quality assessment should be considered as equally essential as that of its quantity (Bashir *et al.*, 2015). Thus, a need to assess water quality for domestic, agriculture and industrial production on the Mount Kilimanjaro slopes is essential.

Sustainable water resources management requires developing knowledge on the impacts of historical and future changes in climate and land use/cover on the water balance of a watershed. Studies in Heihe River Basin, Northwest China, show that land use and climate changes are adversely impacting watershed hydrology (Zhang *et al.*, 2016). These impacts are expected to increase worldwide in the future due to anthropogenic activities and global warming (Fischer, 2013). Hence, it is essential to study the future implications of climate and land use changes to the water balance of the watersheds.

Mount Kilimanjaro is hydrologically important (Agrawala *et al.*, 2003; Hemp, 2005); the mountain is named a water tower for the East African region (Viviroli *et al.*, 2007). The local populace on the mountain slopes of North-eastern Tanzania and South-eastern Kenya predominately depends on freshwater supplies for domestic, hydropower production, industrial, and irrigation (Agrawala *et al.*, 2003; Kishiwa *et al.*, 2018). Further, the mountain harbours the most effective water source in the fog interception zone along the thick forest reserve (Hemp, 2005). Therefore, impacting the water balance of Mt. Kilimanjaro will affect the attainment of the local, regional and global sustainable development milestones.

Kikafu, Weruweru and Karanga (KWK) watershed is one of the mountainous watersheds along the southern slopes of Mount Kilimanjaro and the northern part of the Pangani river basin. Being located on the mountain slopes with greater human activities, KWK experiences tremendous land cover changes. This triggers the need to quantify the impacts of land cover changes on the water balance for sustainable water resources management. However, despite the growing need, simulation of hydrological processes using water balance components,

such as surface runoff in mountainous areas with irregular terrain and complex hydrologic processes, is challenging (Abudu *et al.*, 2012). Also, estimation of the hydrological simulation model (SWAT) parameters is hampered by the variation of temperature and precipitation with elevation and spatial variability due to complex terrain (Anand *et al.*, 2018a).

This study used a soil and water assessment tool (SWAT) for assessing the impacts of land cover changes on the water balance components of the KWK watershed on the southern slopes of Mt. Kilimanjaro. The SWAT has been tested and used to solve complex watershed management problems in many regions all over the world (Anand *et al.*, 2018b; Hyandye *et al.*, 2018; Kishiwa *et al.*, 2018; Shawul *et al.*, 2019; Twisa *et al.*, 2020). The need for a comprehensive analysis of the historical and future land cover dynamics and its impacts on the hydrological processes on the slopes of Mount Kilimanjaro is important.

The issues discussed above prompt the need to quantify the amount and water utilization and assess the sustainability of the water under changing climate and land use/cover. Furthermore, to assess the future ground and surface water interaction, to understand the extent, trends, and future implications of future climate and the land use changes on the water balance of critical watersheds. Thus, the need for site-specific impacts studies is essential for designing future mitigation options for meeting broader community needs.

1.2 Statement of the Problem

Kilimanjaro region is often reported as an early indicator of climate change impacts and rapid changes in land use (Mckenzie *et al.*, 2010). The current climate variability trend and anthropogenic activities have opposing surface and groundwater quality and quantity implications (Kashaigili, 2010; MacDonald *et al.*, 2009b; Mckenzie *et al.*, 2010). Initiatives to address climate change impacts over Kilimanjaro are reported to have started late in the 18th century. From that time, the primary focus of the researchers has been on glacier retreat as a result of climate change (Kaser, 1999; Kaser *et al.*, 2004; Mölg *et al.*, 2008; Mölg *et al.*, 2009; Thompson, 2000; Thompson *et al.*, 2002) and forest cover changes impacts on glacier retreat (Agrawala *et al.*, 2003; Hemp, 2005). Climate variability is reported to have caused a drought that has affected regional life forms, agriculture and vegetation (Mölg *et al.*, 2009). Mckenzie *et al.* (2010) warn that the impacts of climate change on the Kilimanjaro

hydrological system are still not well understood. Most of the recent studies in the country used were of lower resolution, which missed details in KWK.

Studies report the significant attenuating trend in the investments in the management and development of water resources within the Weruweru-Kiladeda sub-catchment in Kilimanjaro (Chiwa, 2012). Some of the most recent studies around Kilimanjaro systems focused on its impact on water quality (Mckenzie *et al.*, 2010), surface water abstraction (Chiwa, 2012), and glacier retreat (Agrawala *et al.*, 2003; Hemp, 2005). However, the link between the present and the future land use/cover changes and water balance over Kilimanjaro taking into account population and food production, is missing in all studies.

Kilimanjaro region was named the eighth most densely populated region with 124 people per square Kilometer and a 1.8% average annual population growth rate from the year 2002-2012 (National Bureau of Statistics [NBS], 2012). This creates pressure on water resources which directly impact the hydrological system (Mul, 2009). Population pressure creates a demand for more shelter, fibre and water for various uses, which in turn, leads to changes to forests, farmlands and waterways (Byerlee *et al.*, 2014; Foley *et al.*, 2005).

Kilimanjaro functions as a water tower of the East Africa region; hydrological balance of Mount Kilimanjaro is reported to be seriously affected by forest fires (Agrawala *et al.*, 2003), which resulted from a loss of nearly a third of the Kilimanjaro forest cover during the last 70 years (Hemp, 2005). This resulted in replacing the fog intercepting cloud forests, which is important in the mountains water budgets (Agrawala *et al.*, 2003; Fairman *et al.*, 2011). It is postulated that changes in specific humidity are likely linked to the ongoing glacier imbalance.

The local communities have increasingly continued converting the land to agricultural land; the assumption has been that the more land is converted to agricultural land, the higher the crop production. Reports show the conversion of other forms to agricultural land on the Kilimanjaro slopes at different spatial and temporal scales (GITEC, 2011; Mbonile *et al.*, 2003; Misana *et al.*, 2012; Soini, 2005b). However, the effectiveness of this conversion in terms of actual yield and potential projections in maintaining the production of the main staple food crops is poorly known.

The limits to the current knowledge discussed above trigger the need to study the impacts of present and future climate and land use/cover changes on the surface and groundwater

hydrology of Kilimanjaro and its future implication. This research, therefore, is proposed to develop a conceptual understanding of the impacts of present and future climate variability and human activities on surface and groundwater resources on the Mount Kilimanjaro slopes and identify sustainable management options. Detailed analysis of the impacts of changing climate and land use in hydrological processes in Kilimanjaro will account for the vulnerability of the Kilimanjaro water catchments (Chiwa, 2012). Also, and a conceptual understanding of the overall availability and predictability of water resources in rivers and groundwater of the Kilimanjaro for sustainable improved livelihood and food security (Rowhani *et al.*, 2011) are discussed in various sections of this study.

1.3 Rationale of the Study

There exist divided opinions on the effectiveness of expanding agricultural land for increasing food production. This phenomenon has never been tested before; thus, this phenomenon creates the need to assess the link between expansion in agricultural land and food production. Furthermore, the land use/ cover classes exhibit multicollinearity; hence changes in one or more classes will necessitate changes in other classes. These changes might also necessitate changes in the hydrological parameters of the catchment. Thus, addressing current and future issues of optimal water use, demand and supply, and prioritization will require a thorough analysis of the link between land use/cover changes and the water balance of the catchment. Climate and land use/cover changes occur in tandem; thus, there is a need for creating an understanding of the water availability under the current climate change scenario. This information will help in addressing future issues of water availability, energy production, and environmental sustainability. On the other hand, crop yield requires good quality water for irrigation, soil productivity, soil structure, and permeability. All these are a subject of the exchangeable ions present in irrigation waters. This phenomenon creates the need for assessing irrigation water quality for sustainable food production and environmental protection. Thus, this study is important not only for the scientific community but also to water managers, the farming community, and policymakers.

1.4 Objectives of the Study

1.4.1 General Objective

The general objective of this study was to develop a conceptual understanding and management of the impacts of present and future climate variability and anthropic activities on food production, surface, and groundwater resources on the southern slope of Kilimanjaro.

1.4.2 Specific Objectives

- (i) To assess the historical and future land use/cover dynamics and association to food production on the slopes of Mount Kilimanjaro.
- (ii) To evaluate the impacts of the present and future land use/cover changes on the water budget of Mount Kilimanjaro slopes.
- (iii) To assess the impacts of the present and future land-use changes on water quality, surface-groundwater interactions, and suitability of water for irrigation on the slopes of Mount Kilimanjaro.
- (iv) To assess the impact of past, present, and future climate changes on the water budget (surface and groundwater) of the Mount Kilimanjaro slopes.

1.5 Research Questions

The following research questions guided this study:

- (i) How is/are the historical and future land use/cover changes, and what is the association with food production on the slopes of Mount Kilimanjaro.
- (ii) How do the changes in land use/cover impact the surface and groundwater hydrology of the southern slopes of Mount Kilimanjaro?
- (iii) How do spatial and temporal land use/cover changes influence the surface and groundwater resources of Kilimanjaro, and how are the surface and groundwater suitable for irrigation?

- (iv) How do surface and groundwater hydrology respond to changes in future climate on the selected rivers and aquifers of the Kilimanjaro?

In order to achieve the aforementioned objectives and answer the research questions, several activities and methods were adopted and parameterized, as summarized in Fig. 1.

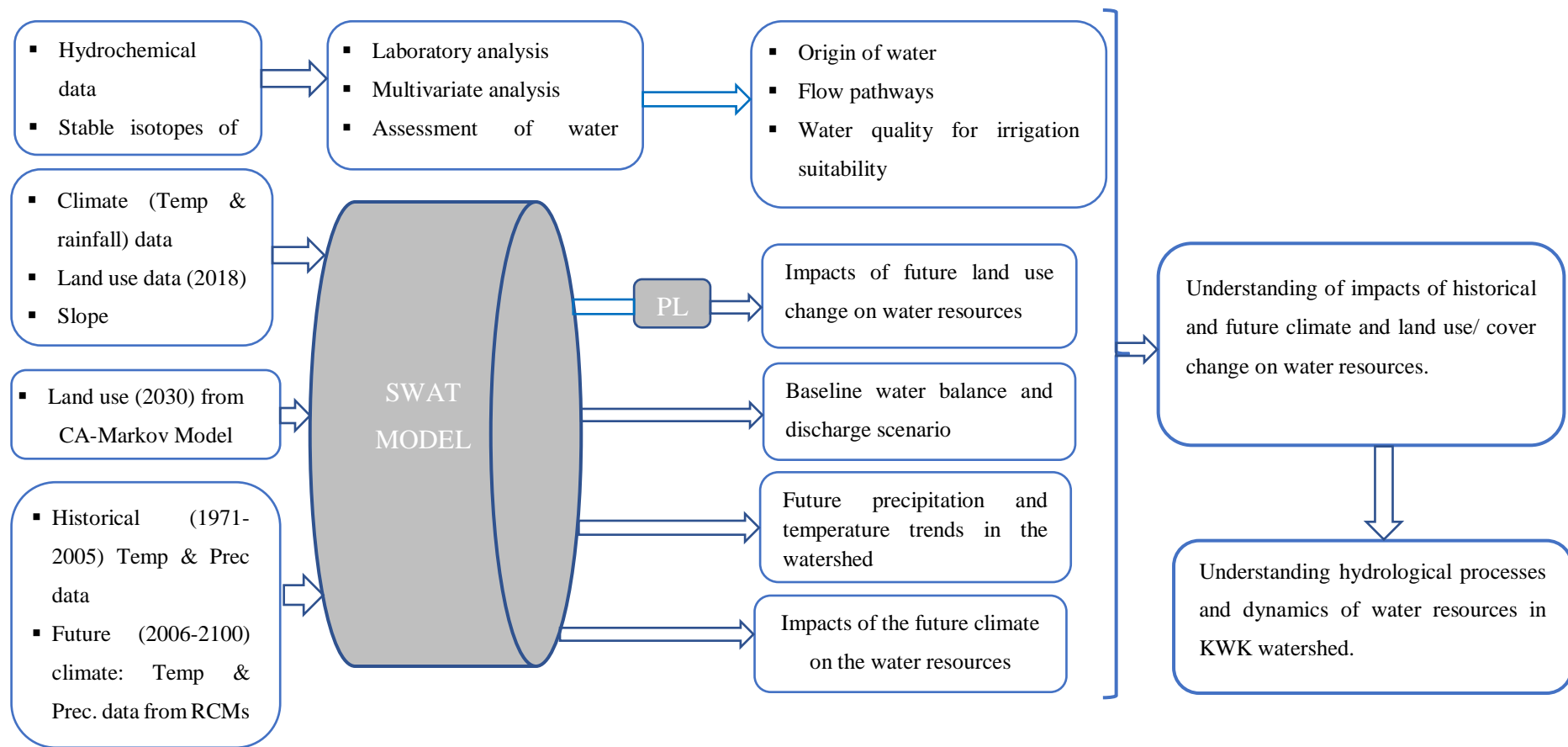


Figure 1: The conceptual framework of data, activities, steps and processes used in this study

1.6 Significance of the Study

1.6.1 Overall Significance

This study is expected to contribute knowledge to the local and regional hydrogeological information and provide an in-depth understanding of surface and groundwater vulnerability to human activities and climate change on the southern slope of Kilimanjaro. However, some of the proposed methods have been applied in parts of the study area before; a combined approach of the techniques is viewed to provide a more comprehensive understanding of the local and regional responses to climate change and anthropogenic activities. Understanding the hydrology of the area will identify the recharge zones and most vulnerable areas for pollution through human actions and changes in climate variables; this will help water managers and users design effective conservation and water management strategies. Furthermore, this study will provide the future hydrological situation based on the future projected precipitation, land-use changes, and changes in population.

The projected surface and groundwater scenario will help develop the management plans for sustainable supply; this will help address issues related to optimum use, land use plans, and pollution management. Also, the findings of this study are useful for the advancement of our policies, practices, and management practices aimed to attain environmental and water resources sustainability. Moreover, the information gathered in this study can be used to help drive progress toward the Sustainable Development Goals (SDGs) and the objectives of the Paris Agreement (COP 21).

1.6.2 Scientific Contribution

Prior to this study, the relationship between expansion in agriculture land and increase in food production, land use/cover changes and hydrological fluxes, land use/cover changes and water quality and climate change and hydrological fluxes on the southern slopes of Kilimanjaro were of limited understanding. Limited previous studies were conducted on spatial and temporal scales (Agrawala *et al.*, 2003; Mmbaga *et al.*, 2017; Soini, 2005b); however, none of these studies linked ongoing land use/cover trend to food production. This study brought in the confirmation that the expansion of agricultural land does not necessarily guarantee an increase in crop production.

This study argued that studying the current state of the art is not just enough. A detailed analysis of the future drivers and trends of land use/cover and climate changes were assessed and documented. Furthermore, the future implication of these drivers to hydrological fluxes was also analyzed and documented. Noticeably, the future of water resources in terms of quality and quantity under the current land use/cover drivers and climate changes necessitate replanning. These management strategies need to be integrated into and implemented in soil and water management plans to sustain food production, hydropower plants and water resources.

It is a common understanding that modelling a mountainous watershed is a challenging activity. However, taking into account the vast ecosystem services offered at the Mount Kilimanjaro slopes, it was necessary to understand the current and future watershed dynamics for proper management. For the first time, this study brought a high-resolution analysis of the current and future land use/cover and climate changes using the current drivers. This study provides an opportunity for water users on the mountain slopes to integrate specific measures precisely for the sustainability of water-intensive activities that account for the day-to-day livelihood on the mountain slopes.

In most cases, the focus of the current study was to use primary data than historical information. The generated data added knowledge on the mountainous watershed with hydrological fluxes of limited understanding. Also, most of the deep and shallow wells used for irrigation activities are of unknown water quality with regard to irrigation suitability. This study brought in the information on the quality of water for irrigation suitability, providing useful information that is informative for small- and large-scale irrigation activities on the mountain slopes.

Furthermore, the hydrology of the East African region is reported to be impacted by land use and climate changes. However, most of these studies are site-specific due to the site-specific nature of drivers. However, illegal wells development increases the data collection challenge due to fear of legal actions. Yet, it was necessary to engage local residency under current and future sustainability to gather enough information for analysis. Thus, this study challenges that in order to balance between conservation and utilization of water resources, water users and water managers need to work together to understand the needs and challenges and design a sustainable management framework. However, in most cases, the two are difficult to meet and plan together due to little understanding of the future implications of the current actions

(in users) and enforcement of the laws and regulations (on the managers' side) without mutual agreement.

1.7 Delineation of the Study

This study aims to develop an understanding of the surface and groundwater dynamics under changing climate and increased anthropogenic pressure on the southern slopes of Mount Kilimanjaro, Tanzania. Historical and near future land-use changes and their impacts on the surface water and the groundwater dynamics are discussed in detail. This dissertation is divided into five chapters; Chapter one consists of the background information, statement of the research problem, rationale of the study, objectives, research questions, and the significance of the study. Chapter two presents the literature review in which major issues impacting surface and groundwater on the slopes of Mount Kilimanjaro are discussed. Chapter three covers the methods and techniques used to investigate land use, surface, and groundwater changes under changing climate and anthropic activities. Chapter four presents the results and discussion of changes in climate and land use/cover and the association to food production, surface, and groundwater dynamics. Chapter five presents the conclusion and recommendations. Although translating the results of this study into an integrated climate and anthropogenic resilient water management system would have produced impressive output, this component has not been carried out. This limitation makes a research gap for future studies of this type. The scope of this study spanned towards understanding changes in surface and groundwater dynamics under the influence of climate and anthropogenic pressure. However, it is worth mentioning that the studied watershed is located on the southern slopes of Kilimanjaro, which makes it a component of the northern part of the Pangani Basin. This equally forms the limitation of the study; further studies could focus on the entire basin to obtain the complete scenario throughout the basin and other similar basins.

CHAPTER TWO

LITERATURE REVIEW

2.1 Introduction

Climate change is a challenge afflicting human beings, animals, and plants worldwide; its associated impacts and susceptibility vary from country to country and even from individual to individual. Developing countries are the most affected by climate change impacts (Kurukulasuriya & Mendelsohn, 2008). East Africa region is among the regions reported to be impacted by changes in climate (Adhikari *et al.*, 2015). The rainfall pattern over the eastern Africa region is highly fluctuating both on temporal and spatial scales. The consequences of unpredictable climatic conditions range from floods to droughts, likely linked with regional climate changes (Anyah & Qiu, 2012).

Climate change and quantified impacts on river basins is a global challenge. Climate change is observed, and its presence is identified globally. Scientific evidence of climate change and its importance first came into the picture by the first IPCC reports of 1990. Later the second in 1995, third in 2001, fourth in 2007, and fifth (AR5) was published in parts between September 2013 to November 2014, based on the representative concentration pathways (RCPs). Many climate change evidence studies are available regionally, countrywide, and globally (Hijioka *et al.*, 2014; IPCC, 2014c; Otte *et al.*, 2016).

In tropical Africa, climate change is predicted to cause adverse impacts on freshwater resources (Pervez & Henebry, 2015; Serdeczny *et al.*, 2016). Tanzania is one among African countries with the most substantial climate change impacts (Hatibu *et al.*, 1999); whereby shifting of cropping season and reduced water availability is expected to impact the farming sector. However, little consideration is given to the impacts in planning future water resource use and management (McCartney *et al.*, 2012). As a result, studies of the impacts of climate change on water resources are promoted in order to ensure their long-term viability. Furthermore, it is expected that the farming sector will be impacted more, resulting in decreased crop production.

Climate variability has affected food security in Tanzania by directly impacting agricultural production (Munishi *et al.*, 2015). The impacts are more felt due to the fact that 80% of agricultural production in the country is rainfall-dependent (Shemsanga *et al.*, 2010). The

majority of the country's population is ranked to have low means of adapting to the impacts of climate change and variability (Agrawala *et al.*, 2003). Climate change results in a spatial and temporal shift in rainfall regime, affecting natural recharge, soil cover properties, and land cover (Shah, 2009). Modern climate change is hypothesized to be dominated by anthropogenic influences, hence inducing changes in atmospheric composition that exceed natural variability (Karl & Trenberth, 2003).

Historical analysis of climate trends in Tanzania shows evident areas of drying in northeast parts and much of southern Tanzania between 1981 and 2016 (Hemp, 2005). Simultaneously, reasonable wetting trends occurred in central parts and remarkable wetting trends in the northwest of the country (Conway *et al.*, 2017). This triggers the need to generate a site-specific analysis and future precipitation and temperature projections to ascertain the impacts on water resources and food production. However, IPCC (2014b) shows the reduced focus on research that links the climate change impacts on groundwater. Moreover, only a few results were site-specific (Kundzewicz *et al.*, 2009), calling for more information and data from other areas of the world.

The efforts to study the impacts of climate change in the Kilimanjaro glacier started in 1887 (Kaser, 1999). Records indicate the decreases in rainfall observed in the three stations around Kilimanjaro mountain by 34%, 27%, and 39% for the periods 1902–2004, 1911–2004 and 1922–2004, respectively (Hemp, 2005). This decrease reflects changes in river flows in response to changing rainfall regime and its variability, which in turn influences the natural recharge rates of Kilimanjaro (Kundzewicz *et al.*, 2009). It is reported that changes in temperatures and rainfall influence growth rates and leaf size of plants affect groundwater recharge (Kundzewicz *et al.*, 2009). The impact on groundwater recharge will be reflected by crop failure due to low rainfall and the emergence of animal, crop, and human diseases (Mtalo *et al.*, 2005b). Changes in mountain weather and climate are hypothesized to cause significant implications for regional water resources and ecological sustainability. Thus, understanding the magnitude of the damage by anthropogenic and natural climate forcing and their relations is therefore significant (Fairman *et al.*, 2011).

2.2 Land use Change on Mount Kilimanjaro Slopes

Land use change has the potential to impact the regional climate of Kilimanjaro (Nair *et al.*, 2010). Studies indicate that the weather and climate of the mountain respond to climate variability and change. It is hypothesized that both natural and anthropogenic forcing are responsible for accounting for the current trend (Nair *et al.*, 2010). However, the information on the nature and magnitude of these forcing is missing (Nair *et al.*, 2010). Climate-induced forest fires and montane forest losses through anthropogenic activities resulted in a notable drop and increased the variability of the Kilimanjaro catchments' water yields. This is due to the loss of the most effective water source in the fog interception zone, affecting the water needs of over 1million people hence going beyond the hydrological magnitudes of the loss of the glaciers to the greater extent (Hemp, 2005).

Most of the previous land use characterization only partially accounts for the additional land use change that has occurred in recent years (Fairman *et al.*, 2011). However, integrating simulation of future changes in land use into management plans is expected to address future management plan issues. Fairman *et al.* (2011) simulated hypothetical deforestation to study the impact of the land use change in Kilimanjaro climate using one dry month of August. However, the simulations did consider predicting future land use/cover scenarios using the current land use/cover change drivers. It is worth noting that changes in government policies, socio-cultural, climate, and population increase influence land use/cover changes on the slopes of Kilimanjaro (Mbonile *et al.*, 2003).

2.1.1 Land Use and Hydrology of Kilimanjaro

Land use change has significant impacts on water resources. However, quantifying its impacts is among the challenging activities in hydrology (Stonestrom *et al.*, 2009). Data scarcity is among the research problems during the quantification of land use impacts on the hydrology of a watershed. The tropical environment experiences a high degree of hydrological data scarcity. However, it is worth mentioning that most of the data generating hydrological studies are focused on large rivers (Example Pangani river), leaving behind small streams that supply water for a large populace dwelling on mountainous slopes (Mölg *et al.*, 2012). Thus, the knowledge on the hydrology of small tropical mountainous watersheds is still limited.

The hydrological balance of Mount Kilimanjaro is seriously affected by forest fires (Agrawala *et al.*, 2003). Nearly a third of the Kilimanjaro forest cover was lost during the last 70 years (Hemp, 2005). This land cover conversion resulted in the replacement of the fog intercepting cloud forests, which is essential in the mountains water budgets (Agrawala *et al.*, 2003; Fairman *et al.*, 2011), and it is postulated that changes in specific humidity are likely linked to the ongoing glacier imbalance. There is a need to develop a conceptual understanding of the overall availability and predictability of water resources in rivers and groundwater aquifer of the Kilimanjaro for sustainable improved livelihood and food security (Rowhani *et al.*, 2011).

Mount Kilimanjaro slopes are typical landscapes with the highest recorded land cover dynamics, and their consequences on water resources, food, and energy production have been reported in previous studies (Said *et al.*, 2019). Changes in land cover in most of the areas surrounding Mt. Kilimanjaro slopes have the potential to impact water resources (Chiwa, 2012; Mbonile *et al.*, 2003; Misana *et al.*, 2012; Mmbaga *et al.*, 2017; Ngugi *et al.*, 2015; Soini, 2005a). These changes trigger the need to understand land cover change trajectories and surface-groundwater interaction among the critical requirements in water management practices in the area. Surface-groundwater interaction affects water management and water rights, nutrients loading from aquifers to streams, and in-stream flow requirements for aquatic species at a watershed scale (Bailey *et al.*, 2016). The knowledge regarding land use/cover changes in relation to water balance components on the slopes of Mt. Kilimanjaro is of utmost importance due to limited information regarding groundwater flow (Mckenzie *et al.*, 2010).

Land degradation and land cover changes have contributed to the decline in surface water resources around Mount Kilimanjaro slopes (Ngugi *et al.*, 2015). Human activities are reported as the main contributor to the rapid land cover changes around the same area. The activities include encroachment due to logging, agricultural expansion, and settlements, which in turn have created significant changes in the land cover (Shishira & Yanda, 2018). Indeed, the increased anthropogenic activities are mainly driven by the fast-growing population, which also strengthens the pressure on the available water resources on a day-to-day basis (Gao *et al.*, 2017). Other drivers include socio-economic development and land pressure for expansion in agriculture (Lambin *et al.*, 2003).

Management of the surface and groundwater resources at a catchment level requires a deep understanding of the hydrological processes; this can improve the productivity in smallholder

farms (Bohté *et al.*, 2010). The chief factors affecting the predictability of hydrological responses in sub-Saharan Africa include increasing population densities and the resultant land-use changes and spatial and temporal climate variations (Mul *et al.*, 2007b). Also, inadequate observed discharge data because most of the catchments are ungauged due to limited resources (Mazvimavi, 2003). The composition of runoff components affects the pollution of waters (Bishop, 1991). The pathway length and permeability of the respective flow system affect the chemical reaction of the infiltrating waters in the organic and mineral matrix of the soil (Hooper & Shoemaker, 1986).

In the Mount Kilimanjaro slopes, pollution of water sources is substantial at varying amounts despite the regulation governing the conduction of activities close to the water sources. Discharges from residents along the river banks are the main source of liquid and solid-waste pollution in water sources along the Rau, Weruweru, and Kikuletwa rivers, among others. This results from discharges released from major settlements living along the river banks (Mbonile *et al.*, 2003). The local populace relies on streams and rivers as a primary water source for their daily water needs (Mckenzie *et al.*, 2010). The water needs range from domestic, industrial, and agricultural needs. More than 200 million m³ of water is extracted through 1800 km of channels to meet their domestic and agricultural needs (Grove, 1993).

2.3 Groundwater-Surface Water Interaction

Understanding Surface water-groundwater interaction is one of the key requirements in water management, taking into account that there is very little information with regards to groundwater flow in Kilimanjaro (Mckenzie *et al.*, 2010). Estimating groundwater recharge is an important water management practice that habitually denotes the success or failure of the groundwater management pattern (Van Camp *et al.*, 2013). Despite all the initiatives so far, the recharge is not measured directly to date. Estimation of recharge is more challenging in semi-arid regions; this is because, in some instances, recharge could be as low as 1% of the total precipitation (Andersen, 2008). In these regions, evapotranspiration takes a countable amount of water infiltrating the soil, and effective recharge depends largely on solely extreme rainfall events (Andersen, 2008).

Stable isotopes complement the traditional physical and chemical groundwater data by delineating the provenance and movement of both solute and water masses (Clark & Fritz, 2000; Hchaichi *et al.*, 2014). Stable isotopes of H₂O ($\delta^{18}\text{O}$ & δD) provide past groundwater

behaviour and provides an easy prediction of the future groundwater understanding of surface water-groundwater dynamics (Kendall & MacDonnell, 1998). Isotopic signatures of water change significantly as water moves between reservoirs as a result of fractionation; this makes it easy to trace its provenance and dynamics (Clark & Fritz, 2000).

The use of stable isotopes of hydrogen and oxygen is due to their resistance to environmental changes and water quality degradation (Barbieri, 2019). Therefore, the behaviour of water body movement, assessment of hydrological environments (Kendall & McDonnell, 2012), and interactions between various water bodies can be established using these isotopes. Changes in the natural hydrological environment can be studied through isotope ratios of hydrogen and oxygen. Isotopes can be applied in recharge processes and groundwater flow mechanisms (Liu *et al.*, 2016), atmospheric precipitation models (Gorski *et al.*, 2015), establishing mutual surface-groundwater interactions (Zhan *et al.*, 2016), and groundwater salinization mechanisms (Carreira *et al.*, 2014). Isotopes of oxygen and hydrogen may chiefly be used to examine the movement of water in the soil and the source of moisture in soil absorbed by plants (Wu *et al.*, 2016). Furthermore, Isotopic studies can be applied in monitoring groundwater flow pathways (Ma *et al.*, 2017) and unsaturated porous layers (Rothfuss *et al.*, 2015).

Dating together with isotopic abundances of H and O have been used to trace temporal and spatial water circulation in various reservoirs (Al-Manmi, 2008). This makes isotopes an essential tool in studying ground-surface water interaction. The basis behind this is that the isotopic content of rain is primarily affected by altitude, latitude, air temperature, and ocean proximity (Al-Manmi, 2008). Hence, this technique is important in establishing groundwater recharge, even if it took place far away. Thus, aquifers recharged by local precipitation could be demarcated from the ones recharged by local lakes and rivers, known to have different isotopic compositions due to evaporation effects (in the lake) or river meandering through different altitudes and latitudes (Clark & Fritz, 2000).

2.4 Land Use and Crop Production on Mount Kilimanjaro Slopes

Agricultural production on the slopes of Kilimanjaro is a historical phenomenon, with small-scale agriculture production to sugarcane and rice plantations along the southern plains. Previous reports show rapid expansion in agricultural land along the mountain slopes (Mbonile *et al.*, 2003; Misana *et al.*, 2012; Soini, 2005b). Drivers towards the escalation of agricultural production along the mountain slopes are water availability in rivers and streams, especially on the southern slopes (Mckenzie *et al.*, 2010). Further, fertile soils rainfed agriculture is still supporting a relatively large group of smallholder farmers and agro-pastoralists, occupying around 85% of the arable land (Fisher *et al.*, 2010; Lein, 2004). However, information on the contribution of the expansion in agriculture land on staple food production is scanty or missing.

Agriculture is an essential factor that influences communities' livelihood prosperity in villages and suburbs on the slopes (Munishi *et al.*, 2015). Factors affecting crop production per unit area include rises in ambient temperature, reductions in precipitation, and uneven spatial distribution of rainfall during the cropping season (Munishi *et al.*, 2015). Further, inadequate land management due to flood and drought (Mbonile, 2005). Further, lack of agricultural inputs affects production per area (Mbonile 2005). However, the efforts of the farming community seem to be focused on expanding the farm area rather than addressing these challenges to intensify production per unit area.

2.5 Changes in Forest Land and Agricultural Land Conversion

Mount Kilimanjaro is a unique ecosystem harbouring natural vegetation, home gardens, agroforest trees, and savannah in the lowlands. Previous reports in the study area show increased forest degradation on the southern slopes from 1606 ha to 5170 ha between 1973 and 2000 (Mbonile, 2005). Reports further show closed and open forests decreased by 56% and 64%, respectively (Munishi *et al.*, 2009). Degradation of more than 41 km² of the forest between 1952 and 1982 (Yanda & Shishira, 2001). Land under agroforestry decreased by 25%, while that under annual crops increased by 41%. Grasslands increased by 116%, and riverine vegetation decreased by 53% (Munishi *et al.*, 2009). These changes trigger the need to establish past and future LULC trends on the southern slopes of Mount Kilimanjaro.

Conversion of other LULC types to agricultural land is a continuous phenomenon. Reports show the conversion of 53 km² of shrub and grassland and sparse vegetation to maize and

vegetable cultivation from 1987 to 2005 in Kahe plains (GITEC, 2011). Further, about 49.97 km² (32.8%) of shrubs and bushland was converted to agriculture and other uses from 1961 to 2000 in the Kirua Vunjo division (Soini, 2005b). In the southern slopes, cultivated land increased from 54% (in 1973) to 63% in 2000 on the southern and eastern slopes (Misana *et al.*, 2012). Also, conversion of about 39.5% of bushland to agriculture between 1973 and 2000 (Mbonile *et al.*, 2003). This conversion prompts the need to establish a link between increased agricultural land and food production.

2.6 Land Use/Cover Changes Detection

On the southern slopes of Mt. Kilimanjaro, several LULC change studies have been conducted on various spatial and temporal scales (Fairman *et al.*, 2011; Mbonile *et al.*, 2003; Misana *et al.*, 2012; Mmbaga *et al.*, 2017). However, none of the previous studies took into account the potential LULC scenario in the area. Furthermore, local communities have continued to convert land to agriculture, with the presumption that the more land (from other types such as a forest) converted to agricultural land, the higher the yield. However, the success of this conversion in terms of actual yield and potential projections in maintaining the production of the main staple food crops is poorly known. Thus, it is necessary to ascertain the future land use/cover dynamics for sustainable water, food, and energy production through hydropower dams.

The past land use changes may be used to establish a model to predict the future land use change trend (Liping *et al.*, 2018). In doing this, land-use change models may be used (Verburg *et al.*, 2004). The LULC change models may be classified into; Empirical and statistical models, such as Markov chains and regression models. Dynamic models, such as the Cellular Automata (CA) model, and integrated models, such as the integrated Grey wolf optimizer (GWO) and Cellular Automata (CA) model (Cao *et al.*, 2019a), as well as the Conversion of Land Use and its Effects model (CLUE-S) (Guan *et al.*, 2011), may also be used. The best models for predicting potential LULC changes are dynamic and interconnected models like CA.

Since the Markov Chain Analysis method alone has been found to have shortcomings, recent studies have used a combination of Cellular Automata and Markov Chain Analysis. Markov Chain is a statistical method that explains the likelihood of land-use change from one time to the next through statistical relationships, according to Al-Bakri *et al.* (2013) and Memarian

et al. (2012), but it is rather insensitive to space and has a high degree of inefficiency in accounting for the causes of land cover change. As a result, the combination of Cellular Automata and Markov Chain (CA-Markov) aids in the avoidance of constraints. Although CA-Markov can simulate multiple land cover and complex patterns, it is also simple to use (Memarian *et al.*, 2012). However, CA Markov does not have the capacity to integrate the social and economic dynamics in its simulations (Arsanjani *et al.*, 2013), but the addition of logistic regression will improve CA-Markov's ability to model urban expansion (Arsanjani *et al.*, 2013). Due to its capacity to account for both spatial and temporal components of land cover dynamics, the CA-Markov model has been suggested for land cover change detection and simulations (Baysal, 2013; Behera *et al.*, 2012). Furthermore, CA-Markov is effective in simulating multiple land cover, and complex patterns have a high level of effectiveness in data-scarce areas and need little calibration (Memarian *et al.*, 2012).

2.7 Climate Change and its Impacts

The impacts of climate change are pronounced in all sectors; the impacts in agriculture and food production, precipitation, temperatures, and water resources, land cover distribution, glacier retreat, and provision of ecosystem services are pronounced and detailed in sections 2.7.1-2.8.

2.7.1 Climate Change and Hydrology on the Southern Slopes of Kilimanjaro

Kilimanjaro region keeps meticulous records of fluctuations in precipitation and temperature. This is due to the fact that rainfed and irrigated agriculture requires different amounts of rainfall. According to meteorological records on the mountain slopes and proxy data analysis, the annual precipitation trend is declining. The above decline indicates a 150 mm drop in annual precipitation between 1880 and 1900 (Agrawala *et al.*, 2003). Four stations on the slopes of Mount Kilimanjaro have shown a decrease of between 2.5 and 12 mm per year over the last 60–100 years (Agrawala *et al.*, 2003; Hemp, 2005). The Lyamungo station on Mount Kilimanjaro's southern slope (about 1200 meters above sea level) also shows an increased number of dry months with less than 30 mm of precipitation (Agrawala *et al.*, 2003).

According to Hay *et al.* (2002) spatially averaged temperatures in Kilimanjaro rose between 1951 and 1960, and between 1981 and 1995, with the period in between showing relatively stable temperature patterns. The records reveal a correlation between temperature inversion,

precipitation decline, and the occurrence of wildfires. Climate change causes the latter, which is exacerbated by anthropogenic activities (Agrawala *et al.*, 2003). In most parts of the country, the recorded trends have resulted in significant changes in the yields of important crops. The decrease in maize yields in Hai district was recorded by Munishi *et al.* (2015). Increased temperature and decreased precipitation, as well as spatial distribution, are related to the pattern. This has implications for the region's food security and puts the livelihood of the local population in jeopardy.

Precipitation, land cover, recharge and discharge all change at the same time. Rainfall, which is affected by changes in the climate of a region, is needed for both recharge and discharge (Kundzewicz *et al.*, 2009). In Tanzania, there is mounting evidence of diminishing dry season discharges for some perennial rivers (Ndomba *et al.*, 2008b; Valimba, 2007; Yanda & Munishi, 2007). Physical entities such as the reduction in river flow discharges and water levels in rivers, the decline in domestic and agricultural water supplies, and the intensification of drought all contribute to community perceptions of climate change and water resources (Kangalawe, 2017; Tagseth, 2010). These entities directly impact water supply, food production, and power generation, and thus on the livelihood of a large population that relies on these services. In Kikuletwa, along the Pangani River Basin, a major reduction in river discharges has been recorded (Lalika *et al.*, 2015). According to projections, the annual runoff in the Kikuletwa river within the Pangani basin is expected to decrease by 9% for all months. Monthly variations are expected in the Pangani basin, with an annual runoff reduction of around 6% (Agrawala *et al.*, 2003). Both of these are located on Kilimanjaro's southern limb. Mahoo *et al.* (2015) emphasize the importance of comprehending rainfall and water distribution on the decadal scale in Tanzania. This is due to the inadequacy of such studies in the country and the suitability of decadal-scale knowledge in evaluating rainfall dynamics (Brunsell, 2010).

Irrigation agriculture and domestic uses are the two main water users along the mountain slopes (Viviroli *et al.*, 2007). According to reports, 13 000 hectares of forest were converted to agricultural land between 1976 and 2000. The reduction in surface runoff of approximately 58.4 hm³/year is related to this conversion (Grossmann, 2008). Clouds water intercepted by trees and other plants provides a significant portion of overall runoff and may also contribute to groundwater recharge, as observed elsewhere (Prada *et al.*, 2009; Prada *et al.*, 2010). Between 1973 and 2000, 39.5% of the bushland was converted to agricultural land (Mbonile

et al., 2003). As a result, it is clear that these massive changes had a direct impact on groundwater recharge and surface runoff in Kilimanjaro's lower plains.

Water resource disputes are increasing, resulting from increasing demand and decreasing supply. Water allocation conflicts, for example, between the Lower Moshi irrigation scheme built in the 1980s and the restoration of the Pangani fall hydropower project, between the rural and urban population in water use, between upstream and downstream users, farmers and pastoralists (Mbonile, 2005) demonstrate increased water demands and decreased availability. As a result, changes in water supplies have an effect on food, water, and power generation, impacting the livelihoods of thousands of people living downstream.

2.7.2 Mount Kilimanjaro Glacier as an Indicator of Climate Change

Researchers have been studying the effects of climate change on Kilimanjaro glaciers for decades (Cullen *et al.*, 2013; Kaser *et al.*, 2004; Mölg *et al.*, 2008; Thompson, 2000), for aesthetic purposes (Adhikari *et al.*, 2015) and as a tourist attraction. Conceivably, the contribution of the glaciers to the region's hydrology should be the most important subject. According to studies, the glaciers of Kilimanjaro contribute just 5% of the annual water input to the region's hydrology (Hemp, 2005). This percent implies that the importance of glaciers as a water source is either marginal or non-existent (Mölg *et al.*, 2014). The dense Kilimanjaro forest reserve, on the other hand, is the source of many rivers and streams (GITEC, 2011), and draws in more moisture than the lower mountain areas.

While the use of glaciers as a global warming proxy has been challenged (Mote & Kaser, 2007), historical observations continue to point to Kilimanjaro Mountain as one of the region's climate change hotspots. Perhaps this is because glaciers of recent origin are known to be particularly vulnerable to climatological variables. This is due to year-round ablation below the glacier equilibrium line in tropical glaciers, as well as a strong vertical balance gradient in each individual type, resulting in a significantly high sensitivity to the Equilibrium Line Altitude increase. As a result, changes in basic climate parameters are reflected in the variability of tropical glaciers (Kaser, 1999).

Since 1887, researchers have been studying the retreat of Mount Kilimanjaro's glaciers. Researchers have focused on the effects of forest cover shifts on glacier retreat (Kaser, 1999; Kaser *et al.*, 2004; Mölg *et al.*, 2008; Mölg *et al.*, 2009; Mote & Kaser, 2007; Thompson,

2000; Thompson *et al.*, 2002) and the influences of forest cover changes on glacier decline (Fairman *et al.*, 2011; Hemp, 2005). For decades, most research focused on the effects of climate variability on Kilimanjaro's glacier retreat, such as solar radiation, humidity, and temperature.

Kaser *et al.* (2004) observed that the glacier retreat on Kilimanjaro Mountain may have been caused by an extreme decrease in atmospheric moisture at the end of the 19th century. The estimated loss of a third of Kilimanjaro's forest cover over the last 70 years has been linked to the mountain's glacier retreat (Hemp, 2005). Global glacier retreat has also been related to air temperatures. However, scientific evidence of this relation in tropical glaciers is thought to be lacking (Houton *et al.*, 2001) and can only partially explain the retreat of Kilimanjaro's glaciers (Kaser, 1999). The ongoing glacier imbalance has also been attributed to changes in air moisture, but there is insufficient evidence of this connection in the Kilimanjaro glaciers (Cullen *et al.*, 2013). However, Kaser *et al.* (2004; 2010) and Mölg *et al.* (2003) have recorded compelling evidence of a correlation between solar radiation and plateau glacier ice mass shrinkage.

The rapid decline in precipitation (Cullen *et al.*, 2006; Kaser *et al.*, 2004) and air temperature inversion are responsible for the “named” faster recession of Kilimanjaro's glacier. The latter has been suggested as a major factor in the decline of Kilimanjaro's ice mass. However, Duane *et al.* (2008) vote no confidence because the ice field's observed air temperature was too low to affect glacier loss. This ensures that cloud cover and humidity play a key role in Mount Kilimanjaro's ice mass retreat. In some cases, the retreat of the Kilimanjaro glaciers is seen as a melting process, with a downhill flow likely to recharge groundwater and lead to springs and river discharges. Nonetheless, the isotopic composition of glacial meltwater varies significantly from that of lowland spring water (Mckenzie *et al.*, 2010). However, according to Mote and Kaser (2007) sublimation is the primary cause of glacier loss on Kilimanjaro. The mass balance of the mountain tops and a decline in atmospheric moisture support this theory as the cause of the observed glacier recession.

Depending on their forms, glaciers respond to changes in climate variables in a variety of ways (Kaser, 1999). As a result, glaciers can be classified according to their shapes: Bed and slope shapes. Similarly, the thickness of the glaciers must be considered (Cullen *et al.*, 2013). In Kilimanjaro, there are two types of glaciers: Tabular-shaped plateau glaciers (mostly

formed at 5700 m.a.m.s.l) and slope glaciers (mostly formed at less than 5700 m.a.m.s.l) (Geilinger, 1936).

Some estimates suggested that the Kilimanjaro glaciers would completely disappear between 2015 and 2020 (Thompson *et al.*, 2002), perhaps due to the generalization of glacier forms. Plateau and slope glaciers, on the other hand, respond to climate change in different ways (Geilinger, 1936). As a result, the expected time for tabular-shaped glaciers to vanish is 2046 (Kaser *et al.*, 2010). However, slope glaciers have been confirmed to have a slight tendency to disappear as a result of climate change, implying that complete deglaciation of Kilimanjaro glaciers in the next decade is unlikely (Kaser *et al.*, 2010).

This ambiguity (Table 1) indicates that the accuracy of prediction using physically based models is uncertain, especially in the tropical region, and that the mechanisms of Mount Kilimanjaro's deglaciation are not well understood. This ambiguity reflects the difficulties in establishing long-term sustainability in Water-Energy-Food (WEF nexus) stability in the Kilimanjaro community.

Table 1: Glacier and ice cover retreat in the Mount Kilimanjaro

Reported scenario	Timeframe	References
The ice cover decreased by 75%	1912 and 1989	Hastenrath and Greischar (1997)
The ice cover decreased by 79%	1912 – 2003	Cullen <i>et al.</i> (2006)
The ice cover decreased by 85%	1912 – 2007	Thompson <i>et al.</i> (2009)
The ice cover may disappear	Within the next two decades	Thompson <i>et al.</i> (2009)
Tabular shaped glaciers will disappear	By the year 2046	Kaser <i>et al.</i> (2010)
Complete deglaciation of Kilimanjaro glacier is uncertain	In the next decade	Kaser <i>et al.</i> (2010)

The notable surface runoff across the mountains rainforest belt originates in the centre of the highest rainfall elevation (Røhr & Killingtveit, 2003), implying that glacial melt has a minor impact on the discharge (Mckenzie *et al.*, 2010). However, permanent streams are said to link the Weru-Weru and Kikafu Rivers, which join the Pangani River, to glaciers on the Kibo peak's southwest side (Agrawala *et al.*, 2003). Furthermore, the report by Mckenzie *et al.* (2010) used isotopic signatures to demonstrate that the contribution of ice melt to river discharge is negligible. The small number of springs between the ice cap and the forest belt suggests that meltwater percolation through the permeable surface volcanic ash is also

limited. As a result, the valleys above 3600 meters are dry for the majority of the year, except below the southwest Kibo glaciers (Downie & Wilkinson, 1972).

2.7.3 Climate and land Use/Cover Changes and Implication on Food Production along Kilimanjaro Slopes

Food production and ecological systems are chiefly affected by changes in cultivated land (Cao *et al.*, 2019b). Studies indicate the increasing urbanization, farming, and demand for more water to satisfy the needs of a growing population. The eighth most densely populated Kilimanjaro region has an annual growth rate of 1.8% and 124 people per square kilometer (National Bureau of Statistics, 2012). Increased farm fragmentation due to the applicable land tenure system in the region, soil erosion, and land degradation (United Nations Development Programme [UNDP], 2014) are among the essential factors that can largely explain this trend. The observed sharp decrease in banana production may have resulted from converting banana farms into short seasonal crops such as maize and bean fields due to low prices in the world market, which rendered banana unprofitable (Soini, 2005a).

An increase in the population is expected to increase food demand. As a result, the future agricultural expansion would not be a strange phenomenon. Instead of increasing the area under agriculture, the best farming technologies can be used to increase production per unit area, thereby meeting high food demand. The majority of grassland, desert land, and lower-elevation forests are expected to be converted to built-up and agricultural lands. Rapid population growth and agricultural expansion, especially in the lowlands, have also been recorded in previous studies (Chiwa, 2012; Mbonile *et al.*, 2003; Misana *et al.*, 2003; Soini, 2005b).

Increased pressure on arable land leads to increased land degradation and lower agricultural yields (Country Environmental Profile [CEP], 1995). The declining productivity of highland gardens has changed the balance, and lowland plots have taken on greater significance in recent years, providing food for both livestock and people. The lowlands, on the other hand, are much drier and necessitate modern agronomic techniques. Significant nutrient mining, combined with high inputs, fertilizer, and seed costs, has resulted in declining soil productivity in the lowland, accelerating soil degradation in the area (UNDP, 2014). To improve fertility and productivity in the lowlands, restoration and fertilizers are needed, but

most smallholder farmers cannot afford the associated costs. As a result, the available land for crop production becomes less productive and usable.

Land use and environmental degradation are two factors that could reduce the amount of water available in the Pangani basin for food production (De Wit & Stankiewicz, 2006). Munishi *et al.* (2015) found that a decrease in precipitation and unequal rainfall distribution during the cropping season are important determinants of maize, bean, and banana yield in the region. Hemp (2005) found that annual precipitation levels on Mount Kilimanjaro have decreased by 600-1200 mm over the last 120 years, while temperatures have risen dramatically since 1976. These would result in a major increase in irrigation demand, which would have an impact on crop production in the region (Munishi & Sawere, 2014).

Small-scale farming and mostly rainfed agriculture are the most common forms of agriculture in Kilimanjaro, resulting in a major mismatch between cropping area and crop yield. According to Mmbaga *et al.* (2017) climate change has resulted in an increase in minimum temperatures, which has resulted in local coffee extinction. Apart from impacting food crops (Munishi *et al.*, 2015), cash crops like coffee have also been confirmed to be severely impacted (Craparo *et al.*, 2015). Coffee production is expected to decline much further into the 2060s if current land use changes and climate change patterns are not reversed (URT, 2012). A more integrative study based on the generation of high-quality data on food production, food demand, climate, pests, and diseases is needed to bring issues closer to practice.

The impact of climate change directly affects rain-fed crops and water supply; this will intensify the pressure on the water availability for irrigation (Rao *et al.*, 2007). Thus, posing a direct and indirect impact on the supply of the basic needs for the increasing population, socio-economic activity across the continent. However, it is worth mentioning that the main challenge in coping with increased demand for food lies in production practices (Lyle, 1996). It is necessary to adjust production techniques in order to achieve a balance between environmental land use and food production. Rather than expanding farm scale, the emphasis should be on developing more innovative techniques that increase productivity in small areas. However, as the core issues of sustainability, sustainable land use necessitates consideration of environmental, social, and economic concerns (Loures, 2019). On the southern slopes of Kilimanjaro, low rainfall, particularly in drier lowlands, combined with poor agronomic practices can lead to nutrient mining and, as a result, lower per capita output. The survey,

however, reveals that the dynamics of land use for agriculture on Kilimanjaro's slopes are all about intensification on the higher slopes and expansion on the lower slopes. This means that the adaptive capacity of the smallholder farmers will be equally reduced (Eriksen *et al.*, 2008). Farming systems will compete with other uses of water to complement the limited water availability. This triggers the need for Land use options that increase the adaptive capacity of smallholder farmers, and are less vulnerable to climate change impacts (Berrang-Ford *et al.*, 2011).

Climate change has resulted in drastic shifts in the yields of important crops in most of the regions in the country. The decrease in maize yields in Hai district was recorded by Munishi *et al.* (2015). Increased temperature and decreased precipitation, as well as spatial distribution, are related to the pattern. This has implications for the region's food security and puts the livelihood of the local population in jeopardy. Globally, land use and climate change are projected to have an effect on food production, posing a threat to food security (Lobell & Field, 2007). This necessitates the creation of a research translation program aimed at converting research-based evidence of locally adapted sustainable food production practices into community-led behaviour.

2.7.4 Climate Change and its Implications on River Discharge

Climate change is projected to significantly lower water availability in the watersheds (IPCC, 2007, 2014e). Projections show that between 75 to 250 million people in developing countries will be exposed to climate change-induced water stress (IPCC, 2007). Rainfed and irrigated agriculture both rely on rainfall in varying amounts in the Kilimanjaro region, so records of precipitation and temperature changes are significant. According to meteorological records on the mountain slopes and the study of proxy data, the annual precipitation trend is decreasing. Between 1880 and 1900, annual precipitation decreased by 150 mm (Agrawala *et al.*, 2003). For the last 60–100 years, four stations on the slopes of Mount Kilimanjaro have shown a decrease of between 2.5 and 12 mm per year (Agrawala *et al.*, 2003; Hemp, 2005). On the southern slope of Mount Kilimanjaro, the Lyamungo weather station (about 1200 meters above sea level) reports an increase in the number of dry months with less than 30 mm of precipitation (Agrawala *et al.*, 2003). As a result, there is a chance that river flow will change as rainfall decreases, necessitating a review of current conditions and projections for the future. Climate change changes the flow system of rivers (Conway *et al.*, 2017); this

includes the magnitude, duration, frequency, rate, and timing of discharge events (Kiesel *et al.*, 2019). Studies show that the future precipitation dynamics in the Kilimanjaro region will primarily be regulated by both global climate and local land-cover change (Otte *et al.*, 2016). Generally, Climate change results in changes in precipitation regime and evapotranspiration rates; thus, they are expected to affect surface water resources in time and space (Kumar *et al.*, 2017). These changes are expected to affect both ecosystem services provision, water availability, food and energy production. This triggers the need to generate high-resolution spatial data for the overall availability and predictability of water resources at the watershed scale.

Hay *et al.* (2002) found that spatially averaged temperatures in Kilimanjaro rose between 1951 and 1960 and 1981 to 1995, with the period in between showing relatively stable temperature patterns. The records show a correlation between temperature inversion, precipitation decline, and the occurrence of wildfires. The latter is a product of climate change and is aided by anthropic activities at the same time (Agrawala *et al.*, 2003). Increased temperature levels are expected to impact the hydrological cycle by increasing evapotranspiration regimes. Thus, affecting the hydrological cycle. In the long run will affect water availability, food, and energy production.

Precipitation, land cover, recharge and discharge all change at the same time. Rainfall, which is affected by changes in the climate of a region, is needed for both recharge and discharge (Kundzewicz *et al.*, 2009). In Tanzania, there is mounting evidence of diminishing dry-season discharges for some perennial rivers (Ndomba *et al.*, 2008b; Valimba, 2007; Yanda & Munishi, 2007). Physical entities such as the reduction in river flow discharges and water levels in rivers, the decline in domestic and agricultural water supplies, and the intensification of drought all contribute to community perceptions of climate change and water resources (Kangalawe, 2017; Tagseth, 2010). These entities directly impact water supply, food production, power generation, and the survival of a large population that relies on these water resources.

Changes in precipitation in the Kilimanjaro forest reserve are linked to past and ongoing land use/cover changes, which triggers the need for further investigation (Mölg *et al.*, 2012). The observations in other mountains of the earth indicate potential impacts on water reservoirs and runoff variability (Roa-García *et al.*, 2011). Fluctuations in water balance are of particular interest; since variations in the local hydrological cycle will likely have a wide

range of effects on the ecosystem, local populace's livelihood on the mountain slopes, and a wide range of regional ecosystems (Mölg *et al.*, 2012). This takes into account the communities living within the catchment and surrounding suburbs.

Changes in rainfall patterns and humidity within the past 80 years have led to anomalies in vegetation and ecology in many parts of Mount Kilimanjaro, especially at lower altitudes and on the northern slope of the mountain (Hemp, 2005). These irregularities mostly take the form of delayed rainfall onset, which extends the dry season and creates agricultural yield uncertainties and food insecurity in the agrarian society that has depended on mountain amenities for centuries (Agrawala *et al.*, 2003).

In Kikuletwa, along the Pangani River Basin, a major reduction in river discharges has been recorded (Lalika *et al.*, 2015). According to projections, the annual runoff in the Kikuletwa river within the Pangani basin is expected to decrease by 9% for all months. Monthly variations are expected in the Pangani basin, with an annual runoff reduction of around 6% (Agrawala *et al.*, 2003). Both of these are located on the southern limb of Mt. Kilimanjaro. Both of these falls on the southern limb of Kilimanjaro Mountain. Due to the suitability of decadal-scale knowledge in assessing the dynamics of rainfall (Brunsell, 2010) and the inadequacy of such studies in Tanzania. Mahoo *et al.* (2015) insist on the need to understand rainfall and water discharge predictability on a decadal scale in Tanzania.

Irrigation agriculture and domestic uses are the two main water users along the mountain slopes (Viviroli *et al.*, 2007). According to reports, 13 000 hectares of forest were converted to agricultural land between 1976 and 2000, resulting in a drop in surface runoff of approximately 58.4 hm³/year (Grossmann, 2008). Clouds water intercepted by trees and other plants provides a significant portion of overall runoff and may also contribute to groundwater recharge, as observed elsewhere (Prada *et al.*, 2009; Prada *et al.*, 2010). Between 1973 and 2000, about 39.5% of the bushland was converted to agricultural land (Mbonile *et al.*, 2003). As a result, it is clear that these massive changes had a major impact on groundwater recharge and surface runoff in Kilimanjaro's lower plains.

Conflicts over water resource are increasing, resulting in increased demand and reduced supply. Water allocation conflicts, for example, between the Lower Moshi irrigation scheme built in the 1980s and the redevelopment of the Pangani fall hydropower project, between the rural and urban population in water use, between upstream and downstream users, farmers

and pastoralists (Mbonile, 2005) demonstrate increased water demands and decreased availability. As a result, changes in water supplies have an effect on food, water, and power generation, impacting the livelihoods of thousands of people living downstream.

2.8 Climate and Land Use Change and Implications on Water-Food-Energy (WFE nexus)

Land use and climate change are unarguably connected through the hydrologic cycle (Stonestrom *et al.*, 2009). The past and future land use and precipitation patterns are used to address issues related to the hydrologic cycle, and human sustainability in a broad perspective. In areas where surface water is insufficient, water users have shifted to groundwater uses to sustain their demand. Although, groundwater is still impacted by climate change mostly through recharge, and evapotranspiration. However, natural groundwater recharge solely depends on precipitation patterns (Shah, 2009). As a result, water managers have shifted the focus into the development of the groundwater system for domestic uses and agricultural production (Kumar, 2016).

The decrease in frequency and increase in severity of precipitation events are also projected in future. These changes will impact freshwater ecosystems and water availability for humans. There is now a shred of growing evidence showing that even at +2°C levels of warming, agricultural productivity is expected to decline across the globe, but mostly throughout tropical areas (Challinor *et al.*, 2014). In most African countries, food production would necessitate more research on drought-resistant crops (Ramírez & Thornton, 2015). These changes trigger the need to consider the projected future climate changes in future water resource planning and food production.

The link between climate and land use and hydrology of an area appears both intuitive and complicated (Schulze, 2000). Røhr (2003) describes the dynamic and unknown processes of interdependence and control between irrigation, vegetation, and river discharge. Since climate change, water supply conditions, and land use/cover changes all affect one another, understanding the effect of climate change on the water cycle necessitates a multifaceted study of its dynamic and nonlinear interrelated processes (Xia *et al.*, 2017). Many possible impacts on the hydrological system are anticipated as a result of ongoing local and global changes in the climate system of Kilimanjaro, according to researchers (Mckenzie *et al.*, 2010). Studies show that population pressure creates a demand for more shelter, fibre, and

water for various uses, which in turn leads to changes in forests, farmlands, and waterways (Byerlee *et al.*, 2014; Foley *et al.*, 2005; Mul, 2009). However, the country highly depends on rainfed agriculture; climate change increases the risk of crop failure due to a shortage of water as a result of reduced precipitation (Enfors *et al.*, 2011; Makurira *et al.*, 2011). Reduced precipitation is expected to affect water availability for ecosystem supports and human needs. Mckenzie *et al.* (2010) postulate that projected climate changes and variability will impact water resources over Kilimanjaro. There is a need to incorporate future climate changes in future water resource management. Therefore, a need for a study that will integrate the population in addressing the future state of surface and groundwater resources over Kilimanjaro is therefore important.

Missing/flimsy knowledge on hydrology, meteorology, and groundwater exploration discovery of the Kilimanjaro slopes hindered economic planning for water supplies in the Kilimanjaro slopes (Mwende, 2009). Initial runoff forecasts display monthly variations in both time and space. The Pangani and Kikuletwa rivers, on the other hand, are expected to have a decrease in discharge by around 6% and 9% annually, respectively (Agrawala *et al.*, 2003). However, by the 2050s, precipitation amounts along the Pangani river are expected to increase by 16 to 18%, resulting in a 10% increase in runoff despite lower peak flows (Kishiwa *et al.*, 2018). This mismatch in runoff estimation highlights the need for high-resolution impact studies in order to improve management strategies.

For domestic and agricultural needs, the local population on the slopes of Mt. Kilimanjaro depend solely on streams and springs (Mckenzie *et al.*, 2010). Smallholder farmers and conventional agro-pastoralists, who depend primarily on rainfed agriculture, control about 85 percent of arable land (Lein, 2004). Weather and climate changes on Mt. Kilimanjaro would have an effect on regional water supply and ecological sustainability (Fairman *et al.*, 2011). This shift affects water and water use, which is related to social, economic, political, and historical ties and processes in Kilimanjaro and the Pangani River (Lein, 2004). This necessitates the creation of a conceptual understanding of water resources overall availability and predictability (Rowhani *et al.*, 2011).

Agriculture, with small-scale to large-scale rice plantations and sugar cane irrigation plantations along the Kahe plains, is the largest water extractor along Pangani and the region. (Lalika *et al.*, 2015). However, the Pangani basin's water supply capacity is less than 1200 m³ per person per year (water-stressed), and irrigation system water efficiency is less than

15% (PWBO/IUCN). This necessitates a replan of the water sustainability for commercial agriculture.

Population growth and immigration in the Pangani basin are linked to the availability of fertile soil and rainfall for staple food production along the Pangani basin (Fisher *et al.*, 2010). Among the climate-dependent practices, Turpie *et al.* (2003) identified zero grazed livestock on densely populated mountain slopes. These various activities need much water to run, putting pressure on both rain-fed and irrigated agriculture, resulting in increased water demand and conflicts among water users in the area (Andersson *et al.*, 2006; Burton & Chiza, 1997; Tagseth, 2010). As a result, climate change would have an effect on a wide variety of community members, from households to plantation agriculture. As a result, there is a pressing need to discuss future resilience.

Climate change has hampered food production and causing drying that has harmed regional life forms, agriculture, and vegetation (Mölg *et al.*, 2009). Other considerations include decreased river discharges and water quality in the Pangani river during both the dry and wet seasons (Mtalo *et al.*, 2005a). As factors affecting output per unit farm area, rainfall fluctuations, floods, and drought have an effect on land management (Mbonile, 2005). According to Mbonile *et al.* (2003), the southern slope of Kilimanjaro has an over-dependence on agriculture and a lack of agricultural inputs, which affects output per field. Crop failure and reduced water availability for hydropower generation, industrial and domestic needs are affecting the livelihoods of the surrounding population and industries (Mbonile, 2005).

According to Mbonile *et al.* (2003), the southern slope of Kilimanjaro has an over-dependence on farming and a lack of agricultural inputs, which affects output per farm area. Crop failure and reduced water availability for hydropower generation, industrial and domestic needs are affecting the livelihood of the local population and industries (Mbonile, 2005). Munishi *et al.* (2015) reported a significant and robust correlation between climate change and lower maize, bean, and banana yields in Hai district. According to the study, the pattern is caused by increases in air temperature, decreases in precipitation, and unequal spatial distribution of rainfall during the cropping season. Compared to 2011, the water demand deficit for irrigation and livestock production is expected to rise by 71.12% and 1.41%, respectively, by the 2060s (Kishiwa *et al.*, 2018). This means that people in the

lowlands who depend on irrigation for food and commercial farming must reconsider their livelihoods.

Crop failure would have a greater effect in these areas because the agriculture sector employs more than 80% of the local population. The study goes on to state that consistent agriculture output is the most important factor affecting the region's livelihood prosperity (Munishi *et al.*, 2015). As a result, it is critical to comprehend the current situation and establish long-term strategies to ensure food security in the future.

Since the country is heavily reliant on hydroelectric power, climate change will have an equal effect on the energy sector as it will on agriculture (Munishi *et al.*, 2015). Water efficiency for hydropower production is currently as low as 35% of full capacity, which means that as climate change impacts become more serious, future environmental degradation and disputes among water users are almost certain (PWBO/IUCN).

In Tanzania, Cole *et al.* (2014) projected a rise in the average hydropower power output from dams. Their study goes on to state that the only factor that must be addressed when building hydropower dams is climate instability. The findings under this study suggest that anthropogenic influence has a significant effect that should not be neglected. The findings by Cole *et al.* (2014) also contradict those of Lalika *et al.* (2015) on the declining trend in rainfall and river discharges. Kishiwa *et al.* (2018) used 2011 as a base year to estimate future water supply for hydropower development along the upper Pangani river (in the 2050s). However, despite increased stream flows of 10%, the study predicts that future water demands for hydropower output will decrease by 27.47% due to lower peak flows. This finding differs from that reported by Cole *et al.* (2014), which was likely due to the use of a coarser resolution dataset. Given the country's desire to develop an intensive industrial economy, the expected hydropower output deficit would have a major impact on meeting the intensive industrial economy's energy demands. As a result, prospective government and private proposals should include an emphasis on renewable energy sources to meet future demand. This also emphasizes the importance of gathering high-quality data for high-resolution impact studies in order to determine the reality of future scenarios.

A few studies in Tanzania have attempted to measure the hydrological responses to potential climate conditions (Adhikari *et al.*, 2017). However, in many parts of the country, the scarcity of high-quality data remains a major issue. This makes it challenging to comprehend the

observed changes and improve the efficiency of hydrological models around the world. This phenomenon hampers gaining a better understanding of the observed changes and improving the efficiency of hydrological models around the world (Kundzewicz *et al.*, 2007). Runoff reconstruction, for example, is hindered by both data access and data quality (Gedney *et al.*, 2006; Peel & McMahon, 2006).

Water, food, and energy resource availability and suitability projections for the Kilimanjaro slopes under climate change and anthropogenic activities is hampered by several factors. One of the most significant factors is a lack of ground-based data from which to deduce temperature patterns at various altitudes on the mountain (Agrawala *et al.*, 2003; GITEC, 2011; McKenzie *et al.*, 2010). Furthermore, there is a scarcity of data on rainfall distribution with elevation, with just a few observations made above 1500-1600 m.a.m.s.l (Røhr, 2003). In most of the models, the details of water demand for each land use plan and representation of each vegetation type are approximate and mostly generalized (Røhr, 2003). Future research should focus on generating high-quality hydrological data at the watershed scale and incorporating local mitigation and adaptation strategies into future decision support systems.

2.9 Motivation

As a water tower, Mount Kilimanjaro feeds major river systems, especially on the southern slopes. The mountain supplies water for agriculture activities along the highly populated southern slopes (Hemp, 2005). Moreover, the mountain harbours a wide range of endemic species (Hemp, 2006b; Myers *et al.*, 2000). Thus, variation in precipitation and the future climate dynamics in the region are of particular interest.

The tropical river basins are facing hydrological extremes (Drought and floods), increased water conflicts and water quality due to anthropogenic activities. Climate and land use changes are linked through its impacts on the hydrologic cycle of the watersheds. The hydrological balance of Mount Kilimanjaro watersheds has been seriously affected by forest fires that are responsible for the loss of a third of the Kilimanjaro forest cover during the last 70 years. Furthermore, there is an expansion in agricultural land driven by the passion for increasing food production to feed the rapidly expanding population. However, the concept of increasing production by expanding agricultural land has never been tested in the KWK watershed. It is evident that there is scope for developing an understanding between climate, human activities, and sustainable water management under climate and land use change

scenarios. Further, an understanding that will enhance agricultural production to feed the increasing population in these river basins under changing climate. The management framework in these river basins needs to incorporate parameter and operational uncertainties for sustainable agriculture production.

Quantification of ground and surface water resources is the first step of the conjunctive water use plan. Further, quantifying the impacts of climate change on hydrological fluxes (both surface and subsurface) has not been done for the KWK watershed. Moreover, the identification of agriculturally suitable water potential zones is required for sustainable irrigation practices. Thus, a set of methodologies were developed, including performance evaluation, to address the aforementioned issues.

2.10 Evaluation of the Impacts of Climate and Land Use Changes on Water Resources

A modelling approach is typically the best method to assess the impacts of land use/cover and climate changes on the water balance. Models can be used to evaluate the historical and future implications of land use/cover changes on the hydrology of a catchment (Huisman *et al.*, 2009). This study used the soil and water assessment tool (SWAT) to assess the impacts of land cover and climate changes on the water balance components of the KWK watershed on the southern slopes of Mt. Kilimanjaro. The SWAT has been tested and used to solve complex watershed management problems in many regions all over the world (Anand *et al.*, 2018b; Hyandye *et al.*, 2018; Kishiwa *et al.*, 2018; Shawul *et al.*, 2019; Twisa *et al.*, 2020). Further, partial least square regression (PLSR) can be used to investigate the impact of land cover changes on the streamflow and establish the impact of the individual land cover type on the streamflow using PLSR modelling. This study provides a comprehensive analysis of the historical and future land cover dynamics and their impacts on the hydrological processes. Further, future climate scenarios can be generated by using Regional Climate Models (RCMs).

2.10.1 The Hydrologic Simulator

Soil and Water Assessment Tool (SWAT) is one of the popular physical-based hydrological models. It is used to simulate hydrologic processes within the watershed (Gassman *et al.*, 2007). The SWAT was developed by the United States Department of Agriculture (USDA).

Since its development, SWAT has been used to predict the impact of management practices on water, sediments, and agricultural chemical yields in large data-scarce basins (Arnold *et al.*, 2012). The SWAT provides a flexible framework that allows the simulation of watershed processes under a wide range of watershed management practices (Ullrich & Volk, 2009). The SWAT has been used to assess the impacts of anthropogenic activities that degenerate the natural river basin systems. Land-use and cover changes being the primary factor impacting the water balance of a watershed (Lam *et al.*, 2011; Yevenes & Mannaerts, 2011). The application of SWAT has been successful in many parts of the world. In recent years, the SWAT has been widely used in many countries (Hyandye *et al.*, 2018; Meaurio *et al.*, 2015; Shawul *et al.*, 2019; Twisa *et al.*, 2020; Wang *et al.*, 2014); and has been tested to inspect the management strategies on watershed hydrology, and water quality (Shawul *et al.*, 2013). SWAT operates on a daily time step with optional monthly or annual output. The model divides a catchment into a set of a unique combination of soil and vegetation types which provides the basic unit for computation of flow accumulation. The SWAT simulates the hydrological cycle using the water balance equation (Equation 1).

$$SW_t = SW_0 + \sum_{i=1}^t (R_i - Q_i - ET_i - G_i - B_i) \quad (1)$$

Where SW_t (mm) is the final soil water content, SW_0 is the initial soil water content on day i , t is the time, R_i is the precipitation amount on the day i . Q_i (mm) is the amount of surface runoff on day i , ET_i (mm) is the evapotranspiration (ET) amount on day i . G_i (mm) is the amount of water entering the vadose zone from the soil profile on day i , and B_i is the amount of return flow on day i .

The snow module in SWAT captures and simulates the snowmelt hydrology. The module allows delimitation of up to ten elevation bands with different precipitation and temperature lapse rates (Grusson *et al.*, 2015; Qi *et al.*, 2016). In this process, SWAT uses the temperature of the near-surface air to characterize liquid and solid rainfall. During this process, the snowfall and snowmelt are estimated when the temperature drops below the snowfall threshold. These processes can be distinguished in space using the elevation, which allows users to add lapse rate for both precipitation (PLAPS in mm H₂O/km/yr), and temperature (TLAPS in °C/km). However, previous studies suggest the absence of isotopic signatures in springs and river discharges of the study area (Mckenzie *et al.*, 2010). Thus, the contribution of snow was not accounted for its contribution to the annual runoff in this study. Variation of temperature and precipitation with elevation and spatial variability due to complex terrain are challenges during estimation of the model parameters (Anand *et al.*, 2018a).

2.10.2 Partial Least Squares Regression Analysis

Partial least squares regression (PLSR) analysis of Land Cover change impact on water balance components is widely applied in performing multivariate regression analyses for collinear predictors (Shi *et al.*, 2013b). In PLSR modelling, two data matrices X and Y are related by a linear multivariate model. A model parameter is estimated as a slope of a simple bivariate regression between a matrix column or row as the Y-variable; and another parameter vector as the X-variable; this is done for each variable (Wold *et al.*, 2001). The PLSR offers a quantitative modelling platform for complex relationships between predictor variables with problems (Wold *et al.*, 2001). The background of the statistics behind PLSR modelling is well documented in the previous studies (Abdi, 2010; Godoy *et al.*, 2014; Tenenhaus *et al.*, 2005; Wold *et al.*, 2001). The PLSR is an extension of a multiple linear regression model. In the simplest form, a linear model specifies the relationship between a dependent variable y, and a set of predictor variables x, as shown in Equation 2.

$$y = k_0 + k_1x_1 + k_2x_2 + \dots + k_nx_n \quad (2)$$

Where; k_0 is the regression coefficient for the intercept, and k_i values are the regression coefficients (for variables 1 to n) computed from the data.

The predictive quality of the model can be improved by running a series of PLSR models. In each run; the Q^2 cumulated (Q^2_{cum}) can be used to eliminate variables with the least influence until the largest Q^2_{cum} was attained. Generally, Q^2_{cum} above 0.5 is considered an excellent predictive power (Shi *et al.*, 2013b). The cross-validated root mean squared error (RMSECV) was used to avoid skewness by the data points, especially when there are outliers. The Model's predictive power was measured by using the global goodness of fit (R^2) and the cross-validated model quality index (R^2_{cross}). The R^2 is a fraction of variance in the dependent variable which can be predicted by the model; whereas, R^2_{cross} measures prediction goodness. Generally, the importance of predictors (for all variables) is measured by the variable importance for the projection (VIP), where the larger the values, the higher the predictor relevance.

In determining the land use types that interact with hydrological components than the other, the regression coefficients (RCs) and the variable importance of the projection (VIP) are used. Those predictors with large VIP values can best explain the dependent variable (Ai *et*

al., 2015; Wold, 1995), the values >0.8 are most pertinent, whereas the values <0.5 show insignificance in explaining the variable (Shi *et al.*, 2013b; Wold, 1995; Woldeesenbet *et al.*, 2017). For the RCs shows the direction and strength of the impact of each independent variable. Generally, a small RC and large VIP show the importance of the variable in prediction in that direction, whereas the small RC and small VIP indicate insignificance of the particular variable, thus, it can be omitted from the model.

The PLSR method associates Principal component analysis (PCA) and multiple linear regression features (Abdi, 2007). The method is suitable when the predictors show multicollinearity. Generally, land use data exhibit collinearity because an increase in the percentage/area of one type will automatically decrease the percentage/area of one or more of the other land use types (King *et al.*, 2005). Thus, it is appropriate in many studies because it eliminates co-dependence among the variables; further, it provides a more unbiased view of the contribution of the changes in water balance components at the watershed scale.

2.10.3 Historical and Future Climate Change Simulation

The ongoing impacts of climate change are expected to substantially impact water resources in many regions of the world (MacDonald *et al.*, 2009a). Because the future climate parameters like precipitation and temperature are vital parts of the water cycle, modelling these impacts needs high-resolution regional rainfall scenarios as input to impact models. The General Circulation Model (GCMs) have been used to model future global-scale climate change trends. However, the current generations of GCMs have a major weakness in producing information at a coarser resolution in impact studies (Hu *et al.*, 2012a; Schmidli *et al.*, 2006). Furthermore, GCMs cannot represent sub-grid scale features and dynamics, namely topography and convections, all of which are vital in climate change impacts on a basins scale (Hu *et al.*, 2012b). In order to overcome these shortcomings, downscaling methods have been established to correlate coarser GCMs data to finer scales relevant for the basin level (Hu *et al.*, 2012b; Hu *et al.*, 2012a; Schmidli *et al.*, 2006).

Downscaling refers to the general term used to name a procedure used to make predictions at a catchment scale by taking information known at large scales (Wilby & Wigley, 1997). The GCMs downscaling approaches can be classified into dynamic and statistical downscaling (Tripathi *et al.*, 2006). Dynamic downscaling uses Regional Climate Models (RCM) or Limited-area Models (LAM), which is embedded into GCM to produce high-

resolution outputs (Mearns *et al.*, 2003); these are believed to better represent topography and land use as compared to GCM (Sunyer *et al.*, 2010). However, it has some limitations that it strongly depends on GCM boundary forcing and has a limited number of scenarios ensembles, computationally intensive and initial boundary conditions affect final results (Wilby & Wigley, 1997).

On the other hand, statistical downscaling models use the fundamental concept that regional or local climate strongly depends on large scale atmospheric variables (such as mean sea level pressure, geopotential height, and wind fields). It has advantages of having the ability to directly incorporate observations into the method, easily transferability to other regions, and the ability to provide point scale climate variables (Wilby & Wigley, 1997). One advantage of the statistical downscaling method is that they provide site-specific information which can be used in many climate change studies (Wilby *et al.*, 2004). The procedure involves screening of potential downscaling predictor variables, assembling and calibration of Statistical Downscaling models, then ensembles of current weather data are synthesized using GCM-derived predictor variables and finally, the observed data and climate change scenario (Wilby *et al.*, 2004).

The RCMs have gained the attention of recent researchers due to their capacity to provide high-resolution climate simulations (Pan *et al.*, 2012; Roux, 2009). However, these simulations are subject to various uncertainties arising from boundary conditions, domain integration size and natural variability within the RCMs and RCM formulation (Min *et al.*, 2013). For example, evaluation in East Africa reported better RCMs simulation in one region and poor in another region within the same temporal scale (1990 to 2008) (Endris *et al.*, 2013). Also, in Southern Africa, the report shows that the performance of the RCMs in simulating precipitation differed over different regions (Shongwe *et al.*, 2014).

The use of RCMs (Regional Climate Models) has been one of the best and robust methods to obtain high-resolution climate information, taking into account regional patterns and indigenous knowledge. The RCMS runs on a limited geographical area using boundary conditions from GCMs (Daniels *et al.*, 2012; Min *et al.*, 2013). The lateral boundary conditions hardly affect the bias of the RCM for all seasons and over most of the African continent. For example, even when numerous GCMs are downscaled, RCA-RACMO is independent of the driving GCM dry over equatorial Africa; in contrast, Climate Limited area Modeling (CCLM) shows a dry bias over the eastern coast of Guinea Gulf (Dosio *et al.*,

2019). The finer spatial resolution of RCMs allows simulation of local climate under greater detail through taking into consideration orographic impacts (coastlines, mountains, water bodies, vegetation) and land-use, and small scale dynamical and boundary layer processes (Luhunga *et al.*, 2016).

One major proposed strategy to minimize the impacts of climate change on water resources is to develop a working adaptation plan (Mutayoba *et al.*, 2018). However, insufficient evidence on the future climate change impacts on water resources afflicts the development of water resources adaptation strategies. Furthermore, developing evidence of climate change on water resources is one among the challenging activity (Muerth *et al.*, 2013). For example, many uncertainties are worth considering when simulating the impacts of climate change on streamflow (Melsen *et al.*, 2018). These climate models perform differently among ecoregions (Kotlarski *et al.*, 2014). Thus, it is necessary to assess these models in different regions.

Thus, it is necessary to assess the performance of climate change data in different ecoregions. One of the best methods to analyse climate change impacts in a watershed is to use a combined analysis of both Climate and hydrologic models. However, hydrologic models themselves introduce uncertainty through parameters (Merz *et al.*, 2011), and model conceptualization. This means care should be taken during model parameterization scenario simulation at the watersheds.

CHAPTER THREE

MATERIALS AND METHODS

3.1 The Study Area Characteristics

3.1.1 Background Characteristics

The mount (Mt.) Kilimanjaro is the highest peak in Africa at 5895 m.a.s.l., located 300 km south of the equator in Tanzania on the border with Kenya between 2°45' and 3°25' South and 37°00' and 37°43' East (Fig. 2). It is located in the northern part of the Pangani River basin (Røhr & Killington, 2003). The Mountain is surrounded by natural forests belt with an area of around 1000 km² (Hemp, 2005). The slopes are dominated by the eroded remnant of an ancient volcano, starting from the savanna plains (700 m. a.s.l) to 5895 m elevation, which is snow and ice (Hemp, 2005).

The Kikafu, Weruweru, and Karanga (KWK) watershed originates from the pick of Mount Kilimanjaro and extend southwards through the thick mountain forest on the Mount Kilimanjaro slopes (Fig. 2). The watershed joins the Kikuletwa networks before entering the Nyumba ya Mungu dam. The area is mostly under rainfed and irrigated agriculture as the primary means of production. The KWK watershed is one of the mountainous watersheds along the southern slopes of Mount Kilimanjaro and the northern part of the Pangani river basin. Being located on the mountain slopes with greater human activities, KWK experiences tremendous changes in its land cover (Fairman *et al.*, 2011; Mbonile *et al.*, 2003; Mmbaga *et al.*, 2017; Soini, 2005b). Further, climate change has for long named to influence the supply of ecosystem services at varying degrees (Mckenzie *et al.*, 2010; Misana *et al.*, 2003; Mölg *et al.*, 2008; Mulangu & Kraybill, 2013; Munishi *et al.*, 2015; Thompson *et al.*, 2002). Thus, necessitating quantifying the impacts of climate and land use/cover changes on the water balance for sustainable water resources management.

3.1.2 Rainfall and Temperatures

The climate of Mount Kilimanjaro is influenced by its proximity to the equator. Thus, its climate is influenced by trade winds and controlled by meridional displacement of the intertropical convergence zone (Duane *et al.*, 2008). It is typical of an equatorial climate; the rainfall and temperatures vary with elevation (Hemp, 2005). The rainfall pattern follows the

bimodal regime and is influenced by trade winds (Coutts, 1969). Generally, the precipitation in the Kilimanjaro tropical rainforests comprises a mixture of rainfall, throughfall, and fog (Otte *et al.*, 2017). There are two distinct seasons in the hydrological year, the March to May (Masika) and October to December (vuli) wet seasons and the January to February and June to September dry seasons (Appelhans *et al.*, 2015; Otte *et al.*, 2016). Variations of the rainy season from one year to another are controlled by Indian Ocean Dipole (IOD) and meridional displacement of Intertropical Convergence Zone (ITCZ) (Otte *et al.*, 2016). Precipitation on the southern slopes is approximately 2500 mm compared to less than 1000 mm on the northern slopes (Hemp, 2005). On the southern slopes, the annual precipitation amount varies with elevation, 900 mm at 800 m.a.s.l. Thereafter, increasing linearly to a maximum of approximately 2700 mm/year at 2200 m. a.s.l dropping linearly until the freezing point level to 750 mm at roughly 3750 m.a.s.l with a continual decline up to the summit (Hemp, 2005).

The Mean annual temperature is 23.4°C at 813 m elevation in Moshi (Walter *et al.*, 1975), decreasing to about -7.1 at the summit (Thompson *et al.*, 2002). The mean annual temperature decreases linearly upslope with a lapse rate of 0.56°C per 100 m (Hemp, 2006a), from 23.4°C at the foothills in Moshi at 813 and declining to 7.1°C at the top of Kibo. The daytime variability ranges between 23°C and 9°C along the elevation gradient (Otte *et al.*, 2017), and derives the mean annual temperatures more than seasonality (Duane *et al.*, 2008), and range between 23 and 9 °C along the elevation gradient.

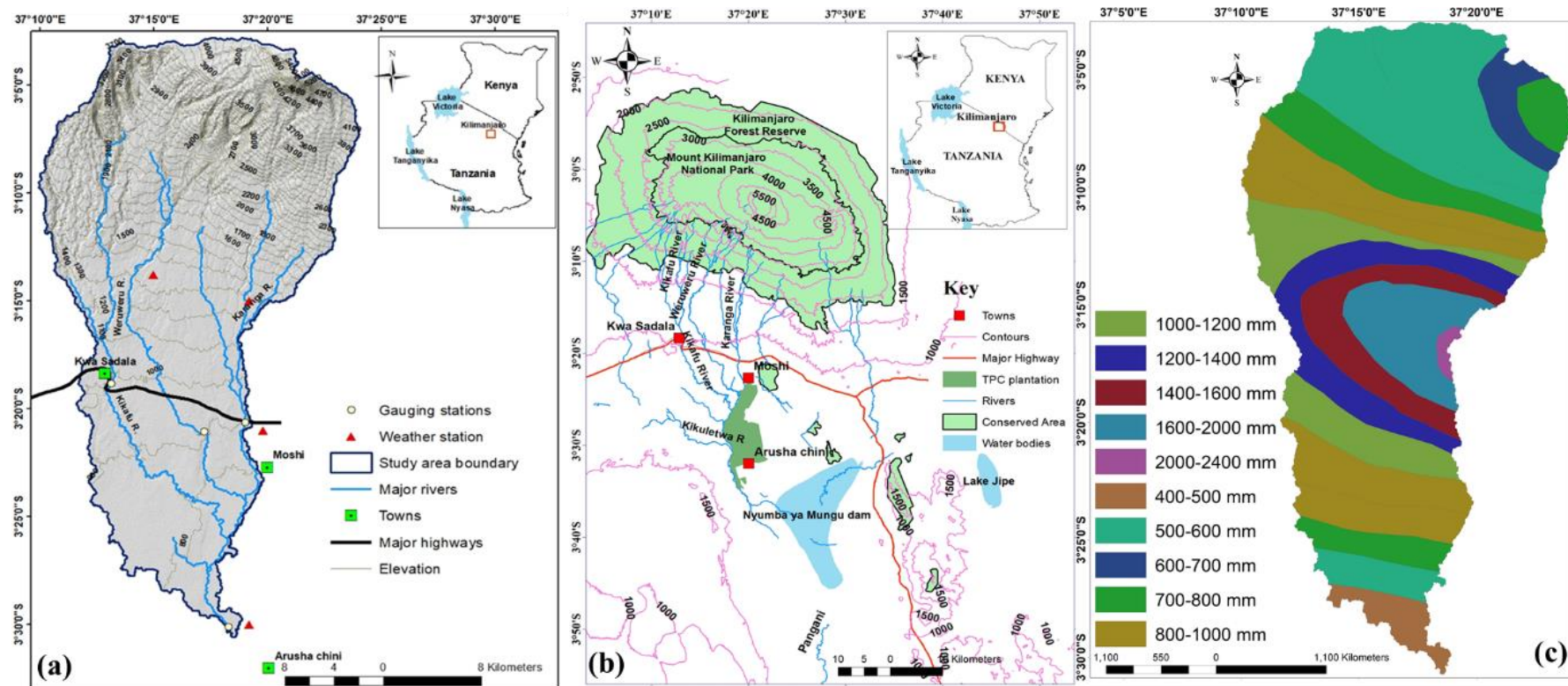


Figure 2: The study area, weather and gauging stations (a), features and elevation (b), and annual rainfall distribution (c)

3.1.3 Geology and Soils

The Geology and soils of the KWK watershed are depicted in Fig. 3 (d) and 3 (e), respectively. The soil erosion is high on the higher slopes as most of the soils are carried to the lower slopes making more than 200 m thickness of unconsolidated materials as overburden (Mwende, 2009). The report by Mwende (2009) further shows that the weathered mantle has been eroded and transported to lower plains. Glacial sands obscure the volcanic rock near the summit from around 3000 to 5000 m.a.s.l (Downie *et al.*, 1956).

According to Food and Agriculture Organization (FAO), the soils of the Kilimanjaro region are categorized into four groups which makes the basis of the variation in soil fertility. The Humic nitisols and humic andosols; chromic cambisols and associated eutric cambisols; orchric and andosols, and chromic cambisols and vitric andosols; mollic andosols and associated eutric nitosols (Fig. 2(b)). The soils are chiefly of volcanic origin, mostly rich in Mg and Ca (Nkya *et al.*, 2015), and silica which might be originating from chemical and physical weathering of rocks and high in water and organic matter (Mwende, 2009). Thus, the soils are predominantly clay, with gravel beds deposits in some areas (GITEC, 2011). Clay soils are predominant throughout most parts of the plain, and the gravel bed is formed as a fan deposit in some areas.

The rocks around Mt. Kilimanjaro are mainly nephelinites, phonolites, olivine and alkali basalts, pyroclastics and trachytes (Schlüter, 2006). Many of the subsequently developed soils are Andosols formed on top of lava and ash flows (Little & Lee, 2006). According to lithological classification criteria by Meinzer (1923), the aquifer is chiefly composed of Neogene alluvials, weathered Neogene volcanics, and fissured Precambrian metamorphics. Most of the lowland areas are covered by alluvial plains, resulting from huge deposits from floods during heavy storms; for example, the alluvial deposits are mostly concentrated on the lowland areas along Kikuletwa River and Kahe plains. Kahe plains are chiefly formed by Kilimanjaro volcanics and alluvial deposits resulting from erosion in highland areas and rivers (GITEC, 2011). The large smooth mass of Kibo lahar is a boulder deposit with typical mounded that covers a large area of the plains south-west of Moshi at heights of below 915 m. In places, it shows a typical mounded landscape, this deposit was formed by enormous debris flows during the development of the Kibo. The southern slopes are dominated by a mass of glaciated valleys that dissect along the southern slopes compared to other slopes, these mass sections increases in depth southwards.

3.1.4 Hydrogeological Setting

Theoretically, the Kilimanjaro aquifer is composed of Neogene alluvials, the weathered Neogene volcanic, and fissured Precambrian metamorphics (Mwende, 2009). The Kilimanjaro groundwater system behaves comparably to that of the regional Pangani (Mul *et al.*, 2007) with shallow (through sediments) and regional flow systems (controlled by regional geology) (Mckenzie *et al.*, 2010; Mul *et al.*, 2007a). The groundwater system is older with connection to the surface water system. The river system is inextricably linked to groundwater and precipitation (Mckenzie *et al.*, 2010). Submontane (1600 m.a.s.l), montane zone (1600–2800 m. a.s.l), subalpine zone (2800–3900 m. a.s.l), and alpine zone (>3900 m. a.s.l) climatic zones result from temperature and precipitation stratification with elevation on Mt. Kilimanjaro (Hemp, 2006b).

The southern slopes of Mount Kilimanjaro are home to rivers and streams that contribute significantly to the Pangani river basin, as well as hydropower generation at Nyumba ya Mungu, Pangani, and Hale stations, as well as Tanganyika Planting Company (TPC). Small to large scale agriculture production projects and rice production at the lower Moshi Irrigation scheme are also found in the study area (Sarmett & Faraji, 1991). Fishing is also enhanced by the Nyumba Ya Mungu Dam, which has a maximum catch yield of around 4000 tonnes per year. The Amboseli ecosystem, which supports Masai pastoralists and a diverse wildlife population, receives water from the northern slopes as well (Agrawala *et al.*, 2003). In comparison to the other slopes, the southern slope of Mount Kilimanjaro is more fertile and wet. As a result, the southern slope is relatively densely populated and intensive agricultural practices (National Bureau of Statistics, 2012, 2018; Røhr & Killingtveit, 2003).

3.1.5 Population and Economic Activities

The population of the Pangani catchment area has grown by 32% in the last decade and a half, from 2.4 million people in 1988 reaching 3.2 million people (Fisher *et al.*, 2010). The slopes of Mt. Kilimanjaro have been continuously inhabited by humans for over 2000 years (Schmidt, 1989). The slopes of Mt. Kilimanjaro are currently surrounded by five neighbouring districts (Moshi Rural, Moshi Urban, Rombo, Hai and Siha districts). The total population of the districts has increased over time (Table 1), indicating increased demand on land, which contributes to environmental degradation (Daluti, 1994; Tagseth, 2010). This

means that land cover shifts, changes in surface and groundwater quantity and quality, and soil degradation are more likely to increase.

The population of the Kilimanjaro region has an average annual growth rate of 1.8%, making it the country's eighth most densely populated region (National Bureau of Statistics, 2012). The population density in the area is 124 people per square kilometer (National Bureau of Statistics, 2012), increasing to 650 people per square kilometer on the southern slopes (Zongolo *et al.*, 2000), and nearly 300 people per square kilometer on Mount Kilimanjaro's southern slopes (Mbonile *et al.*, 2003). In an ideal world, population pressure leads to increased demand for shelter, fibre, and water for different purposes, resulting in changes in forest, farmland, and water supplies (Byerlee *et al.*, 2014; Foley *et al.*, 2005). This demonstrates the presence of water resource pressures that have a direct effect on the region's hydrological system (Mul, 2009). The characteristic compacted surface of urbanized areas raises surface runoff and decreases groundwater recharge to a greater degree (Zomlot *et al.*, 2015). As a result, population patterns and behaviour must be considered because they affect land use/cover change and, as a result, potential water supply.

The Pangani river basin and the Kilimanjaro region population are centered on the Kilimanjaro and Pare mountain slopes and flat highlands, with sparsely populated lowlands (Adams *et al.*, 2010; Tagseth, 2010). In lowland areas, the majority of farms and intensive irrigation activities are carried out; furrow irrigation with small farms is a dominant historical water usage on Mt. Kilimanjaro slopes (Gillman, 1932; Raum, 1940), and mixed rainfed/plantation irrigation is common in lowland areas. According to Teale and Gillman (1935), the settlement's geographical setting on Kilimanjaro is influenced by water availability Teale and Gillman (1935). This means that changes in water management will affect how Kilimanjaro region residents interact with nature and the environment; as a result, the observed hydrological changes are a result of historical and current water management practices.

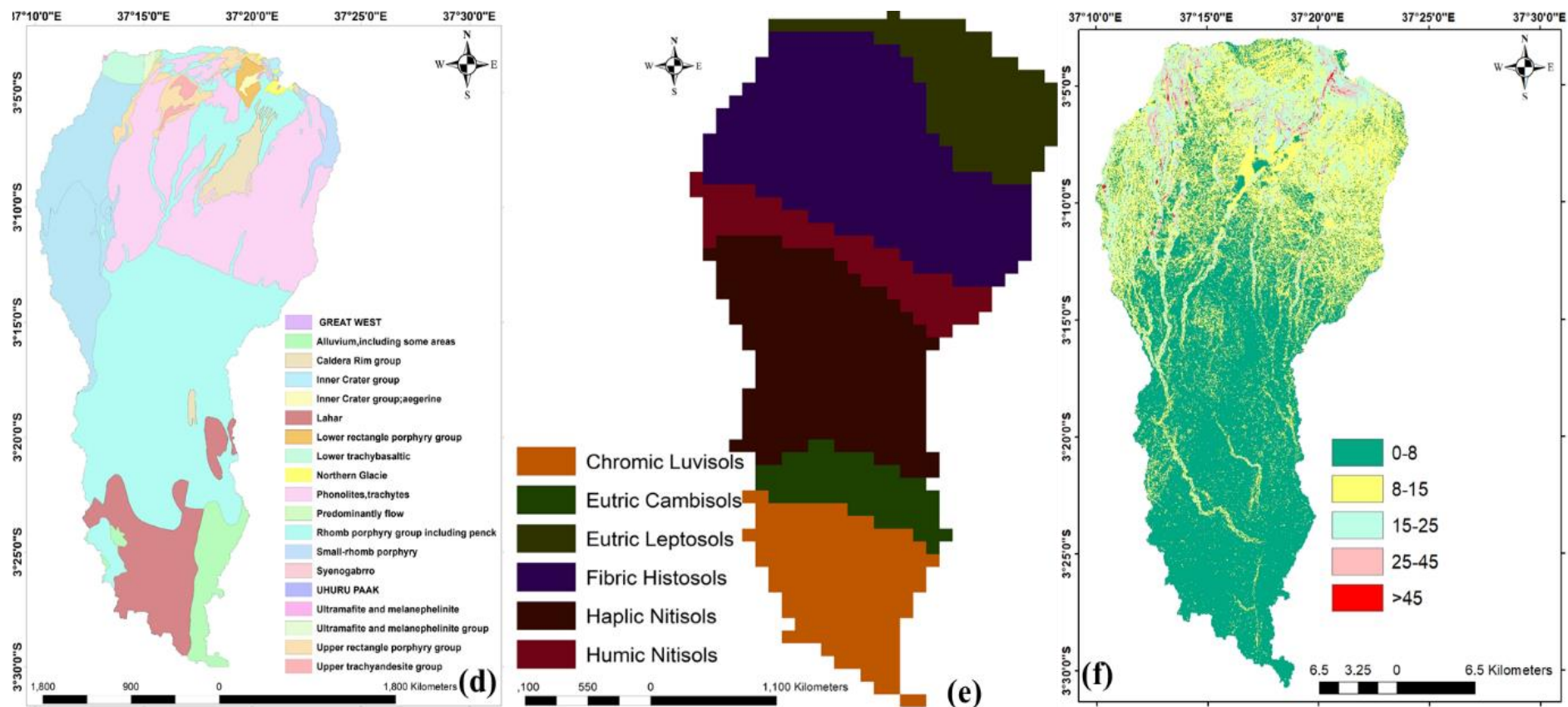


Figure 3: Geology (d), Soils (e) and Slope (f) maps of the study area

3.2 Assessment of the Historical and Future Land Use/Cover Dynamics on Mt. Kilimanjaro Slopes

In this objective, the main targets were three folds: (a) to map LULC in three historical periods (1993, 2006 and 2018) on the southern slopes of Mt. Kilimanjaro, (b) to project LULC in 2030 and to assess variations from the current LULC conditions, and (c) to investigate the impact of the LULC changes on the selected staple food production. The past LULC maps were extracted from satellite images through image classification, then aligned with population data, mean annual rainfall data, and other factors and constraints (Table 4) to generate suitability maps that were used for future (2030) LULC prediction.

In general, the procedures for this objective were as follows: (a) land-cover mapping in 1993, 2006, and 2018 using time-series satellite images (Maximum likelihood), (b) Calculation of transition area matrix obtained from the Markov procedure, which indicates the number of pixels that are likely to migrate from each land-cover class to another class over a given time interval (1993-2006), (c) Using Markov chain and Multi-Criteria Evaluation (MCE) model to prepare LULC transition suitability images. The suitability images depict the cells that are suitable for a specific land cover, (d) Comparing observed and predicted maps for the year 2018 to assess the model's predictive power, (e) Using the CA–Markov module in integrated geographic information system (GIS) and remote sensing software (IDRISI software) to simulate the land-cover change of 2030. Furthermore, (f) Using historical and current crop production data and potential agricultural land to align the results of available cropland and selected staple food production using linear interpolation. Figures 2 and 3 show a summary of these procedures.

3.2.1 Data Acquisition and Image Pre-Processing

The historical land-use data (1993, 2006, and 2018) of the catchment were obtained by classifying their respective Landsat (4, 7, and 8) level 1 images. The satellite images were freely available on the United States Geological Survey (USGS) website's Global Visualization Viewer (<https://glovis.usgs.gov/>). Landsat images from the Operation Land Imager (OLI) for 2018, Landsat 7 for 2006, and Landsat 4 for 1993 were used for land use/cover classification in this study. To reduce seasonal variability, all the images used in

this analysis were from the same season. Both images were resampled to a cell size of 30 m x 30 m, and atmospheric and geometric errors were corrected in ArcGIS.

The projections of these images were converted to local projections of the study area spatial data, as defined previously by Liang *et al.* (2018), in order to align them with other spatial data from the study area, including ground-truthing coordinates for accuracy assessment. Before extracting the necessary study area using the polygon boundary, individual bands from the images were extracted, and band composites were created. Mount Kilimanjaro and the dense forest of Kilimanjaro National Park occupy the upper part of the study area due to its geographical setting. Most of the time, particularly during the rainy season, this area is obscured by clouds. As a result, cloud-free images were difficult to acquire, particularly during the rainy season of 2018. To address this data quality issue, the cloudy areas of the image (which are mostly rock and snow that do not change significantly over time) were sliced out and replaced with cloud-free observations extracted from the satellite image of September 23, 2016 using ArcMap's Mosaic feature (Said *et al.*, 2021). Before the images were transferred to ArcGIS for further processing, the Landsat 7 scan line errors were corrected by filling in the missing data with scan line correction data using the "fill no data" feature in Quantum GIS (QGIS).

Other data used in this analysis included the Digital Elevation Model (DEM), road and stream networks, railway lines, and Protected areas shapefiles, in addition to satellite photos. These data came from a variety of sources. The data types used, and their characteristics are summarized in Table 2.

Table 2: Characteristics of the data used

Category	Data	Year	Data source
Satellite image	LT04-1993-02-17 (path 168/row062)	1993	https://glovis.usgs.gov/
Satellite image	LC07-2006-02-05 (path 168/row062)	2006	https://glovis.usgs.gov/
Satellite image	LC08-2016-09-23 (path 168/row062)	2016	https://glovis.usgs.gov/
Satellite image	LC08-2018-02-29 (path 168/row062)	2018	https://glovis.usgs.gov/
DEM	Digital elevation model	2018	https://glovis.usgs.gov/
Roads	All main and minor roads	2018	Survey and Mapping unit
Streams	All streams and rivers	2018	Pangani Basin Water office
Parks	Protected areas	2018	Tanzania National Parks
Demographic	Crops production	2018	Statistics Unit-Ministry of Agriculture

Field surveys were conducted to collect ground-truthing points with a hand-held GPS receiver in order to validate the land-use and land-cover change (LULCC) categories created. A set of 50-70 points (depending on accessibility) were randomly collected for each land use/cover class with uniform distribution in the area. These points were used to determine land use/cover classification accuracy, which was done by combining expert knowledge with field observations. It was possible to confirm the cover types and match them with the processed data from satellite images. Using Google Earth, the coordinates of features in remote montane forests, Kilimanjaro National Park, and high mountain areas were collected. The image processing software used in this analysis was ArcGIS 10.6 student edition and IDRISI Selva v17.0.

3.2.2 Image Classification and Accuracy Assessment

Land cover was divided into ten (10) major categories (Table 3), which include both natural and non-natural protected areas. This means that both natural and human-induced changes were included. Prior to image classification, the expert was guided by ground-truthing points to make an on-screen selection of the areas to select pixels to be used as training samples. Where identifying a land cover class on a satellite image was difficult or features were ambiguous, ground truth points were overlaid on Google Earth images to identify ambiguous features and train the past (1993 and 2006) images, allowing the opportunity to mark the

training sample and assign a particular land class. Following that, the signature file was generated using the training samples. The images were then created using a supervised classification algorithm with a maximum likelihood algorithm to generate land cover maps for the region in 1993, 2006, and 2018. Since supervised classification resulted in certain pixels being positioned in incorrect spatial areas; for example, agricultural land on top of Mt. Kilimanjaro, expert knowledge was used to correct these wrongly classified features. A raster calculator feature was used in this study to determine at what elevation a specific land-use class should appear. Expert classification was used because it is based on expert knowledge of the study field. The procedure is outlined in detail by Taweek and Thammapala (2005). To enhance classification accuracy, expert classification was used to combine remote-sensed data with other georeferenced data sources such as DEM, land use data, and spatial texture.

Table 3: Land use/cover classes and their description

S/N	Land use/cover class	Description
1	Built-up area (BU)	Tarmac and gravel roads, concrete areas, urban and rural settlements
2	Agricultural land (AGR)	All land with crops
3	Water (WAT)	Water in wetlands, rivers, fishponds, and water in agricultural areas.
4	Forest (FOR)	Thick canopy, areas with closed trees, both natural and planted forests.
5	Bare land (BAR)	Quarry areas, bare soils, eroded soils, and sands.
6	Grassland (GRA)	Tall to short grasses, sometimes bare soils in the dry season.
7	Wetland (WET)	Areas with lands partially submerged in water and grasses.
8	Shrubland (SHB)	Wooded areas with a more open canopy.
9	Rocky surface (ROS)	Areas covered with bare rock and less vegetation
10	Glacier ice (GLI)	Areas covered with Glacier ice

To determine the degree of agreement between the classified images and the ground features, an accuracy assessment was performed. Ground truthing points and other reference points found from satellite and Google Earth images were used as ground-truthing points. In addition, interviews with local residents were conducted with the aim of enhancing the

accuracy of historical images classification (1993, 2006). During fieldwork, a total of 50 to 70 ground-truthing points were obtained and used to determine the precision of each land-use class. The producer's, user's and overall accuracy, as well as Kappa coefficient, were determined. The number of samples correctly identified divided by the reference totals was used to determine producer accuracy, while the number of samples correctly identified in each class was divided by the classified totals to determine consumer accuracy (Foody, 2008). The total number of correctly classified pixels divided by the total number of sample points used in accuracy assessment yielded the overall classification accuracy of each image (Foody, 2008). The coefficient of agreement, or Kappa statistics, was calculated using Equation 3. The Kappa coefficient is a measure of the overall statistical accuracy of an error matrix between a classified map and reference data; it accounts for non-diagonal components. Figure 4 summarizes the image classification and accuracy evaluation method.

$$\Lambda K = \frac{N \sum_{i=1}^n x_{ii} - \sum_{i=1}^n (x_{i+} \times x_{+i})}{N^2 - \sum_{i=1}^n (x_{i+} \times x_{+i})} \quad (3)$$

Where N is the total number of observations in the entire error matrix, n is the number of rows, x_{ii} is the number of points correctly classified for a specific land use category, x_{i+} and x_{+i} are marginal sums for row and column i associated with the category (Bishop *et al.*, 1975).

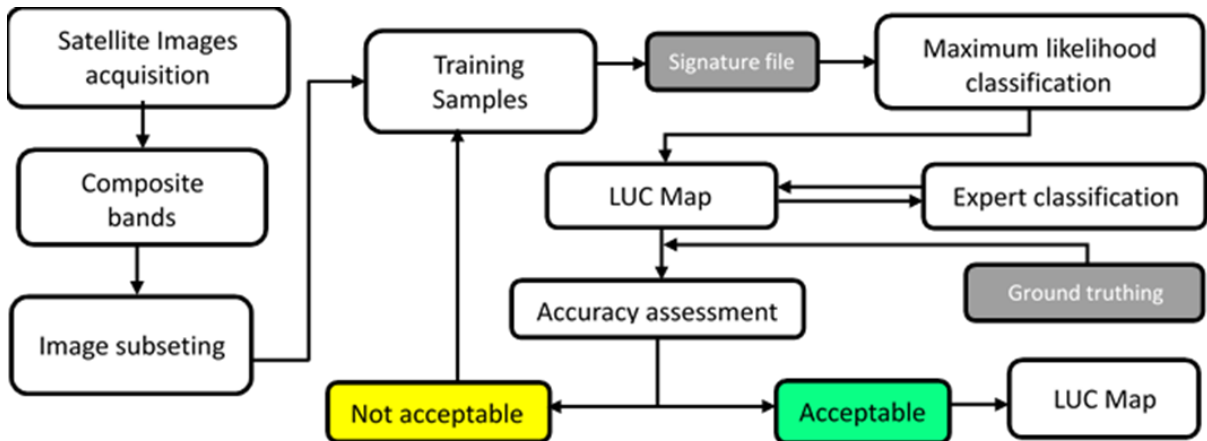


Figure 4: Image classification and accuracy assessment workflow

3.2.3 Data Preparation and Future Land-Use and Land-Cover Projection

(i) Criteria Development and Generation of Land-Use Suitability Maps

The factors involved in the simulation of land-use change were identified by Barredo *et al.* (2003). A factor is a criterion that influences the suitability of a specific land cover in a specific location. The values of the factors differ, but land use cover change forecasts are typically stretched from 0-255 (Musa *et al.*, 2018). Environmental factors, that is, constrained areas, local-scale neighbourhoods, that is, one land use influenced by another, and spatial characteristics of towns, that is, distance and access to the city centre, are the five categories of factors. Other factors include land-use zoning status, urban planning regulations, and factors related to individual interests, social-economic development, and political systems, such as population growth trends. These variables were evaluated in order to monitor their behavior in the study area; however, the current model does not account for potential changes in urban plans and policies.

Since they drive the spatial patterns of the simulations, land-use class suitability maps are important and play a central role in CA-Markov modeling. Suitability images are used to determine the suitability of each cell for a specific land cover. As a result, much like the other phases in modeling, their training necessitates detailed awareness and technique (Tattoni *et al.*, 2011). Suitability maps were created in this study using factors and constraints gathered from field surveys in the study area. For each land-use class, factors and constraints were created (Table 4).

Table 4: The criteria used in the preparation of suitability maps

LULC suitability class	Factors	Membership function	Membership function shape	Control points	Constraints
Built-up area	Distance from built-up area	MD	J shaped	c = 200, d =Maximum	Existing water surfaces, river course(60 m buffer), protected areas
	Distance from the road	MD	Linear	a = 1, b =6800	
	Slope	MD	Linear	c= 0.1, d =35	
	Elevation	MD	Linear	c= 600, d =1900	
	Distance from the river	MI	S shaped	a = 60, b =11 000	
Agriculture land	Slope	MD	Linear	c= 0.1, d =20	River course (60 m buffer), existing built-up area, existing road network, existing protected area
	Distance From built-up area	Symmetric	Linear	a = 50, b =500, c= 4000, d =7500	
	Elevation	Symmetric	Linear	a = 300, b =1000, c= 1200, d = 1700	
	Population	MD	Linear	c= 12300, d =16 000	
	Distance from the river	MI	Linear	a = 60, b =10 000	
Water	Existing water network (Boolean)	No fuzzy	-	-	River course network
Forest	Distance from the road network	MI	Linear	a = 100, b =10 000	Existing agriculture land, road network, existing buildup area
	Slope	Symmetric	Linear	a = 10, b =30, c= 40, d =68	
	Elevation	Symmetric	Linear	a = 1700, b =2300, c= 2300, d =3200	
	Annual rain	MI	Linear	a = 600, b =1000	
	Slope	MD	J shaped	a= 10, b =30	
Barren land	Distance from Built-up area	Symmetric	Linear	a = 20, b =40, c= 40, d =5500	River course network, road network, existing built-up area
	Elevation	Symmetric	S shaped	a= 700, b =800, c= 800, d =1000	
	Annual rain	MD	Linear	c= 400, d =1200	
	Soil types	Do not fuzzy	-	-	
	Distance from the road	MI	J shaped	a= 30, b =maximum	
Grassland	Slope	MD	Linear	c= 0.3, d =30	Existing built-up area, river course network.
	Elevation	MD	J shaped	c= 800, d =1100	
	Population	MD	Linear	c = 4000, d =26 000	
	Elevation	MD	S shaped	c = 400, d =980	
	Slope	MD	Linear	c = 0, d =2	
Shrubland	Distance from the road	MI	S shaped	a = 50, b =maximum	River course network, road network, existing built-up area
	Distance from built-up area	MI	Linear	a = 1000, b = 13 000	
	Elevation	Symmetric	S-Shaped	a = 2000, b =3500, c= 3500, d =3700	
Rocky surface	Elevation	Symmetric	Linear	a = 3800, b = 4300, c= 4300, d =5800	Existing shrub land, existing forest

LULC suitability class	Factors	Membership function	Membership function shape	Control points	Constraints
Glacier ice	Elevation	MI	J shaped	a = 3800, b = maximum	Existing shrub land, existing forest, existing built-up area

MI-Monotonically increasing; MD- Monotonically decreasing

The approach used to prepare the factors and constraints has been well outlined by Hyandye and Martz (2017). To arrive at the person assessment index (suitability maps), the Multi-Criteria Evaluation (MCE) function was used to combine information from different criteria (El-Hallaq & Habboub, 2014).

Factor maps were generated in ArcGIS v.10.6 and then imported into IDRISI Selva v.17 for further processing. In Idrisi Selva, all constraint maps were generated by editing the existing values in the feature class(es) and setting the targeted constraint of the feature class to zero. Tanzania National Roads Agency, Pangani Basin Water Office (PBWO), classified satellite photos, and Tanzania National Parks GIS unit provided vector layers of proximity to highways and waters, accessibility to existing settlements, and forest reserves, respectively. Before importing the DEM data into Idrisi Selva, the slope map was generated in ArcGIS. The Tanzania Meteorological Agency (TMA) provided annual precipitation records for the stations in the study region, while soil types were created using soil data from PBWO. The population density map was generated using the formula in Equation 4 and population figures projected from the 2012 National Population Census.

$$N_t = Pe^{rt} \quad (4)$$

Where N_t is the population at a future date, P is the current population, e is the natural logarithm base of 2.71828, r is the rate of increase divided by 100, and t is the time.

In ArcGIS, all vector files were rasterized and imported into the IDRISI Selva software. Factor maps were standardized and given a continuous suitability scale from 0 to 255, with 0 representing unsuitable sites and 255 representing the most suitable sites, using a decision support tool in IDRISI Selva Software.

This was accomplished by employing various fuzzy memberships and control points (Table 4). There are no medium values in constraint maps since they apply to the restricted areas for growth. The values are either 0 (inappropriate) or 1 (appropriate) (Eastman, 2012). In these characters, the constraints were allocated as Boolean images characters of 0 and 1, with 0 indicating areas not suitable for future development and 1 indicating area suitable for future development. The control points were used to assess a pixel's degree of membership in a factors layer; they were chosen based on the relationship between a factor and urban development (Eastman, 2012).

In this analysis, Sigmoidal, J-shaped, and Linear membership functions were used as fuzzy membership functions. These shapes typically determine the shape and pattern (decreasing, increasing, or symmetric) (Eastman, 2012; Eastman, 2009). When the factor value rises and the suitability of a specific land cover rises, the pattern is said to be 'monotonically increasing'. When the value of the factor rises and the suitability of a specific land cover class falls, it is said to be 'monotonically decreasing'. As the value of the factor increases, the suitability of a given land cover class increases from a given point reaches maximum suitability at a given point and then starts to decrease; it is said to be 'symmetric'.

Suitability maps (Fig. 6) were created using standardized factors and constraints for each land cover group. Using the Analytical Hierarchy Process (AHP) and pairwise comparisons, weights were allocated to each factor to show their relative importance. Other methods can be customized or equal weights (Eastman, 2012). Each factor's importance was determined by assigning values ranging from 1/9 (less significant) to 9 (extremely important). The final weights of each factor were then calculated using the principal eigenvector. The pairwise matrix was evaluated using a consistency threshold of less than 0.10, with everything above the threshold requiring re-evaluation (Lin *et al.*, 2014).

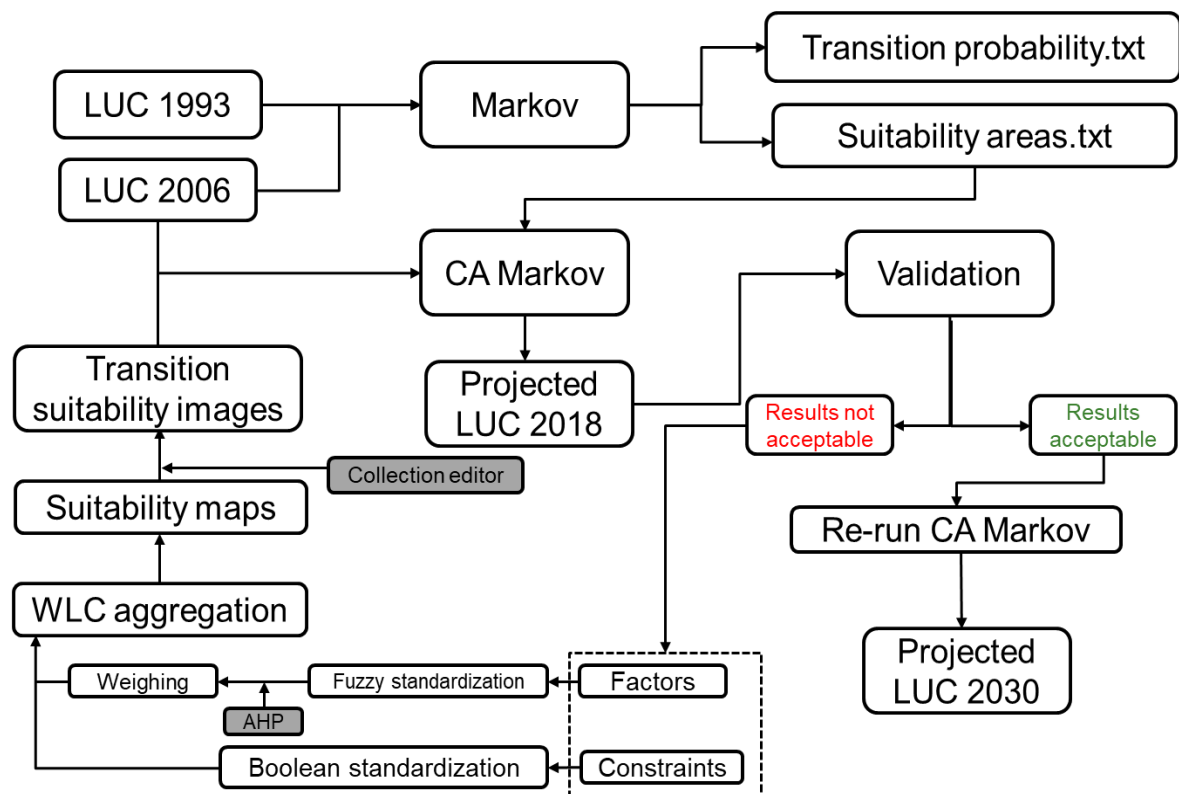


Figure 5: A summary of the procedures used to simulate land-use and land-cover map of the year 2030

The MCE module was used to combine all the factor layers to create the suitability maps for each land-cover class (Fig. 6). In this study, Weighted Linear Combination (WLC) was used (Fig. 5). The WLC (Weighted Linear Combination) was used in this analysis (Fig. 5). The WLC uses linear features to overlay standardized factors based on their significance weight of importance, where total factor weights equal one (Eastman, 2012).

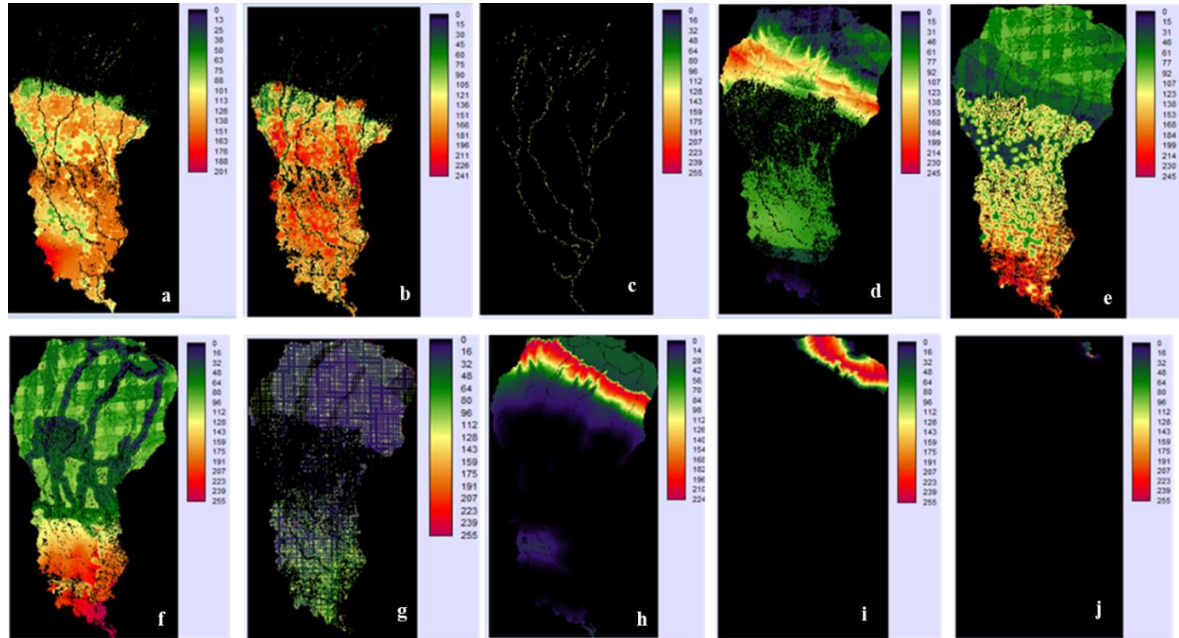


Figure 6: Land use/cover classes suitability maps for Built-up area (a), Agricultural land (b), Water (c), Forest (d), Barrenland (e), Grassland (f), Wetland (g), Shrubland (h), Rocky surface (i), Glacier ice (j)

(ii) Future Land Use/Cover Changes Prediction and the Relationship with Crop Production in the Kikafu, Weruweru and Karanga Watershed

A Markov model was run using the 1993 land cover image (t-1) and the 2006 land cover image (t=1), which produced two files: Transition probability and transition areas. The transition probability indicates the likelihood that a pixel will change land use/cover in the future (or remain constant). A transition area matrix, on the other hand, displays a total area with the probability of changing the next time (Eastman, 2012). Table 5 displays the 1993 (t-1) categories in rows, with the 2006 (t=1) categories in the column. The CA-Markov model was run using a 5 x 5 contiguity filter using the Markov model outputs together with the suitability maps. The simulated map for the year 2030 is the model's production.

The validation of models is an essential part of the modeling process (Memarian *et al.*, 2012). The kappa coefficient and Cramer's V are two of the several methods for conducting model validation that is available in the literature (Baysal, 2013). Among the available validation,

methods are quantity and distribution disagreements (Brown *et al.*, 2013), chi-square, and F-test of observed and simulated images (Katana *et al.*, 2013), as well as relative operating characteristics (ROC) (Pontius & Schneider, 2001). The Validate feature embedded in IDRISI selva software was used to investigate quantity and allocation disagreements in this analysis. The simulated and observed land cover maps had a kappa coefficient of 0.61 or higher, which was considered sufficient agreement (Eastman, 2012). After reaching the minimum kappa coefficient, the model was deemed suitable for further processing and was used to simulate the future land cover map of 2030. According to Eastman (2012) this approach involves using statistical algorithms to analyze both the degree of agreement in quantity and the position of cells between the simulated and observed land cover maps.

Integrating model results with agriculture production for the selected staple food crops is critical in determining the viability of expanding cultivated land for production. Because of the high fragmentation and complexity of the farming system practiced in the study field, secondary data were used to divide agricultural land into LULC for each of the selected crops. These figures were obtained from the Kilimanjaro region's agriculture division, which produced estimates of cultivated land and crop yields for each crop. Thus, the crop production and agricultural land were linked from the model performance by computing the proportion of land size for each crop from the known proportion of arable land from the Kilimanjaro region's agriculture department's long-term records of agricultural production.

3.3 To assess the Impacts of the Present and Future Land Use/Cover Changes on the Water Budget of Mount Kilimanjaro Slopes

The main targets of this objective were, therefore, three folds, namely: To set-up, parameterize and calibrate the SWAT model in terms of streamflow. Further, to investigate the impact of land use/cover changes on the streamflow and establish the impact of the individual land use/cover type on the streamflow using partial least square regression modelling.

The approach in this study employed both the historical and the near future (2030) land-use change analysis (from section 3.3). Several studies suggest that there might be potential impacts of land-use changes on the hydrology of Mt. Kilimanjaro that is of limited knowledge. Thus, with a high population rate in the KWK watershed, it was worth to analyze these impacts. This study is an integrative work done in a GIS environment and statistical

analysis at a watershed scale. Field surveys and the interviews (not shown here) were also done to acquire community information on water demand, withdrawal and crop management. Where necessary, precise locations of some of the features were determined using a hand-held Garmin global positioning system (GPS) for further analysis. The ArcSWAT embedded in ArcGIS version 10.5 was used to build the model, and calibration was done in SWAT Calibration and Uncertainty Procedures (SWAT CUP). The PLSR was done using the statistical package for social science (SPSS) version 21 and XLSTAT add-in tool.

3.3.1 Input Data Collection and Processing

The Model inputs required to run SWAT include the Digital Elevation Model (DEM), land use, soil, and weather data. The Arc GIS interface of the SWAT model was used to discretize the catchment area and extract the input files to be used in SWAT12. All data types are summarized in Table 5.

(i) Digital Elevation Model

The 30 m resolution topography data used for this study was obtained from the Shuttle Radar Topography Mission (SRTM) accessed freely from the USGS database at <https://earthexplorer.usgs>. The DEM was used to delineate the watershed, generate a stream network, and provide topographical parameters, such as overland slope and slope length for each catchment of the basin. Burning of the digitized stream network from the Google earth interface was opted to eliminate errors due to DEM. In this option, the stream network was overlaid onto DEM to force alignment of the stream to follow the specific path. This was done to resolve discrepancies in the topographic and hydrographic data.

(ii) Land Use/Land Cover

Land use/cover is another vital segment of data that is essential for hydrological simulation of the basin. The land use maps for the years 1993, 2006, and 2018 were classified from satellite images. Further, the near future (2030) land use map was predicted using the Markov Chain, and Cellular Automata (CA) models embedded in Idrisi Selva; this procedure is detailed in Said *et al.* (2021). These maps were independently used to simulate the hydrological impacts of land-use changes at the watershed scale. The SWAT codes were given for all land use classes in order to meet the SWAT model requirement of four digits land-use codes.

(iii) Soil Type and Characteristics

Soil data is essential for hydrological simulations with SWAT. Soil physical and chemical properties (texture, organic carbon, bulk density, soil available water content, hydraulic conductivity and bulk density) in soil layers help as determining factors for surface runoff (Gashaw *et al.*, 2018). Harmonized World Soil Database v 1.21 Soil data was freely accessed online through http://www.waterbase.org/download_data.html, the FAO Harmonized global soils database website. The soil data from the FAO soil database of the African soils slice was extracted using the watershed boundary. Due to the fact that the ArcSWAT12 soil database's "user soil" table only includes USA soils, the attributes of these soils in Fig. 7 were modified using a "user soil" table from the MapWindow SWAT12 database. The lookup table contains files that link soil map and soil database in SWAT as described by Abbaspour *et al.* (2019).

(iv) Weather Data

Precipitation data was obtained from the four ground-based weather stations (Kilimanjaro International airport (KIA), Lyamungu, Moshi Airport, and Kibosho Mission); these were combined with the Climate Forecast System Reanalysis (CFSR) global weather data for SWAT. The KIA is slightly out of the watershed; but, it contains good quality and is located in influential area data that necessitated its inclusion in this study. The Tanzania Meteorological Authority provided the ground-based gauging station data, whereas the CFSR weather data were freely accessed from <http://globalweather.tamu.edu/>. The use of the CFSR data was due to the unavailability of some parameters (wind speed, solar radiation, and relative humidity) in the three stations which are within the watershed. The CFSR data often captures the rainfall pattern very well; however, it often overestimates the gauged rainfall (Worqlul *et al.*, 2017). Hence, Kilimanjaro and Lyamungu stations were used to perform bias correction of the CFSR precipitation data. The CFSR of the National Centres for Environmental Prediction (NCEP) provides ready to use weather data with a good resolution between 1979 and 2014 (Roth & Lemann, 2016). The bias of the CFSR data was corrected by a linear bias correction approach which is well described by Worqlul *et al.* (2017). This approach reduces the volume difference between CFSR and gauged rainfall data while keeping the pattern. The two datasets (uncorrected CFSR and gauged rainfall data) involved in the linear bias correction process covered the same time window (1979–2014). The annual volume difference between the observed and bias-corrected data was minimized to zero. The

collected data were added to the SWAT weather database table (User-made). The stations are as observed in Fig. 1.

(v) Discharge Data

The discharge data for model calibration and validation period with varying time length ranging from 1979 to 2018 for Kikafu, Weruweru and Karanga rivers at their gauging station were obtained from the Pangani Basin Water Office. Data cleaning revealed two anomalies; the data discontinuity (gaps) which might be due to inadequate gauge reading and or records keeping and abnormally high discharge values. The abnormal high discharge values were deleted during data cleaning, and gap-filling was done using the simple interpolation and linear regression methods (Koch & Cherie, 2013). However, calibration was only done at one station in the outlet due to data quality issues. The data types and the sources are summarized in Table 5.

Table 5: Description of data types and sources

Data type	Description	Resolution	Source
Topography map	Digital Elevation Model	30*30 m	ALASKA satellite facility
Land use	Land use maps	30*30 m	Classified image
Soil Map	Soil types		https://www.2w2e.com/home/GlobalSoil
Weather data	Daily precipitation	6 stations	Tanzania Meteorological Agency (TMA)
Weather data	Max and Min air temp	6 stations	Global weather data for SWAT
Weather data	Relative humidity	6 stations	Global weather data for SWAT
Weather data	Solar radiation	6 stations	Global weather data for SWAT
Hydrometric	Daily streamflow	4 stations	Pangani Basin Water Office (PBWO)

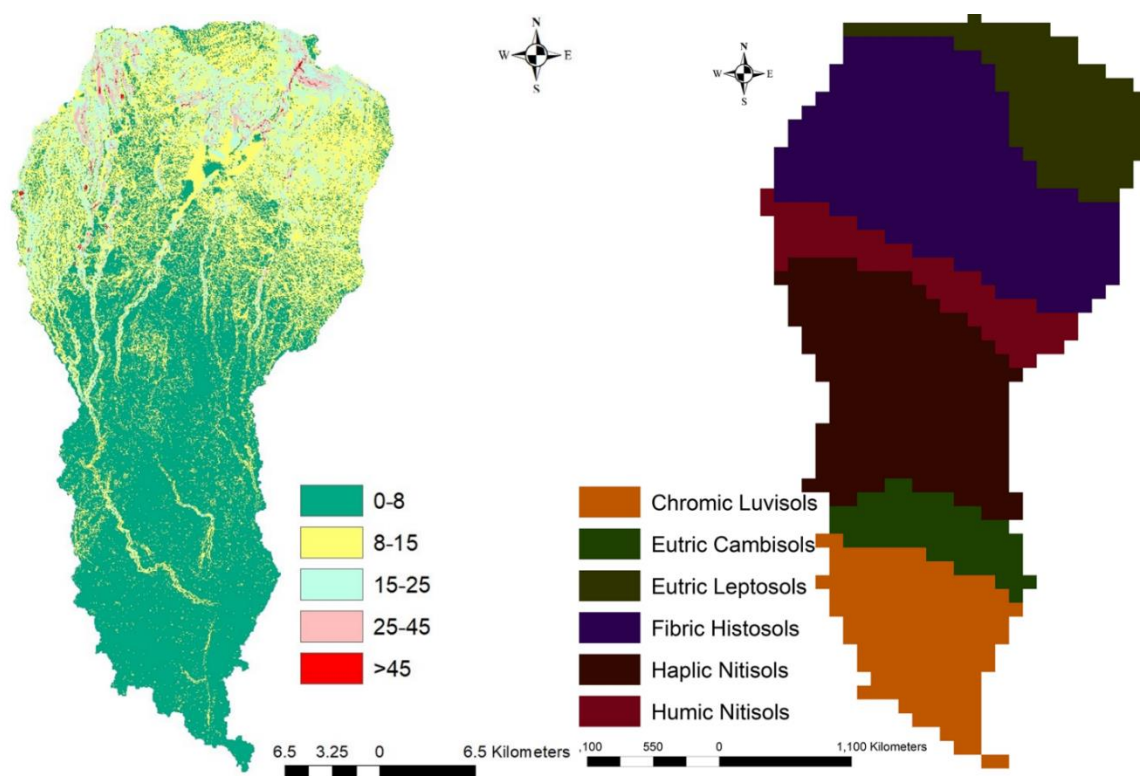


Figure 7: Slope and soil maps

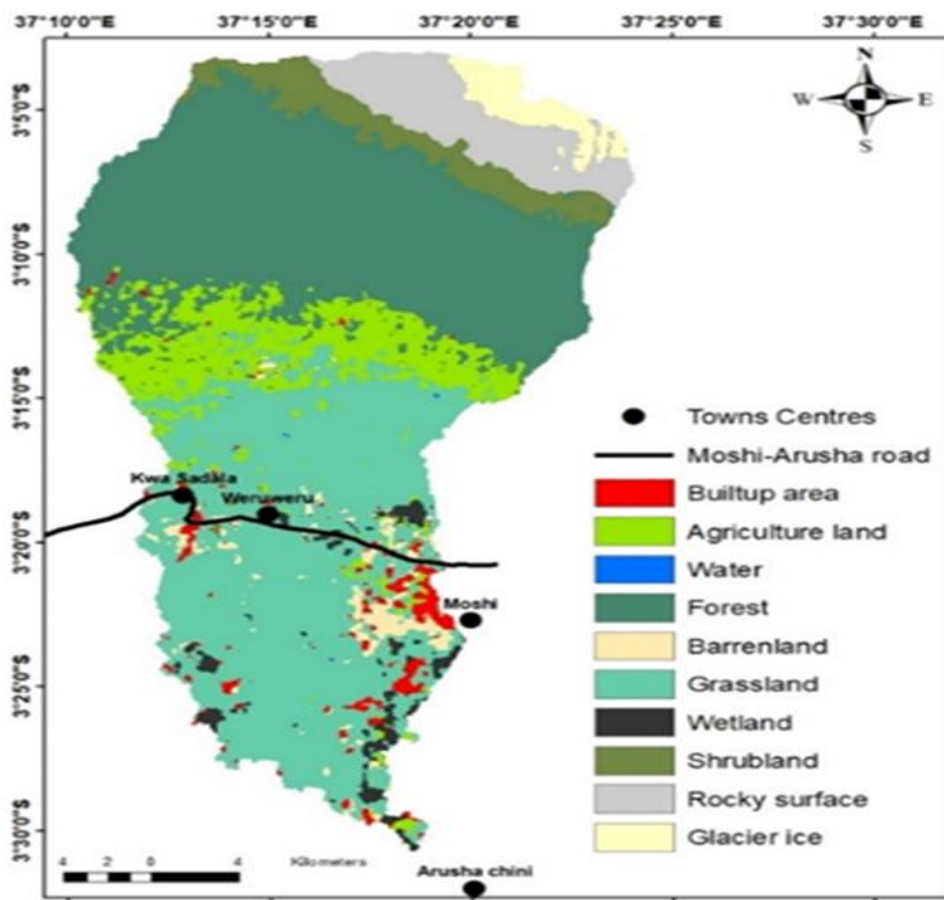


Figure 8: Land use map for the year 2006

3.3.2 Model Set-up and Parameterization

A total of 33 sub-basins and 532 Hydrologic Response Units (HRU) were delineated. The HRU are the areas with a combination of unique soil, slope and land use. This unique combination helps to account for differences in evapotranspiration and other hydrological conditions with different land covers, soils and slopes (Setegn *et al.*, 2008). The model was edited to include management activities such as cropping season in the watershed area, especially in agricultural land. The Digitized stream network was extracted from the topographic data; this network was used to construct a hydrographical network and discretize the sub-basins. Land-use maps were prepared and classified into ten (10) categories, whereas soil map comprised six categories. The slope map was reclassified into five categories, i.e. <0-8%, 8–15%, 15-25%, 25-45% and >45%. Runoff is the most important factor for management in the whole catchment since the catchment falls under mountains area with higher runoff, especially in the pick rain seasons. Estimation of the potential evapotranspiration was done using the Hargreaves method, while the runoff was estimated using the curve number method.

3.3.3 Calibration and Validation of the Soil and Water Assessment Tool Model

The SWAT model calibration and uncertainty procedure (SWAT-CUP) (Abbaspour, 2011) was used for calibration of the model. Model calibration and sensitivity analysis were done at the outlet due to data quality issues. Simulations that were set up using the 2006 LULC map were used to calibrate monthly and daily streamflow from 1987 to 1993. After calibration, the simulations that were set up using the same LULC map were used to validate the monthly and daily streamflow from 1994 to 2000. Sensitivity analysis was carried out in SWAT CUP, 22 flow parameters were used, and the model was run for 1000 iterations. The significance of sensitivity was determined using t-stat and p-value (Chanapathi *et al.*, 2018). The higher the absolute t-stat values among the parameters and the smaller p-values, the higher the sensitivity, usually close to 0; and 0.05 acceptable (Abbaspour, 2015). The t-stat is used to identify the relative significance of the parameter, whereas the p-value is used to ascertain the sensitivity significance (Chanapathi *et al.*, 2018). After automatic calibration using SWAT CUP, the final calibrated model was attained by multiplying, adding, or subtracting the default values by a factor guided by a manual calibration helper.

Generally, the calibration process was based on varying the hydrological parameters iteratively. The simulated and observed streamflow agreement was used as a decision tool for the final parameter variation. The model performance was evaluated comparatively using the streamflow hydrograph for simulated and observed streamflow for both calibration and validation periods. Statistical evaluation of the model was done using per cent bias (PBIAS), Coefficient of determination (R^2), the Nash and Sutcliffe simulation efficiency (NS) as shown in Equation 5, 6, and 7. The root means square error (RMSE)-observations standard deviation ratio (RSR). The R^2 is a measure of the extent of uniformity between observed and simulated data, R^2 ranges from 0 to 1, with higher values indicating high suitability; however, values higher than 0.5 are considered acceptable for simulation (Van Liew *et al.*, 2003). The NS show the extent that observed and simulated data fit each other (Nash and Sutcliffe, 1970), where $NSE = 1$ is the best value. Per cent bias (PBIAS) measures the average tendency of the simulated data to be larger or smaller than their observed values for a given quantity over the calibration or validation period; the value becomes the best as it comes to zero. The RMSE-observations standard deviation ratio (RSR): Standardizes RMSE using the observations standard deviation; generally, the best simulation performance is considered to have relatively lower RSR and hence lower RMSE. The details of model evaluation can be found in Moriasi *et al.* (2007).

$$NSE = 1 - \frac{\sum_{i=1}^n (O_i - P_i)^2}{\sum_{i=1}^n (O_i - O')^2} \quad (5)$$

$$R^2 = \left\{ \frac{\left(\sum_{i=1}^n (O_i - O')(P_i - P') \right)^2}{\sum_{i=1}^n (O_i - O')^2 \sum_{i=1}^n (P_i - P')^2} \right\} \quad (6)$$

$$PBIAS = \frac{\sum_{i=1}^n (O_i - P_i)}{\sum_{i=1}^n O_i} \times 100 \quad (7)$$

Where, n is the number of measured/observed data; O_i and p_i are measured and predicted data at the time i , respectively; O' and P' are the mean of observed and predicted data, respectively. More near the value of NSE and R^2 to 1, the better the model performance. The NSE lies between $-\infty$ and 1, with more positive values indicates very good agreement between observed and simulated values. Also, co-linearity between simulated and observed values was interpreted using R^2 , the range is from -1 to 1. The higher the value indicates better performance. The PBIAS positive value indicates an underestimation of bias and the negative value indicates an overestimation of bias (Abbaspour, 2015).

3.3.4 Streamflow Validation

The calibrated flow parameters were used to check the model capacity to simulate measured streamflow results. The streamflow validation of the model was done using a new streamflow dataset without any adjustment in the calibrated flow parameters. Evaluation of the Model performance was done using PBIAS, R^2 , and ENS, respectively.

In this study, PLSR modelling was used to determine the association between the simulated hydrological components and land use/cover classes. The predictors are the land-use classes, while the response function is meant to be the annual hydrological components. The PLSR is one of the robust multivariate regression methods, especially when there are collinear predictors, high correlated predictors, numerous predictors equal to or higher than observations and many independent variables (Shi *et al.*, 2013). Thus, the predictors in this work are land-use classes, whereas the response function was annual hydrological components. Land use/cover types are colinear when the fraction of one type increases, the fraction of one or more land use/cover types will also be affected (King *et al.*, 2005). These analyses were done using the statistical package for social science (SPSS) version 21 and the XLSTAT add-in tool (Huisman *et al.*, 2009).

3.3.5 Model Application for Scenarios Simulation

The impacts of LU changes on the hydrological variability was based on historical LU inputs for the years 1993, 2006 and 2018; the future LU scenario analysis was done using the LU map for the year 2030. The calibrated and validated SWAT model was used to perform these analyses. The impacts of land management practices at Scenario analysis concerning LC change is essential to understand the effect of land management practices at the basin and

subbasins scale; these practices increase the impact of hydrologic variability on the society and ecosystem (Shawul *et al.*, 2019). The analysis of LC changes on the water balance of a watershed was done using both temporal and spatial variation of land-use scenarios. In introducing the scenarios in the SWAT model, the land use/cover maps were varied (1993, 2006, 2018, and 2030), simulations were done for each land use/cover and the results were recorded. Where comparison was necessary, the changes in water balance components were done using consecutively two land cover maps and the corresponding simulated water balance components.

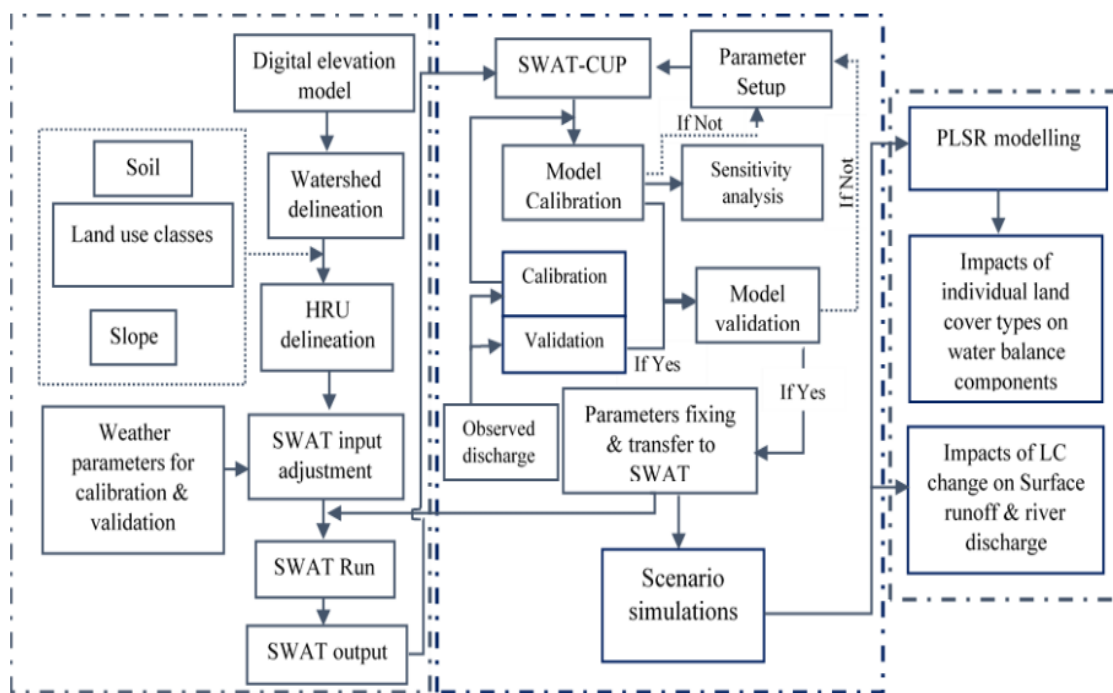


Figure 9: Conceptual diagram for application of soil and water assessment tool model in assessing impacts of land cover on the hydrology of Kikafu, Weruweru and Karanga watershed

3.4 To Assess the Impact of Past, Present, and Future Climate Changes on the Water Budget (Surface and Groundwater) of the Mount Kilimanjaro Slopes

3.4.1 Climate Data from the Coordinated Regional Climate Downscaling Experiment Regional Climate Models

This objective has three targets: (a) to assess how precipitation and temperature (maximum and minimum) have changed in the past 30 years, (b) to assess how precipitation and temperature will change in the future period, and (c) to assess the implication of the changes in precipitation and temperature (maximum and minimum) on the hydrology of the KWK

watershed. Specifically, it has the following objectives: (a) evaluate the historical runs of two RCMs–GCMs at the catchment scale; (b) analyze the climate change signal for the future period of 2021–2100 compared to the reference period of 1979–2005; (c) evaluate the ability of the climate models to reproduce the historical discharge; and (d) assess the impacts of climate change on the hydrology of the KWK watershed by the middle of the 21st century.

Two regional climate models in the Coordinated Regional Climate Downscaling Experiment (CORDEX) database were used to generate rainfall simulation data. The online repository <http://cordexesg.dmi.dk/esgf-web-fe/> was used to access the data. The CORDEX RCM outputs are quality checked and should be used in accordance with the terms of use (<http://wcrp-cordex.ipsl.jussieu.fr/>). Monthly rainfall data were extracted from two CORDEX RCMs stated in Table 6 over a 35-year period (1971-2005).

The choice of regional climate models was based on their ability to simulate the historical (1971-2005) climate condition in most regions over Tanzania with relatively minimum error (Luhunga *et al.*, 2016). According to the evaluation by Luhunga *et al.* (2016) RACMO2T driven by Irish Centre for High-End Computing (ICHEC) show better rainfall simulation results in most of the unimodal and bimodal regions as compared to other RCMs regardless of the driving GCM. The study further recommends that CCLM4 and RCA4 RCMs driven by MPI, CNRM and ICHEC GCMs can be used to simulate temperature over most stations in Tanzania. The choice of these models is due to relatively similar errors among the evaluated models. Details of the regional climate models and their driving general circulation models are described in Nikulin *et al.* (2012). Thus, in this study, CCLM4 and RACMO CORDEX RCMs and their driving GCMs written in short forms as (CNRM) for the CNRM-CERFACS-CNRM-CM5, and (ICHEC) for the ICHEC-EARTH respectively were used (Table 6). The RACMO22T Regional Climate Model from the Coordinated Regional Climate Downscaling Experiment (CORDEX-RCM) was retrieved from the Royal Netherlands Meteorological Institute (KNMI) node, whereas CCLM4 was retrieved from Climate Limited-Area Modelling (CLM) Community node.

Two-time slices were chosen to attain these targets, with the historical period spanning from 1970-2005 while the future period spans from 2020-2100. Moreover, “all regional climate models use a similar domain and spatial resolution of 0.44° by 0.44° which correspond to approximately 50 km by 50 km, and are driven by the European Centre for Medium-Range Weather Forecasts Interim Re-Analysis (ERA-Interim from 1989 to 2008) as lateral

boundary conditions” (Nikulin *et al.*, 2012). Simulations were run under the Representative Concentration Pathway (RCP) 4.5 (intermediate emissions) and RCP 8.5 (business as usual). The selection of the two RCP was based on the realization that the differences in outcomes between the RCPs are often minimal until mid-century. The climate system responds relatively slowly to changes in greenhouse gas concentration. So the choice of RCP is not essential until midcentury. For analyses after mid-century, it is essential to distinguish between different RCPs. The RCP8.5 gives a much more rapid warming and more pronounced changes in important indicators such as river flow, water temperature and precipitation. The nature of the study area did not favour the use of RCP 2.6, although its difference with 4.5 remains relatively small until the end of the century. Thus RCP 4.5 and 8.5 were analysed to produce a more pronounced view of the changes to the selected water balance components. The RCP is labelled after a possible range of radiative forcing value in the year 2100 relative to pre-industrial values.

Table 6: Coordinated regional climate downscaling experiment regional climate modelling used in the study

No.	RCM	Model Centre	Short Name of RCM	GCM
1	RACMO22T	Royal Netherlands Meteorological Institute (KNMI)	RACMO22T	ICHEC
2	COSMO-CLM (CCLM4)	Climate Limited-Area Modelling (CLM) Community	CCLM4	CNRM

Bias correction of the RACMO22T and CCLM4 simulations under RCP 4.5 and RCP 8.5 were performed by using Climate Model for hydrological modeling (CMhyd) software. Moreover, bias correction requires daily precipitation and temperature (maximum and minimum), which were acquired from Tanzania Meteorological Authority (TMA) (Table. 7). The information in Table 7 assisted in the creation of the location files (for precipitation and temperature) that were loaded into the CMhyd software during bias correction. The choice of these stations was based on the availability of long-time data and altitudinal spatial distribution.

Table 7: Daily weather data used in the study area

Station code	Name	Lat	Long	Elevation (m)	Period	Source
9337004	Moshi	-3.35	37.33	813	2004-2009	TMA
9337005	Kibosho	-3.25	37.32	1478	1979-2014	TMA

The Coordinated Regional Climate Downscaling Experiment (CORDEX) program, founded by the World Climate Research Program, provides high-resolution regional climate projections. These projections can be used to evaluate future climate change impacts at the regional level (Giorgi *et al.*, 2009). However, RCMs has to be bias-corrected before they are used for generating downscaled projections of the future climate.

3.4.2 Bias Correction

Bias correction in climate change modeling reduces problems associated with Regional Climate model outputs such as under or overestimation of rainfall, maximum and minimum temperatures (Christensen *et al.*, 2008). Thus, bias correction methods assist the adjustment of simulated temperature and precipitation in the RCM. The corrected biases may develop due to systematic model errors resulting from imperfect conceptualization, discretization and spatial averaging within grid cells (Teutschbein & Seibert, 2012). Furthermore, bias correction was performed through a specific algorithm that is specific for each climate variable (i.e. precipitation and temperature) as described in equation 8 and 9. In this study, linear scaling (multiplicative) and linear scaling (additive) method were adopted for bias correction of precipitation and temperature (maximum and minimum), respectively.

3.4.3 Linear Scaling for Precipitation

Linear scaling for precipitation uses monthly correction values resulting from the differences between observed and present-day simulated values. The ratio is calculated from long term observed monthly mean precipitation and that of RCM simulations (control run data) (Zhang *et al.*, 2018). The corrected RCM simulations should perfectly agree in their monthly mean values with the observations (Teutschbein & Seibert, 2012). Equations 8 were used to perform linear scaling for precipitation.

$$\left. \begin{aligned} P_{con,cor(d)} &= P_{con(d)} * \left(\frac{P_{obs(m)}}{P_{con(m)}} \right) \\ P_{sec,cor(d)} &= P_{sec(d)} * \left(\frac{P_{obs(m)}}{P_{con(m)}} \right) \end{aligned} \right\} \quad (8)$$

Where,

$P_{con, cor(d)}$ = Corrected daily rainfall in the corresponding month during the control period.

$P_{sec, cor(d)}$ is the same as $T_{con, cor(d)}$ during the future period.

$P_{con(d)}$ =Uncorrected daily rainfall in the corresponding month during the control period.

$P_{sec(d)}$ is the same as $P_{con(d)}$ during the future period.

$P_{obs(m)}$ = Observed monthly mean rainfall in the corresponding month during the control period.

$P_{con(m)}$ = Simulated monthly mean rainfall in the corresponding month during the future period.

3.4.4 Linear Scaling for Temperature

Bias correction for temperatures was achieved with an additive term, which represents the difference between long-term monthly mean observed temperature and control run data (Teutschbein & Seibert, 2012). The factors applied are supposed to remain the same even for future conditions (i.e. stationarity). Equation 9 was used to perform linear scaling for temperature.

$$\left. \begin{aligned} T_{con,cor(d)} &= T_{con(d)} + (T_{obs(m)} - T_{con(m)}) \\ T_{sec,cor(d)} &= T_{sec(d)} + (T_{obs(m)} - T_{con(m)}) \end{aligned} \right\} \quad (9)$$

Where,

$T_{con, cor(d)}$ = Corrected daily temperature in the corresponding month during the control period.

$T_{sec, cor(d)}$ =Same as $T_{con, cor(d)}$ during the future period.

$T_{con(d)}$ = Uncorrected daily temperature in the corresponding month during the control period.

$T_{sec(d)}$ = Same as $T_{con(d)}$ during the future period.

$T_{obs(m)}$ = The observed monthly mean temperature in the corresponding month during the control period.

$T_{con(m)}$ = The simulated monthly mean temperature in the corresponding month during the future period.

3.4.5 Trend Analysis

Trend analysis was performed using a non-parametric test, the Mann-Kendall trend test (Rodrigo & Trigo, 2007). This rank-based procedure is widely used to assess the influence of the outliers and extreme values. In this test:

The null hypothesis H_0 is that there is no trend in the data, is tested against.

The alternate hypothesis H_1 is that there is a trend in the data.

Thus, the alternate hypothesis assumes that the data are independent and identically randomly distributed. The Mann Kendall is estimated using a time series of n data points and two subsets of data, x_i , and x_j , where $i=1, 2, 3, \dots, n-1$ and $j=i+1, i+2, i+3, \dots, n$. As an ordered time sequence, the values were evaluated. Each data value is compared to all subsequent data values, and the statistic K is increased by one if a data value from a later time period is higher than a data value from an earlier time period. Similarly, if a later period's data value is lower than an earlier period's data value, K is decremented by 1. The final value of K is the sum of all such increments and decrements. Equation (10) is used to calculate the Mann-Kendall K Statistic, and the test is calculated using Equation (11):

$$K = \sum_{n=1}^{n-1} \sum_{j=i+1}^n \text{sgn}(x_j - x_i) \quad (10)$$

$$\text{sgn}(x_j - x_i) = \begin{cases} +1 & \text{if } (x_j - x_i) > 0 \\ 0 & \text{if } (x_j - x_i) = 0 \\ -1 & \text{if } (x_j - x_i) < 0 \end{cases} \quad (11)$$

where x_i , and x_j are annual values in years i and j , are the annual values in years i and j , $j > i$ respectively. When the sample size n is less than 10, the value of K , is compared directly to the theoretical distribution of K derived by Mann and Kendall (calculated using Equations

(10) and (11)) and is asymptotically normal (Hirsch & Slack, 1984). The two-sided test is used, at certain probability level, H_0 is rejected in favour of H_1 if the absolute value of K equals or exceeds a specified value $K\alpha/2$, where $K\alpha/2$ is the smallest K which has the probability less than $\alpha/2$ to appear in case of no trend. A positive value of K designates an “increasing trend”; likewise, a negative designates decreasing trend. For $n \geq 10$ the statistic K is approximately normally distributed with the mean and variance as follows:

$E(K) = 0$; the variance δ^2 , for the K statistic, is defined as follows:

$$Var(K) = \left(\frac{n(n-1)(2n+5) - \sum_i t_i(i-1)(2i+5)}{18} \right) \quad (12)$$

Where t_i is the number of ties to the extent i . The summation term in the numerator is used only if the data series contains tied values. The standard test statistic Z_k is calculated as follows:

$$Z = \begin{cases} \frac{K-1}{\sqrt{Var(K)}} & \text{if } K > 0 \\ 0 & \text{if } K = 0 \\ \frac{K+1}{\sqrt{Var(K)}} & \text{if } K < 0 \end{cases} \quad (13)$$

The test statistic Z is used as a measure of the significance of trends. In fact, this test statistic is used to test the null hypothesis, H_0 . If Z_k is greater than $Z\alpha/2$, where α represents the chosen significance level (e.g. 5% with $Z 0.025 = 1.96$) then the null hypothesis is invalid, implying that the trend is significant. In this study, the Mann-Kendall test is used to detect if a trend in rainfall in monthly time series is statistically significant at 99% and 95% levels over the period of 1979-2005.

The SEN's Slope Estimator is used to estimate the gradient of the trends in rainfall (Sen, 1968). This method provides a more robust slope estimate than the least square method because it is sensitive to outliers or extreme values. The slope is estimated as follows:

$$T_i = \frac{x_i - xy}{j - y} \text{ for } i = 1, 2, 3, \dots, N \quad (14)$$

where x_j and x_y are data values at time j and y and $j > y$ correspondingly. The median of these N values of T_i is considered as Sen's estimator of the slope which is given as:

$$Q_i = \begin{cases} T_{\frac{N+1}{2}} & N \text{ is odd} \\ \frac{1}{2} \left(T_{\frac{N}{2}} + T_{\frac{N+2}{2}} \right) & N \text{ is even} \end{cases} \quad (15)$$

Sen's estimator is calculated as $Q_i = T_{(N+1)/2}$ if N is odd, furthermore, $Q_i = [T_{N/2} + T_{(N+2)/2}]/2$ if N is even. Also, Q_i is estimated by the two-sided test by $100(1 - \alpha)\%$ confidence interval. Furthermore, a true slope can be derived by the non-parametric test Q_i with a positive value indicating an upward or increasing trend. In contrast, a negative value of Q_i signifies a downward or decreasing trend in the time series.

3.4.6 Assessment of the Impacts of Climate Change on the Hydrology of Kikafu, Weruweru and Karanga Watershed

In this study, the impacts of climate change on the hydrology of KWK watershed was carried out by comparing the parameters simulated from historical (1971-2005) and the future (2006-2030, 2031-2050, 2051-2070, 2071-2100) under two emission scenarios (RCP 4.5 and RCP 8.5). However, it is worth mentioning that one of the uncertainties may arise from the tendency of the different CORDEX regional climate models to simulate the climate variables at one location differently (Dosio *et al.*, 2019). Thus, this may be one of the potential sources of uncertainty in hydrological parameters simulation. This tendency necessitated the ensemble average of two CORDEX regional climate models driven by two different GCMs was built. Outputs from the constructed ensemble average for RCP 4.5 and RCP 8.5 emission scenarios were used as input into the SWAT model to simulate the stream flows and water balance components during historical (1971–2005), and future (2006-2100) climate. The SWAT model was calibrated using the procedure described in section 3.4.3. The calibrated SWAT model was used to simulate the historical and future hydrology of KWK watershed under RCP 4.5 and 8.5, respectively.

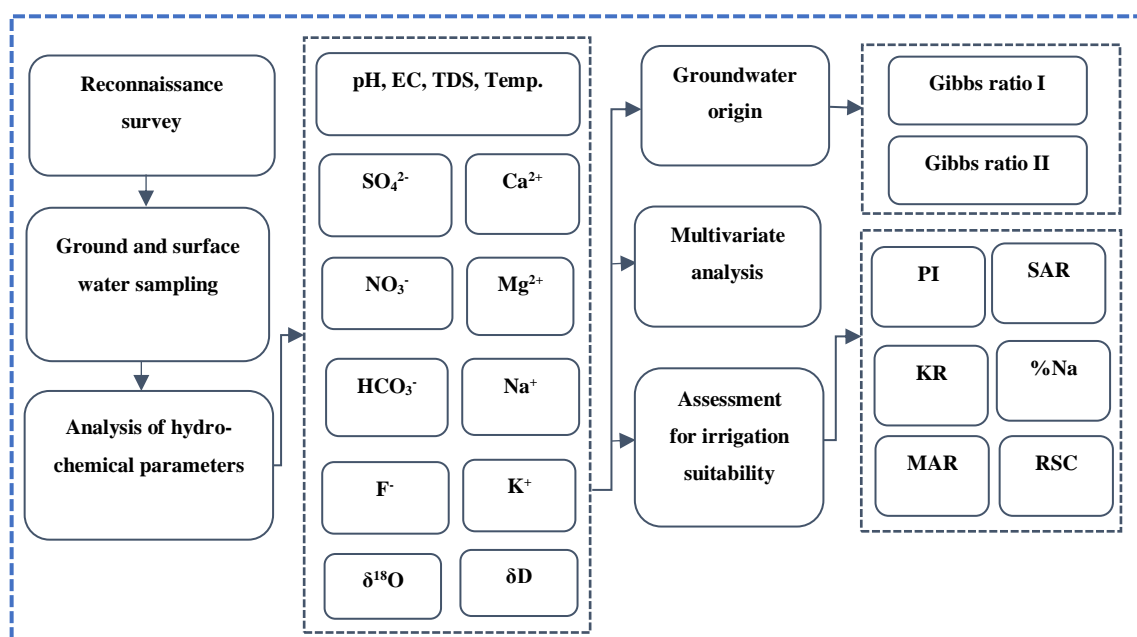
In simulating the hydrological parameters under RCP 4.5 and 8.5, ensemble outputs were used. The projected dataset involving four-time slices and two RCP scenarios (a total of four datasets) were used to derive hydrological fluxes using the SWAT model. This procedure was done by upgrading its climate-specific input parameters as scheduled. The projected

changes of all hydrological parameters are subject to the changes in the projected rainfall and precipitation patterns under 4.5 and 8.5 RCPs.

3.5 To Assess the Impacts of the Present and Future Land-Use Changes on Water Quality on the Slopes of Mount Kilimanjaro

3.5.1 Sample Collection

Surface and groundwater samples were collected from rivers, boreholes, shallow wells, and reservoirs, making a total of 54 stations. These stations were sampled twice, during the dry season (August 2019) and the rainy season (April 2019). The GPS (global positioning system) was used to locate sampling sites. High-density polyethylene (HDPE) sampling bottles of 1L size were used for sampling, and amber glass bottles of 10 mL size were used for isotope samples. Duplicate samples were collected from the middle of the rivers and reservoirs so as to avoid local anthropogenic influence in the river/reservoir banks, and pumping for 15 minutes was effected before sampling in deep wells aiming to avoid sampling the stagnant water. The sampling bottles were rinsed thrice using distilled water, deionized water and finally sampled water before sampling. Isotope samples were filled and capped while in water to avoid air bubbles. The Hanna multiparameter probe (model number HI-9829) was used to measure physical parameters such as pH, temperature (°C), Electrical conductivity (EC) ($\mu\text{S}/\text{cm}$), dissolved oxygen (DO)(mg/L), and total dissolved solids at the point of collection. 2mls Nitric acid was used to acidify samples for cations analysis, whereas no acid was added in samples for isotopes analysis. Cool boxes with ice packs were used for temporary sample storage during transportation, and samples for NO_3^- and NO_2^- were analysed in the same day. Further, samples were refrigerated at 6°C before analysis. The steps applied in this objective are summarized in Fig. 10.



PI- Permeability Index, MAR- Magnesium Adsorption Ratio, SAR-Sodium Adsorption Ratio, KR- Kelly Ratio, RSC- Residual Sodium Carbonate, %Na-Sodium Percent

Figure 10: Summary of the methods applied in determining the impacts of land use on water quality

3.5.2 Samples Analysis

(i) Laboratory Analysis

Determination of the composition of Stable isotopes of Oxygen and Hydrogen was done using an off-axis integrated cavity output spectroscopy (OA-ICOS); model DLT-100, laser isotope analyzer at the Department of hydrological investigations, the National Institute of Hydrology, Roorkee-India. The results are reported in δ -notation relative to Vienna Standard Mean Ocean Water (VSMOW). The $\delta^{18}\text{O}$ and δD results were compared with the Local Meteoric Water Line (LMWL) which was established using isotope data in precipitation from different parts of Tanzania. The precipitation isotopes data were freely sourced from the Global Network for Isotopes Precipitation (GNIP), available online through www.iaea.org/water, and previously published works (Ghiglieri *et al.*, 2012; McKenzie *et al.*, 2010; Nkotagu & Mwambo, 2000).

Determination of the major dissolved ions (K^+ , Na^+ , Mg^{2+} , Ca^{2+} , Cl^- , CO_3^{2-} , SO_4^{2-} , F^- , and was carried out at the water laboratory located at the Ngurdoto Defluoridation Research station, in northern Tanzania. The samples were measured twice to increase the precision and accuracy of the results. Atomic absorption Spectrophotometer(AAS), and spectrometer were used to determine ions concentration in water. Also, Titration was used for total alkalinity,

total hardness, Cl^- , Ca^{2+} , whereas spectrophotometer was used for SO_4^{2-} . The K^+ and Na^+ and Mg^{2+} were analyzed using Atomic Absorption Spectrophotometer (AAS), while, HCO_3^- and CO_3^{2-} were determined using equation 17 and 18 (Trussell *et al.*, 1989). Piper trilinear, Wilcox and Durov diagrams were plotted in Schlumberger Aquachem 2011.1 software package. Determination of irrigation suitability parameters was done by calculation using the relations equations 19-25 (meq/L). Various water quality standards were used to determine the quality of water for irrigation suitability:

$$\text{HCO}_3^- = \frac{\text{Total alkalinity} - 5.0 * 10^{(pH-10)}}{1 + 1.94 * 10^{(pH-10)}} \quad (17)$$

$$\text{CO}_3^{2-} = 0.94 * [\text{HCO}_3^-] * 10^{(pH-10)} \quad (18)$$

(ii) Geostatistical and Spatial Data Analysis Framework

Multivariate statistical analysis and Cluster analysis were carried out in Statistical Package for Social Science (IBM SPSS v26) and Paleontological Statistics (PAST) Software Package (Hammer *et al.*, 2001). This analysis aims to uncover the relationship or differences between variables from different sampling sites in terms of water quality. The correlation analysis was carried out for hydrogeochemical characteristics of analyzed water samples, and the significance of correlation coefficients was tested using the statistical software. A geographical Information System (GIS) Software Package, ArcGIS version 10.6, was used to generate various maps in this study. Clusters were established based on similarities of variables under consideration. One-way ANOVA, single factor was used to compare means of various parameters between river and groundwaters.

(iii) Data Quality Assessment

All devices were calibrated before use in order to ensure the quality of hydrochemical data. All titration samples were standardized prior to use; thereafter, a control sample (of a known concentration) was analysed before analysis of other samples. Deionized water was used as a blank sample during calibration spectrophotometer. For the isotopes samples, the results were checked using the standard deviation. The quality of isotopic water analysis results was checked by using the standard deviation values ($\delta^{18}\text{O} < 0.3\text{‰}$ and $\delta^2\text{H} < 2\text{‰}$), whereby samples with a standard deviation greater than these values were reanalyzed. The accuracy of geochemical analysis was done through the water balance calculation of the ion balance,

and a range of $\pm 0.01\%$ was used (Aleke *et al.*, 2016). The equation according to Hounsflow (1995) is represented as:

$$\%Parameter = \frac{\text{Individual Parameter}}{\text{Total Parameter}} * 100 \quad (19)$$

Where the cation-anion ratio of $1:1 \pm 0.01$, the geochemical analysis was regarded as accurate.

3.5.3 Groundwater Quality for Irrigation Assessment

The quality of irrigation water is important for ensuring crop maximum productivity. The groundwater suitability for irrigation in this study area was evaluated using residual sodium carbonate (RSC), sodium absorption ratio (SAR), sodium percentage (Na%), magnesium hazard (MH), and permeability index (PI). Other measures were Wilcox Diagram and Kelly's ratio (KR).

(i) Residue Sodium Carbonate

Residual sodium carbonate is used to identify carbonate and bicarbonate hazards. The CO_3^{2+} and HCO_3^- react with Ca^{2+} and Mg^{2+} and precipitate as calcite and magnesite. The presence of exchangeable Sodium per cent and sodium hazard in the soil is enhanced by residual sodium carbonate (RSC), which is expressed by equation 20 and ions concentrations were expressed in meq/l. The RSC is calculated using Equation 20:

$$RSC = \left[(\text{HCO}_3^-) + (\text{CO}_3^{2-}) \right] - \left[(\text{Ca}^{2+}) + (\text{Mg}^{2+}) \right] \quad (20)$$

Irrigation water can be categorized into four categories based on RSC values, the value less than zero (No hazard), the value between 0 and 1.25 (safe for irrigation), the value between 1.25 to 2.5 (Slight to moderate carbonate hazard), and a value greater than 2.5 (unsuitable for irrigation).

(ii) Sodium Adsorption Ratio (SAR)

This is the measure of the amount of Na^+ in water relative to Mg^{2+} and Ca^{2+} for irrigation purposes. Sodium Adsorption Ratio (SAR) was calculated using Equation 21 (Bashir *et al.*, 2013):

$$SAR = \frac{Na^+}{\sqrt{\frac{Ca^{2+} + Mg^{2+}}{2}}} \quad (21)$$

The introduction of water quality classes with regard to the sodicity hazard is challenging than salinity problem. The SAR=0-10, indicate low sodium water (S1) and can be used for irrigation for all types of soils. Nevertheless, sensitive crops may be affected by the continuous application of low concentrations of sodium water. The SAR value ranging from 10-18 indicates medium sodium water (S2), which possesses sodium hazard for certain crops in fine-textured soils. The medium sodium water may be used on coarse textured soils and organic soils with good drainage conditions. High SAR (18-26) water (S3) can potentially release a harmful amount of exchangeable sodium for uptake by plants, which can hinder plant growth. Thus, it requires special soil management strategies, such as high drainage and organic manuring. Very high sodium (SAR>26) is unsuitable for irrigation because it will affect crop growth, reducing yield.

Salinity is represented by the electrical conductivity of water (EC), expressed in dS/m, or in mS/m or $\mu\text{S/cm}$ at a standard temperature of 20°C. Based on the ranges of electrical conductivity value, salinity status was categorized into four classes (Richards, 1954). Low salinity ($\text{EC} < 250 \mu\text{S/cm}$) water (C_1) can be used for all crops in all soil types for irrigation purpose. Medium-salinity (EC to $750 \mu\text{S/cm}$) water (C_2) can be utilized to moderately salt tolerance crops in soil types with a moderate amount of leaching capacity. High salinity ($750 < \text{EC} < 2250 \mu\text{S/cm}$) water (C_3) can be used only for salt tolerance plants with high drainage facility. Very high salinity ($\text{EC} > 2250 \mu\text{S/cm}$) water (C_4) is not suitable for irrigation under ordinary conditions. Water having high salinity, negatively impacts crop yield, degrade the land and finally pollute the groundwater.

(iii) Magnesium Adsorption Ratio

The Magnesium hazard (MH) or Magnesium Adsorption Ratio (MAR) index was developed by Paliwal (1972) to quantify magnesium hazard in the water. Usually, calcium and magnesium maintain a state of equilibrium in most of the natural waters (Nagaraju *et al.*, 2014). With the presence of dolomite, the chance of magnesium hazard is more likely. The magnesium content in water is related to infiltration during irrigation, and the chance of the presence of magnesium (mg^{2+}) is more for water-rock dominance areas. The crop yield is highly affected by more magnesium in water. It is essential to quantify magnesium with

respect to calcium (Ca^{2+}) (meq/L) to save the crop from magnesium hazard. Magnesium hazard is given by Equation 22:

$$MAR / MH = 100 * \left(\frac{Mg^{2+}}{Mg^{2+} + Ca^{2+}} \right) \quad (22)$$

(iv) Exchangeable Sodium Percent

Wilcox diagram (Wilcox, 1948) is widely used for the evaluation of groundwater suitability for irrigation use. It is a scatter chart of exchangeable sodium per cent (ESP) on Y-axis versus salinity hazard (EC) on X-axis. The ESP determines the ratio of exchangeable sodium to total capacity (Total cations including sodium, potassium, calcium and magnesium) expressed in equivalents per million. Equation 23 was used to calculate ESP:

$$ESP = \frac{Na^+}{(Na^+ + K^+ + Ca^{2+} + Mg^{2+})} \times 100 \quad (23)$$

For irrigation uses, ESP in water should not exceed 60%. The ESP value greater than 15 results to the soil being saline-sodic to sodic. The $ESP < 15$ indicates saline soil. Using Wilcox (based on ESP and EC values), groundwater can be classified as Excellent to good, good to permissible, permissible to doubtful, doubtful to unsuitable and unsuitable for irrigation based.

(v) Kelly's Ratio

Kelly's ratio (Kelley, 1963) is an important indicator for irrigation water quality measures. Kelly's ratio is measured considering ions concentration (meq/L) of sodium against calcium and magnesium. Kelly's ratio (KR) was calculated by using Equation 24:

$$Kelly's \text{ Ratio} = \frac{Na^+}{(Ca^{2+} + Mg^{2+})} \quad (24)$$

Generally, Kelly's ratio of more than 1 indicates an excess level of Na^+ in water. If Kelly's ratio is more than 3, the water is considered unsuitable for irrigation. Water with Kelly's ratio less than one is considered suitable for irrigation.

(vi) Sodium Per cent (Na%)

Kelly (1940) and Wilcox (1958) have also been used to ascertain the hazardous effect of sodium on water quality for irrigation usage in terms of Kelly's ratio (KR) and sodium percentage (SP/Na%). Sodium per cent relates directly to soil structure and is computed using Equation 25.

$$Na\% = \left(\frac{Na^+ + K^+}{Na^+ + K^+ + Ca^{2+} + Mg^{2+}} \right) \times 100 \quad (25)$$

(vii) Permeability Index

Permeability index (PI) is calculated using Equation 26. Soil permeability is affected by long term use of high salt irrigation water. The presence of Na^+ , Ca^{2+} , Mg^{2+} and HCO_3^- (meq/L) in irrigation water influences PI. Classifying water based on PI was proposed by WHO aimed at assessing the suitability of groundwater for irrigation purpose. The classes are as follows, class I is the water with more than 75% of the maximum permeability, which is the best quality for irrigation. Further, class II is the water with PI ranging between 25 and 75% of the maximum permeability is acceptable and can be applied for irrigation with certain measures, class III is the water with less than 25% of the maximum permeability is unsuitable for irrigation.

$$PI = \frac{Na^+ + \sqrt{HCO_3^-}}{(Na^+ + Ca^{2+} + Mg^{2+})} \times 100 \quad (26)$$

3.5.4 Data Analysis

Hydrochemical analysis of water chemistry data was done using Principal Component Factor Analysis (PCA), Hierarchical Cluster Analysis (Yidana *et al.*, 2008), and Analysis of Variance (ANOVA). The ANOVA test was followed by a Tukey HSD test to compare means of the water chemistry data. Furthermore, Piper trilinear (Piper, 1944) was used to classify water based on major cations and anions contents. The Gibbs diagram (Gibbs, 1970) and ionic ratios of some parameters such as Ca^{2+}/Mg^{2+} , Na^+/Cl^- , Na^+ versus Cl^- , and Durov diagram were used to determine the chemical and ionic exchange processes controlling dissolved ions content of water. The bivariate scatter plots of $\delta^{18}O$ versus δ^2H were used to assess the source of water in various water sources as well as the mixing pattern among them.

This was done so as to establish hydrological characteristics of the watershed such as the flow patterns, source origins, hydrological connections and chemical histories of surface and subsurface water masses.

CHAPTER FOUR

RESULTS AND DISCUSSION

4.1 Current and Future Land Use/Cover Changes and the Association to Food Production

4.1.1 Assessment of Classification Accuracy and Generation of Land-Cover Maps

The overall accuracy assessment of the supervised image classification by maximum likelihood algorithm was 85.32%, 87.23%, and 88.77% for the years 1993, 2006, and 2018, respectively (Table 8). These percentages meet the minimum accuracy requirement of 85% for effective and accurate land use/cover change analysis and modeling (Ahmed *et al.*, 2013; Araya & Cabral, 2010). According to Jensen (2007) the findings of this analysis are suitable since the Kappa values are greater than 80%.

Table 8: Accuracy assessment results of the classified images

Year	Overall Accuracy (%)	Kappa Coefficient
1993	85.32	0.9012
2006	87.23	0.9231
2018	88.77	0.9621

Clouds patching at high altitudes can affect the classification of images and, as a result, the discrimination of glacier ice on Mount Kilimanjaro. In the long run, this has an effect on how training samples are prepared, which has an impact on classification accuracy. Clouds and cloud shadows block the glacier, snow cover, and glacier surface debris cover in most instances (Rastner *et al.*, 2019). Despite the fact that the results of satellite image classification accuracy exceed the minimum criteria of 80%, it is worth noting that the interpretation of the glacier ice results in this study may have been influenced by the clouds cover problem. This problem can be solved by finding a new image date that is close to the desired year (i.e. 1994, not 1993, but the same season); or, more possibly, by collecting high-resolution clouds free satellite images, which are usually not free.

4.1.2 Patterns of Land Use/Cover Changes

Figure 12 shows the maps of the KWK watershed's classified land use/cover images. Table 9 summarizes the findings of the historical land use/cover change study, which included selected spatial area gain/loss. In general, the land use/cover change results (Table 9) show an exponential rise in built-up area from 1993 to 2018, a gain of 7.59% of the total watershed area, and a nearly identical pattern for agricultural land, with a gain of 10.94% of the total watershed area. According to the findings, water and rocky surface areas have decreased slightly (0.06% and 0.24%, respectively). When grasses covering the rocks decrease, most of the rocky area is exposed; hence spectral signatures under the rocky category are recorded, which count on increasing the rocky surface. The areas of all other groups suffered losses of varying degrees. For example, barren land and grassland suffered the greatest overall losses (4.51% and 8.50%, respectively). Forest, wetland, shrubland, and glacier ice have lost a small amount, with losses of 2.28, 1.62, 1.43, and 0.29%, respectively.

Table 9: Losses/gains in land use/cover areas (km²)

LU Classes	Year			Percent change		
	1993	2006	2018	1993-2006	2006-2018	1993-2018
Built-up area	32.88	59.57	89.85	3.56	4.03	7.59
Agricultural land	80.26	118.68	162.40	5.12	5.82	10.94
Water	11.84	10.32	11.36	-0.20	0.14	-0.06
Forest	242.33	231.77	225.22	-1.41	-0.87	-2.28
Barren land	78.84	69.27	44.95	-1.27	-3.24	-4.51
Grassland	167.12	140.82	106.31	-3.50	-4.60	-8.10
Wetland	21.96	17.08	9.80	-0.65	-0.97	-1.62
Shrubland	42.23	35.76	31.53	-0.86	-0.56	-1.43
Rocky surface	69.32	65.36	67.55	-0.53	0.29	-0.24
Glacier ice	3.84	1.99	1.65	-0.25	-0.05	-0.29

Negative sign means loss

The growing population trend is reflected in the rise in built-up area (Fig. 12). According to studies, future population growth in the catchments is linked to the urbanization of more land, including areas along sideways, the road network, and urban suburbs (Hyandye & Martz, 2017). The development of the Siha district is proof of this; studies show that several new villages have sprouted along the road on Mt. Kilimanjaro's slopes (Soini, 2005b).

It is also worth noting that the population coincides with rising food demand, resulting in increased agricultural production. There was a slight proportional (7.04%) reduction of forest land from 1993 to 2018, compared to what was present in 1993 (2.28 km²). This may be due

to the growth of settlements along the forest buffer zone region, as well as the shrinking of the riverine forest as agriculture land expands. In some areas of Mt. Kilimanjaro's slopes, encroachment into the forest reserve and the replacement of natural vegetation with farmed crops has been recorded (Mbonile *et al.*, 2003).

The findings of this research support the notion of revisiting the enforcement of laws and regulations regulating protected areas. Evidence from other countries on land use change, particularly near protected area boundaries, indicates research directions and the need for policymakers to re-design policies and their implementation in protected areas (Tesfaw *et al.*, 2018). Drought may be to blame for the 1.62% decrease in wetlands, particularly in lowland areas. Drought is one of the main causes for farmers and pastoralists invading wetlands (Mbonile *et al.*, 2003). Furthermore, prolonged drought can result in drying wetlands.

Similar LULCC trends were observed on the slopes of Mt. Kilimanjaro in other studies. Between 1987 and 2005, the Kahe plains lost 53 km² of shrub and grassland, as well as sparse vegetation, to maize and vegetable cultivation (GITEC, 2011); increased forest loss on the southern slope from 1606 ha to 5170 ha between 1973 and 2000 (Mbonile, 2005); and conversion of about 39.5% of bushland to agriculture between 1973 and 2000 (Mbonile *et al.*, 2003). Furthermore, between 1952 and 1982, more than 41 km² of the forest was degraded (Yanda & Shishira, 2001); between 1961 and 2000, about 49.97 km² (32.8%) of shrubland and bushland in the Kirua Vunjo division was converted to agriculture and other uses (Soini, 2005b); and on the southern and eastern slopes, cultivated land increased from 54 percent in 1973 to 63% in 2000 (Misana *et al.*, 2012). Bushland is being replaced by cultivated fields on a regular basis. Bushland occupied 40% of the area in the Kirua Vunjo division on the southern slopes in the early 1960s, but had been reduced to 7% by 2000 due to conversion to cultivated fields (Soini, 2005b).

In the past, the highlands were more densely populated than the lowlands, this is because the lowlands are relatively dry as compared to highlands. Agriculture expansion is said to have produced a new and distinct community of farmers who have settled in the dry lowlands previously deemed unsuitable for permanent settlement by the Chagga due to insufficient rains and malaria (Soini, 2005b). Despite the low rainfall levels in the lowlands, the lowlands are actually home to the majority of intensive agriculture activities. Floods and flowing rivers make the lowlands the most active and productive areas in irrigated areas throughout the season and throughout the year. As a result, there is a need to invest in advanced agrarian

technology in order to increase output per unit area. It is also important to concentrate on non-agricultural activities to complement agricultural production (Soini 2005; Mbonile 2003).

Due to increasing demand for cultivable land, the scarcity of the land increased; even the most peripheral areas were cultivated, such as along riverbanks, despite existing bylaws. Agriculture expansion took its path to the lowlands at a high pace after the enactment of the agriculture policy in 1983 (Mbonile *et al.*, 2003), the policy aims to promote food production in the Tanzania. Annual crops such as maize and horticultural crops have largely replaced perennial crops, this is due to decrease in prices of the perennial crops such as coffee. Lowlands and highlands have been intensively cultivated since that period.

The patterns found in this study are similar to those recorded globally. According to previous studies, tropical savannas have declined by more than half due to conversion to cultivated land (Assessment, 2005). About 20% of the savanna vegetation in Sub-Saharan Africa has been transformed to cropland (UNDP, 2000). In addition, the Food and Agriculture Organization (FAO) predicts that natural savanna areas will continue to be converted to small-scale subsistence agriculture (Zhou, 2011). Agricultural land, plantation forests, and settlement all increased by 18%, 93%, and 125%, respectively, in Ethiopia's upper Suha watershed. The study also indicates a 54%, 82%, and 16% decline in natural forest, shrubland, and grassland, respectively (Mekuriaw *et al.*, 2019).

4.1.3 Projection and Validation of Land Use/Cover Change on the Slopes of Kilimanjaro

By contrasting the observed and simulated land use/cover maps of 2018 (Fig. 11), the model's ability to accurately simulate the year 2030 (Fig. 13) land use/cover maps were validated. In terms of the spatial distribution of all land use categories, the two maps have a fair degree of similarity. With slight adjustments in intensity and alignment, the corresponding land use/cover groups in Fig. 6 d and e showed a strong fit in terms of spatial distribution.

The Validate module in IDRISI Selva generated the kappa coefficients (κ), which were used to assess the predictive power of the simulation model. The overall simulation accuracy (κ -no) was found to be 78.78%; the model's ability to accurately specify the location (κ -location) was found to be 73.86%. Table 6 depicts the agreement and disagreement measures between

the observed and simulated LULC of 2018. The total agreement between the simulated and observed maps (κ -standard) was found to be 0.7286. The quantity and allocation disagreements were low (12.83% and 14.31%, respectively).

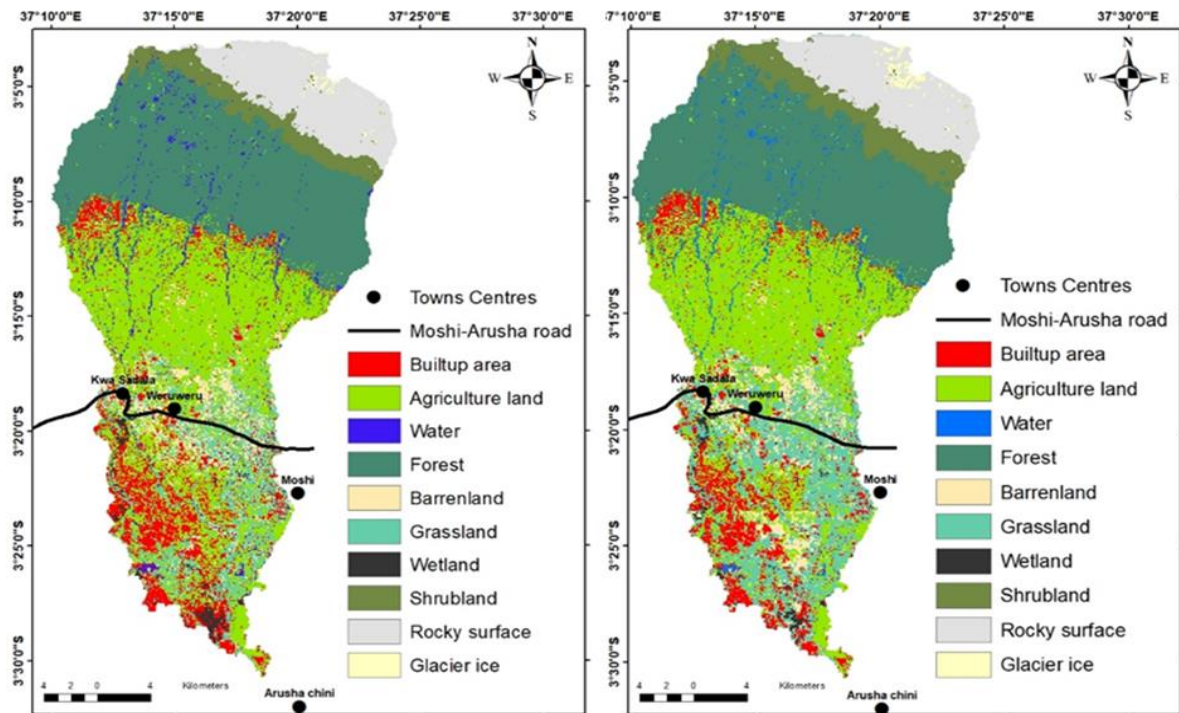


Figure 11: Observed (left) and simulated (Right) land-use and land-cover maps for 2018

The kappa coefficients (k), which were used to assess the simulation model's predictive ability, were developed by the Validate module in IDRISI Selva. The model's ability to correctly specify the position (-location) was found to be 73.86%, and the overall simulation accuracy (-no) was found to be 78.78%. The agreement and disagreement indicators between the observed and simulated LULC of 2018 are presented in Table 11. The cumulative agreement (-standard) between the simulated and observed maps was 0.7286. Disagreements in quantity and distribution were minimal (12.83% and 14.31%, respectively).

Table 10: Components of agreement/disagreement between the observed and simulated Land-use and land-cover maps of 2018

Agreement/disagreement	Value
Quantity disagreement	0.1283
Allocation disagreement	0.1431
Quantity agreement	0.5073
Allocation agreement	0.1064
Change agreement	0.1149

In terms of the quantity and position of cells in each land use category, the accuracy values during validation indicate that the simulated map did not vary significantly from the observed map. The error (disagreements) may have resulted from the transient nature of most LULC classes, with the exception of a few that are permanent and often located in the upper part of the Kilimanjaro National Park, which is protected by law. Memarian *et al.* (2012) found a similar level of quantity and allocation inconsistency. In most cases, errors are caused by inadequate land use suitability maps and image classification overgeneralization. The shape of the chosen contiguity filter also has an effect on the suitability maps. This may be due to inefficient digitization of some of the dataset, as well as other variables and limitations that could have affected the outcomes (Musa *et al.*, 2018). Inefficient georeferencing and geometric correction of the comparison map are another popular source of cell-by-cell error (Eastman, 2012). High-quality datasets, such as satellite images and other spatial data, are needed to enhance these validation results. In addition, advanced methods must be incorporated into the development of more accurate suitability maps; logistic regression is one of the suggested methods. However, the findings of this study follow the criteria for use set forth by Pontius and Millones (2011), and are suitable for use in simulating potential land use/cover for 2030.

Before being used for land use forecasting, suitability maps can be checked. Relative Operating Characteristic (ROC) method can be employed. The spatial structure of the model's achievements and errors is not taken into account by ROC, however. All of the data for the ROC comes from contingency tables, which display only cell-by-cell analyses of the relationship between a map of real change and a map of simulated change, with each grid cell representing a single homogeneous category (Pontius & Schneider, 2001).

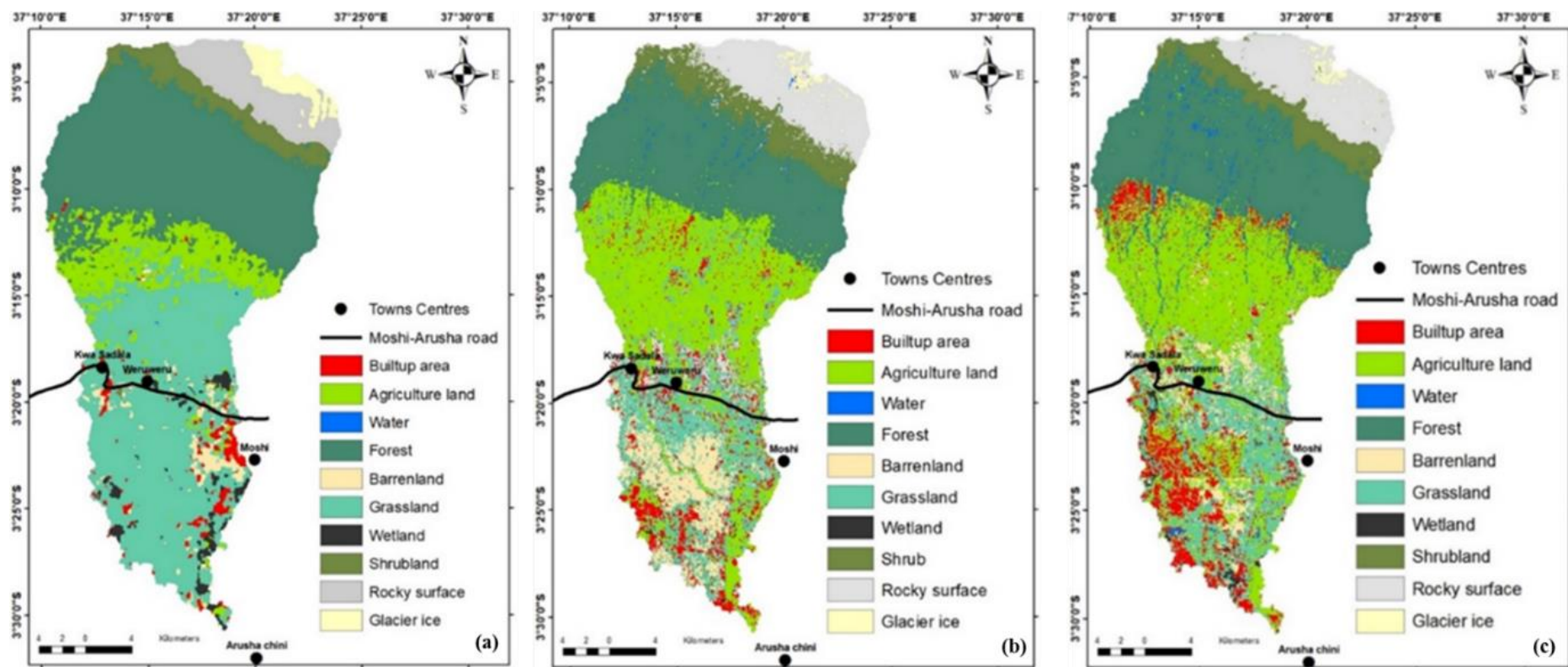


Figure 12: Classified land use/cover image maps for the year 1993 (a), 2006 (b) and 2018 (c)

The ROC approach is unable to show a spatially based uncertainty in the prediction maps. To show the magnitude of the agreement between the maps, ROC includes other statistics such as Cohen's kappa index (Vakhshoori & Zare, 2018). As a result, a visual comparison and additional measures of association that account for the spatial pattern must be supplemented to ROC (Costanza, 1989). As a result, the model was validated in this work using a methodology proposed by Pontius and Millones (2011), which advocates for quantity and allocation agreement and disagreement for accuracy evaluation. However, it is worth noting that suitability maps were twisted several times (as depicted in the procedure in Fig. 5) before arriving on the acceptable Kappa index.

4.1.4 The Transition Matrix of Land Use/Cover Change on the Slopes of Kilimanjaro

Table 10 shows the probability transition matrix created by the Markov model for the land use/cover maps of 1993 and 2006. The total cells to be converted into another group in the next time period are shown in the transformation matrix areas (Eastman, 2012), it is a stochastic matrix whose (i, j) entry gives the probability that an element moves from the j th category to the i th category during the next phase of the process (Andrilli & Hecker, 2010). The LULC for the year 2018 was simulated using this probability transfer matrix. Table 10 displays the land use/cover classes for the earlier date $t-1$ (1993), while the columns show the likelihood of the current date's land use/cover classes. Table 10 shows the land use/cover classes for $t-1$ (1993) (earlier date), while the columns display the likelihood of the land use/cover classes for the current date, $t=1$ (2006).

Table 11: Probability transitional matrix of Land-use and land-cover of 1993 and 2006 for simulation of land-use and land-cover of the year 2018

Given: Probability to change to:										
	Built	Agric	Water	For	Barr	Gra	Wet	Shr	Rock	Glac
Built	0.2371	0.2124	0.0000	0.0012	0.0529	0.4103	0.0092	0.0319	0.045	0.0000
Agric	0.0508	0.4010	0.0012	0.0041	0.3122	0.2232	0.0001	0.0035	0.0039	0.0000
Water	0.0008	0.4134	0.1634	0.0000	0.0041	0.2807	0.099	0.001	0.0376	0.0000
For	0.0076	0.1384	0.0082	0.6537	0.0001	0.1093	0.0000	0.0795	0.0032	0.0000
Barr.	0.4364	0.278	0.0000	0.0000	0.1093	0.1181	0.0014	0.0132	0.0436	0.0000
Gra	0.1100	0.3126	0.0001	0.0000	0.1857	0.3345	0.001	0.0081	0.048	0.0000
Wet	0.0872	0.3639	0.011	0.0351	0.0562	0.3798	0.0167	0.0266	0.0235	0.0000
Shrubland	0.0033	0.0043	0.0006	0.0044	0.0001	0.0116	0.0000	0.7818	0.1939	0.0000
Rocky	0.0000	0.0000	0.0011	0.0000	0.0000	0.0001	0.0003	0.0057	0.9791	0.0137
Glacier	0.0000	0.0000	0.0033	0.0000	0.0000	0.0000	0.0052	0.0000	0.7460	0.2455

Built =Built-up area, Agric =Agricultural land, For =Forest, Barr =Barrenland, Gra =Grassland, Wet. =Wetland, Shr =Shrubs, Rock =Rocky surface, Glac =Glacier ice.

The majority of the LULC classes were unstable. However, for rock surface (0.9791), shrubland (0.7818), and forest (0.6537), the probability of remaining unchanged was high; agriculture had a moderate probability of remaining unchanged (0.4010). Other groups were found to have a low likelihood of being unstable in the future. Other land use groups could not shift to water, according to the probability transfer values in Table 11.

Furthermore, wetland conversion to grassland (0.3798) and wetland conversion to agriculture (0.3639) had a higher likelihood than agriculture and grassland conversion to wetland. There is also a high likelihood (0.4134) that water will be converted to agriculture and a 0.2807 risk that water will be converted to grassland. The probability transformation values revealed that the likelihood of other land use groups changing to glaciers is almost zero, with the exception of glaciers disappearing and being replaced by rocky surfaces (0.7460).

The lower probability of rock surface, shrubland, and forests changing to other groups can be due to the fact that the upper part of Kilimanjaro National Park, which is a conservation area protected by statute, is mainly shrubland (Soini, 2005b). Tourism and other conservation activities are the only human activities allowed in the area. The high likelihood of remaining unchanged in agriculture may be attributed to the fact that some lowland areas practice irrigation agriculture and that all of the images were taken during the same season. Agriculture has long been a part of the history of the area, and most of the suitable areas have been used by the locals, who mainly live at higher elevations. More grasslands and barren land areas being converted to agriculture and urbanization indicate a need for more investments in non-agricultural economic activities. The rapid conversion of wetlands to grassland and cultivation is likely due to the rapid growth of vegetables and short-term crops in seasonal wetlands. Moisture fluctuations due to variations in annual precipitation amount, which primarily affect wetlands, grassland, and bare lands, may have accounted for the stability of grassland and glaciers LULC classes (Hyandye & Martz, 2017). However, since the probability values recorded in this analysis are dependent on the magnitude and direction of change in land use, future changes in magnitude and direction may produce a different pattern.

4.1.5 Projected Land Use/ Cover Changes on the Slopes of Kilimanjaro

Figure 13 shows the LULC map simulate using CA-Markov model for the year 2030. To determine the quantitative changes in land use, the total areas of LULC groups in 2030 were

compared to the total areas of the real land cover map in 2018 (Table 12). The results in Table 8 show that, under the current scenario for 2018-2030, the built-up area will increase by 32.55% (29.25 km²), while agricultural land will grow by 39.52% (64.18 km²). A significant proportion of grassland (53.92% /57.16 km²) and forest (7.46%/9.82 km²) will be transformed to agriculture land, while 10.52, 5.34, and 13.22 km² of all built-up areas will have been converted from agriculture, forest, and barren land, respectively. The glacier ice is predicted to shrink by 18.79 percent (0.31 km²). According to the model, grassland, wetland, and barren land would decrease by 57.24%, 39.29%, and 15.8%, respectively, by 2030.

Table 12: Land-use and land-cover change matrix between 2018 and 2030 (km²)

		2018										
	LUC CLASS	BUI	AGR	WAT	FOR	BARR	GRA	WET	SHR	ROS	GLAC	TOTAL
2030	BUI	52.35	12.47	0.07	1.26	35.10	8.32	0.00	0.53	0.00	0.00	119.10
	AGR	8.52	103.47	0.10	9.82	3.10	57.16	1.41	0.00	0.00	0.00	226.58
	WAT	0.51	0.52	7.85	0.07	0.00	0.00	0.92	0.00	0.30	0.02	10.18
	FOR	5.54	7.30	0.00	194.33	0.00	0.00	0.00	2.78	0.00	0.00	210.88
	BARR	8.22	5.33	0.00	0.59	17.65	12.01	0.88	2.47	0.00	0.00	37.85
	GRA	7.90	2.18	2.01	4.15	0.12	25.60	2.75	0.00	0.00	0.02	45.46
	WET	0.02	0.31	0.09	3.60	0.03	1.51	3.89	0.00	0.00	0.00	5.95
	SHR	0.00	0.00	0.10	10.41	0.00	0.00	5.00	5.23	5.14	0.00	25.37
	ROS	0.00	0.00	0.00	0.00	0.00	0.00	0.71	17.60	61.90	0.49	67.91
	GLAC	0.00	0.00	0.01	0.00	0.00	0.00	0.00	0.00	0.21	1.12	1.34
	Total	89.85	162.4	11.36	225.22	44.95	106.31	9.8	31.53	67.55	1.65	750.62
Change (%)	+32.55	+39.52	-0.39	-6.37	-15.80	-57.24	-39.29	-9.54	0.53	-18.79		

In comparing the simulated future map with the historical trend, there is no specific approach to follow (Jokar & Kainz, 2011). Arsanjani *et al.* (2011) detailed a technique that was used in this work. The feasibility of occurrence on the predicted sites was used to determine the position of the predicted cells for various land uses/covers. Simply visualization of the LULC maps from 1993, 2006, and 2018 (Fig. 11), it is clear that the built-up areas in the KWK catchment have grown dramatically. The observed changes between 2018 and 2030 are significantly higher than those previously observed. This increase might be due to exception of import tax for agricultural machinery, which reduces costs of farm preparation thus, sharp increase in agricultural land. Furthermore, the introduction of new districts which increased number of people hence increased the need for residential areas may account for a sharp increase in builtup areas. The transition probability between 1993 and 2006 may be the source of the observed trend. Nonetheless, the model validation results indicate that it correctly captured the driving factors. Adding more years to the model training and validation process will improve the performance of the model as suggested by Ndomba *et al.* (2008a). This model included the majority of the factors that contributed to the changes in land use on Mt. Kilimanjaro's slopes. On the other hand, the model findings are based on the premise that current drivers will continue to behave in a similar manner without major adjustments. Changes in government policy or the introduction of major projects that occur between the base year (2018) and 2030 are not included in the model simulation.

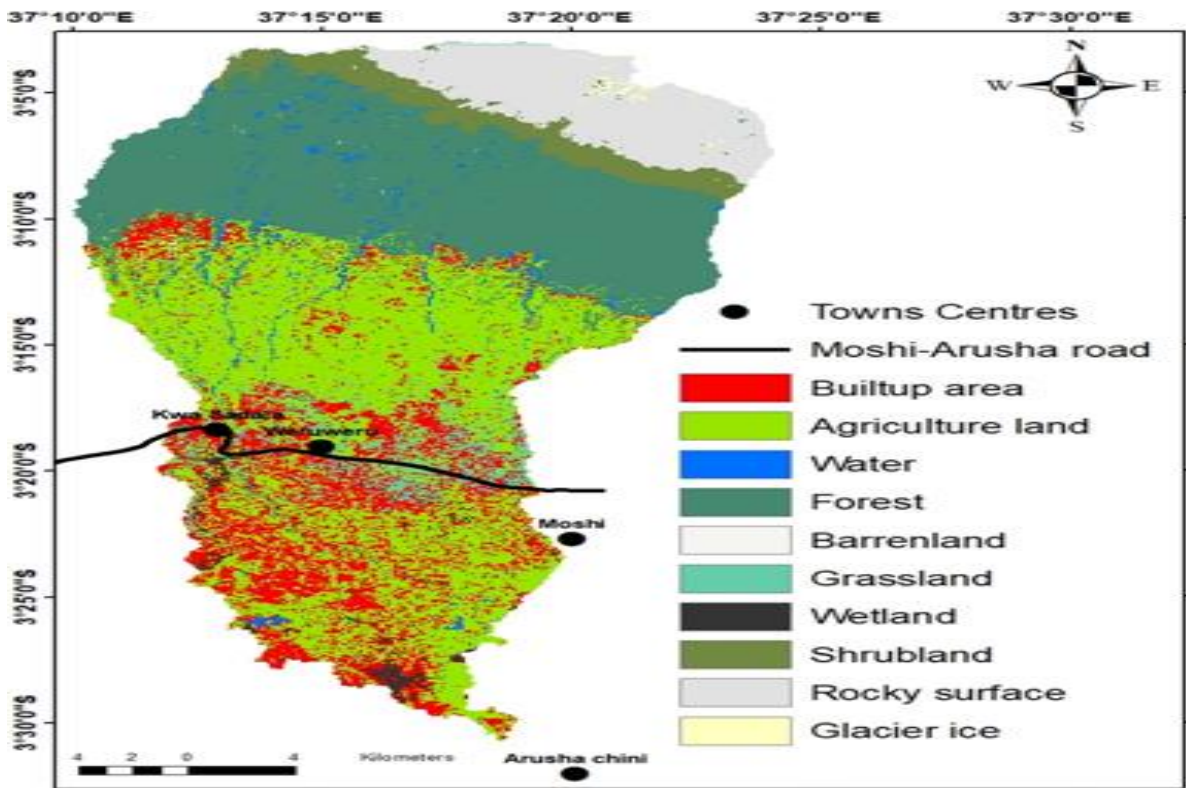


Figure 13: Simulated land-use and land-cover map of the year 2030

Figure 13 also shows that glacier ice will increase in 2030. However, this increment should be interpreted with caution since the factors for de-glaciation and re-glaciation are more likely related to glacier type and climate changes (Geilinger, 1936; Kaser *et al.*, 2010), all of which are not included in this model (except precipitation). It is also worth noting that this model only represents a small portion of Mt. Kilimanjaro's entire glacier.

The findings of this study are in line with a study by Hyandye and Martz (2017) in Usangu catchment. The study reported increase in urban area by 8.2%, decrease in forest area by 20.6%; also 19.6% grassland and 8.5% of agricultural land in 2013 was expected to be converted to urban land by 2020. The global trend reported by Cao *et al.* (2019b), which shows rises in agricultural land from 2010 to 2100 in all three scenarios studied. Forest, grassland, and shrubland areas are also declining, according to the survey. In Doha, the LULC forecasts a 20.1% increase in built-up areas from 2010 to 2020 (Hashem & Balakrishnan, 2015). In addition, estimates indicate that forest destruction will continue in the immediate future (2026) in the Long Island Sound Watersheds of the United States (Zhai *et al.*, 2018).

Taylor *et al.* (2013) depict that land use has a greater impact on terrestrial hydrology than climate change. Changes in land use on Kilimanjaro are likely to have an effect on the mountain's water balance, as the mountain is regarded as an East African water tower (Viviroli *et al.*, 2007). The mountain provides water to South-eastern Kenya and North-eastern Tanzania, where freshwater demand for domestic, hydropower, commercial, and irrigation is expected to rise rapidly (Agrawala *et al.*, 2003). The mountain is important for regional climate regulation and provides ecosystem services to communities living on its slopes (Hemp, 2005). In the fog interception zone of Mt. Kilimanjaro, LULC adjustment also means the loss of the most powerful water source (Hemp, 2005). The Kahe catchment aquifer was also grouped among the depleted mountain catchments due to rapid rises in deforestation and expansion of agricultural activities (Grove, 1993). Agriculture increased from 23% to 58% of the area in other catchments, such as the Lake Babati catchment, from 1960 to 1990, accounting for a recharge decline from around half to a quarter of the annual rainfall (Sandström, 1995). As a result, it was important to study the effects of LULC changes on Mt. Kilimanjaro slope hydrology.

Mount Kilimanjaro slopes habitats and ecosystems provide a unique avenue for both local and global society in terms of wildlife conservation (Msoffe *et al.*, 2020), water supply (Agrawala *et al.*, 2003; Hemp, 2005) and tourism (Anderson, 2015). According to reports, the highlands' vegetation is increasingly dwindling, and the snow cover is vanishing, raising the risk of losing

Mt. Kilimanjaro's tourist attraction for the rest of the world (Mbonile, 2005). The land use and cover change study for the slopes of Mt. Kilimanjaro leads to a deeper understanding of potential landscape changes and related impacts that affect both the immediate local population and the global at large. As a result, this research offers critical future-based knowledge for the protection of Mt. Kilimanjaro's slopes ecosystem, which benefits both the local and international communities. These ecosystem services are important not only for the local community but also have the potential to stymie the achievement of local, regional, and global sustainable development goals.

With the current changes in climate, it is worth noting that changes in precipitation and temperature patterns result from the relation between land use and climate change. Finally, these changes in precipitation and temperature patterns affect the United Nations sustainable development targets, such as food security (Goal 2), poverty eradication (Goal 1), electricity for all (Goal 7), climate change mitigation and adaptation (Goal 13), and biodiversity loss (Goal 15) (Nations, 2019). As a result, the findings outlined in this work are critical for better planning and protection of the habitats and landscapes of Mt. Kilimanjaro's slopes, so that life support benefits to both the local and global communities can continue to be harnessed.

4.1.6 Food Production and Expansion in Agricultural Land

Along the Mount Kilimanjaro slopes, maize, rice, bananas, and beans are staples and cash crops. The crops chosen are among the six most important crops globally (Lobell & Field, 2007). When the results of this analysis were combined with averaged food production figures from the five districts of the study region (Rombo, Hai, Siha, Moshi district council, and Moshi urban district councils) recorded by URT (2018). Maize, rice, banana, and bean production was projected to increase by 28.33% from current records. However, as shown in Fig. 14 (Left hand side), the available record does not reflect the rise in crop production as agricultural land increases. In Fig. 14 (Right hand side), the observed trend for banana indicates a declining trend. Around 2005 and 2008, there was a significant drop in banana production, which continued until 2017. Despite the increase in agricultural land reported in this study, the output of maize, rice, bananas, and beans is less than 200 000 tons, as depicted in Fig. 14.

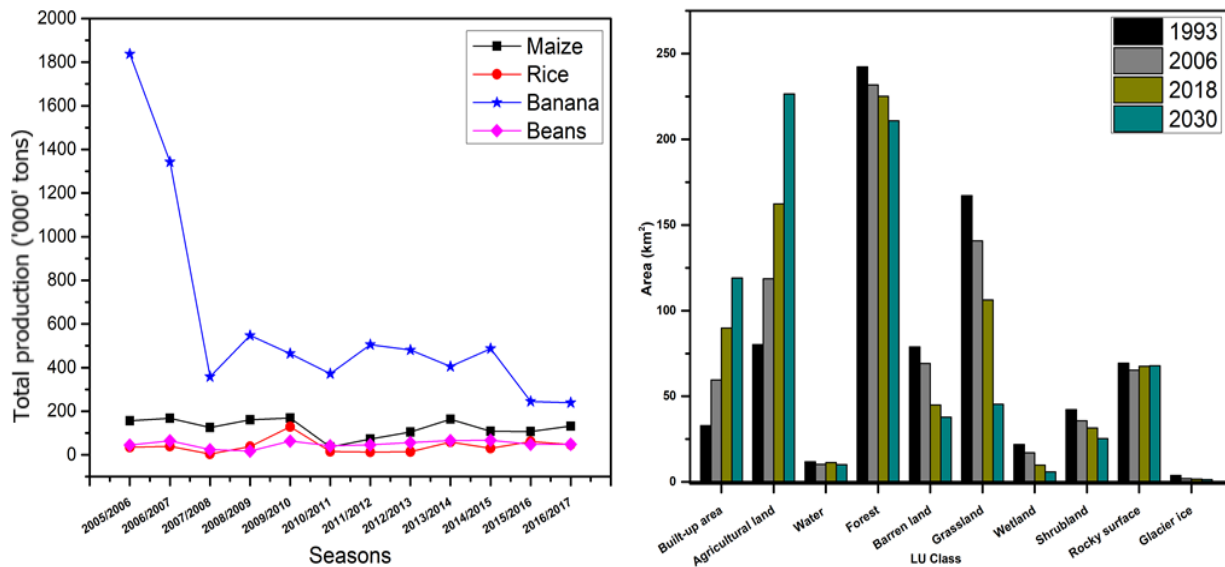


Figure 14: Total food production in five districts along the study area and the land use change trend

Changes in cultivated land have the greatest impact on food production and ecological processes (Cao *et al.*, 2019b). Despite the expansion of agricultural land, the yield of selected staple food crops does not reflect the expansion of agricultural land (Fig. 14). There is no direct connection between increased cropland and increased food production. However, this increase in LULC is based on the assumption of a uniform spatial increase and favourable weather, pests, and disease conditions throughout the area. On the other hand, the observed mismatch demonstrates that expanding the output area does not guarantee an increase in crop yield. Furthermore, the findings indicate that other factors influencing crop yield include good agronomic practices, suitable weather, fertile soils, and pest and disease management practices. Increased farm fragmentation as a result of the region's land tenure system, soil erosion, and land degradation (UNDP, 2014) are among the key factors that contribute to this disparity. Due to low prices on the world market, banana farms may have been converted into short-season crops such as maize and bean fields, resulting in banana farms being unprofitable (Soini, 2005a). On the southern slopes of Kilimanjaro, however, low rainfall, particularly in drier lowlands, and poor agronomic practices can result in nutrient mining and, as a result, lower per capital output. The survey, however, reveals that the dynamics of land use for agriculture on Kilimanjaro's slopes are all about intensification on the higher slopes and expansion on the lower slopes.

The demand for more food increases as the population grows. As a result, agricultural expansion would not be a surprising phenomenon in the future. Increasing output per unit area rather than expanding agricultural land will help meet rising food demand. The majority of grassland, barren

land, and lower-elevation forests are expected to be converted into built-up and agricultural land. Some previous studies have also recorded rapid population growth and agricultural expansion, especially in the lowlands (Chiwa, 2012; Mbonile *et al.*, 2003; Misana *et al.*, 2003; Soini, 2005b).

Increased pressure on arable land leads to increased land degradation, which results in lower agricultural yields (CEP, 1995). The declining productivity of highland gardens has changed the balance, and lowland plots have taken on greater significance in recent years, providing food for both livestock and people. The lowlands, on the other hand, are much drier and necessitate modern agronomic techniques. Significant nutrient mining, combined with high prices for inputs, and fertilizers, has resulted in declining soil productivity in the lowlands, accelerating soil degradation (UNDP, 2014). In order to improve fertility and productivity in the lowlands, restoration and fertilizers are needed, but most smallholder farmers cannot afford the associated costs. As a result, the available land for crop production becomes less productive and usable.

Land use and environmental degradation are two factors that could reduce the amount of water available for food production in the Pangani basin (De Wit & Stankiewicz, 2006). Munishi *et al.* (2015) found that decreased precipitation and uneven rainfall distribution during the cropping season are important determinants of maize bean and banana yield in the region. Annual precipitation levels on Mount Kilimanjaro have decreased by 600-1200 mm over the last 120 years, whereas temperatures have risen significantly since 1976 (Hemp, 2005). These changes in precipitation and temperature patterns would result in a major increase in irrigation demand, which would negatively impact crop production in the region (Munishi & Sawere, 2014). Small-scale farming and mostly rainfed agriculture are the most common forms of agriculture on Kilimanjaro, resulting in a major mismatch between cropping area and crop yield. According to Mmbaga *et al.* (2017), climate change has resulted in an increase in minimum temperatures, which has resulted in local coffee extinction. Aside from food crops (Munishi *et al.*, 2015), cash crops like coffee have also been confirmed to be severely impacted (Craparo *et al.*, 2015). Coffee production is expected to decline much further into the 2060s if current land use changes and climate change patterns are not reversed (URT, 2012). To bring issues closer to practice, a more integrative study centered on generating high-quality data on food production, food demand, environment, pests, and diseases is needed.

This study agrees with the findings by Lyle (1996) that the key challenge lies in production practices and not in the farm sizes. It is necessary to adjust our production methods in order to

achieve a balance between environmental land use and food production means. Rather than expanding farm scale, the emphasis should be on developing more innovations that increase productivity in small areas. On the other hand, sustainable land use necessitates the consideration of environmental, social, and economic problems as core issues of sustainability (Loures, 2019).

Land use and climate change are projected to affect global food production, posing a threat to food security (Lobell & Field, 2007). A research translation program focused on translating research-based evidence of locally adapted sustainable enhancement of food production practices into community-led actions to reverse land degradation while simultaneously increasing and diversifying productivity will be needed to achieve food security. This study stresses the need for the greater agency in incorporating this knowledge into the decision-making process in the face of global and local changes in LULC, population growth, and decline in food production. This decision-making process is essential for local support of sustainable food production as well as land restoration. The intervention in the decision-making process will counteract local and global changes and practices that threaten food production and environmental sustainability. A detailed understanding of community needs, goals, policies and activities can also be used to strike a balance between development and environmental sustainability. As a result, local adaptation efforts should focus on these issues.

4.2 The Impacts of the Present and Future Land Use/Cover Changes on the Water Budget

4.2.1 Sensitivity Analysis

The sensitivity analysis showed that there are nine most sensitive KWK SWAT model parameters that minor changes in their values were found to influence river flow are shown in Fig. 15. These parameters were those with p-value ≤ 0.05 . The parameters include a_CN2.mgt, v_ALPHA_BF.gw, a_HRU_SLP.hru, v_GWQMN.gw, a_CH_K2.rte, a_SOL_AWC().sol, a_SLSUBBSN.hru, v_GW_REVAP.gw, a_CANMX.hru and SOL_K().sol. The t-statistical values of the parameters are used to rank the parameters in the order of magnitude of their influence on the streamflow. According to Abbaspour (2015) the higher the absolute t-test values, and low p-values, the more sensitive the parameter. The information regarding parameters sensitivity analysis is always helpful in making modellers' work easy as it highlights which parameters to fine-tune during calibration of a hydrological model.

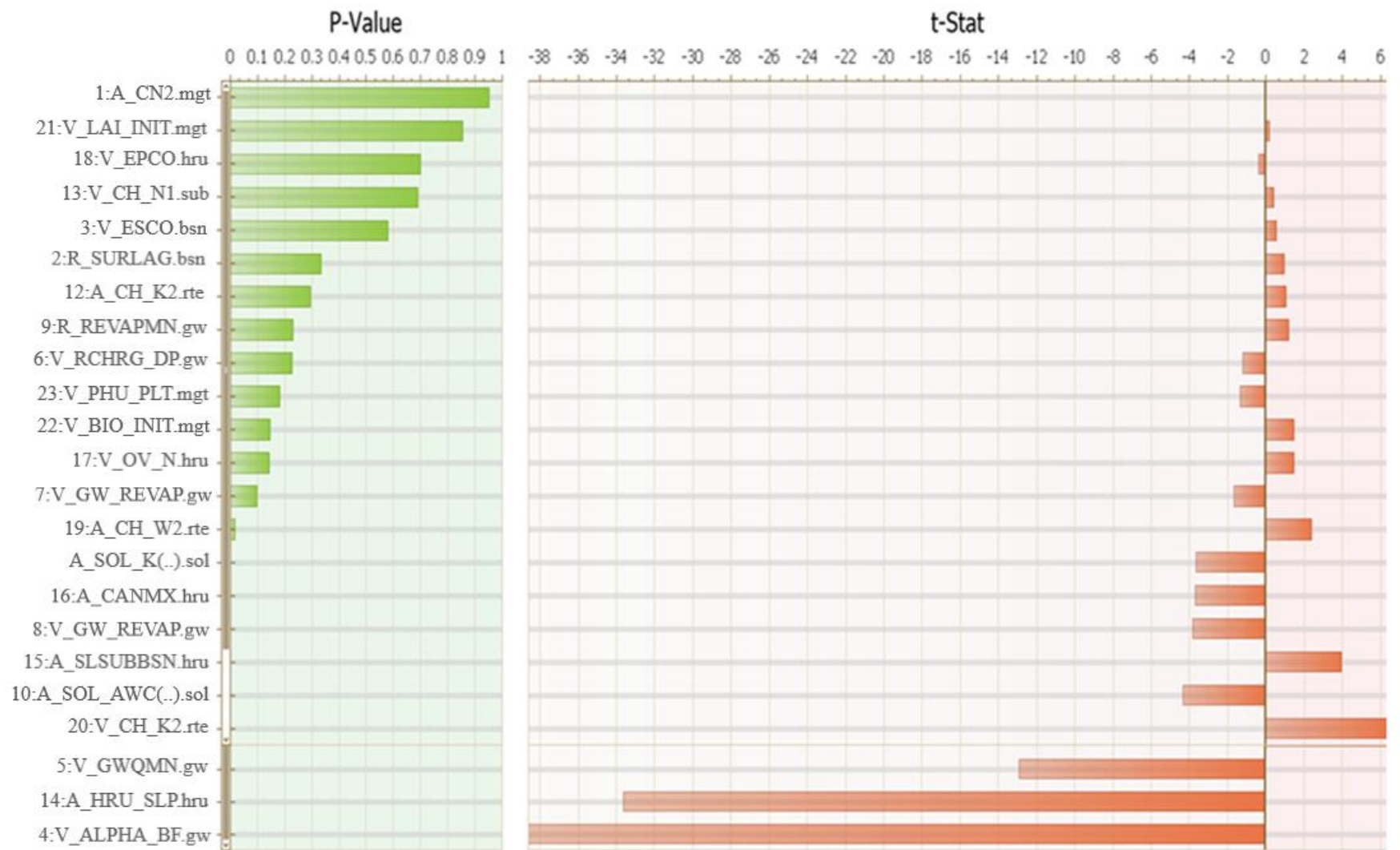


Figure 15: Results of parameter sensitivity analysis (P-value and t-stat)

Previous hydrological studies by Ndomba *et al.* (2008) and Kishiwa *et al.* (2018) have also reported on the most sensitive flow parameters in Pangani. The parameters SURLAG, GWQMN, RCHRG_DP, SLOPE, soil depth (SOL_Z), ESCO, SOL_AWC, SOL_K, and ALPHA_BF, CH_N, CH_K2, SLSUBBSN, GW_DELAY, SOL_ALB, and GW_REVAP. Among these previously reported parameters were also crucial in this study, although with different levels of sensitivity. Contrary to previous studies, the maximum canopy storage (CANMX.hru) was not reported to influence the model output.

4.2.2 Model Parameters, Calibration and Validation

The calibration and validation curves plotted together with mean monthly rainfall are shown in Fig. 16.

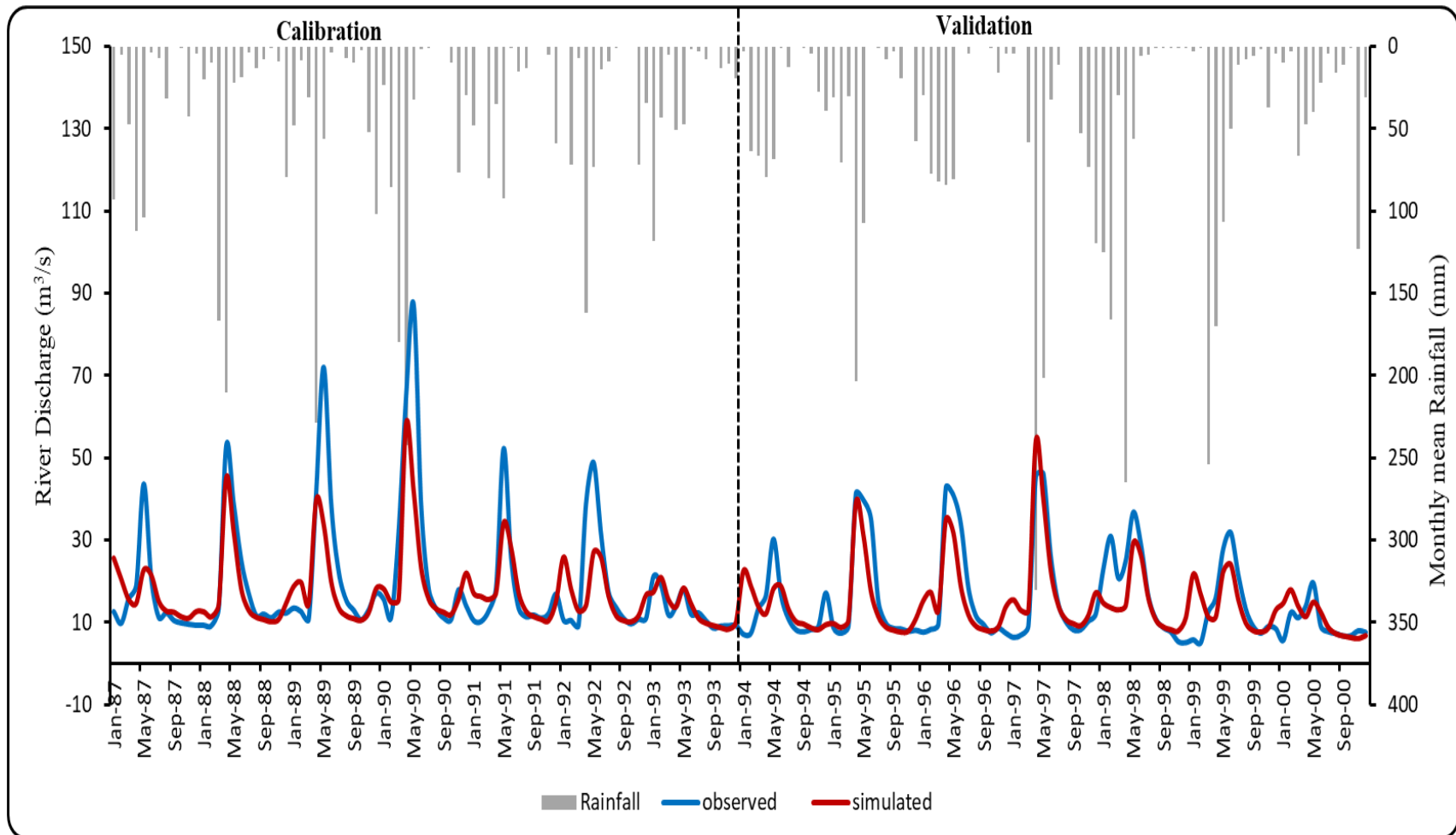


Figure 16: Comparison between the simulated and observed monthly discharge of Kikafu, Weruweru and Karanga watershed

The model calibration parameters that were used for calibration and their default range are summarized in Table 13.

Table 13: Parameters sensitive to streamflow, their default range, fitted value during calibration and final values used

Parameter	Description	SUFI2 fitted value	Default range	The final value in SWAT model
r_SURLAG.bsn	Surface runoff lag time (days)	0.02	0.05 – 24	0.02
v_ESCO.bsn	Soil evaporation compensation factor	0.65	0.01 - 1	0.65
v_GWQMN.gw	Threshold depth of water in the shallow aquifer for return flow to occur (mm H ₂ O)	382.88	0 – 5000	382.88
v_GW_REVAP.gw	Groundwater “revap” coefficient	0.27	0.02 - 0.2	0.05
r_REVAPMN.gw	Threshold depth of water in the shallow aquifer for "revap" to occur (mm H ₂ O)	2.01	0 – 1000	750
v__ALPHA_BF.gw	Baseflow alpha factor (days)	0.11	0 – 1	0.13
v__RCHRG_DP.gw	Deep aquifer percolation fraction	0.22	0 – 1	0.63
v__GW_DELAY.gw	Groundwater delay (days)	579.52	0 – 500	18.25
v__CH_N1.sub	Manning’s ‘n’ value for the tributary channels	0.69	0.01 – 30	0.69
v__EPCO.hru	Plant uptake compensation factor	0.83	0.01 – 1	0.83
a__OV_N.hru	Manning’s “n” value for overland flow	0.10	0.01 – 30	0.10
a__CANMX.hru	Maximum canopy storage (mm H ₂ O)	0.077	0 – 100	10.78
a__SLSUBBSN.hru	Average slope length (m)	75.11	10 – 150	75.11
a__HRU_SLP.hru	Average slope steepness (m/m)	-0.38	0.3 - 0.6	0.47
a_SOL_AW().sol	Available water capacity of the soil layer	-0.02	0 – 1	0.12
a_SOL_K().sol	Saturated soil hydraulic conductivity (mm/h)	515.59	0- 2000	515.59
a_CH_k2.rte	Effective hydraulic conductivity in main channel alluvium (mm/h)	192.66	0 500	85.56
a_CN2.mgt	Initial SCS runoff curve number for moisture condition II	6.35	35-98	92.13
a_CH_W2.rte	Average width of main channel at top of bank (m)	-2.97	0 – 1000	54.21
v__CH_K2.rte	Effective hydraulic conductivity in main channel alluvium (mm/h)	463.10	-0.01 - 500	467.39
v__LAI_INIT.mgt	Initial leaf area index	5.21	0 – 8	5.21
v__BIO_INIT.mgt	Initial dry weight biomass (kg/ha)	661.20	0 -1000	661.20
v__PHU_PLT.mgt	Total number of heat units or growing degree days needed to bring plant to maturity	2228	0 – 3500	2228

a_means absolute; given value is added to the existing parameter value during calibration; v_means replace; the existing parameter value is to be replaced by a given value during calibration and r-refers the default parameter values are multiplied by a factor of (1 + r).

The rainfall and monthly river discharge in Fig. 16 show that the model well captured the hydrologic processes within the watershed. Generally, Fig. 16 shows that the simulated flow reflected the observed flow. Further, the parameter values for NSE, PBIAS, and R^2 in Table 14 are 0.61, 0.59, and 0.68, respectively, for calibration; and 0.66, 0.54, and 0.67, respectively, during validation showed satisfactory results.

Table 14: Model performance statistics for the calibration and validation periods

Period	Average monthly flow (m ³ /s)		Evaluated statistics			
	Observed	Simulated	NSE	r-factor	PBIAS	R ²
Jan 1987-Dec 1993	19.16	17.23	0.61	0.56	10.1	0.68
Jan 1994-Dec 2000	14.06	15.06	0.66	0.69	3.3	0.67

The NSE value >0.5 , $PBIAS < \pm 10$ < $PBIAS < \pm 15$, and $R^2 \geq 0.6$ (Moriasi *et al.*, 2007; Santhi *et al.*, 2001) indicate that the model is acceptable for the hydrological simulations. In this regard, the calibrated SWAT model used in this study could efficiently and reliably be used in simulating the hydrological impacts of land-use changes in KWK watershed for 1993 to 2030 time-step.

4.2.3 The Impact of Land Cover Changes on the Hydrology of the Kikafu, Weruweru and Karanga Watershed

The influence of land cover changes on the hydrology of a watershed is indicated using changes in vegetation that signify changes in Curve Number (CN) in different decades. Decrease in forest area and changes in other vegetation changes in CN of a watershed. Studies show that increases in built-up area and increase in population decrease vegetation cover (Kundu *et al.*, 2017). Continuous demand for space and other natural resources can influence people to shift and settle in forested areas, which will result in forest degradation and increased surface runoff in these areas.

Generally, the results of the impact of land cover changes on the hydrology of the KWK watershed showed that the LC fluctuations in the catchment for the past 25 years (1993-2018) impacted the annual basin water balance component values (Table 15). The results show higher annual variation in GWQ as compared to LatQ and WatQ. The predicted LC changes of 2030 will result in lower values for almost all selected hydrological parameters than in previous years (1993-2018). It is expected that expansion in agricultural land and built-up areas, reduction of grassland and shrubland increases SurfQ and streamflow and consequently reduces GWQ (Marhaento *et al.*, 2017). Furthermore, the correlation among hydrological components was also

studied (Table 15). The results show a relatively high positive correlation among the hydrological components at varying degrees. Ideally, the results suggest that changes in one hydrological component result in the change in the value of other components.

Table 15: Area land-use change, annual basin values (mm) for different consecutive years in the study area (Note: Rocky surface and Glacier ice were not used in this analysis)

LU	Selected areal LC classes (%)								Annual basin values (mm)				
	BULT	AGRL	WATR	FORR	BARR	GRSL	WTL	SHRL	SurfQ	LatQ	GWQ	ET	WatQ
1993	4.38	11.63	1.44	33.08	11.17	23.18	2.93	5.89	295.39	38.86	168.93	502.0	513.00
2006	6.47	17.68	1.54	31.01	9.23	19.97	2.28	5.03	275.69	38.97	176.28	492.0	512.17
2018	10.34	23.29	1.54	31.13	4.58	16.96	1.44	4.20	345.23	36.3	205.91	571.2	672.29
2030	14.93	30.54	2.00	30.54	1.46	9.24	1.06	4.44	292.94	38.67	174.33	498.6	516.06

BULT-Built-up area, AGRL-Agriculture land, WATR-Water, FORR-Forest, BARR-Barren land, GRSL-Grassland, WTL-Wetland, SHRL-Shrubland, SurfQ-Surface runoff, LatQ-Lateral flow, GWQ-Groundwater flow, ET-Evapotranspiration, WatQ-Water yield

The exponential increase in annual values for the selected hydrologic parameters is observed between the 1993 and 2018 years. SurfQ increased by 16.87%, whereas GWQ also increased by about 21% between 1993 and 2018 years. Likewise, WatQ has also increased exponentially from 1993 to 2018 and is expected to decrease in the near future (2030). Values show a decrease of about 0.2% between 1993 and 2006 and a sharp increase of approximately 31.3% from the year 2006 to 2018 and is expected to decrease by 23.2% by 2030. However, despite this increase, LatQ was observed to exhibit an almost negligible rise between 1993 and 2006, while it shows a slight increase between 2018 and 2030, meaning that the impact of LU changes on lateral flow is minimal.

The results show that land cover has changed throughout the study period within the catchment, previous studies also show that land use has changed on the entire slopes of Mt. Kilimanjaro (Mbonile *et al.*, 2003; Misana *et al.*, 2012; Soini, 2005a; Stump & Tagseth, 2009; Tagseth, 2008). The possible reasons for the escalation of agricultural land and the built-up area may be due to higher population growth rate and social-economic development such as the fair prices for horticultural crops in the lowlands. Thus, more people are engaging in growing crops in the catchment. Further, the influx of people from outside and highland areas has resulted in an increase of cropland and extension of the built-up areas to the lowland areas that were previously considered comparatively dry and less productive. Perhaps there could be experienced more decrease in the area under forest; however, most of the forest area falls in the upper area of the Kilimanjaro National Park, which is protected by the law. Although reports still show anthropogenic activities such as logging, forest burning, charcoal making, the establishment of new villages, livestock keeping and cultivation, landslides, and quarrying across the protected forest reserve (Lambrechts *et al.*, 2002). Also, the conversion of the lower montane forest into coffee plantation are among the factors contributing to forest loss (Gütlein *et al.*, 2017).

Despite the conservation activities, it is worth stating that there is still a flimsy decrease in the area of forest area, especially close to the forest borders and in the lowlands (Mbonile *et al.*, 2003). Thus, observation shows that the magnitude of variation in ET values is small despite the change in LC with time. However, monthly fluctuations in ET support that the model perfectly captures cropping season that is expected to have relatively higher ET values during vegetative stages; although in general agreement with the fact that seasonal crops (agricultural land) have less ET than perennial trees (Deng *et al.*, 2015; Woldeesenbet *et al.*, 2017). Studies show that

evapotranspiration takes a countable amount of water infiltrating the soil in semi-arid regions, and effective recharge depends solely on extreme rainfall events (Andersen, 2008).

The expansion of agricultural land, built-up areas, and shrinking of grassland may have resulted in increased surface runoff in the KWK watershed, especially in the lowlands. The changes in WatQ as a result of changes in vegetation is due to changes in CN values. The CN values increased with an increase in built-up areas, bare agricultural lands and decreased forest areas (Kundu *et al.*, 2017). Although the variation in land use results in changes in hydrological processes, the soil types, geological conditions, and slope are among the factors governing the impacts of land-use changes on the water balance components (Bruijnzeel, 2004). Thus, KWK being located on the mountain slopes is expected to be affected by these factors. Other studies reported a similar trend in the basin. For example, Kishiwa *et al.* (2018) predicted an increase in the annual streamflow by 10% in the year 2060 and steady growth in the streamflow annually, taking 2001 as a baseline year.

Generally, in a situation where most of the vegetation is converted to built-up areas and the expansion in agricultural land, compaction causes lower permeability and storage capacity resulting in a lower infiltration capacity. This transforms a substantial fraction of rainfall into surface runoff. The SurfQ and GWQ increases as the areas with cleared vegetation for agriculture and built-up areas increases. A similar observation was reported in South Africa, that SurfQ is higher and GWQ is lower in bare lands, with no vegetation (Gyamfi *et al.*, 2016); GWQ is higher in the forest and other vegetative places due to increased infiltration into the shallow and deep aquifers. Reduced infiltration increases surface runoff, which may be a reason for flood reoccurrence in lowland areas, especially at the beginning of the season, where there are no plants in the farms.

4.2.4 The Variations of Individual Land Cover Changes on Water Balance Components

Results of the Partial Least Squares Regression (PLSR) model of the hydrological components in the KWK watershed presented in Table 16 indicates a strong correlation between land cover changes and the variations in water balance components. That is, the cumulative explained variations in Y, and Q^2 cum corresponds to the correlations between the explanatory (X) variable (Land use) and dependent (Y) variables (Water balance components), with the components are all close to 1. Variation in the hydrological components (Cum explained variation in Y (%)) were

94.1%, 96.8%, and 98.6% for component number 1, 2 and 3, respectively. These high correlation values indicate that the PLSR model captured well both the X and the Y variables.

Table 16: Results of the partial least squares regression model of the hydrological components in the Kikafu, Weruweru and Karanga watershed

Response Variable Y	Variation in response	Q²	Comp	Explained variation in Y (%)	Cum explained variation in Y (%)	Root Mean PRESS	Q² Cum
Hydrological components (ET, WatQ, SurfQ, GWQ, LatQ)	0.951	0.901	1	94.1	94.1	0.272	0.9953
			2	2.7	96.8	0.432	0.9926
			3	1.8	98.6	0.561	0.9937
			4	1.4	100	0.624	0.9481

The PLSR variable importance of the projected values (VIP) and weights of the independent variables are given in Table 17. The highest VIP value was obtained in agricultural land (VIP = 1.57); built-up area (VIP = 1.28), barren land (VIP = 1.13), shrubland and grassland (VIP = 1.10). It can be noted from Table 17 that forest has a comparatively lower influence in impacting the selected water balance components (VIP 0.89). Nevertheless, the forest is still important in influencing water balance components, whereas wetland and water were of minor importance. The relative importance of predictors (VIP) shows that water and wetland exert comparatively less significance (VIP less than 0.8). Component 1 was dominated by agricultural land and built-up areas on the positive side, whereas water, forest, barren land, grassland, wetland and shrubland were on the negative side. In component 2, all land use/cover classes were negative sided except forest, which was on the positive side. Component 3 was also dominated by the negative sided classes except for forest and grassland, while the positive side included water, barren land, wetland and shrubland, agricultural land and built-up areas.

Table 17: Variable importance for the projection values and partial least squares regression model weights for independent variables in the Kikafu, Weruweru and Karanga watershed

Variable	VIP	w*1	w*2	w*3
BUILT	1.28	0.316	-0.878	0.444
AGRL	1.57	0.445	-0.597	-0.449
WATR	0.69	-0.374	-0.742	-0.491
FORR	0.89	-0.465	0.371	0.913
BARR	1.13	-0.325	-0.410	-0.337
GRAL	1.10	-0.386	0.324	0.493
WETL	0.65	-0.206	-0.236	-0.3530
SHRL	1.11	-0.228	-0.264	-0.4818

4.2.5 Hydrological impacts of individual land cover changes on the selected water balance components

The areal changes under built-up, agriculture, as well as water positively attributed to the changes in Evapotranspiration (ET), Surface runoff (surfQ), Water yield (WatQ), groundwater flow (GWQ) as well as lateral flow (LatQ) (Table 17). The correlation coefficient values for the built-up area for all water balance components ranged from 0.89 to 0.94. Specifically, for agricultural land, the correlation coefficient values were 0.79 (ET), 0.86 (SurfQ), 0.85 (WatQ), 0.94(GWQ), and 0.86 (LatQ). Furthermore, water surface coverage was slightly positively correlated to SurfQ (0.54), WatQ (0.54), GWQ (0.69) as well as LatQ (0.54). In contrast, the change in SurfQ was negatively attributed to changes in the areas under barren land (0.96), grassland (0.86), wetland (0.90) and shrubland (0.86). Water yield, on the other hand, is negatively attributed to the areal

changes in barren land (0.96), grassland (0.86), wetland (0.89) and shrubland (0.86). The GWQ is slightly negatively attributed to changes in the forest area (0.62), but, highly attributed to changes in the areas of barren land (0.99), grassland (0.94), wetland (0.97), and shrubland (0.94). Similarly, the change in latQ was negatively attributed to changes in the areas of grassland (0.86), wetland (0.89), shrubland (0.86) as well as barren land (0.96). On the other hand, ET was negatively attributed to changes in the areas under barren land (0.92), grassland (0.79), wetland (0.84), and shrubland (0.79). Although Glacier ice is one of the land-use types, it is worth mentioning that the contribution of the snow was not taken into account as a contributor to the annual runoff. The motive behind this decision is that previous studies suggest the absence of isotopic signatures in springs and river discharges (Mckenzie *et al.*, 2010). Further, the rocky surface was also omitted during VIP tests.

Water balance is and has been a critical component to be understood in carrying water management issues skillfully. In this study, changes in the area under natural vegetation such as forest, shrubland, wetland, and grassland were negatively correlated with SurfQ at varying degrees (Table 18). These land covers were found to be in the decreasing trend (Table 15). These correlation results in Table 18 would mean that improving the vegetation cover on the hillside and abandoned land area could help to reduce the direct surface runoff in the KWK watershed. In turn, improving vegetation on the hillside will help reduce flooding recurring in the area, affecting most of the people in the lowlands. Most of the previous studies have shown that an increase in vegetation cover, particularly forests, leads to decreasing SurfQ and flood occurrence (Gashaw *et al.*, 2018; Shawul *et al.*, 2019). According to Siriwardena *et al.* (2006) clearing of forest by 45%, increased the SurfQ by around 40%. Also, increased in runoff due to replacing rangeland through expansion in agriculture land and built-up areas was reported from 2000 to 2013 in the Olifants basin, south Africa (Gyamfi *et al.*, 2016).

Increased ET and increased runoff may be a result of the conversion of vegetated areas to agriculture and built-up areas. However, the increased agricultural lands lead to higher water abstraction (Wagner *et al.*, 2013). This increase might be the reason for the slight decrease in ET in the near future (Table 15). Increased SurfQ due to increased built-up area was reported in some previous reports (Du *et al.*, 2012; Tavakoli *et al.*, 2014). Therefore, it is envisaged that the observed reduction in ET reflects the conversion to agricultural lands, which increases water use. Also, conversion to agricultural land increases the CN value, thus and reducing ET. Memarian *et al.* (2014) also observed that an increase in a built-up area and agricultural land increases CN, thus reducing ET.

Further, an increase in cultivated lands at the expense of other vegetation covers resulted in increased runoff was also reported by Gashaw *et al.* (2018) in the Andassa watershed, Blue Nile Basin, Ethiopia, Woldesenbet *et al.* (2017), and Karamage *et al.* (2017) in Rwanda. Contrary to these results, Twisa *et al.* (2020) in the Wami Ruvu basin revealed a negative influence on surface runoff and water yield by natural forest, woodland, bushland, grassland, water, and wetland. Further, the study reported a negative influence of the built-up area on GWQ and ET. At the same time, natural forests, bushland, woodland, grassland, water, and wetland had a positive influence on ET and GWQ. However, KWK being located on a mountainous place with complex terrain is expected to behave differently from other catchments.

Agricultural land and built-up areas are the main attributes in the changes in WatQ, SurfQ, ET, and GWQ; the expansion in these LULC classes means that with the ongoing expansion in agricultural land and built-up areas, the water balance of a watershed will be affected negatively. This observation supports Anand *et al.* (2018) report, stating that the intensification of urban and cultivated lands is an essential environmental stressor that significantly affects water balance components of a catchment. For instance, an increase in the built-up area has a contribution to a higher proportion of surface runoff and streamflow and lowers the quantity of groundwater flow (Marhaento *et al.*, 2017).

Generally, the increase in runoff may imply increasing soil erosion and sedimentation if left unattended. Twisting land use trends to allowing more vegetation covers will reduce wet season flow, increase dry-season flow, SurfQ, LatQ and GWQ (Gashaw *et al.*, 2017). Techniques such as replacing cereals with fruit trees, intensifying agronomic practices that will advocate increasing productivity of small farms and discourage opening up of more land for agriculture. Further, using soil and water management practices may be useful to increase vegetation cover at the KWK watershed.

The PLSR results in Table 18 show that all land use/cover classes are important in influencing changes in water balance components, with the exception of shrubland and wetland. Thus, regulation of other LC classes should be implemented to regulate the impacts in the hydrology of KWK watershed. The current reported rapid population growth, climate change and expansion in agricultural land, built-up areas, and other economic activities can significantly impact the future if the situation goes unattended (Garcia & Alvarez, 1994; Mondal, 2019). The PLSR results from this study are suitable for designing and carrying out sustainable natural resources management practices at the basin scale and other similar environments (FAO, 2017). Moreover,

the results from this study show the potential of using a combined PLSR and hydrologic modelling framework for impact studies in data-constrained environments.

Table 18: Correlation matrix for the land cover variables and selected hydrologic components

Variables	BUILT	AGRL	WATR	FORR	BARR	GRASL	WETL	SHR	ET	SurfQ	WatQ	GWQ	LatQ
BUILT	1.00												
AGRL	0.98	1.00											
WATR	0.80	0.89	1.00										
FORR	-0.74	-0.85	-0.99	1.00									
BARR	-0.99	-0.97	-0.76	0.69	1.00								
GRASL	-0.98	-1.00	-0.89	0.85	0.97	1.00							
WETL	-0.99	-0.99	-0.85	0.80	0.99	0.99	1.00						
SHR	-0.98	-0.99	-0.89	0.85	0.97	1.00	0.99	1.00					
ET	0.89	0.79	0.44	-0.35	-0.92	-0.79	-0.84	-0.79	1.00				
SurfQ	0.94	0.86	0.54	-0.46	-0.96	-0.86	-0.90	-0.86	0.99	1.00			
WtrQ	0.94	0.85	0.54	-0.45	-0.96	-0.86	-0.89	-0.86	0.99	1.00	1.00		
GWQ	0.99	0.94	0.69	-0.62	-0.99	-0.94	-0.97	-0.94	0.95	0.98	0.98	1.00	
LatQ	0.94	0.86	0.54	-0.46	-0.96	-0.86	-0.89	-0.86	0.99	1.00	1.00	0.98	1.00

Significant value at $p=0.05$, SurfQ =surface runoff, LatQ =Lateral flow, GWQ =ground water flow, ET =Evapotranspiration, WtrQ = total water yield

4.3 The Impacts of the Present and Future Land-Use Changes on Water Quality

In this objective, the main targets were: (a) to carry out water sampling (b) to assess the water quality during the dry season (June to July), due to excessive varied requirements and utilization of scarce water resources (Marghade *et al.*, 2020). Table 19 shows the analytical findings of physicochemical and isotopic parameters from surface and groundwater sources assessed in this study. The main focus was to assess the water suitability for irrigation application, However, descriptive statistics were computed and addressed in Table 20, where Tanzania (TZS) limits and the World Health Organization (WHO) guideline were used to highlight the general drinking water suitability of all tested sources.

Table 19: Analytical results

Source	Code	Depth	DO	Temp	pH	TDS	EC	NO ₃	SO ₄	Ca	Mg	Cl	HCO ₃	K ⁺	Na ⁺	F ⁻	¹⁸ O	² H	d-excess
Weruweru River (WR)	WS1	2.2	6.2	20.3	6.75	94	141	6.6	7	8.8	5.1	10	40	2.5	11	4.14	-4.81	-23.57	14.93
	WS2	1.5	7.1	23.5	6.78	111	166	8.4	10	11.2	4.5	13	39	2.6	15	4.82	-4.72	-22.95	14.77
	WS3	3.1	4.9	25.5	6.73	124	186	16	9	11.8	5.2	8	57	4.5	16	4.72	-4.46	-21.93	13.75
	WS4	1.6	6.3	25	6.74	314	468	12.8	23	32	11	33	155	5.8	46	4.63	-3.69	-16.28	13.22
	WS5	1.0	5.9	28.4	6.94	310	463	17.5	25	40	7.5	30	148	7.4	40	5.5	-4.11	-17.85	15
Karanga River (KR)	KAS1	1.2	3.8	23.3	6.57	319	476	11.3	37	43	9.6	45	97	6.8	36	4.7	-3.48	-16.53	11.6
	KAS2	0.4	7.3	23.8	6.55	250	373	9.7	19	21.4	7.4	39	84	7	42	4.79	-3.5	-16.5	11.53
	KAS3	0.3	5.5	25.2	6.52	350	522	17.3	40	45	11.5	51	95	6.9	41	5.3	-3.51	-16.23	11.86
	KAS4	1.1	4.8	25.4	6.66	279	417	18.4	33	31	8.5	29	101	5.6	40	4.23	-3.18	-14.39	11.06
	KAS5	0.8	6.4	25.9	6.70	458	684	27.9	60	67	14.3	60	122	7.1	47	4.27	-3.35	-15.91	10.86
Kikafu River (K'R)	KIS1	1.0	6.3	29.8	6.80	720	1074	39.1	64	95	36.2	96	256	15.4	58	9.89	-3.73	-17.79	12.03
	KIS2	2.1	5.4	25.2	6.60	168	251	10.8	26	26	4.6	19	43	3.3	16	2.38	-3.68	-15.77	13.71
WR Confluence before	WSX	1.1	5.0	28.0	6.74	405	605	24	32	66	11	72	95	7.7	35	6.79	-4.06	-19.78	12.73
KR Confluence before	KASX	1.2	4.2	27.5	6.69	587	876	25.3	55	85	15.5	76	222	9.4	66	6.43	-3.7	-18.04	11.56
WR+K'R Confluent	KWUSX	0.7	5.4	28.3	6.71	531	794	37.5	48	65	13.6	52	231	11.1	73	7.02	-3.82	-18.56	11.99
WR+KR+K'R Confluence	KWK1	2.3	5.5	28.1	6.64	800	1194	19.4	70	122	30.5	89	382	10	68	7.42	-3.58	-17.23	11.41
Shallow Wells along WR	WSW1	8.0	3.3	27.5	6.77	1480	2212	95	134	24.6	13.7	140	684	36	190	2.46	1.79	3.71	-10.58
	WSW2	5.0	2.9	25.9	6.56	684	1021	51.8	64	88	27.7	77	255	11	73	10.4	-3.84	-21.11	9.59

Source		Code	Depth	DO	Temp	pH	TDS	EC	NO ₃	SO ₄	Ca	Mg	Cl	HCO ₃	K ⁺	Na ⁺	F ⁻	¹⁸ O	² H	d-excess
Boreholes Town	Moshi	BG1	120	0.2	22.3	6.45	429	641	19.8	27	66	5.4	65	160	6	55	5.22	-4.44	-21.59	13.9
		CG	120	0.4	29.1	6.84	294	439	10.3	17	39	9.2	44	119	4.6	35	4.35	-5.18	-27.48	13.99
		IG1	80	0.7	22	6.68	282	422	16.8	21	47	4.7	40	100	5	29	4.07	-4.3	-20.4	13.98
		KVG1	60	1.0	28	6.28	183	273	26	13	21	5.4	24	48	3.2	26	2.04	-3.73	-15.54	14.26
Boreholes K'R	along	KGS1	120	0.2	25.2	6.70	602	898	33.7	36	90	20	68	289	14	53	4.98	-3.73	-17.79	12.03
		KGS2	110	0.1	25.2	6.63	456	680	30.5	29	65	17.7	58	188	8.7	41	3.3	-3.68	-15.77	13.71
Boreholes TPC	within	TG1	80	0.3	26.4	6.78	1170	1749	54.7	75	190	50.3	129	582	14.1	76	7.39	-3.82	-18.47	12.12
		TG2	90	0.2	25.4	6.67	1670	2493	45.5	143	242	87	199	763	12.5	123	5.25	-3.62	-17.16	11.76
		TG3	70	0.3	26.5	6.68	1916	2860	59.5	193	288	52	306	566	16.8	212	9.12	-3.72	-17.75	12.04
Boreholes along WR		WSG1	130	0.1	24.6	6.71	380	568	28.9	26	44	7.2	38	176	6.2	61	7.33	-4.2	-18.93	14.69
		WSG2	80	0.4	28.8	6.08	182	272	8.6	9	20.4	2.7	37	43	5	30	5.13	-4.1	-18.87	14.43
Boreholes from Kahe flood plain		S01	120	1.16	24.3	6.57	222.6	347.8	5.9	18	42.7	15.3	9.3	167	0.09	1.82	0.22			
		S02	125	1.68	24.7	7.16	174.9	273.2	2.8	13	28.6	6.2	20.5	97.4	3.1	15.4	0.2			
		S03	118	1.8	24.7	6.72	224.9	351.4	18.5	17	30.5	11.7	15.8	132	2.4	22	0.24			
		S04	12.6	2.6	24.1	8.41	759.6	1186.8	88	55	118	31.7	50	420	11.9	67.3	0.87			
		S05	115	1.91	23.2	7.21	391.0	610.9	21.6	29	64	15.7	32	234	4.8	32.8	0.33			
		S06	7.3	4.53	25.1	7.98	993.3	1552	3	48.9	138	59.8	29.18	887	9.48	80.31	0.71			
		S07	6.8	1.13	25.4	7.82	1172.9	1832.6	5.1	32.9	180	64	11.7	1166	22.58	76	1.57			
		S08	6.2	1.16	23.1	7.28	531.7	830.8	23	48	101	32	65	246	3.6	11	0.32			
		S09	14.5	1.03	23.7	7.19	791.3	1236.5	30	95	136	47	83	362	4.6	36	0.41			

Source	Code	Depth	DO	Temp	pH	TDS	EC	NO ₃	SO ₄	Ca	Mg	Cl	HCO ₃	K ⁺	Na ⁺	F ⁻	¹⁸ O	² H	d-excess
Boreholes from Kahe flood plain	S10	8.2	1.96	24.3	7.91	299.7	468.3	13	18	50	11.9	29	181	5	23	1.03			
	S11	11.8	4.38	24.7	8.11	507.0	792.1	15.7	51	88	14	58	245	15.5	40	0.78			
	S12	9.3	4.53	24.2	6.71	248.5	388.2	12	11	45	10	17.1	177	7	12.3	0.78			
	S13	16.9	3.78	26	8.05	635.3	992.7	52	12.9	51	31	71	370	11	105.6	0.59			
	S14	10.9	1.49	24.8	7.83	451.5	705.5	18.2	22	20.23	63	5.63	400	8.78	20	0.45			
	S15	13.8	1.21	23.5	8.02	84.2	131.6	7	3	13.4	7.2	4.6	60	0.3	1.2	0.38			
	S16	8.7	2.62	25.3	7.39	124.8	195	4	8	17.2	6.4	2	107	1.7	12	0.23			
	S17	10.3	2.6	24.6	6.69	504.1	787.7	62	11	94	26	16.7	378	2	22	0.57			
	S18	8.6	2.83	26	7.72	456.8	713.8	14	32	103	8.9	32	311	0.7	25	0.59			
	S19	9.7	4.21	27.8	7.41	154.6	241.5	8.6	6	22	8	7	121	2.7	13.2	1.3			
	S20	13.1	3.4	26.8	7.12	189.1	295.5	5	9	28	12	11	146	2	12	1.61			
	S21	22.6	3.78	26.5	6.87	335.7	524.6	5.8	7.9	46	12.3	3.36	330	5.5	40	1.43			
	S22	15.6	3.82	21.9	7.8	279.9	437.4	7	14	51	15.4	14	222	1.8	11.3	1.04			
	S23	17.7	3.69	25.6	7.96	441.4	689.7	26	44	73	26.3	30.2	255	3	23	0.77			
	S24	8.1	3.72	25.2	6.97	898.8	1404.4	43	60	162	50	74.8	560	3.8	39	0.3			
All units are in mg/l except depth (m), Temp (°C) ¹⁸ O (‰), ² H (‰) d-excess (‰), pH (unitless), electrical conductivity (μS/cm)																			

Table 20: Descriptive statistics water quality with drinking guideline

Parameter	Descriptive Statistics			Tanzania Standards	WHO Guideline
	Max	Min	Mean	Drinking (TZS:789 - 2018)	Drinking (2011)
Depth	130.0	0.3	33.8	-	-
DO	7.3	0.1	3.1	-	-
Temp	29.8	20.3	25.3	-	-
pH	8.4	6.1	7.0	5.5 - 9.5	6.5 - 8.5
TDS	1916.0	84.2	495.5	1500	1000
EC	2860.0	131.6	754.2	2500	-
NO ₃	95.0	2.8	24.0	45	50
SO ₄	193.0	3.0	37.8	400	250
Ca	288.0	8.8	69.7	150	-
Mg	87.0	2.7	20.3	100	-
Cl	306.0	2.0	49.3	250	250
HCO ₃	1166.0	39.0	257.7	-	-
K	36.0	0.1	7.2	-	-
Na	212.0	1.2	44.7	200	200
F	10.4	0.2	3.2	1.5	1.5
¹⁸ O	1.79	-5.18	-3.7	-	-
² H	3.71	-27.48	-17.8	-	-
d-excess	15	-10.58	12.0	-	-

4.3.1 The General Insight from Water Samples and Physical Parameters

The depth parameter in surface water samples was defined as the vertical distance at an average central river water surface to halfway middle the water body from riverbeds. Depth in groundwater sources was the well maximum drilled underground length from the earth's surface (the information was extracted from well drilling reports). All water sources presented a mean depth value of 33.8 m, where surface water sources had a 0.3 - 3.1 m depth range, and groundwater depth obeyed 5 - 130 m margin. Depth in all water sources influenced Dissolved Oxygen (DO) concentration, where higher DO values ranged from 3.8 to 7.3 mg/L and 0.1 to 3.3 mg/L for surface-water and groundwater sources, respectively. The mean pH value was 7.0, with a maximum of 8.4 and a minimum of 6.1 values. Electric conductivity (EC) and Total Dissolved Solids (TDS) had mean values of 754.2 mg/L and 495.5 µS/cm. Nitrate values ranged from 2.8 to 95 mg/L with a mean value of 24.0 mg/L.

4.3.2 Water Classification and Hydrogeochemical Facies

Other major cations and anions are presented in the Piper diagram (Fig. 17). Piper diagram was used to graphically represent the chemistry of groundwater samples in the study area (Piper, 1944; Sadashivaiah *et al.*, 2008; Srinivas *et al.*, 2014). It comprises three plots: A ternary diagram in the lower left representing the cations, another ternary diagram in the lower right representing the anions, and a diamond plot in the middle representing a combination of the two ternary diagrams. The diagram was mainly employed to understand and identify different water compositions or types through chemical relationships among ground and surface water samples (Utom *et al.*, 2013). Overall analyses show that most groundwater samples belong to sodium bicarbonate type (NaHCO_3 enrichment) and Mixed CaNaHCO_3 type. Sodium bicarbonate indicates the presence of minerals such as bentonite, biotite, muscovite, and illite, which form the bedrock of the study area (Chegbeleh *et al.*, 2020). By comparison, most surface waters belong to Ca-HCO_3 type, mixed CaNaHCO_3 type with small component of NaCl type. These results suggest the presence of ground-surface water interaction. Other studies reported similar Sodium and Magnesium dominance in groundwater types in Arusha (Chacha *et al.*, 2018; Ghiglieri *et al.*, 2012) and Kilimanjaro aquifers (Mckenzie *et al.*, 2010).

As stated earlier, most groundwater sources belong to the NaHCO_3 water type. However, the arrow pointing from the blue to the red circle of the Piper diagram (Fig. 17) shows the shifting in groundwater quality. Some of the deep groundwater sources become polluted with water from agricultural activities. Thus, most groundwater sources resembling surface water, indicating ground-surface water interaction with the likelihood of groundwater pollution due to small to large scale agricultural activities. The first end member is (shown using the blue circle) represented by long residence water whose class is driven by rock-water interaction (the Na-HCO_3 type), where one of the shallow wells is NaCl type water type with high salinity. Salinity might have accumulated from the prolonged dissolution of salts from irrigation activities.

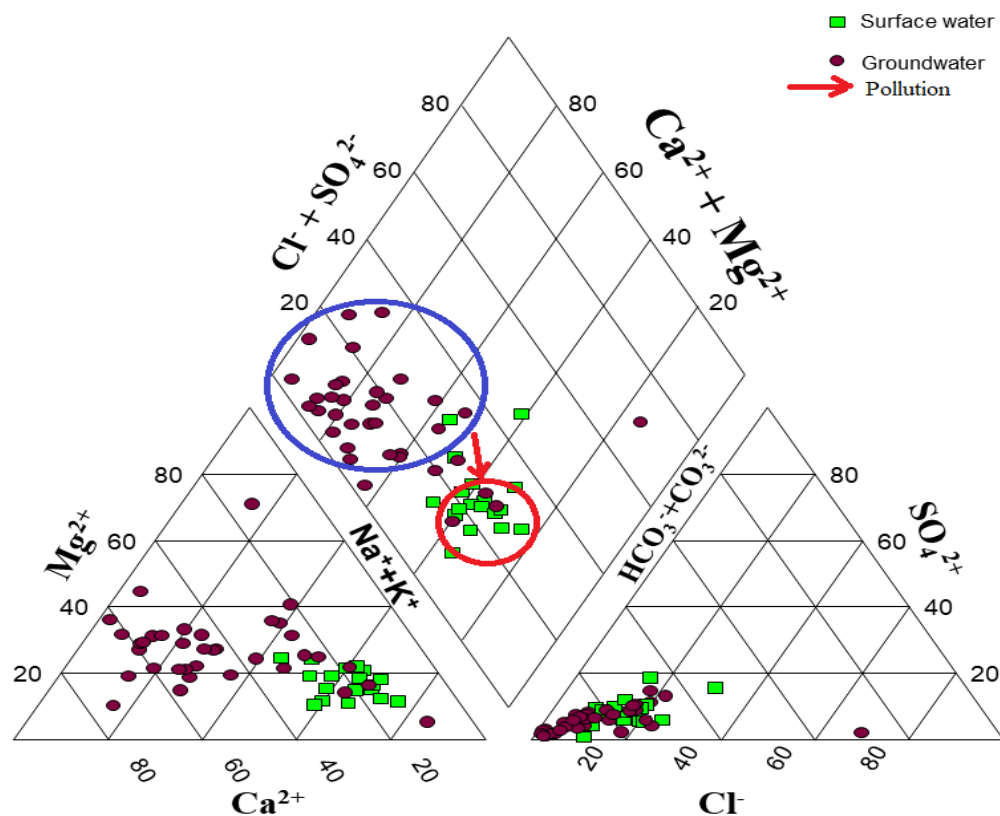


Figure 17: Piper diagram for the chemical composition of surface and groundwater sources

4.3.3 Hierarchical Cluster Analysis of Water Sources

Cluster analysis aims to identify the spatiotemporal similarity of different datasets. The CA helps to interpret a large number of data and indicate the similarity/ dissimilarity of different datasets. Euclidean distance measure was used for measuring the distance among the data samples to find the similarity among the dataset. The final grouping is presented by a dendrogram with a similar hydro-geochemical composition (Fig. 18). In hierarchical clustering, clusters are performed sequentially by starting with the most similar pair of objects and performing higher clusters step by step.

The samples from 54 sampling points were clustered into two main categories/clusters (Clusters I-II) which divided into sub-clusters as depicted in Fig. 18. Generally, HCA assigns the samples from the same region into the same cluster. Cluster 1 constitutes of 22.2% of the total samples and is dominated by groundwater samples (83.3%) and 16.7% surface water. Cluster II is the largest of all the clusters and contains 50% of all the water samples and has 55.6% ground and 45.4% samples from rivers. Cluster III contains 90% groundwater, the groundwater samples in

Cluster III are mostly of Ca-HCO₃ water type and account for 11.1% of the total samples. The distribution of the Cluster indicates the link with the geological setting, which accounts for different hydrochemical processes.

In terms of linkage distance, Cluster I comprises a total of 12 samples which indicated a linkage distance less than 1200; most of these are located in the lower part of the catchment. In cluster I, 10 samples were collected from deep wells, and only one sample from a shallow well and one sample was collected from the confluence of the three rivers. In cluster II, 26 samples with less than 1200 linkage distance (dissimilarity), whereas cluster III comprises ten samples, nine being deep wells (>100 m deep) and one shallow well. On the other hand, Cluster IV comprises all five deep well samples; cluster III and IV have less than 1800 linkage distance (dissimilarity). Generally, twenty-five sampling sites have revealed a similarity above 85% for all sampled groundwater in the dry and wet season.

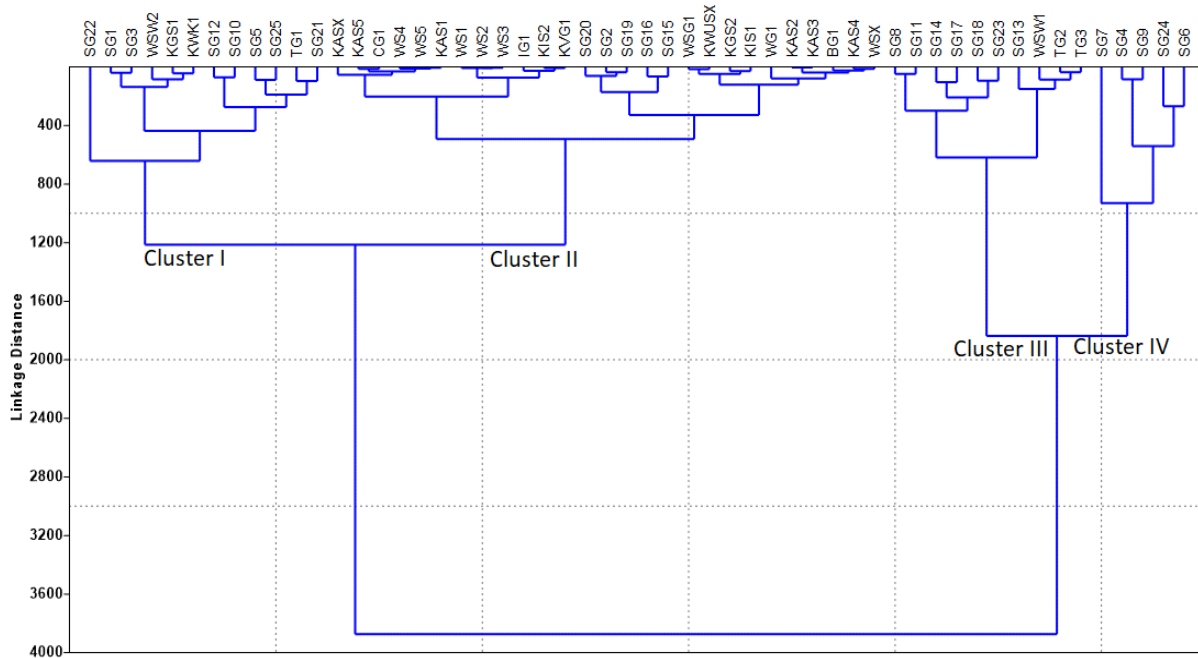


Figure 18: Dendrogram showing a spatial relationship among data collection sites

4.3.4 Origin of Groundwater Sources and Mechanism Controlling Geochemistry

The Gibbs (1970) plot based on ratios of $(\text{Na}^+)/(\text{Na}^+ + \text{Ca}^{2+})$ and $\text{Cl}^-/(\text{Cl}^- + \text{HCO}_3^-)$ as a function of the Total Dissolved Solids (TDS) show that most of the sample points are located in the central part of the plot. The Gibbs plots are useful in addressing water chemistry through the contribution dominance of rock-water interactions, precipitation and evaporation effects. The 38% of samples showed evaporation effect, 62% showed rock-water dominance effect, and none had precipitation features since all samples originate from dry season samplings. The central concentration of the samples reflects that the rock weathering is the dominant process, with a notable influence of evaporation precipitation/crystallization in controlling the geochemistry (Fig. 19). Furthermore, few samples lie on the atmospheric precipitation process. This indicates rock-water interaction dominance, and that groundwater quality is controlled by the chemical weathering of rocks and anthropogenic activities (Gautam *et al.*, 2015). The evaporation-precipitation mechanism may be influenced by high temperature and high humidity level.

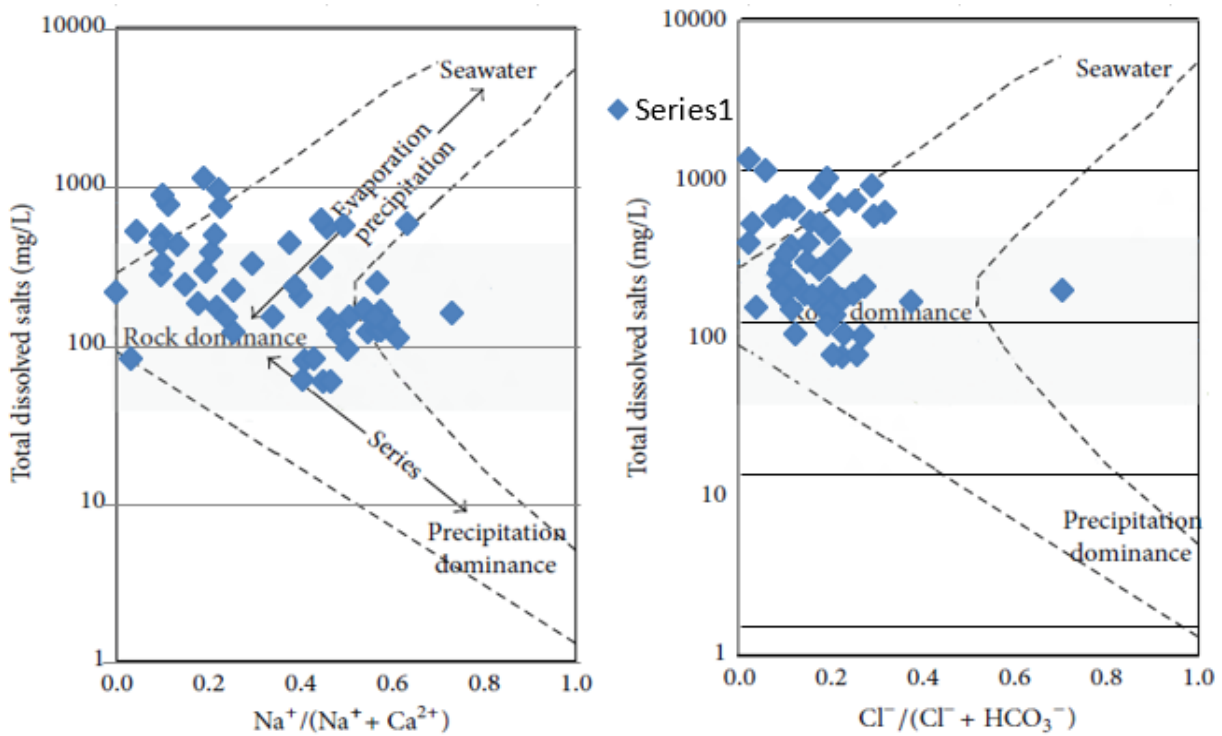


Figure 19: Gibbs plot for (a) Cations and (b) Anions

Figure 27 shows that evaporation is not a dominant effect in the study area as Na/Cl vs EC 's plot portrays variation in the Na/Cl ratio (with constant evaporation dominance effects) with an increase in EC (Jankowski & Acworth, 1997). Salve *et al.* (2008) delineated that decrease in

Na/Cl show alteration of sodium carbonate water through mixing and dissolution with sodium chloride, but chloride increase is from recharge activities. Rock-water interaction effect dominates the study area alerts on how anthropogenic water uses are excessive; this feature calls for immediate integrated water resources management plan to be in place and under operation. Many water chemistry ionic plots confirm that reverse ion exchange water process occurs; and at favourable exchange sites, i.e. Ca^{2+} and Mg^{2+} in the aquifer geology replace Na^+ .

Generally, according to the Durov plot (Fig. 20) the groundwater can be classified as sodium type, although few samples belong to the intermediate type. In terms of anionic classification, the water can be classified into bicarbonate type. The dominant hydrochemical process is Simple dissolution (mixing) and ion exchange. Thus, the geological setting of the area influences the groundwater chemistry. In terms of pH, the sampled groundwater sources has pH ranging from 6 to about 7.2. when the water samples are classified according to Total Dissolved Solids, 3 samples (about 8.3%) have TDS values between 600 and 500 mg/L, whereas 27.8% (10 samples) have TDS values between samples (300-500 mg/L), while majority of the samples (about 63.9%) of the samples possesses TDS values less than 300 mg/L.

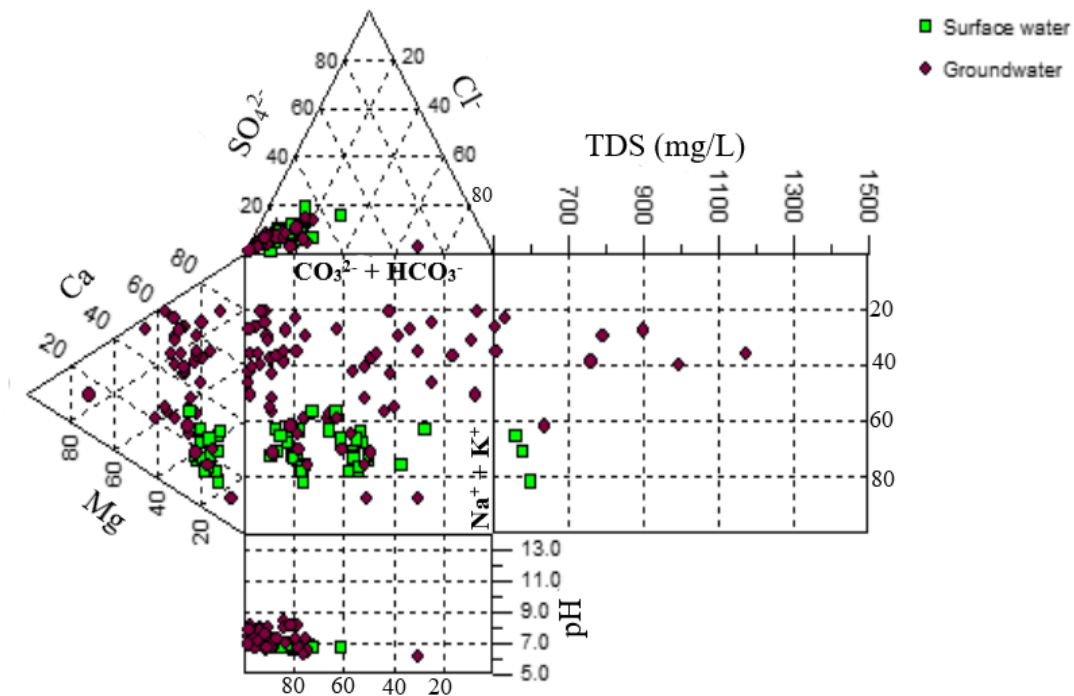


Figure 20: Durov plot for surface and groundwater samples

Surface water samples exhibit a slight different trend, while the samples show dominance as sodium type in terms of cationic classification, and bicarbonate type and mixed type in terms of

anions, one sample fall under chloride type. However, the dominant process is mostly simple dissolution, followed by ion exchange and reverse ion exchange taking only a few samples. This means surface and groundwater interact from upstream to downstream. The pH ranges from 6 to 8.5, and the Total Dissolved Solids for 9 samples (about 47.4%) has TDS ranging from 500-1200 m/L, and 52.6% of the samples had TDS less than 500 mg/L.

The primary ion constituents of the water samples (SO_4 , HCO_3 , Cl , Mg , Ca , Na) in the study area (meq/L) were plotted on a Schoeller diagram (Schoeller, 1965). This diagram shows a semi-logarithmic representation of the concentrations of the samples of the study area (Abbaspour, 2015). The sample concentrations are individually represented using points on six equally spaced lines; a line connects these points. The diagram in this study supports the Piper and Durov diagrams, which revealed Na , and Ca , and HCO_3 as dominant cations and anions, respectively (Fig. 21).

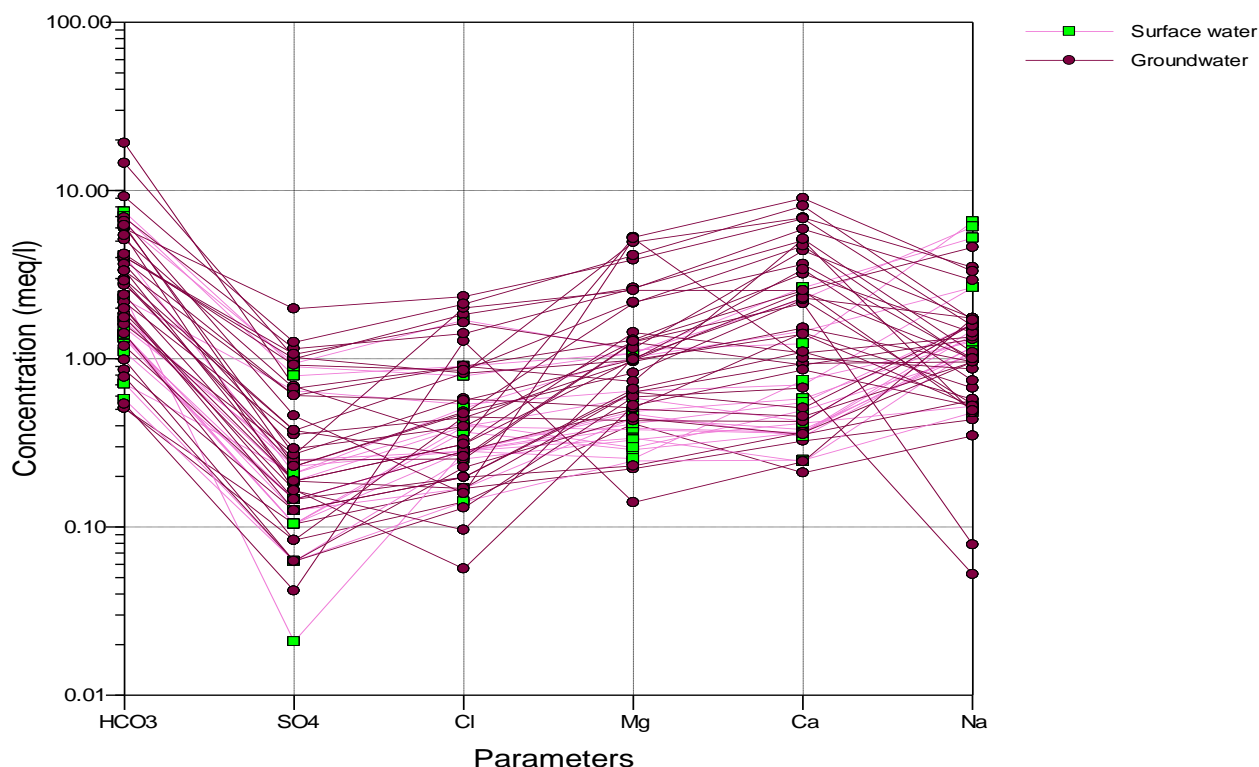


Figure 21: Schoeller plot of the water samples

4.3.5 Isotopic Analysis

The study area comprised two distinct topographical zones; the upper/highland zone (above 800 m.a.m.s.l) had rivers and few groundwater sources where the interaction of surface water and

groundwater was assessed with ^{18}O and ^2H isotopes. The lower/lowland zone (above 800 m.a.m.s.l) had no direct interacting surface water sources, and since it is a flood plain, groundwater recharges are significant at these locations. Isotope characteristics comprised three categories (surface, shallow and deep) of the upper part of the study area. Surface water sources had a maximum and minimum ^{18}O , ^2H and d-excess values of -3.18‰, -14.39‰, 15‰ and -4.81‰, -23.57‰, 10.86‰, respectively. Shallow well water sources had a maximum and minimum ^{18}O , ^2H and d-excess values of 1.79‰, 3.71‰, 9.59‰ and -3.84‰, -21.11‰, -10.58‰, respectively. Deep well (Borehole) water sources had a maximum and minimum ^{18}O , ^2H and d-excess values of -3.62‰, -15.54‰, 14.69‰ and -5.18‰, -27.48‰, 11.76‰, respectively. Isotopic observations and variation are expressed in Fig. 22; most water sources plot close to LMWL except for one shallow well that plots within GMWL. Both zones correspond to different aquifers, and hence their geology (Appendix 3) with controlled minerals during recharges sessions.

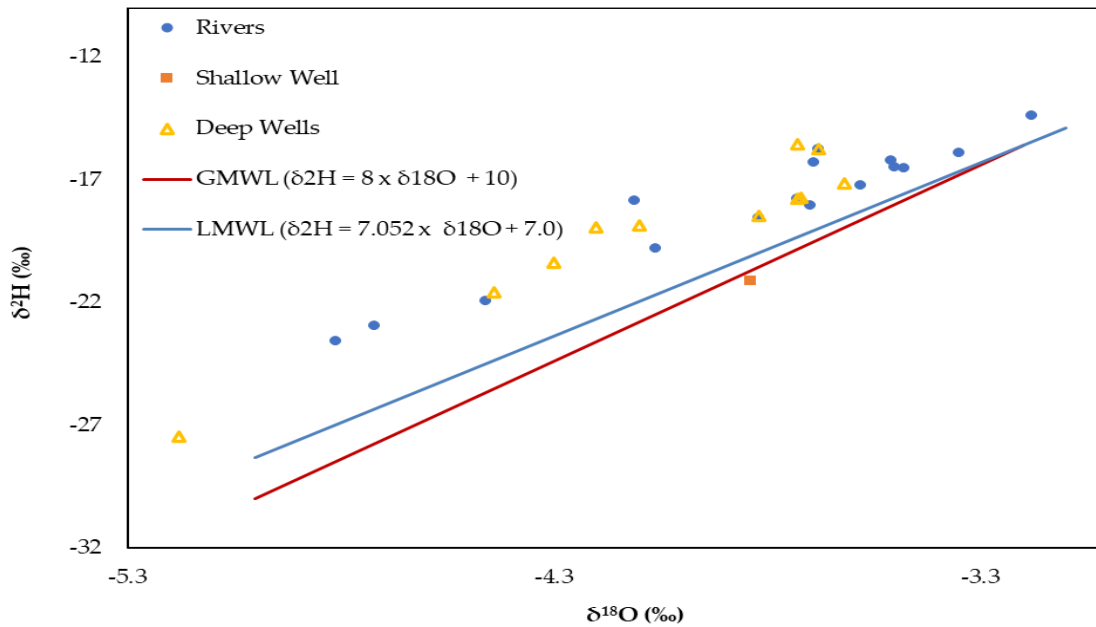


Figure 22: Observational plot of $\delta^2\text{H}$ and $\delta^{18}\text{O}$ for rivers, shallow well and deep wells with global and local meteoric water lines

Figure 22 shows rivers and deep wells plotting above LMWL and GMWL (except for shallow wells). This observation signifies that the sampling area is characterized by warm conditions (Kumar *et al.*, 2018) as the study was conducted during the dry season. Furthermore, such water sources are affected by the evaporation effect (Oyarzún *et al.*, 2015) that acted upon surface water sources, and their vapour masses recharged most of the sampled sources (Clark & Fritz,

1997), which led them to plot above GMWL. These observations prove that water from these sources is not exclusively a direct local rainfall originating from Mount Kilimanjaro, as values of $\delta^{18}\text{O}$ in this study are more depleted than average local rainfall values reported by Bodé *et al.* (2020). Groundwater and surface water have comparable stable isotope values; hence, the groundwater recharge in the study area may not originate from Mount Kilimanjaro's slopes as observed for Arusha city from the slopes of mount Meru (Lugodisha *et al.*, 2020). Thus, the local recharge occurs in the study area with intensive small- and large-scale agricultural activities. D-excess values for deep and surface water sources are above 10, signifying recycled moisture as a source of precipitation in the current water. Recycled moisture in the study area occurs due to a portion of the precipitation water that undergone evapotranspiration from Mount Kilimanjaro slopes and precipitated again before water contribution in the study area. Since $\delta^2\text{H}$ intercept of LMWL is less than that of GMWL, it can be concluded that no external recycled moisture was supplied in the region (Durowoju *et al.*, 2019). Contrasting, two shallow wells (one not shown in Fig. 22) plotted below LMWL and GMWL, which implied direct recharge from local rainfall. Their d-excess values were below ten that characterizes the excessive evaporation effect that has taken place (Oyarzún *et al.*, 2015). This is true as the study area has a micro-climate controlled by agricultural activities that may allow water evaporation and precipitation. Generally, $\delta^2\text{H}$ and $\delta^{18}\text{O}$ values confirmed that; groundwater in the dry season has similar properties to surface water along watercourses, and recycled water is the major recharge means. Contrary, a ten-year ice core study on Mount Kilimanjaro showed a maximum of -5.66‰ $\delta^{18}\text{O}$ (Thompson *et al.*, 2002), whereas the current study had a minimum of -5.18‰ for $\delta^{18}\text{O}$. This observation infers that, as the glacier melts during the dry season on Mount Kilimanjaro (Zawierucha & Shain, 2019), it sustains downstream water availability along the mountain's slope. As water moves from the upper forest to the lower forest of Mount Kilimanjaro, heavier isotopes are enriched following selective utilization of water with lighter isotopes for biotic (plants and animals) and abiotic (e.g. evaporation) activities (Ehleringer & Dawson, 1992). Thus, water reaching down slopes of Mount Kilimanjaro becomes relatively enriched on heavier isotopes than that at glacier origin and could account for another source of groundwater recharge in the study area, i.e. water from melting glacier. This observation is similar to GITEC (2011), which reported that apart from rainfall, glacier melting was another recharge mechanism in the same study area through upland subsurface inflow.

4.3.6 Multivariate Statistical Method

(i) Principal Component Analysis

In this study, Pearson's correlation coefficients between water quality parameters were calculated and presented in Table 21. Fifteen parameters (Temp, pH, TDS, DO, EC, NO₃, SO₄, Ca, Mg, Cl, HCO₃, CO₃, K, Na, F) were used for PCA/Cluster analysis (CA). Pearson correlation matrix (Table 21) was used to elucidate the relationship between analyzed parameters, where the strong correlations ($r > 0.5$, $p < 0.05$ for positive correlation, and $r < 0.5$, $p < 0.05$ for negative correlation) were observed in sampling depth and dissolved oxygen, major ions, as well as pH with fluoride. Principle component, PC (Table 22) loadings were evaluated from the correlation matrix and values from unity comprised a significant component to be used for water chemistry data correlation analysis. Component loading with at least 0.5 values was considered significant with respect to observed proportion/variance. The EC has a strong correlation with TDS and HCO₃ (>0.9). Also, EC has a good positive correlation with SO₄, Ca, and Mg (>0.8), and a good positive correlation with Cl (>0.7). The SO₄ has good correlation with Ca, HCO₃ (>0.8), and Mg (>0.6). Ca has a good positive correlation with Mg, HCO₃, and CO₃ (>0.8). Further, K has a good positive correlation with Na (>0.8). The pH has a reasonably positive correlation with CO₃ (>0.7). Also, DO has a negative correlation with CO₃ (>0.8) and Ca (>0.7). And a negative correlation with pH and TDS. The Mg has a strong correlation with TDS (>0.8), EC, Ca (>0.8) and SO₄ (>0.7).

Table 21: Pearson correlation matrix for studied samples

Parameters	pH	TDS	DO	EC	NO ₃	SO ₄	Ca	Mg	Cl	HCO ₃	CO ₃	K	Na	F
Temp														
pH	1													
TDS	0.45	1												
	-	-0.58	1											
DO	0.69													
EC	0.43	0.99	-0.55	1										
NO ₃	0.10	0.48	-0.13	0.49	1									
SO ₄	0.47	0.86	-0.53	0.86	0.48	1								
Ca	0.60	0.90	-0.72	0.89	0.39	0.85	1							
Mg	0.55	0.88	-0.63	0.87	0.37	0.79	0.87	1						
Cl	0.22	0.74	-0.39	0.74	0.57	0.69	0.62	0.48	1					
HCO ₃	0.48	0.96	-0.56	0.96	0.41	0.82	0.90	0.91	0.57	1				
CO ₃	0.75	0.66	-0.82	0.64	0.18	0.62	0.81	0.76	0.30	0.72	1			
	-	0.44	0.04	0.45	0.20	0.28	0.13	0.19	0.43	0.38	-0.07	1		
K	0.01													
Na	0.03	0.56	0.07	0.58	0.34	0.37	0.27	0.27	0.51	0.50	-0.05	0.81	1	
	-	-0.34	0.71	-0.31	-0.13	-0.42	-0.56	-0.49	-0.20	-0.34	-0.67	0.34	0.37	1
F	0.58													

Significant correlation, $r > 0.5$; Yellow highlight colour = negative correlation; Green highlighted colour = positive correlation

Kaiser-Meyer-Olkin (KMO) and Bartlett's sphericity tests were performed on the parameters correlation matrix prior to PCA in order to examine the validity of PCA. The KMO results show that PCA could be useful to reduce dimensionality (Fig. 21) as all the values are close to 0 at 99.95 significance levels. Principal components were identified, corresponding to eigenvalues greater than 1 (Table 22). Principal component loadings are classified as strong, moderate, and weak, corresponding to absolute loading values of (>0.9 , >0.9 , >0.9).

Table 22: Principal component loadings of analyzed data

Parameters	PC 1	PC 2	PC 3
Depth	0.06	0.03	-0.94
DO	-0.27	0.31	0.83
Temp	0.27	0.49	0.19
pH	0.00	-0.79	0.33
TDS	0.99	-0.09	0.02
EC	0.99	-0.11	0.03
NO ₃	0.69	0.12	0.05
SO ₄	0.91	0.13	0.01
Ca	0.85	-0.22	-0.09
Mg	0.75	-0.44	0.05
Cl	0.88	0.27	-0.14
HCO ₃	0.78	-0.46	0.13
K ⁺	0.76	0.15	0.22
Na ⁺	0.90	0.21	0.05
F ⁻	0.35	0.79	0.00
Eigen value	7.61	2.24	1.80
Difference	5.37	0.43	0.94
Proportion (%)	50.72	14.90	12.02
Cumulative (%)	50.72	65.61	77.63

Multivariate analysis using principal component analysis has identified a strong component loading (PC1) in Table 22, which shows correlated factors governing the major ion chemical composition of analyzed samples. The technique is suitable in interrelated experimental parameters, and PC1 in this study presented a proportion of 50.72% out of 77.63% total loadings. While other parameters were considered less related concerning loading values, pH had an absolute zero value in PC1, which means it was neither related nor controlled by the water chemistry of major ions in the study area during the sampling session. The EC and TDS were strongly related to values 1.00 and 0.99 in the Pearson correlation matrix and principal component analysis, respectively. Their values represent general dissolved chemical content in water and define the suitability based on intended uses guidelines or limits (Table 21).

The EC and TDS for surface water sources significantly increase from upstream to downstream sampling locations. Such observation is justified with the geological setting and anthropogenic activities. Geologically, shallow and deep wells along studied rivers served to deduce groundwater and surface water dynamics. Surprisingly, groundwater sources alongside these rivers had comparable quality characteristics; contaminant smoothly increases from WS1

through WS2 to WS3. The abrupt increase of pollutants is observed from WS4 to WS5, where WSG1 and WSG2 with elevated contaminants are located (Fig. 23). Isotopes also reveal the same trend (Fig. 23 (b)), and values show a considerable decrease at WS4, where WSW1 is located and presents an inverse relationship of isotope values. Further to this, the observed isotopic values decrease as heavier (more enriched) values of WSW1 mix with lighter (more depleted) Weruweru River values at WS4 sampling point region. An observation further confirms the difference of contaminant origin of the shallow well WSW1 being originating from anthropogenic activities that are taking place at the sampled sites.

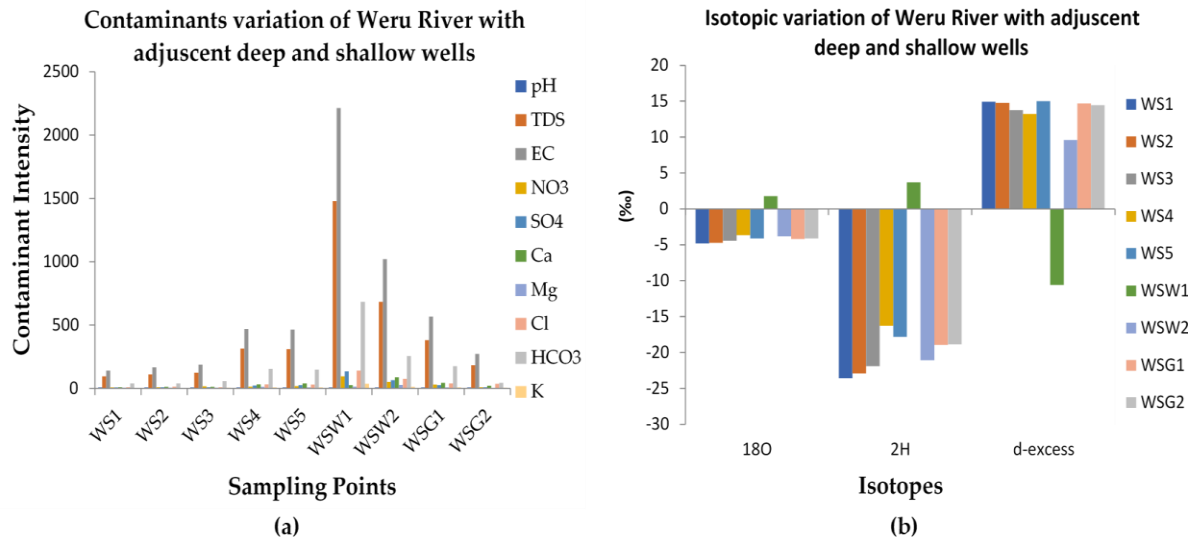


Figure 23: Variation in surface water, shallow water and deep water sources for Weru River (a) Water quality contaminants, (b) Stable isotopes

Another observation of surface water and groundwater dynamic is depicted in Fig. 24; there are no shallow wells due to the limited or absence of anthropogenic activities such as small-scale irrigation activities. Hence, all water quality contaminants and isotopic characteristics had comparable values with available groundwater mixing at KAS5, which is in line with BG1 that corresponds to elevated contaminants of groundwater interaction. Such observations are further addressed under hydrogeochemical processes that delineate contaminant origins, underlying contaminant mechanisms, and prospects with intended uses.

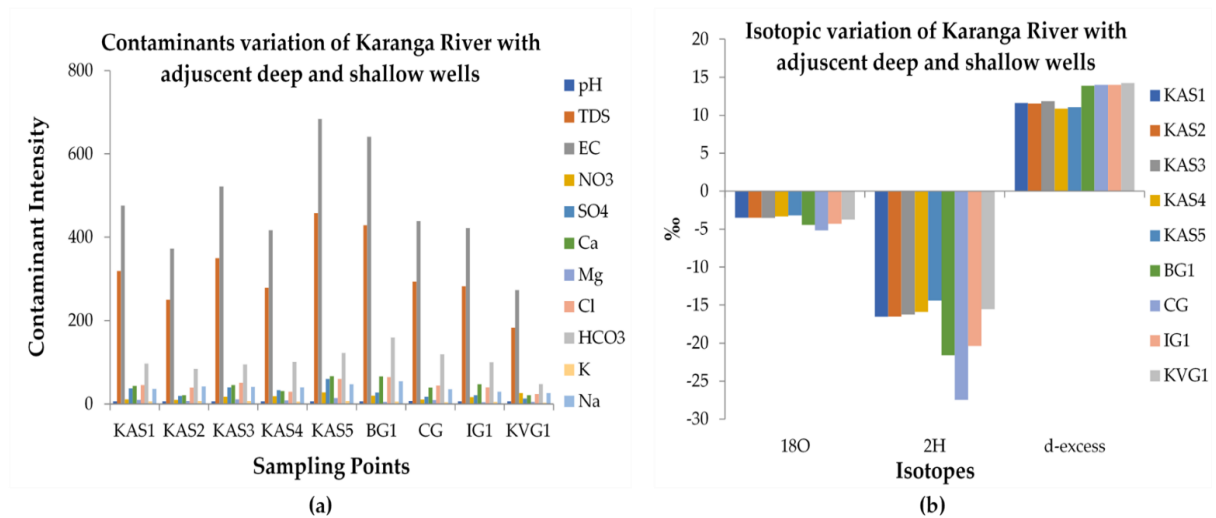


Figure 24: Variation in surface water, shallow water and deep water sources for Karanga River (a) Water quality contaminants, (b) Stable isotopes

Figure 25 shows Chadha's plot where hydrogeochemical processes are categorized into four quadrants, i.e. I - Recharging water, II - Base Ion Exchange Water, III - Sea/End-member Water, and IV - Reverse Ion Exchange Water (Senarathne *et al.*, 2020). Results show that all study area samples fall in I and IV regions, thus controlling hydrogeochemical processes are limited to recharging water and reverse ion exchange water. The upper part of the study area (Fig. 24 (a)), which possesses rivers and adjacent wells, had many samples (93%) plotting in IV where reverse ion exchange processes occur (except borehole 1 and 2 in TPC farm, 7%). The lower part of the study area (Fig. 24 (b)), which is a flood plain with no river, had most samples (89%) plotting in I where recharging water features prevail, and fewer samples (21%) in IV. These observations prove that lowlands are active in recharging processes as most of the water in I were held across flood plains during wet seasons. Highlands have limited recharge durations as water tends to flow spontaneously in this geological setting, and in most cases, results in sustainable surface water flows. Observations from Fig. 23 and Fig. 24 identifies a significant contribution of groundwater to surface water quality and can thus be regarded as a baseflow. Such base flows have modified surface water characteristics since they originate underground, where they took time to realize reverse ion exchange processes and sustain surface water flows in the dry season.

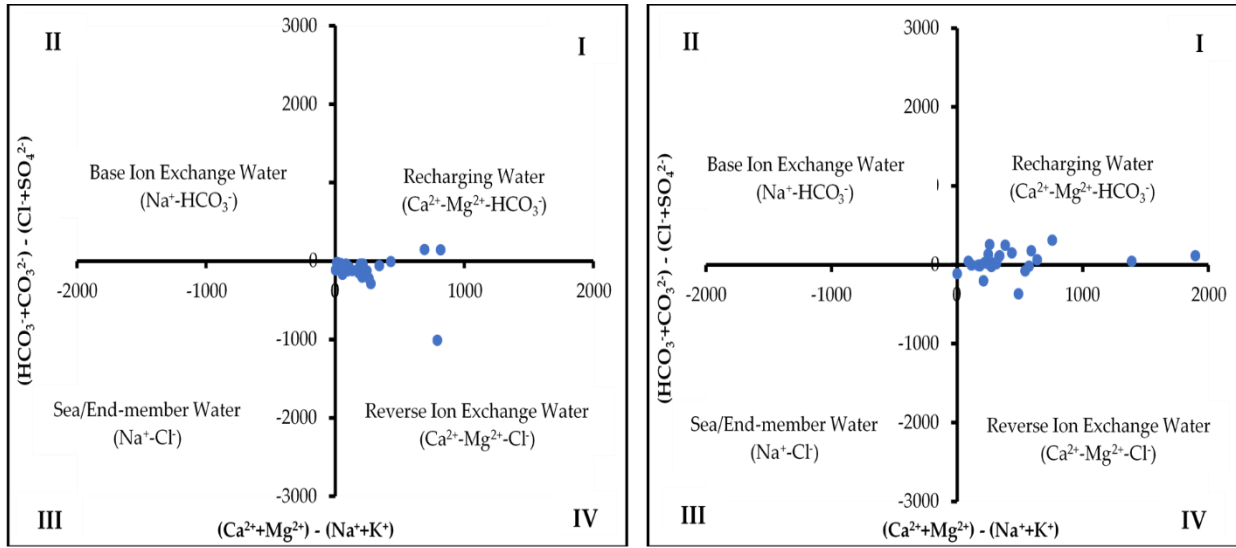


Figure 25: Chadha's classification for the hydrogeochemical process delineation of (left) Upper area, and (right) Lower area, water quality

Figure 26 (left) shows weathering processes as carbonate-based, i.e. dolomite (Vasu *et al.*, 2017), since all samples plot above the equiline, not as silicate-based that would have plotted samples below the equiline, which further proves the reverse ion exchange addressed in Fig. 25 (Marghade *et al.*, 2020). Figure 26 (right) assures the absence of silicate-based weathering, where most samples plots below 0.5 $Mg^{2+}/Mg^{2+}+Ca^{2+}$ ratio, which is the contrary characteristic for silicate-based weathering (Drever, 1997). Only one sample obeyed silicate weathering features and is in the lower part of the study area.

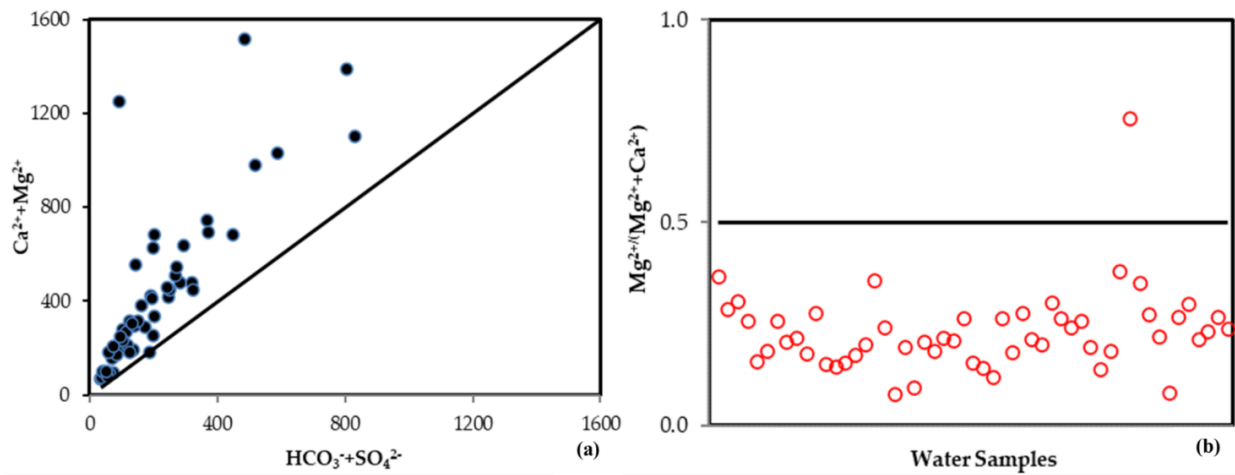


Figure 26: Binary plots of (a) $Ca^{2+}+Mg^{2+}$ vs $HCO_3^-+SO_4^{2-}$, (b) $Mg^{2+}/Mg^{2+}+Ca^{2+}$

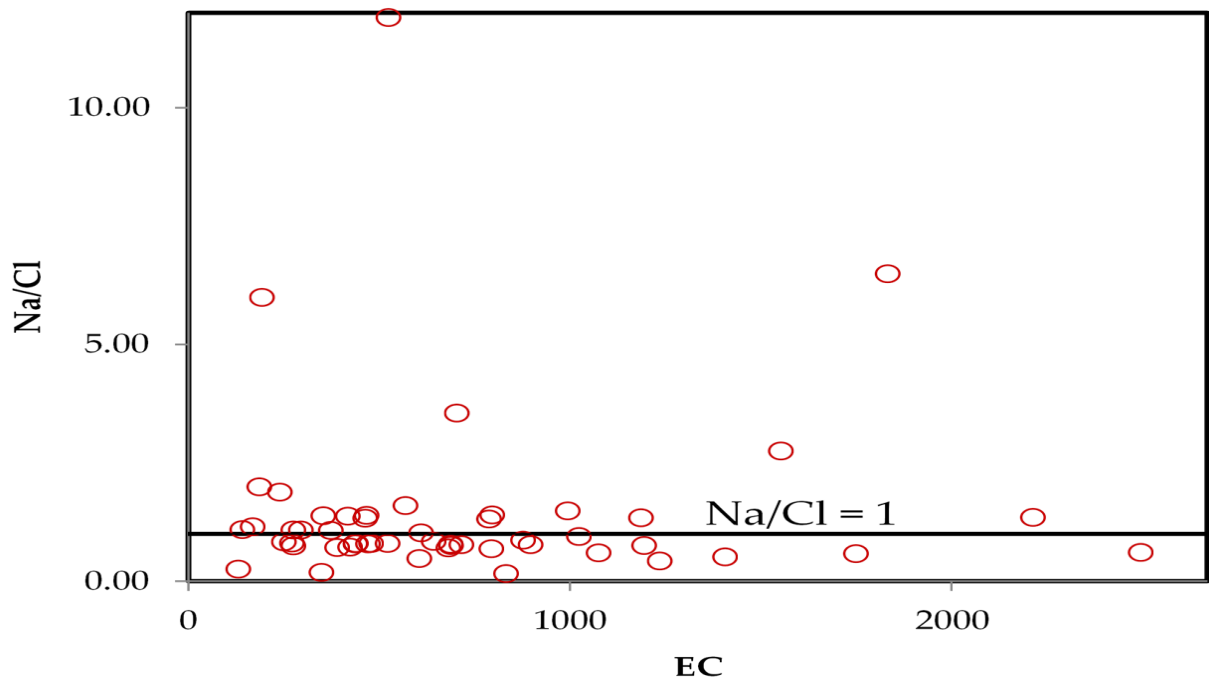


Figure 27: Plot of Na/Cl vs Electrical Conductivity

4.3.7 Potential variations of pH with fluoride, depth and dissolved oxygen

(i) The pH and Fluoride Variation

The principle component loading PC2 (Table 22) expressed a significant correlation between pH and fluoride in an inverse related manner, i.e. -0.79 for pH and +0.79 for fluoride. Karthikeyan and Shunmugasundarraaj (2000) also reported an inverse relationship between fluoride and pH in groundwater. Dobaradaran *et al.* (2009) formulated an equation after multiple regression analysis of groundwater data which showed negative fluoride and pH relationship. Figure 28 shows that high fluoride concentration ($F^- > 2$) in the upper area with relatively low pH values was dominant compared to the lower area ($F^- < 2$) characterized by high pH values. A clear explanation of these observations would mean accelerated dissolutions in the upper part due to corrosive low pH values. Kitalika *et al.* (2017) observed positive correlation of fluoride and pH in the dry season in the same basin, which indicated that fluoride dissolution from the rock was the function of pH.

Contrary, previous research has demonstrated that high fluoride leaching from rocks is attributed by increasing pH values and more prominent in alkaline conditions (Hossain & Patra, 2020; Kitalika *et al.*, 2017; Salve *et al.*, 2008). The underlying principle for these observations is that

two ionic species are likely to undergo exchange reaction if their radii differ by less than 15% (Yehia & Ezzat, 2009). Since fluoride (F^-) and hydroxyl (OH^-) ions obey this rule with 1.36 Å and 1.40 Å radii size, respectively. Furthermore, F^- leaching should increase with the increase in pH, which facilitates OH^- availability for exchange with rock F. Arguably, the current study had no phenol alkalinity (PA) in the upper area which is deduced at $pH \geq 8.3$. The lower area had only one sample with pH 8.4 and is considered negligible for considerable hydroxyl generation effects. Phenol alkalinity could have accounted for the availability of hydroxy ions to realize exchange at high pH values. Its absence indicates that current alkaline conditions are due to carbonates. In this case, leaching by the acidic condition dominates observed high fluoride contents in the study's upper area; furthermore, fluoride discharge from intensive chemical fertilizer application in this highly irrigated zone could be another reason.

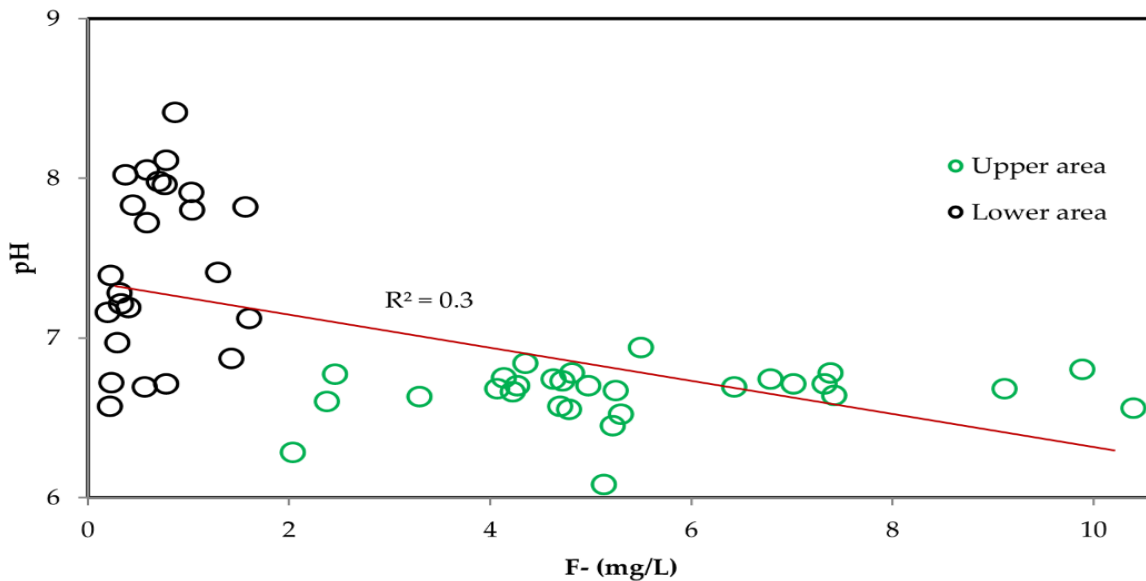


Figure 28: Fluoride (F^-) variation with pH in the upper and lower parts of the study area

(ii) Depth and Dissolved Oxygen

A significant inverse correlation of depth (-0.94) and DO (+0.83) was addressed in Table 22 by principal component loading PC3. Dissolved oxygen saturation is the function of depth and temperature in aqueous systems. The DO concentration in all study area obeyed a Surface-water >>>shallow wells > deep wells trend. Availability of oxygen in water determines the vulnerability to oxic microbial contamination and oxic water reactions with rock materials. In this study, DO in shallow wells portrayed surface and groundwater dynamics, which is essentials for consideration during water resources management and governance at an integrated level. For

instance, trends in the highland area revealed contamination increased from up-river to down-river sampling points, and baseflow accounted for these observations; this trend may be a result of an increased residential area, and hence increased anthropic activities as one moves from the conservation area downslope. Sampling depth in all surface water sources was not uniform due to water level variation, which can be due to varied abstraction rates from most irrigation water users intakes, percolation, and river width changes. A similar observation on water level fluctuation with riparian groundwater oxygenation exists elsewhere (Mächler *et al.*, 2013; Malard & Hervant, 1999; Massmann & Sültenfuß, 2008; Williams & Oostrom, 2000). Variation of groundwater depth and DO is depicted in Fig. 29.

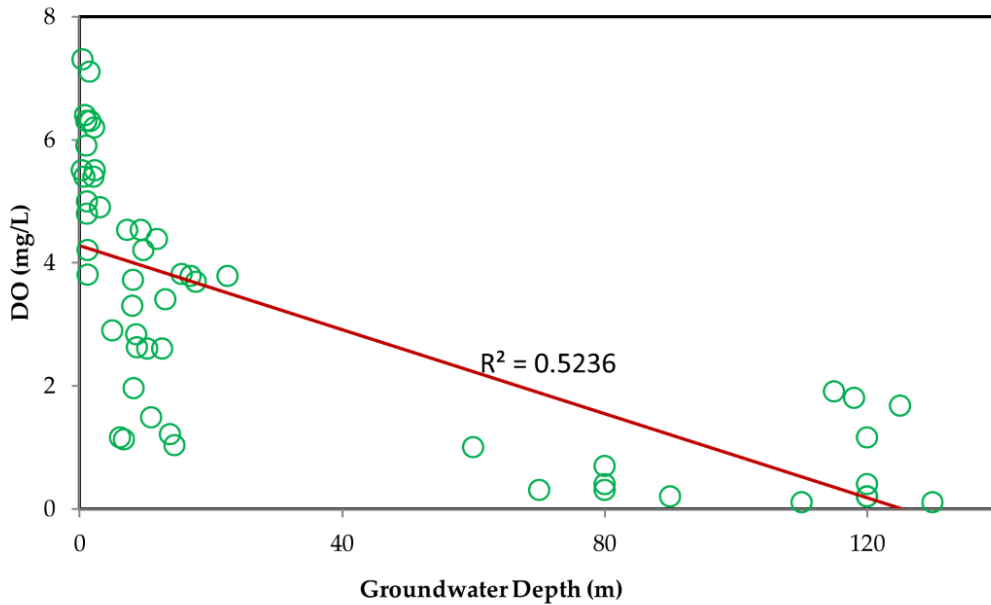


Figure 29: Variation of dissolved oxygen with groundwater sources depth

Figure 30 shows dissolved oxygen (DO) variation with temperature for surface and groundwater sources. The DO variation with temperature is significant in surface water sources than groundwater source. The DO shows an inverse relationship with temperature, i.e. it increases with a decrease in temperature. Thus, cold water can hold more DO than warm water. The DO values in all surface-water sources of the study area satisfies environmental flow criteria and supports aquatic life, which is the second priority of any water resource exploitation after potable water preference (URT, 2002). It is evident that even with intensive anthropogenic pollution activities observed, rivers still assimilate such wastes to acceptable levels of critical parameters like DO. In water quality management, a lesson is given to authorities on the necessity of considering pollution load control rather than current pollution levels after waste discharge into

surface-water reservoirs. It will enable the facilitation of river water assimilation power to account for natural factors (like climate variability and change) that may affect water quality, thereby acting like an adaptation or mitigation measure in-place during water resources management and governance operations.

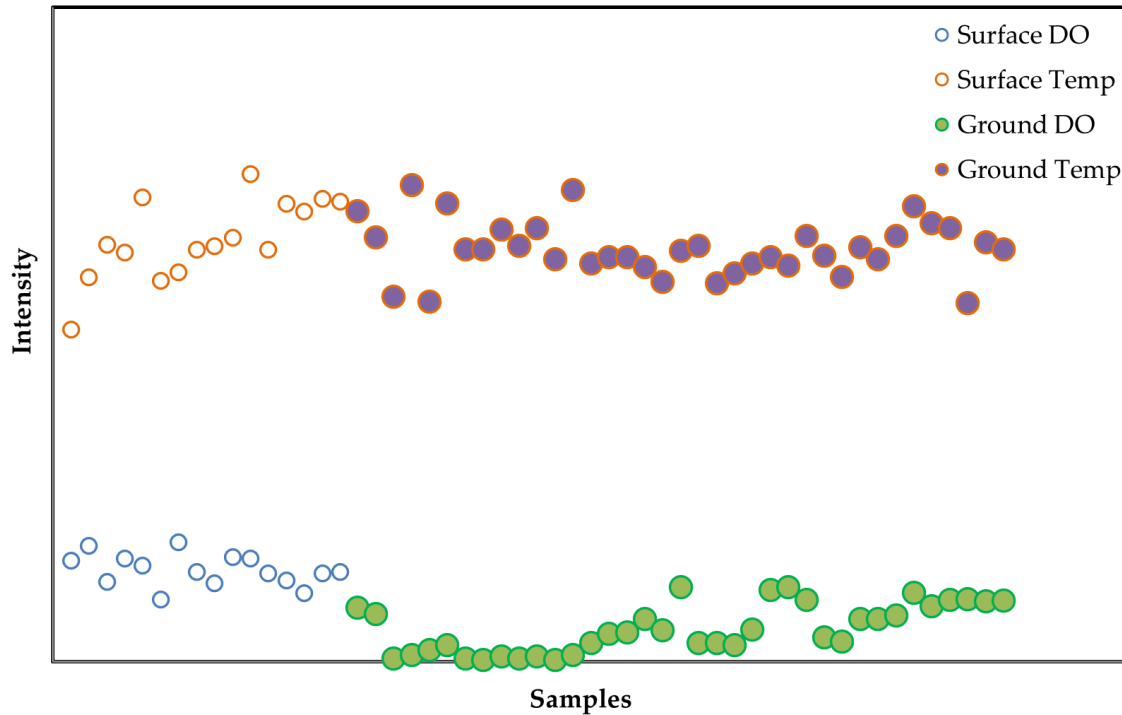


Figure 30: Surface and groundwater variation of temperature (temp) and dissolved oxygen

4.3.8 Water Quality Suitability for Potable Uses

There is a preferential prioritization of potable water uses in any water resources allocation for various socio-economical activities (URT, 2002). The quality of water determines its suitability for potable uses. Where the scarce resource is not suitable for domestic uses, it still receives the same preference, but users have to find treatment means at community and household levels. Table 20 shows average water quality findings from this study where maximum and minimum values serve as references for comments on local and international standards conformity.

(i) pH and Fluoride

The upper area had pH variation averaging at 6.7 with several values below 6.5, whereas the lower area also varied at an average of 7.5. The evaluated mean value for all sites was 7.0, with

maximum and minimum pH values of 8.4 and 6.1, respectively. According to local standards, all pH values conformed to natural potable water use suitability; but WHO guidelines disqualified conformity sources with pH less than 6.5. In water chemistry, pH refers to the potential of hydrogen, which depicts aqueous hydrogen ions concentration. Its scale ranges from 0 to 14 (acidic to alkaline or basic) where 7.0 portrays an acid-base balance and a neutral point. Potable water use with non-conforming quality may result in aesthetic issues such as bitterness taste due to high or alkaline water. This water cannot build scales on exposed plumbing as maximum pH values do not exceed 8.5. However, sources with pH below 6.5 are susceptible to laundry staining, sink and drain stains, and metallic or sour taste aesthetic problems. Furthermore, low pH potable water facilitates minerals leaching from metallic plumbing and can add toxic heavy metals to drinking water. Direct effects upon contact with users include eye, skin, and mucous irritation.

Fluoride dissolution in groundwater from rocks may readily occur through pore spaces between interacting rocks containing sodium, calcium, and silicate-based fluoride compounds. Unlike many communities with fluoride-free water sources that require an intentional addition of fluoride to their drinking water for promoting dental health (Ahmed *et al.*, 2020; Mächler *et al.*, 2013), all potable water supplies in the study area contain naturally occurring fluoride. Fluorination practices mean that fluoride is not a harmful chemical but rather beneficial at low concentrations (≤ 1.5 mg/L). However, fluoride at higher concentrations like those observed in the upper part of the study area has detrimental effects. Prolonged utilization of such polluted water presents dental and skeletal disease characterized by bones' pain and tenderness (Srivastava & Flora, 2020). Furthermore, mottling of teeth (fluorosis) through pitting and brown teeth staining occurs in children with less than ten years due to their teeth being under the development stage (Viteri-García *et al.*, 2020).

(ii) Total Dissolved Solids (TDS)

Technically, TDS is not a pollutant but rather an indication of potential exceedance of other major ions contaminants, i.e. anions such as sulphate, nitrate, chloride, and carbonates; cations such as calcium, magnesium, sodium and potassium. Calcium and magnesium are major components of water hardness and at elevated levels may lead to scale buildup in pipes, impairs the efficiency of water heaters and filters (Karar & Henni, 2020). Unbearable hard water presents aesthetic problems such as bitterness presented with high pH issues and salt taste (Dietrich &

Devesa, 2019). Users not experienced from the water with high TDS values are likely to encounter gastrointestinal discomforts. However, other particular combination of major ions can dominate TDS, i.e., sulphate and allied compounds which present metallic plumbing corrosions, saltiness and bitterness taste; sodium and chloride exhibit corrosion effect in metallic plumbing, and saltiness taste. It is easy to estimate TDS from electric conductivity (EC) water measurements; approximately, TDS is half of EC values (Miraj *et al.*, 2017).

(iii) Chloride and Nitrate

Chloride and nitrate have a close relationship when agricultural activities are major water polluting sources. Intensive irrigation practices characterize the study area with surface and groundwater sources. These activities significantly modify surface water sources that broadly serve potable water uses to all riparian levels at the upper part of the study area. Nevertheless, the Kahe aquifer dominates the lower part of the study area and is also affected by groundwater irrigation activities using (a sole reliant source) and considerably alters potable water use suitability (Lwimbo *et al.*, 2019). Figure 31 shows the relationship between nitrate and chloride in upper and lower study area sites. There is a significant correlation between nitrate and chloride ($R^2 = 0.5$) in the upper part, where rivers are available and the area characterized by many water user associations utilizing surface water sources in their irrigation schemes, and the large scale plantation area for sugarcane. A low correlation between chloride and nitrate ($R^2 = 0.3$) also exists in the lowland areas of the study site.

In either case, naturally occurring chloride interacts with the lithosphere's hydrosphere in many ways. i.e., subsurface groundwater movement through geological deposits, sands, and bedrocks dissolve chloride and other minerals. The chloride concentration varies with water-rock residence time variation, the extent of dissolution, and well depth. Anomaly high chloride concentration to background levels is an indication of anthropogenic activities influence. In this study, the lowland area is characterized by most wells (65%) but with insignificant Nitrate-chloride correlation, meaning natural forcing on chloride leaching from lithosphere are minimal. The upper area has only 35% groundwater sources, but surface and shallow wells had saline water sources. High chloride content observed in the upper area indicates that it originates from anthropogenic activities such as industrial waste (from the sugarcane process industry), artificial fertilizers, and animal manure used in the value addition of irrigation practices. Other sources include bush landfills during farm preparations and sewage from human activities in the area.

On the other hand, elevated nitrate in water sources is mainly due to fertilizer, animal, or human manure pollution. Nitrate beyond maximum limits tends to effectively affect infants below the age of six months through serious illness, that is, dyspnea and methemoglobinemia, or death (Brender, 2020; Wang *et al.*, 2020).

A similar trend has been reported in different studies. Adimalla (2020) showed a good correlation of few studied groundwater samples for nitrate and chloride, indicating agricultural influence and animal waste. Except for their empirical study areas findings, Yu *et al.* (2020) showed a positive correlation between nitrate and chloride which was associated with agricultural productions. Their report further noted that chemical application of fertilizers and faecal pollution tends to increase. Benettin *et al.* (2020) revealed a positive correlation of nitrate and chloride in stream water studies of 12 years during the winter-spring regime. This phenomenon corresponds to the current study season and validates our observations. While a positive correlation of calcium and nitrate indicated chemical fertilizer application, a positive correlation between nitrate and chloride suggests that animal manure and livestock waste influences nitrate content in groundwater (Maurya *et al.*, 2020). Therefore, anthropogenic activities in the upper part play a key role in significant water pollution that inevitably serves potable uses; the lower part has limited anthropogenic effects that could account for groundwater pollution. Hence non-anthropogenic activities may be responsible to a large extent for practical low pollution level; this observation means nitrate pollution is high in industrial and residential areas, especially in areas of minimum manure/fertilizers use in farming activities. Such observations confirm why Lwimbo *et al.* (2019) did not find any pesticide residual in the lower part of our study site.

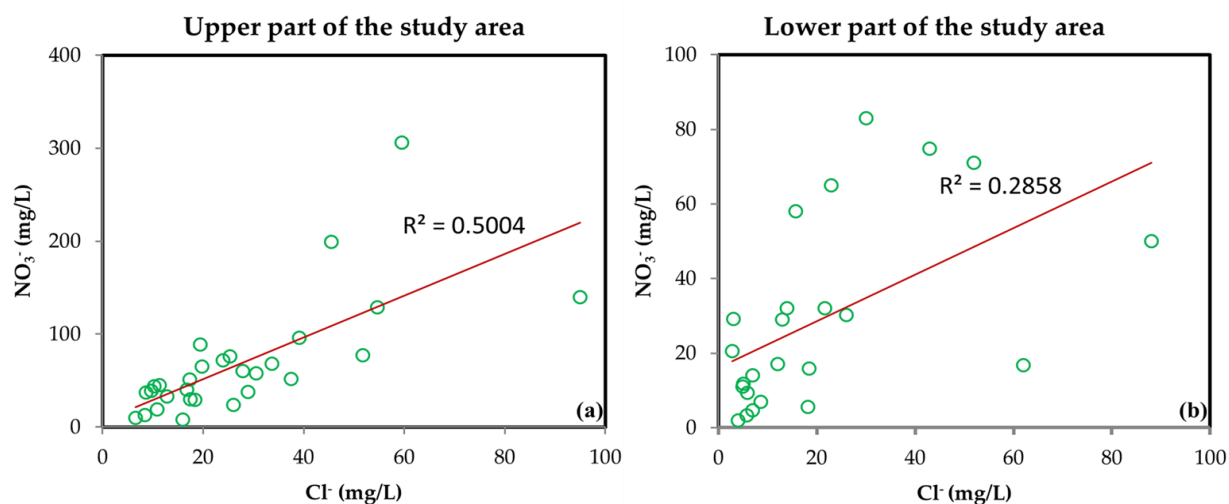


Figure 31: Nitrate and Cl concentration for lowland and upland areas

(iv) Bicarbonates

The observation from Piper and the HCO_3^- concentrations were chiefly dominance than other major anions. It has a minimum concentration of 39.0 mg/L, a maximum concentration of 1166 mg/L, and an average of 257.7 mg/L. High HCO_3^- levels in groundwater resulted from the reaction of CO_2 in the unsaturated soil zone and rainwater (Kumar *et al.*, 2009). However, it is worth stating that no literature documented the standard value of HCO_3^- for drinking purposes; although, values above 200 mg/L are unsuitable for drinking water (Bhardwaj & Singh, 2011; Brindha & Kavitha, 2015). Overall, 52.7 % of the sampled groundwater are permissible for drinking purposes in the watershed.

4.3.9 Suitability of Water quality for Irrigation Application

Evaluation of groundwater quality for irrigation is significantly vital (Adimalla, 2020). Eight indices were used to evaluate 55 sample locations for irrigation quality; the results are as indicated in Table 23. In this study, groundwater quality for irrigation was evaluated using Sodium adsorption ratio (SAR), sodium percentage (Na%), residual sodium carbonate (RSC), Permeability index, and Kelly's ratio (KR). Equations were used to calculate values for each index in water samples.

(i) Sodium Adsorption Ratio

Water samples classification using the Sodium Adsorption Ratio (SAR) index developed by Richards (1954) shows that all the water sources from the sampled stations have excellent water

quality for irrigation. The SAR varied from 0.1 to 5.99, with a mean of 1.81 and a standard deviation of 1.25 (Table 23). The results show that all samples had values <10 (S1), suggesting that 98.15% had excellent quality for irrigation while 1.85% fell under S2, suggesting medium sodium hazard. Continued use of water with High SAR changes soil properties, leading to a breakdown in the physical structure of the soil and reduces Na permeability in the soil, destroying soil structure due to dispersion clay particles. When irrigation water is high Na^+ and low in Ca^{2+} , the soil tends to become flocculated with and become impermeable, causing challenges to cultivate (Ackah *et al.*, 2011). Further, the textured soils (i.e. those high in clay) are the most vulnerable and becomes hard and compacted when dry and increasingly impermeable to water infiltration (Salifu *et al.*, 2017). With high SARs water, adjustments may be needed to maintain soils. Calcium and magnesium, if present in the soil in large enough quantities, will counter the effects of the sodium and help maintain good soil properties (Fipps, 2003). Based on SAR values for the study area, all the groundwaters could be classified as excellent and would be suitable for irrigation.

(ii) Electrical Conductivity

The US salinity diagram (Richards, 1968) with Electrical Conductivity (EC) (as salinity hazard) and SAR (as alkalinity) was used to evaluate the samples (Fig. 32). The results show that 35.19% of the samples fall within the low salinity-low sodium type of water (C1-S1), while 42.59% fall under the medium salinity-low sodium class (C2-S1). Further, 20.37% of the water samples fall under the High salinity low sodium class (C3-S1), and Only 1.85 % (one sample) of the water samples fall within the high-salinity hazard-medium sodium hazard class (C3-S2). The sample falling under C3-S2 is from a shallow well in irrigation fields around Kikafu village. Groundwaters that fall within the C1-S1 and C2-S1 can be used for irrigation on all types of soil with a minor hazard of developing detrimental levels of exchangeable sodium. However, C3-S1 types of water could only be used to irrigate certain semi-tolerant crops (Jafar *et al.*, 2013), whereas C3-S2 cannot be used for irrigation, although it is used for irrigation in the study area. In terms of spatial distribution, SAR is high on the southern side where there is thick alluvial deposit; the concentration decreasing towards the middle of the watershed and extend northwards, and the concentration is low on the eastern and northwestern side (Fig. 33(g)).

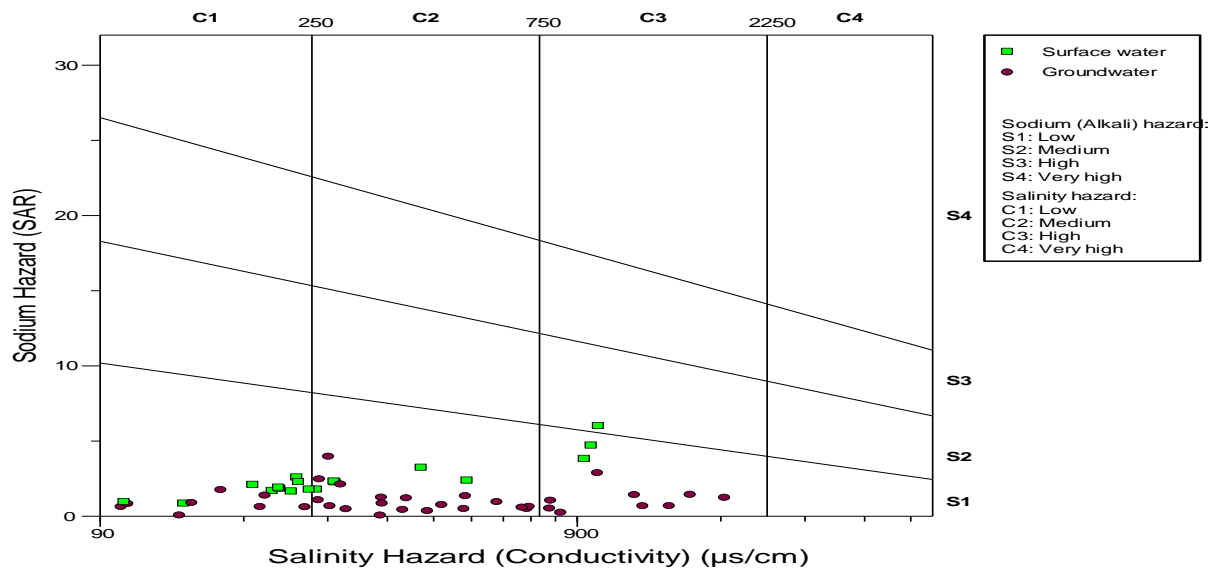


Figure 32: Classification of river water in terms of the degree of suitability for irrigation: Electrical conductivity versus sodium adsorption ratio (Richards, 1954)

(iii) Kelly's ratio

In this study, the total water quality data were used to calculate Kelly's ratio in spatial and temporal scales (Table 23). Kelly's ratio (KR) ranged from 0.05 - 0.54 and had mean and SD values of 0.54 and 0.26, respectively. All samples were less than 1, which shows irrigation suitability; thus, the water quality is suitable for irrigation use. Spatially, most areas in the Eastern side, decreasing towards the middle and northern side (Fig. 33(h)); although all areas had $KR \leq 1$, thus, can be used for irrigation without inflicting problems (Wani, *et al.*, 2014).

Table 23: Indices used to evaluate water samples for irrigation suitability

Sample code	Gibs Ratio I	Gibs Ratio II	RSC	SAR	MAR (%)	ESP (%)	KR	PI
WS1	0.62	0.22	0.12	0.62	66.49	34.34	0.45	108.82
WS2	0.57	0.25	0.04	0.83	40.91	42.38	0.66	116.52
WS3	0.66	0.20	0.07	0.96	50.00	46.92	0.66	126.30
WS4	0.74	0.11	0.56	1.69	54.22	53.01	0.73	110.52
WS5	0.77	0.18	0.50	1.83	57.93	55.12	0.71	118.26
WSW1	0.84	0.21	3.93	5.99	48.14	66.79	0.71	116.46
WSW2	0.79	0.19	0.91	3.23	48.15	62.77	0.85	101.54

Sample code	Gibs Ratio I	Gibs Ratio II	RSC	SAR	MAR (%)	ESP (%)	KR	PI
KAS1	0.76	0.18	0.57	1.91	51.76	55.91	0.80	103.84
KAS2	0.80	0.21	0.72	2.58	44.42	64.37	0.75	120.48
KAS3	0.79	0.22	0.65	2.28	51.57	60.19	0.84	124.20
KAS4	0.69	0.14	0.68	1.78	45.88	51.56	0.78	120.47
KAS5	0.82	0.21	0.51	2.09	58.24	60.75	0.73	110.62
KIS1	0.75	0.11	1.40	2.31	43.10	58.45	0.77	126.85
KIS2	0.56	0.27	-0.04	0.85	44.54	38.96	0.79	122.12
WSX	0.63	0.16	0.53	1.78	25.75	52.14	0.61	107.55
KASX	0.68	0.37	-0.09	1.66	37.81	54.52	0.72	90.88
KWUSX	0.76	0.08	0.71	2.12	55.72	55.79	0.85	93.37
KGS1	0.59	0.08	0.62	1.25	57.93	36.61	0.83	87.76
KGS2	0.50	0.09	0.42	1.08	40.57	36.87	0.83	110.35
KWK1	0.55	0.09	0.82	1.20	57.20	33.69	0.78	102.62
SG1	0.43	0.15	1.34	0.10	92.52	5.39	0.71	107.68
SG2	0.55	0.13	4.21	0.51	50.46	35.52	0.51	85.31
SG3	0.59	0.18	2.70	0.48	72.23	27.14	0.60	93.45
SG4	0.77	0.47	-0.73	2.84	76.37	43.75	0.48	81.89
SG5	0.61	0.07	3.93	0.30	87.50	15.58	0.79	113.33
SG6	0.79	0.03	1.81	0.95	96.53	11.32	0.65	106.57
SG7	0.77	0.04	6.18	1.74	86.62	29.83	0.80	121.07
SG8	0.65	0.10	4.51	0.56	82.70	23.07	0.56	105.64
SG9	0.75	0.06	-2.25	0.54	95.98	10.64	0.92	116.32
SG10	0.74	0.06	4.60	1.79	39.27	58.01	0.06	77.07
SG11	0.77	0.06	3.37	0.97	90.35	23.22	0.54	167.87
SG12	0.70	0.02	1.24	0.16	97.67	4.91	0.35	120.51
SG13	0.78	0.37	2.31	3.24	73.26	46.69	0.51	58.45
SG14	0.78	0.03	9.47	2.60	73.29	46.75	0.18	98.63
SG15	0.78	0.02	9.13	3.13	73.28	46.79	0.12	27.84
SG16	0.78	0.01	10.25	3.67	73.27	46.68	0.35	60.16
SG17	0.77	0.03	-15.29	0.47	98.53	4.62	0.28	87.55
SG18	0.77	0.01	9.59	0.32	98.52	4.61	0.11	30.04
SG19	0.78	0.12	6.64	3.78	50.93	60.55	0.81	182.0
SG20	0.79	0.28	1.77	2.37	85.59	33.46	0.27	60.64
SG21	0.77	0.02	4.15	1.22	87.94	27.99	0.05	42.10
SG22	0.77	0.03	20.52	1.99	87.99	27.93	0.56	68.02
SG23	0.71	0.09	6.95	0.54	91.91	16.34	0.56	81.37
SG24	0.71	0.28	3.07	0.27	91.82	16.42	0.56	77.54
SG25	0.71	0.08	5.88	1.63	82.46	29.48	0.56	72.83
TG1	0.64	0.11	1.61	2.38	41.44	50.02	0.05	15.05
TG2	0.73	0.10	4.11	4.70	32.52	63.00	0.05	24.58
TG3	0.66	0.12	3.26	3.81	29.18	56.30	0.77	96.57
BG1	0.79	0.24	0.55	2.46	50.49	62.11	0.38	52.97
CG1	0.68	0.19	0.22	1.38	52.77	47.72	0.31	64.96
IG1	0.72	0.19	0.26	1.75	39.00	59.36	0.31	50.62
KG1	0.61	0.23	-0.03	0.89	55.90	39.98	0.18	59.96
WG1	0.88	0.70	0.15	3.96	36.64	67.89	0.18	82.50
WSG1	0.79	0.19	0.66	2.26	58.20	57.67	0.34	57.05

Sample code	Gibs Ratio I	Gibs Ratio II	RSC	SAR	MAR (%)	ESP (%)	KR	PI
Maximum	0.88	0.7	20.52	5.99	98.53	67.89	0.92	182
Minimum	0.43	0.01	-15.29	0.1	25.75	4.61	0.05	15.05
MEAN	0.71	0.16	2.40	1.81	63.21	41.15	0.54	91.99
SD	0.09	0.13	4.50	1.25	21.33	18.41	0.26	33.37

(iv) Exchangeable Sodium Percent

Classification of groundwater sources for irrigation was also based on Exchangeable Sodium Percent (ESP) (Table 23). In this study, ESP ranged from 4.61 to 67.89% with a mean value and SD of respectively 41.15 and 18.412%, respectively (Table 23). The results show that 30.71% of the sampled sources fall under C3 (Permissible water quality for irrigation), and 23.80% are in the doubtful quality class (C4), and the final group (C5) carries; that is unsuitable water quality for irrigation application. The rest of the samples fall under excellent water quality and good quality for irrigation. The spatial distribution shows high ESP at the middle of the watershed and extending to the North Eastern side and lower concentrations on the South Eastern side where most of the deep irrigation wells are concentrated (Fig. 33(b)).

(v) Residual Sodium Carbonate

In this study, Residual Sodium Carbonate (RSC) ranged from -15.29 to 20.52, with a mean value of 2.40 and a standard deviation of 4.50 (Table 23). The results further show that 14.81% of all water sources fall under the no hazard category, whereas 35.19% of the water sources fall under the safe category for irrigation. Moreover, 12.96% of all the water sources have a slightly moderate carbonate hazard, while 37.04% of all the assessed water sources are unsuitable for irrigation. This means that the farms irrigated by 37.04% of all the sampled sources will be infertile due to high Na_2CO_3 (Kaka *et al.*, 2011). The smaller the value of Sodium carbonate, the safer the water for irrigation and vice versa. According to Esmaili *et al.* (2013), sodium hazards increase as RSC increases. Waters with high concentrations of HCO_3^- have the tendency to cause the precipitation of Ca^{2+} and Mg^{2+} as the water in the soil becomes more concentrated. As a result, the relative proportion of Na^+ in the water increases in sodium bicarbonate (Sadashivaiah *et al.*, 2008). Also, Ca^{2+} and Mg^{2+} may be precipitated when high Na_2CO_3 water is applied to the soil. Further, salts are concentrated when the soil dries due to precipitation and the removal of Ca^{2+} and Mg^{2+} from the solution. Negative values show the difficulties in Na^+ buildup due to the

presence of sufficient Ca^{2+} , and Mg^{2+} are more than what can be precipitated as CO_3^{2-} (Esmaili *et al.*, 2013). Spatially, RSC is high on the southern side, and moderate concentration extends towards Eastern and North-Eastern side (Fig. 33 (f)). It is worth mentioning that the southern part is dominated by small-large scale irrigation activities. Thus, higher concentrations on the southern parts will likely affect most of the agriculture activities.

(vi) Magnesium Hazard Index/ Magnesium Adsorption Ratio

Generally, calcium and magnesium, in most cases are in keeps a state of equilibrium. It is suggested that MH value of more than 50% intensifies the soil alkalinity and has severe effects on crop yield (Gupta & Gupta, 1997). The MAR in this study ranged from 25.75 to 98.53% with standard deviation and a mean of 21.33 and 63.21%, respectively, using the MAR index. Only 29.63% of the water sources fall under a suitable category for irrigation (MAR of $\leq 50\%$), whereas 70.37% of the water sources fall under unsuitable water quality for irrigation (MR of $\geq 50\%$) (Table 23). Thus, prolonged usage of such waters for irrigation of crop fields may reduce crop yield and destroy soils. Higher values of Ca^{2+} and Mg^{2+} result in soil aggregation and friability (Mohammed *et al.*, 2018). However, these ions are needed for plant growth. Generally, Mg and Ca of more than 10 meq/L is not suitable for irrigation; when these ions are in high concentrations in irrigation water, it increases soil pH and reduces phosphorus availability. Spatially, MAR is high on the Eastern parts close to suburbs with relatively high population, leaving the middle and increasing (Fig. 33 (c)).

(vii) Permeability Index

The Permeability Index (PI) evaluates sodium hazards of irrigation water. Local PI values ranged from 15.05 - 182%, with mean and SD of 91.99 and 33.37 % (Table 23). In most samples, 72.22% of the water sources fall under class I, which is excellent water quality for irrigation. Whereas 22.22% of the water sources fall under class II, which is good water quality for irrigation and can be applied with certain measures; and 5.56% of the water sources fall under category III, which is unsuitable water quality for irrigation. The spatial distribution shows that PI ranged are high on the Eastern, South Eastern, and Western parts of the watershed; these areas are, in most cases small-scale irrigation activities with high production of horticultural crops (Fig. 33(e)). Thus, using this index, only 5.56% of horticultural crops are affected.

(viii) Sodium Percentage (%Na)

The results show that the calculated mean value of the sodium percentage in the groundwater was 20.56 % and ranged between 10.45 % and 46.94 % (Table 23). Furthermore, 6.67% of the sampled sources fall under C1 (Excellent water quality for irrigation), whereas 22.22% fall under C2 (Good quality for irrigation). Also, 33.33% of the sampled sources fall under C3 (Permissible water quality for irrigation), and 25.93% are in the doubtful quality class (C4), and the final group (C5); that is unsuitable water quality for irrigation application. Excess of Na^+ in water does not favour plant growth (Ackah *et al.*, 2011). Also, excess Na^+ leads to a reduction in soil permeability (Mohammed *et al.*, 2018). When excess Na^+ combines with carbonate and chloride form alkali soils and saline soils (Ackah *et al.*, 2011). The spatial distribution shows high Na% in the western part of the watershed, whereas the eastern and northern areas have medium Na% and low Na% can be found on the southern parts of Kahe sub-basin (Fig. 33(d)).

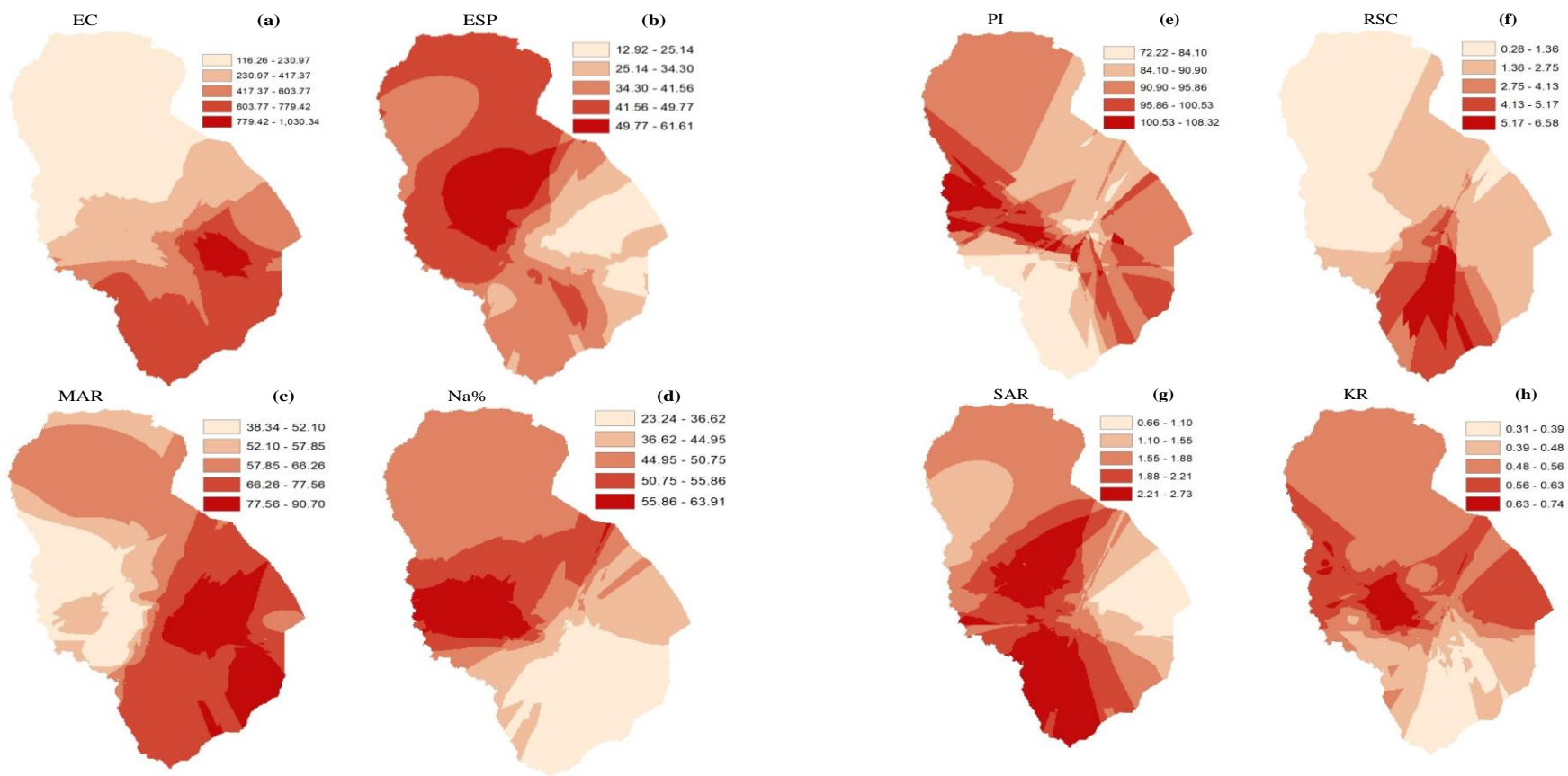


Figure 33: Spatial distribution of the indices used to assess irrigation suitability

4.4 Impacts of Past, Present, and Future Climate Changes on the Water Budget (Surface and Groundwater) of the Mount Kilimanjaro Slopes

In this objective, the climate of the KWK watershed was downscaled in terms of precipitation and temperature using RACMO and CCLM4 RCMs, the discussion is based on the model simulation results and the historical data from the ground-based stations. Thereafter, the temperature and precipitation data were used to force the calibrated SWAT model to simulate the future streamflow. Finally, the impacts of climate change on the selected hydrological parameters were determined using statistical approaches. The selected hydrological parameters include Surface runoff (SurfQ), Groundwater flow (GWQ), Water yield (WatQ), and evapotranspiration (ET).

The rationality between temperature and precipitation is of special concern in hydrology (Muerth *et al.*, 2013). The RCMs have been mentioned the best in simulating the climate change impacts in different areas of the world. However, the regional climate model outputs habitually necessitate bias correction due to biases compared to the observed temperatures and precipitations of a given region. Thus, in order to simulate the historic runoff used in the SWAT model, bias correction has to be carried out even if the corrections change the relationship between temperature and precipitation (Muerth *et al.*, 2013).

4.4.1 Impacts of Climate Change on Precipitation

The annual average spatiotemporal change (percentage) in precipitation under RACMO2T forced by the ICHEC-EC-EARTH GCM scenario is presented in Fig. 32, 33, and 34. The annual mean precipitation and mean monthly temperature of the KWK watershed for the past three decades (1979 to 2005) showed an increasing trend with a 3.3 mm/year increment in highland areas and 8.1 mm in lowland areas (Fig. 32). The watershed was forecasted to have a positive increment in precipitation over all the RCPs in future years as observed for historical precipitation.

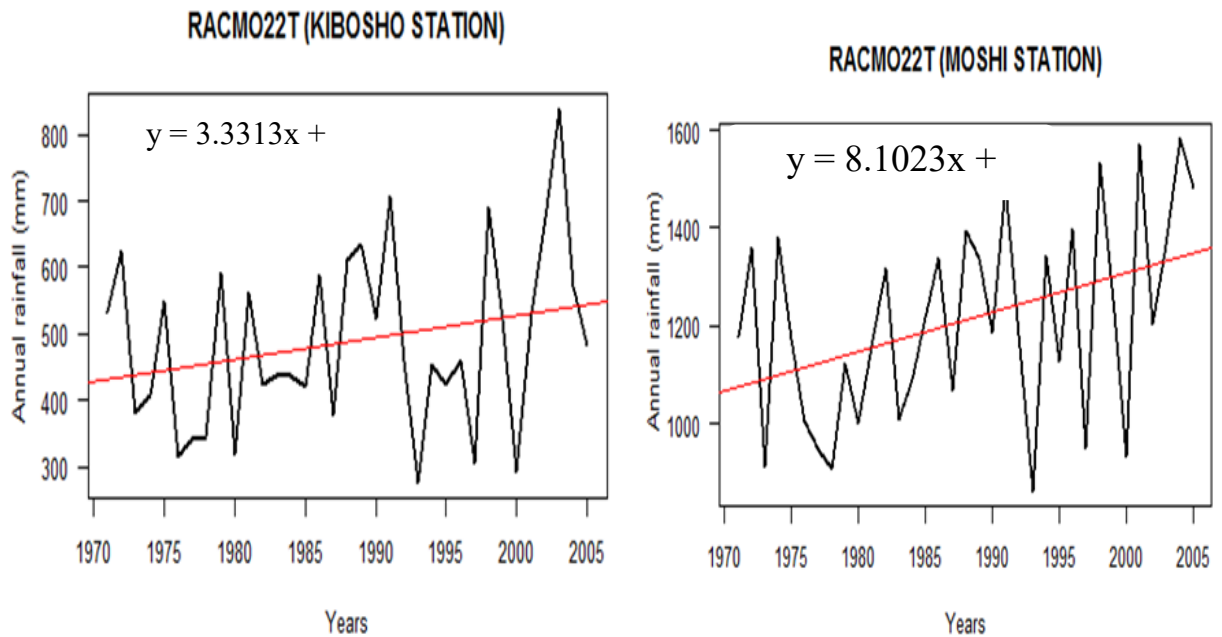


Figure 34: Historical regional atmospheric climate model 22T model for annual rainfall in different weather stations in the Kikafu, Weruweru and Karanga watershed

Generally, the mean annual historical precipitation for the highland station shows an annual increase of about 3.33 mm/year, whereas that of the lowland areas show an annual increase of about 8.1 mm/year. From the year 2006 to the end of 2030, the annual mean rainfall increased by 66.8 mm/year along Kibosho, 13.5 mm/year along Moshi and from 2050 to the end of 2100. For RCP 4.5, the annual mean precipitation for the highland areas typically associated with a relatively high precipitation amount along Kibosho is expected to increase by about 64.53 mm/year from 2051 to 2100 and 20.6 mm/year in Moshi.

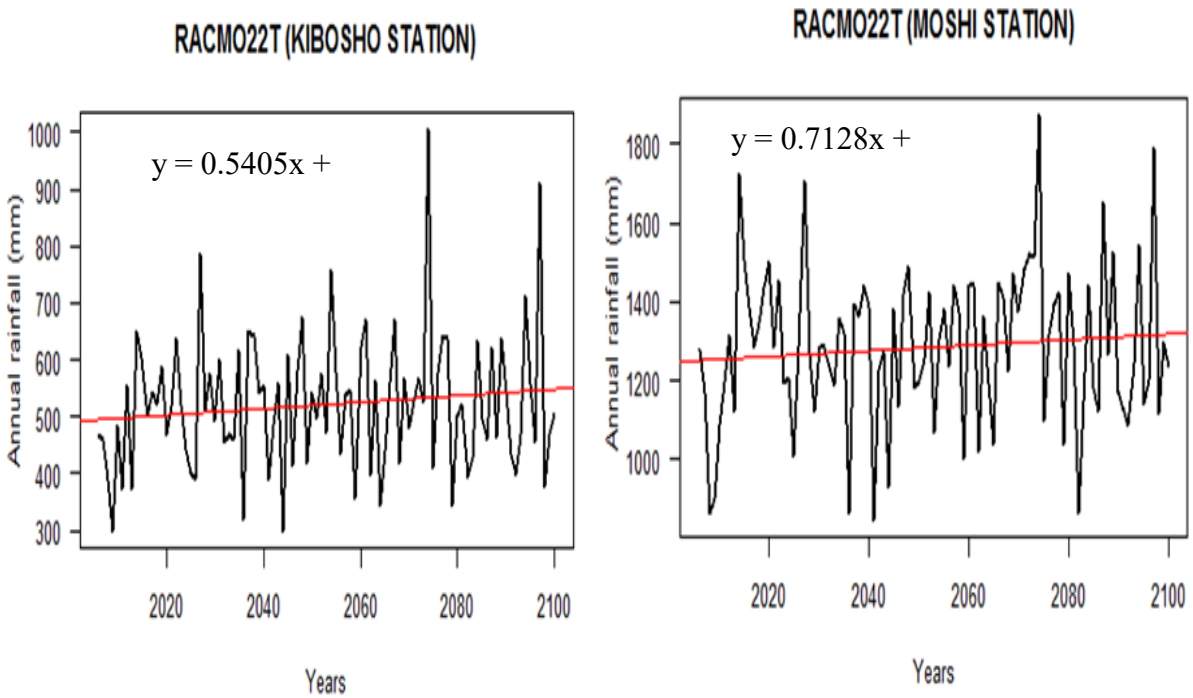


Figure 35: Regional atmospheric climate model 22T model annual rainfall projections under Representative Concentration Pathway 4.5 in the different weather station

For RCP 8.5, the results are presented in Fig. 35. The results show that the annual mean precipitation is expected to increase by about 0.8 mm/year along Kibosho station that represents highland areas, and about 1 mm/year along Moshi station that represent the lowland areas from 2051 to 2100. Further, the mean annual rainfall increased by 110.1 mm/year along Kibosho and 64.63 mm/year along Moshi from 2006 to the end of 2030. However, from 2005 to 2100, the simulated long time future precipitation shows an increase of about 0.77 mm/year in highland areas and 0.94 mm/year in the lowland areas.

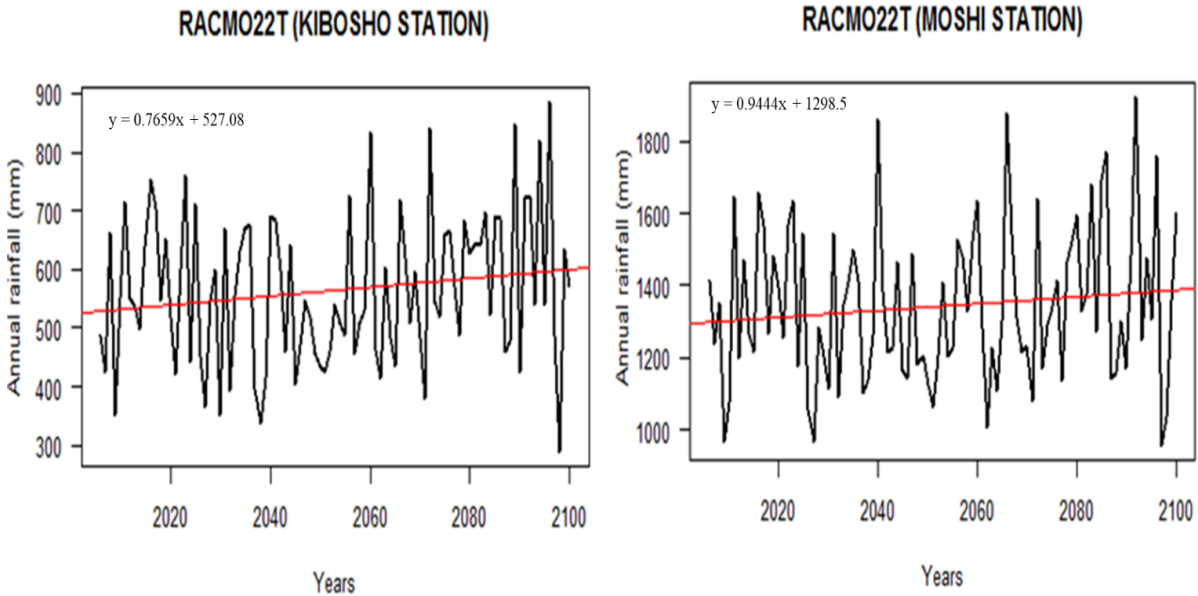


Figure 36: Regional atmospheric climate model 22T annual rainfall projections under representative concentration pathway 8.5 in the different weather station

The results show that the magnitude of increase in rainfall is 0.54 mm/year in highland areas and 0.77 mm/year in lowland areas under RCP 4.5; furthermore, 0.71 mm/year in highland areas against 0.94 mm/year in lowland areas under RCP 8.5. These results suggest that the magnitude of the increase is more vivid under RCP 8.5 than RCP 4.5, and the intensity is higher in lowland areas as compared to highland areas, which might be attributed to the model construction.

However, the result from CCLM4 shows a decreasing trend with a negative slope in both historical and future precipitation records, both for RCPs 4.5 and 8.5. These results are contrary to the results simulated from RACMO model, which show an increasing trend. Thus, there is no consensus on the direction of change in rainfall for the future, even amongst a small selection of two model simulations. Using CCLM4 model for both RCPs, the results show that the rainfall has been decreasing both in highland and lowland areas.

Historical rainfall (1979-2005) shows a decrease of 5.52 mm/year in the highland station and 0.26 mm/year in the lowland station (Fig. 36) under CCLM4 driven by CNRM. This suggests that highland areas are getting drier than lowland areas. These results are contrary to the earlier results derived from RACMO22T RCM. The difference may be linked to the construction of the RCM models.

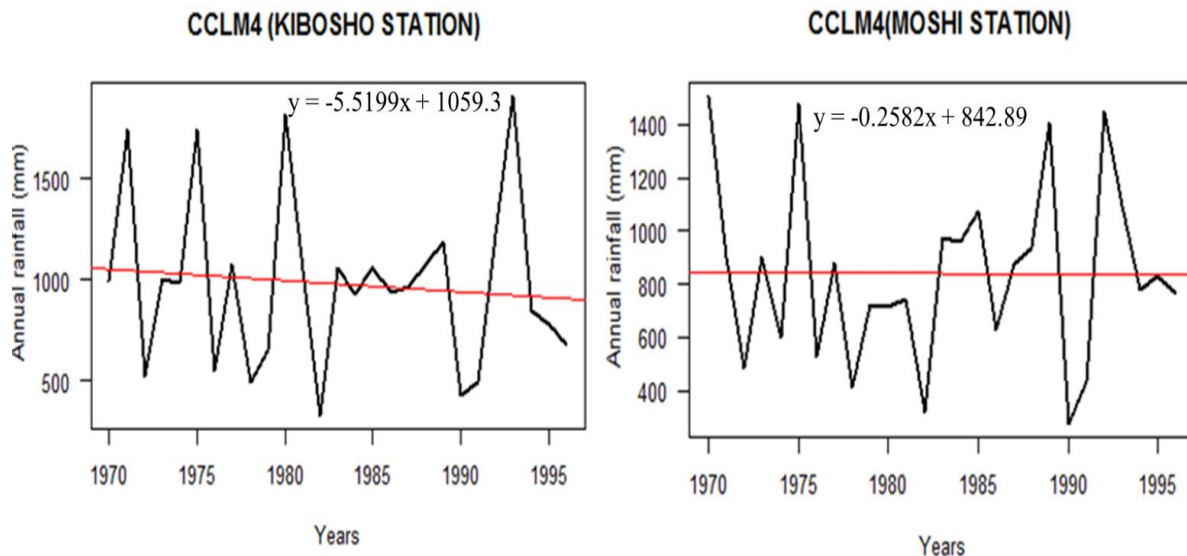


Figure 37: Climate limited area modeling 4 historical rainfall in lowlands and highland

Previous studies show the strongest decline in rainfall amounts of about 6.58 mm/year at $p < 0.05$ that was recorded in the highland areas being represented by Kibosho station (Otte *et al.*, 2016). The results in Fig. 37 show a decrease in annual rainfall amounts of about 5.5199 mm/year, and this figure is more or less close to the reported decline in other studies. The report further shows a decline of about 5.14 mm/yr in the Moshi station but not significant ($p = 0.13$), which show little confidence in the figure. This show that CCLM4 may better simulate the rainfall situation in the study area as compared to RACMO22T. A strong negative trend was also reported by Hemp (2005) for Moshi and Kibosho station. However, most of these studies insist on the importance of carrying out data cleaning (data quality control and gap-filling) due to data irregularities (Hemp, 2005; Lyon & DeWitt, 2012; Otte *et al.*, 2016).

The future projection simulation shows that the future (2005-2100) precipitation exhibit a decreasing trend as depicted in Fig. 37. Under RCP 4.5, the results show that the rainfall will decrease by about 2.2 mm/year in highland areas and 2.7 mm/year in lowland areas. These results suggest that the lowland areas are expected to be comparatively drier than highland areas; it is worth mentioning that much of the agricultural activities are being conducted in the lowland areas. Thus, this decrease reflects the impact on crop irrigation activities in lowland areas, impacting crop production.

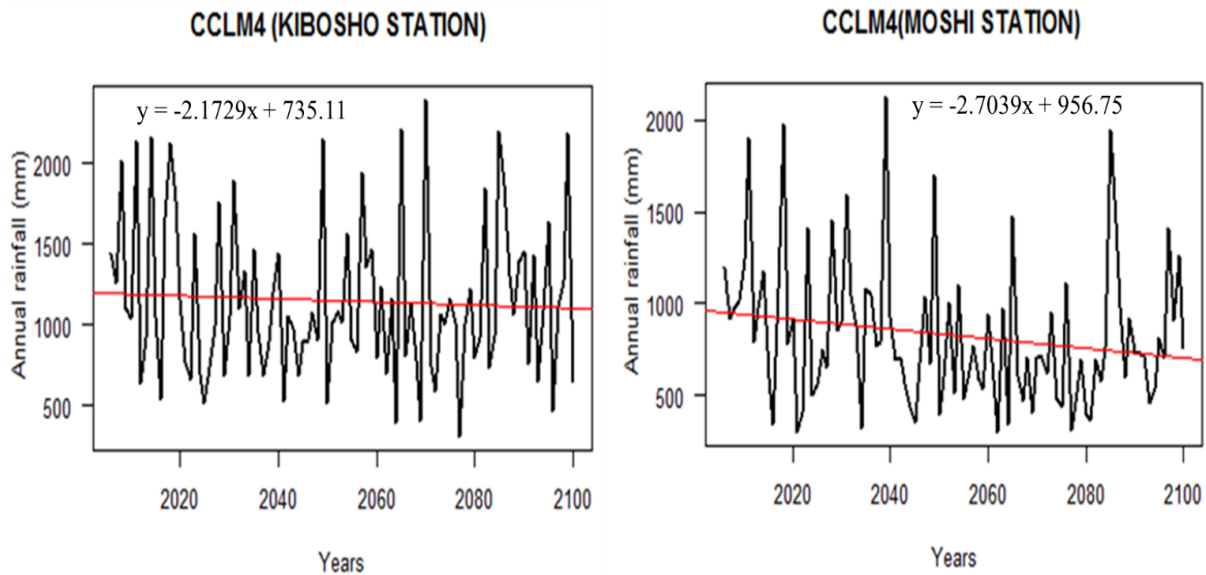


Figure 38: Climate limited area modeling 4 future rainfall projections under representative concentration pathway 4.5

Furthermore, the results show that the rainfall follows a similar decrease under RCP 8.5 (Fig. 38). A comparatively minimal decrease in rainfall is projected under RCP 8.5; about a 0.6 mm/year decrease is projected in the highlands and about 1.1 mm/year in the lowlands. The results mean that the dry lowlands will be drier, and the comparatively wet highlands will be relatively less dry than the lowlands. It is also worth mentioning that the results show a comparatively high decrease in magnitude under RCP 4.5 than RCP 8.5; this might be attributed to the model construction.

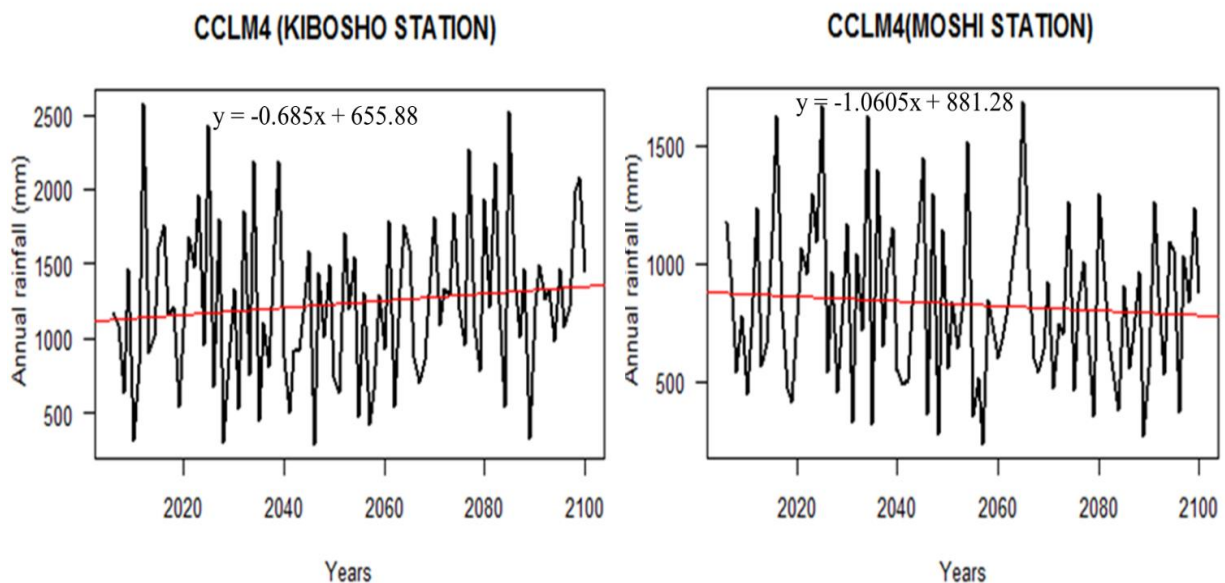


Figure 39: Climate limited area modeling 4 future rainfall projections under representative concentration pathway 8.5

Some of the previous studies reported a similar trend in other areas of Tanzania. Ongoma and Chen (2017) reported the higher negative anomalies in the long rainfall season March-May (MAM) between 1951–2010 in northern regions of Tanzania and Northeastern Kenya. The study further reports the higher negative rainfall anomalies in October-November-December (OND) season than those reported in MAM. Despite that the drying is projected in lowland areas, previous studies suggest that almost all of the moisture in the atmosphere at highland areas comes from the lower elevation through the montane thermal circulation mechanism (Duane *et al.*, 2008).

In the East African region, reports show a decrease in rainfall amounts during the 1979–2005 period (Funk *et al.*, 2008). The intensified drying over East Africa may be due to human-induced activities comparatively improved warming of Indian Ocean Sea Surface Temperatures, which expands the warm pool and Walker circulation westerly, leading to a subsidence anomaly hence the drying (Williams & Funk, 2011). The study further showed that dry phases of the East African long rains are associated with positive SST anomalies over the western tropical Pacific and the opposite to the eastern parts of the ocean. In the detailed analysis of the drivers of the decreased rainfall variability in East Africa, studies reported that the drying trend in East Africa is due to natural decadal variability and not anthropogenic activities (Yang *et al.*, 2014). The report further state that the observed drying trend in the East Africa region is a part of the decadal variability of climate through observations and models.

The decrease in rainfall in the main cropping season (MAM) is envisaged to impact thousands of the farming community due to the fact that this is the main cropping season and that most of the farmers, especially in northern Tanzania, solely depend on rainfed agriculture for their livelihood. Reports alarm that there is medium confidence warns of the intensification of the drought in the present century. This phenomenon result from a decrease in precipitation and/or amplified evapotranspiration over the East African region (Seneviratne *et al.*, 2012). Although this study was not aimed to find the cause of the source of the decline in rainfall amounts, it is worth mentioning that both short and long rains at Mount Kilimanjaro are modified by the individual ENSO and IOD phases. Also, variability in short rains is most vivid, showing a more immediate connection to macroscale mechanisms (Chan *et al.*, 2008; Hastenrath, 2000; Otte *et al.*, 2016).

It is worth mentioning that the intra-annual rainfall distribution cannot be reported as decreasing or increasing over time. The best option may be conceived as seasonal fluctuations of rainfall amount with large intraseasonal variability. However, Otte *et al.* (2016) reported the mean monthly median for the long rains having a significant decrease in the highland and lowland areas around Kibosho and Moshi stations. The study highlights the decline in the peak April values from 254 to 122 mm at KIA, Moshi, and TPC in the lowlands, and from 540 to 348 mm at Kilema and Kibosho in the highlands. Furthermore, the earlier report by Camberlin and Philippon (2002) also reported the decrease in rainfall amounts in the main rainfall season in northeastern Tanzania and Kenya. A decline in rainfall amount during the long rainy season (MAM) in Kilimanjaro was also reported in other studies (Lyon & DeWitt, 2012).

Seasonal rainfall can be conceived in a more mixed feeling. The short rains (OND) are projected to be more variable, while long rains are projected to be variable under different scenarios (Appendix 1 and 2). Under RCP 4.5, the long-term projections show that the rainfall will decrease by 1.28 mm/year and 0.47 mm/year in the highlands and lowlands, respectively. Thus, the lowland areas are projected to be comparatively drier. Furthermore, the long rains (MAM) under RCP 8.5 are projected to decrease by 1.86 mm/year in lowland areas and about 1.2 mm/year in the highlands. The short rains are projected to increase by 0.31 mm/year in the lowlands and 2.77 mm/year in the highlands under RCP 8.5. Under RCP 4.5, OND rains are projected to decrease by about 0.48 mm/year in lowland areas, whereas an increase by about 0.63 mm/year in the highland areas. An increase in short rains in the highlands translates into an increased runoff, hence floods to the lowland areas.

The RACMO22T have shown a more positive trend in historical data contrary to the observation data, this reflects the biases especially when few observation data are used. Thus, for studies of this nature, CCLM4 simulated precipitation comparatively better than RACMO22T. The analysis reports in other areas show that biases in precipitation is a subject of the few observation dataset used, in Greater alpine CCLM biases ranged from +10 to +70%; suggesting that the evaluation of RCM should be carried out using as many datasets as possible for bias calculation and uncertainties reduction (Haslinger *et al.*, 2013). Furthermore, the reports show that over Somalia and northern Tanzania most of the models (> 80%) agree on the sign of the precipitation change; however, as the signal to noise ratio is less than 1, which means that the absolute value of projected change can vary greatly across models (Osima *et al.*, 2018).

4.4.2 Impacts of Climate Change on Temperature

Whereas there is no consensus on the direction of change in rainfall for the future among the selected RCMs. However, there is a much better agreement that temperatures are likely to increase in the future. The minimum and maximum temperatures in the historical (1979-2005) show a similar increasing trend in RACMO and CCLM4 RCMs. Also, in all model simulations, temperatures across the watershed are projected to rise. The historical minimum temperature is presented in Fig. 40; the annual watershed means of the minimum temperature increased by about 0.02°C/year from 1950-2001.

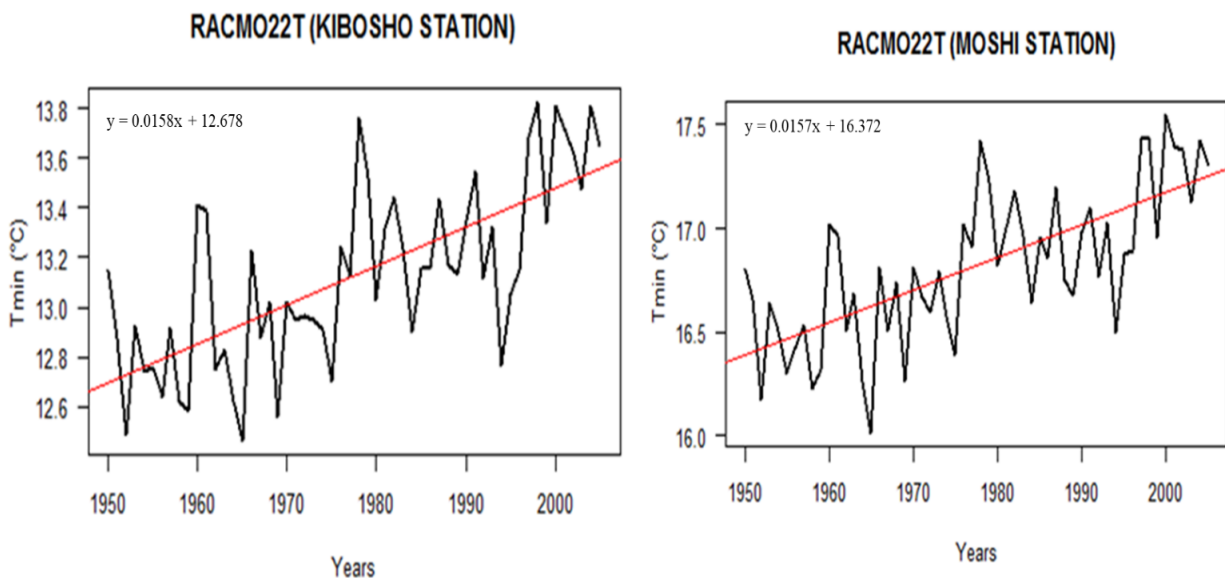


Figure 40: Historical minimum temperature projections for the different weather stations in the Kikafu, Weruweru and Karanga watershed

The minimum temperature projections under RCP 4.5 show increasing temperature in the future (2006-2100). Generally, the minimum temperatures are expected to increase by 0.02°C /year in the highland areas and about the same magnitude in the lowland areas. The minimum temperature of the period between 2030 and 2050 is expected to increase by 0.55°C (from 17.83°C in 2030 to 18.38°C in 2050). Further, from the year 2050 to 2100, the annual means of the minimum temperatures are expected to increase by 0.69°C for lowland areas and about 0.71°C for highland areas. However, it is worth mentioning that the minimum temperatures are lower for the highland areas (represented by the Kibosho station) as compared to lower slopes stations of being represented by Moshi airport (i.e., 13.13°C at the end of 2030, 14.15°C at the end of 2050, and 15.43°C at the end of 2100, respectively). The results are summarized in Fig. 41.

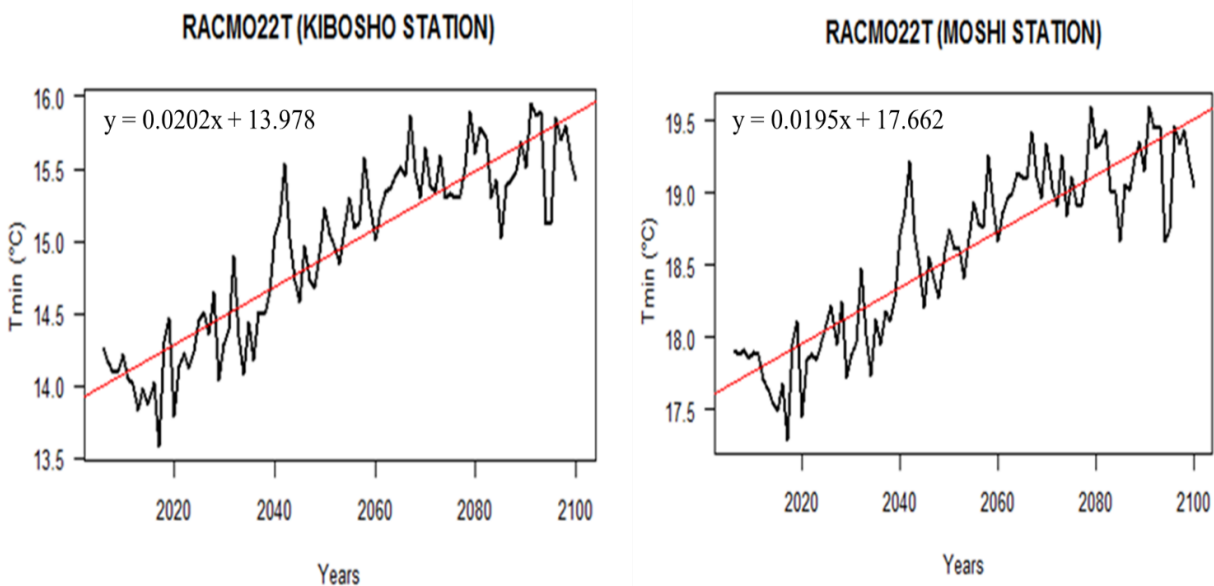


Figure 41: Minimum temperature projections for different weather stations under representative concentration pathway 4.5

The mean minimum temperature is projected to increase by 0.05°C /year in highland and almost the same trend in lowland areas from 2006-2100 under RCP 8.5. This increase is comparatively higher by about 0.03°C /year in highland areas and 0.028°C /year in lowland areas as compared to RCP 4.5.

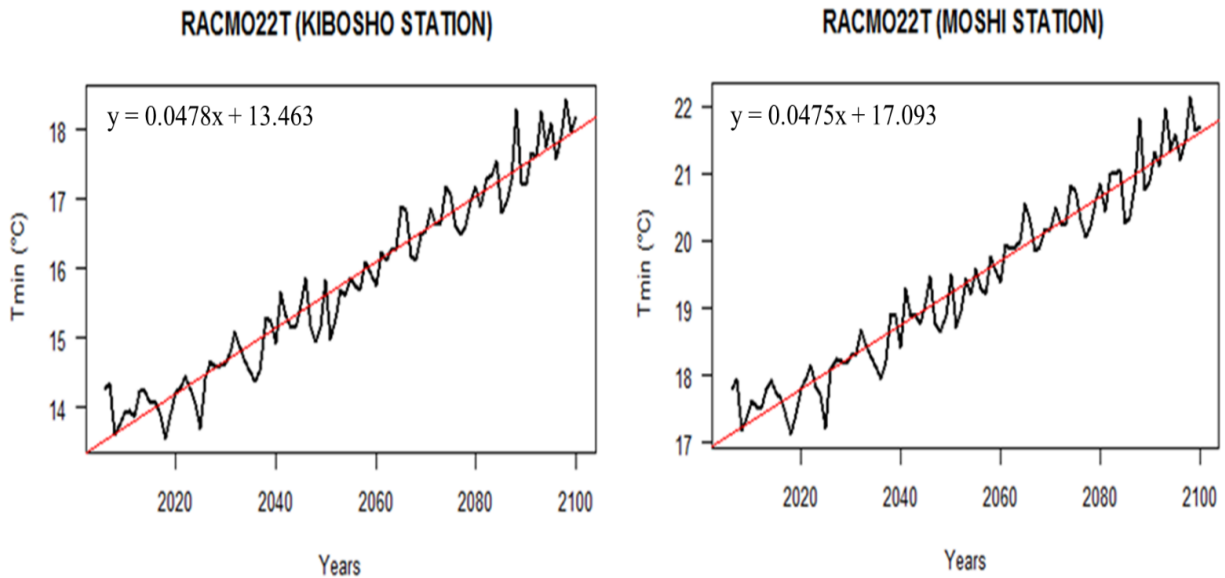


Figure 42: Minimum temperature projections for different weather stations under representative concentration pathway 8.5

The historical maximum temperatures are presented in Fig. 43. The long-time average temperature is simulated to increase by 0.0183°C/year in highland areas, and 0.0179°C/year in the lowland areas. These results translate to hotter daytime in the highland areas as compared to lowland areas.

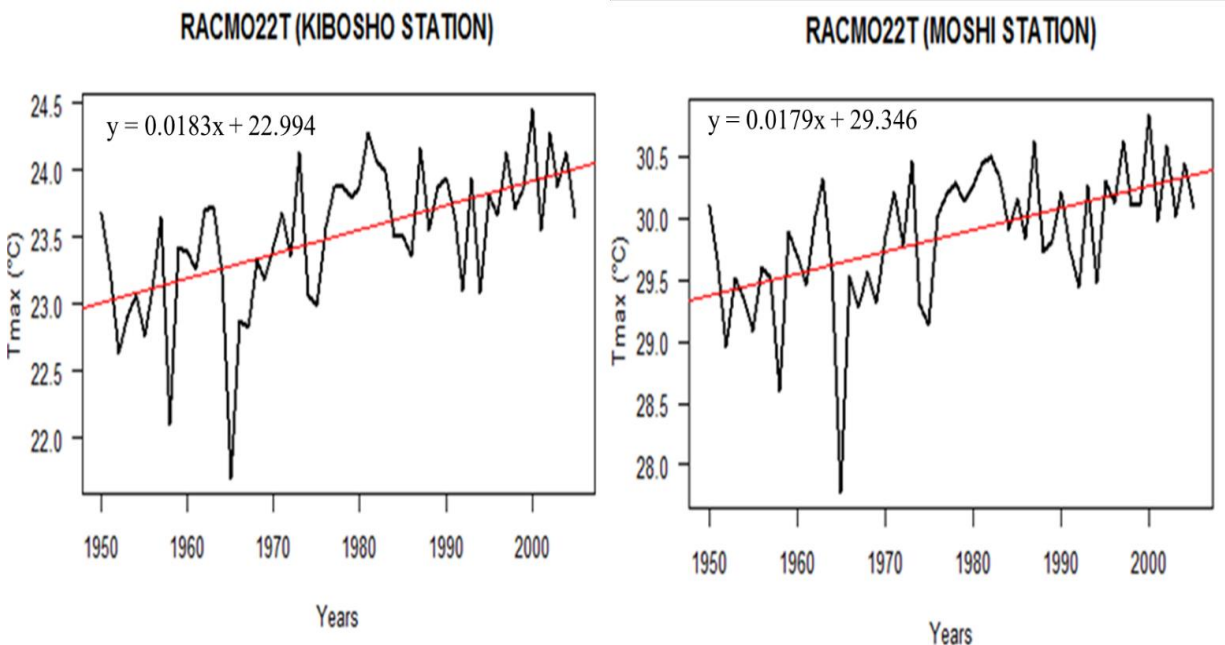


Figure 43: Historical maximum temperature projections for the different weather stations in the Kikafu, Weruweru and Karanga watershed

The annual mean maximum temperatures for the KWK watershed are expected to increase by about 0.02°C for highland areas and almost an equal increment in lowland areas under RCP 4.5. Furthermore, the mean annual maximum temperatures are projected to increase by 0.36°C (from 30.84°C in 2030 to 31.20°C in 2050); this increment is between 2030 and 2050. Also, from the year 2030 to 2050, the annual means of the maximum temperatures are expected to increase by 0.72°C for lowlands and about 0.45°C for highlands. Further, the mean annual maximum temperatures between the years 2050 and 2100 is expected to increase by 0.72°C in lowlands and 0.67°C in highlands. This increment shows that the time between 2030 to 2050 and 2050-2100 is projected to be hot in terms of maximum temperatures; the trend results are presented in Fig. 44.

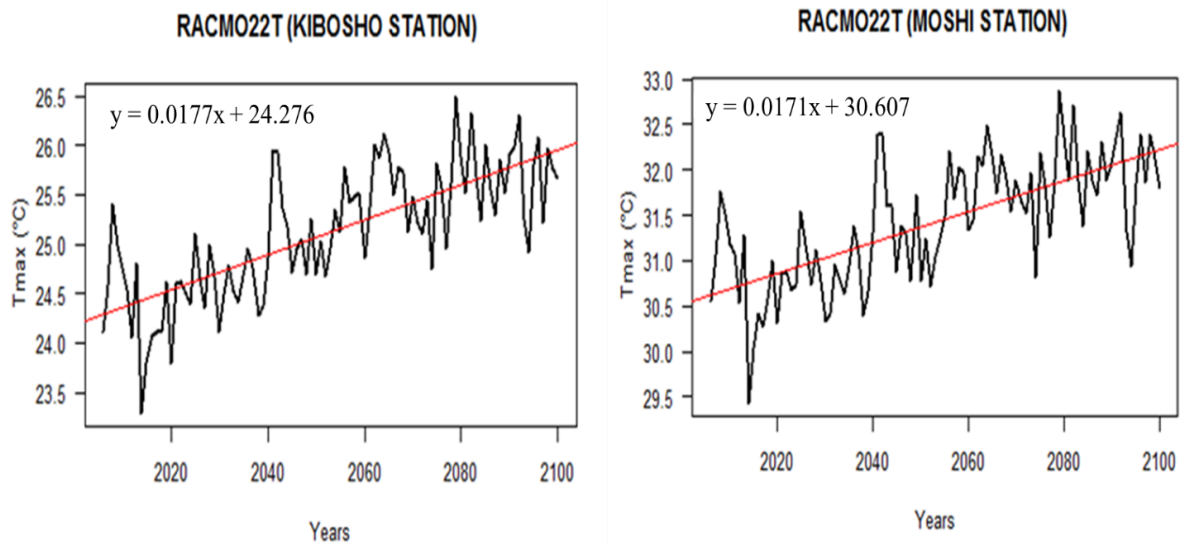


Figure 44: Maximum temperature projections for different weather stations under representative concentration pathway 4.5

The annual mean maximum temperatures projections are presented in Fig. 45. Generally, maximum temperatures are projected to increase by 0.04°C /year in the highlands and almost a similar increment in the lowland areas. Furthermore, the annual means of the maximum temperatures for the KWK watershed under RCP 8.5 between 2030 and 2050 are expected to increase by 1.05°C. i.e., from 33.52°C in 2030 to 30.47°C at the end of 2050 in the lowlands, and 0.97°C, i.e. 24.18°C to 25.15°C in highlands. Furthermore, the mean annual maximum temperatures are expected to increase by from 33.00°C at the end of 2050 to 31.53°C at the end of 2100 in the lowlands; in the highlands, the annual means of the maximum temperatures are expected to increase by 1.66°C by the end of 2100 in the highlands.

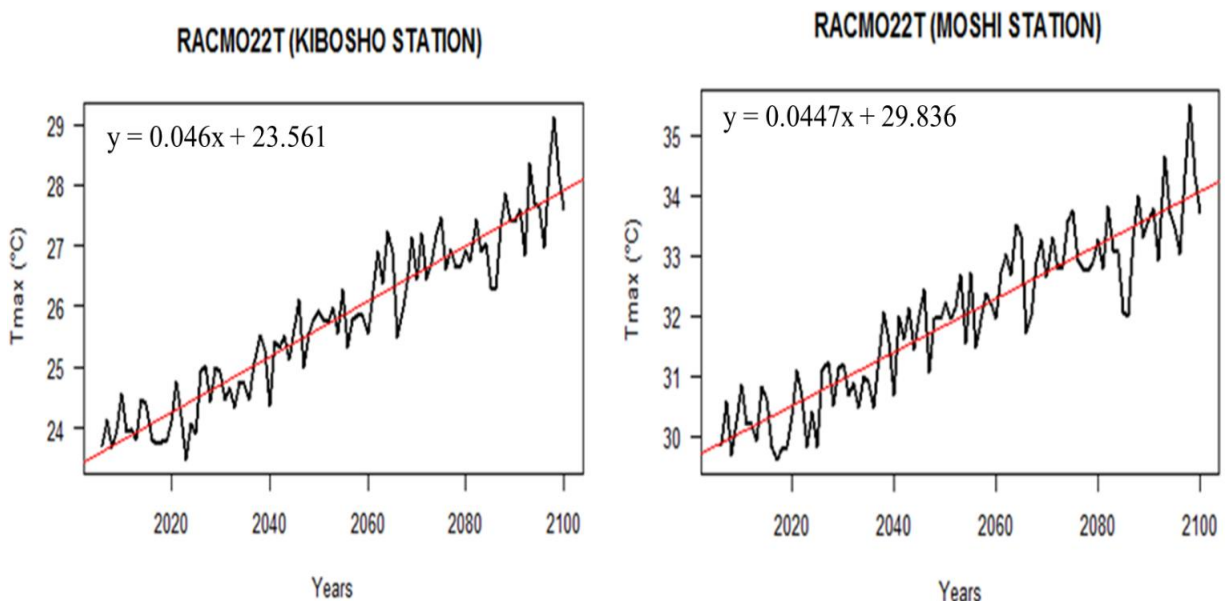


Figure 45: Maximum temperature projections for different weather stations at Kikafu, Weruweru and Karanga watershed under representative concentration pathway 8.5

For CCLM4 RCM, the historical (1950-2005) average minimum temperature for highland areas shows an increase of about 0.0097°C/year in highland areas and 0.0087°C/year in the lowland region (Fig. 46). This means the highland areas are projected to be relatively hotter at night than lowland areas.

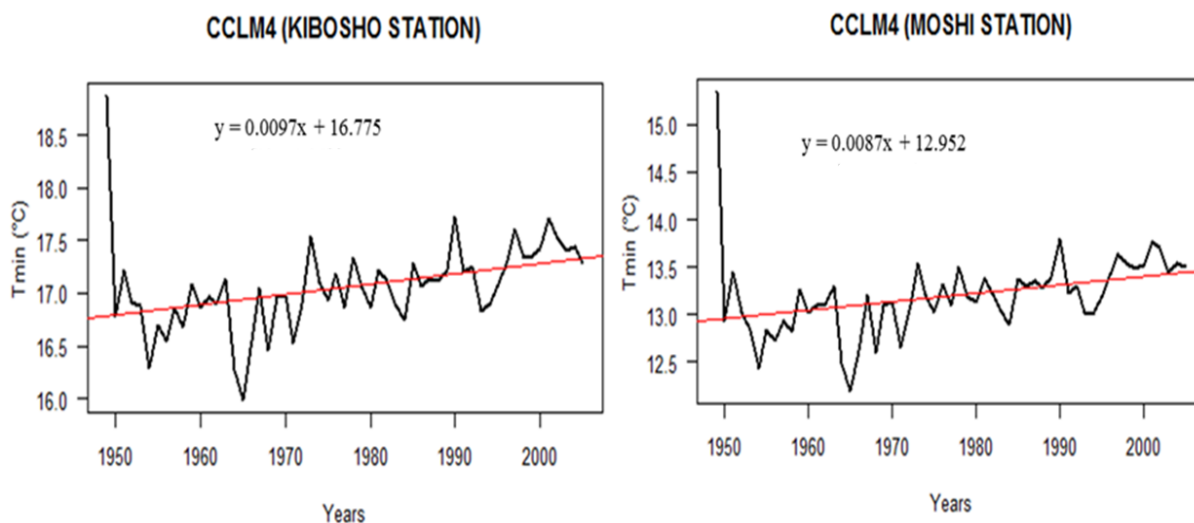


Figure 46: Historical average minimum temperature for climate limited area modeling 4 model

On the other hand, the maximum temperatures from 1950 to 2005 show an increasing trend with a positive slope (Fig. 47). The data show an increase of about 0.012°C/year for highland areas and about 0.016 °C/year for lowland areas. The difference in the change may be attributed to the difference in elevation; generally, the higher the elevation, the lower the temperature.

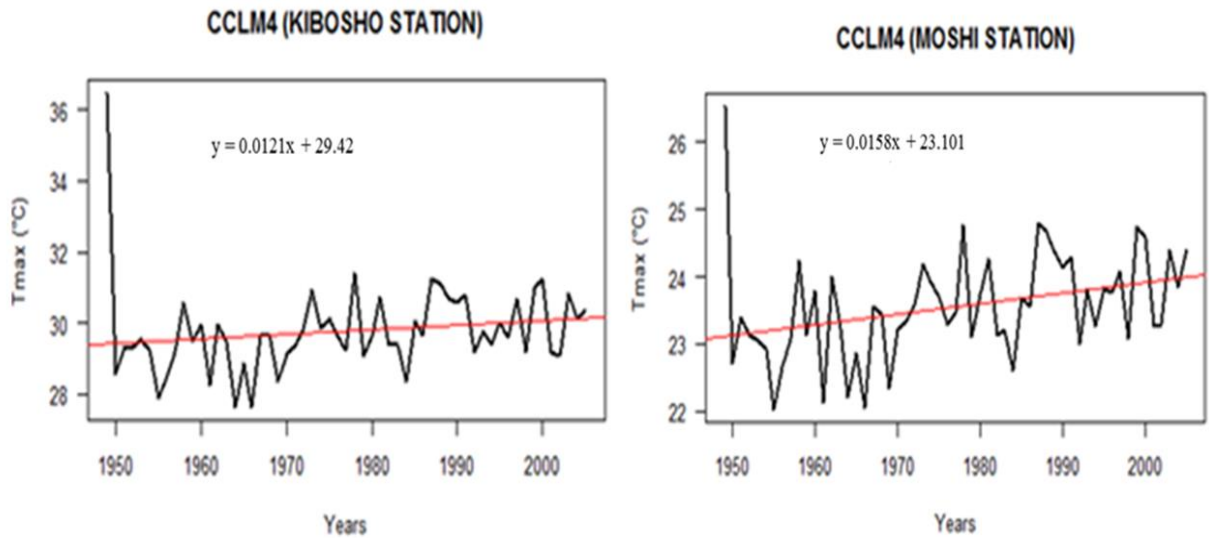


Figure 47: Historical average maximum temperature for climate limited area modeling 4 model

The future average maximum temperatures under RCP 4.5 show that the temperatures are likely to increase by about 0.0227°C /year in the highland areas and 0.0238°C /year in the lowland areas (Fig. 48). This increment is for long term averages and translates to increased hot days and hot nights in the highland and lowland areas in the future.

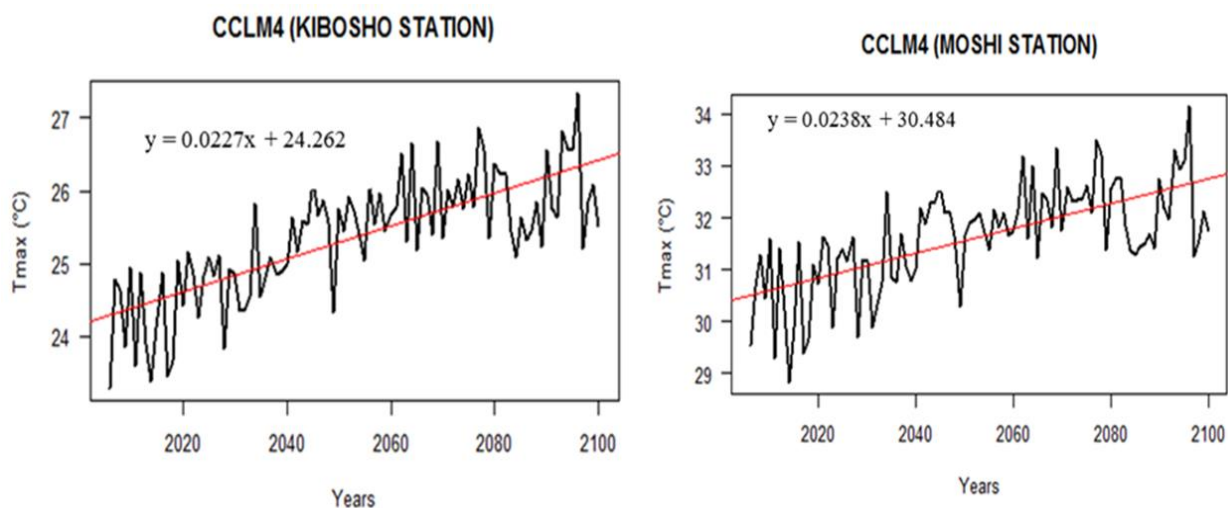


Figure 48: Future average maximum temperature for climate limited area modeling 4 model under representative concentration pathway 4.5

The average long time minimum temperatures under RCP 4.5 show an increase of about 0.018°C/year in highland areas and almost a similar increment in lowland areas (Fig. 46). These results translate to an increase in hot nights in both lowland and highland areas at the same rate.

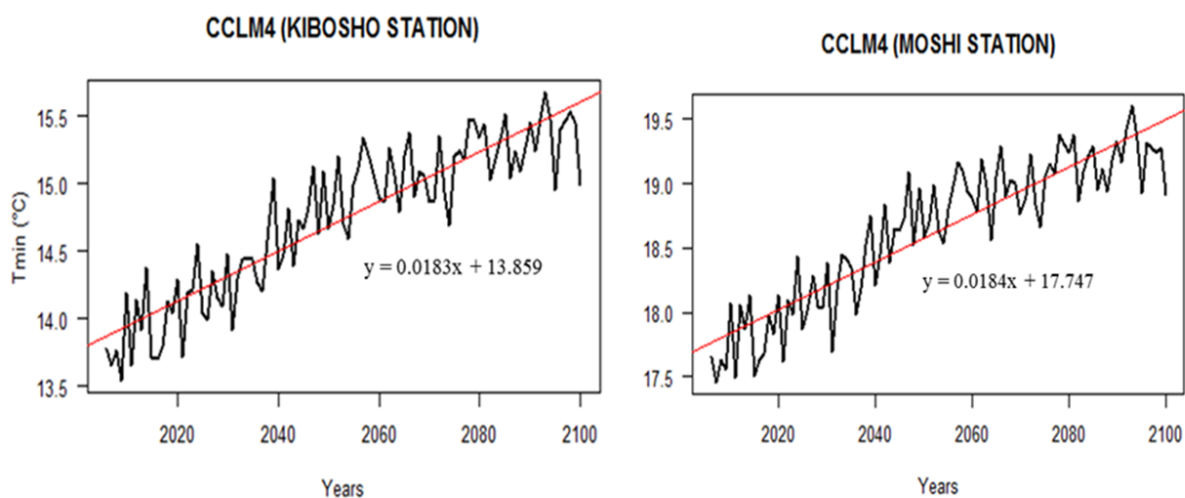


Figure 49: Future average minimum temperature for climate limited area modeling 4 model under representative concentration pathway 4.5

The maximum temperature in the future under RCP 8.5 is projected to increase by about 0.048°C/year, 0.0467°C/year in the lowland areas and highland areas, respectively (Fig. 45). The increment in the maximum temperature in the lowland and highland areas reflects hot days and hot nights.

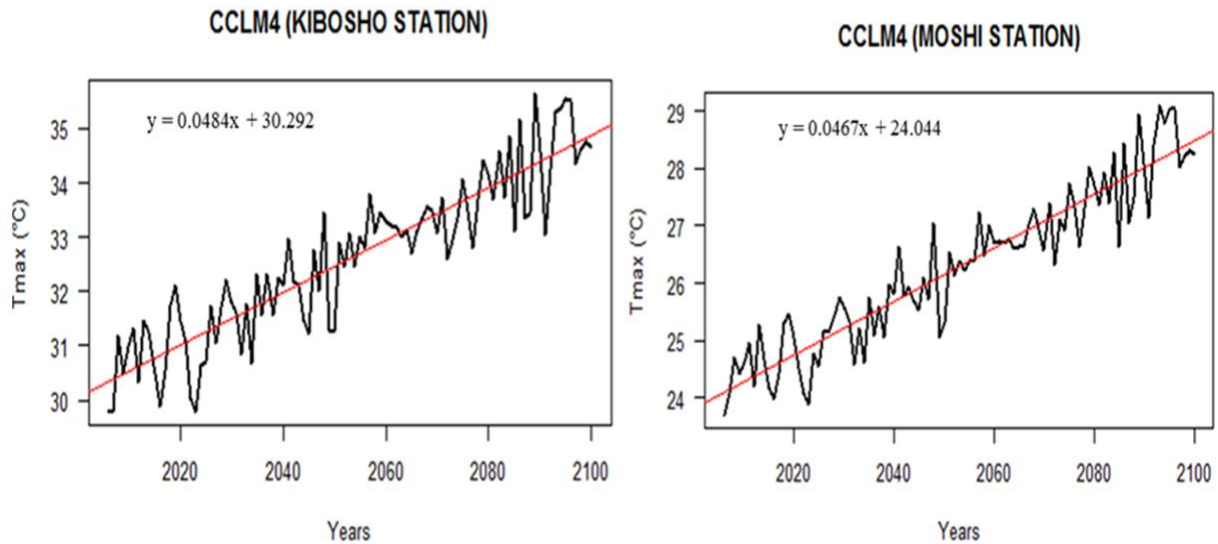


Figure 50: Future average maximum temperature for climate limited area modeling 4 model under representative concentration pathway 8.5

The average minimum temperature under RCP 8.5 also shows an increasing trend with a positive slope. The long time average (2006-2100) show increment of about 0.046°C/year in the highland areas and 0.045°C/year in the lowland areas (Fig. 51). This means the nights are projected to be hotter by an average of about 0.05°C per annum.

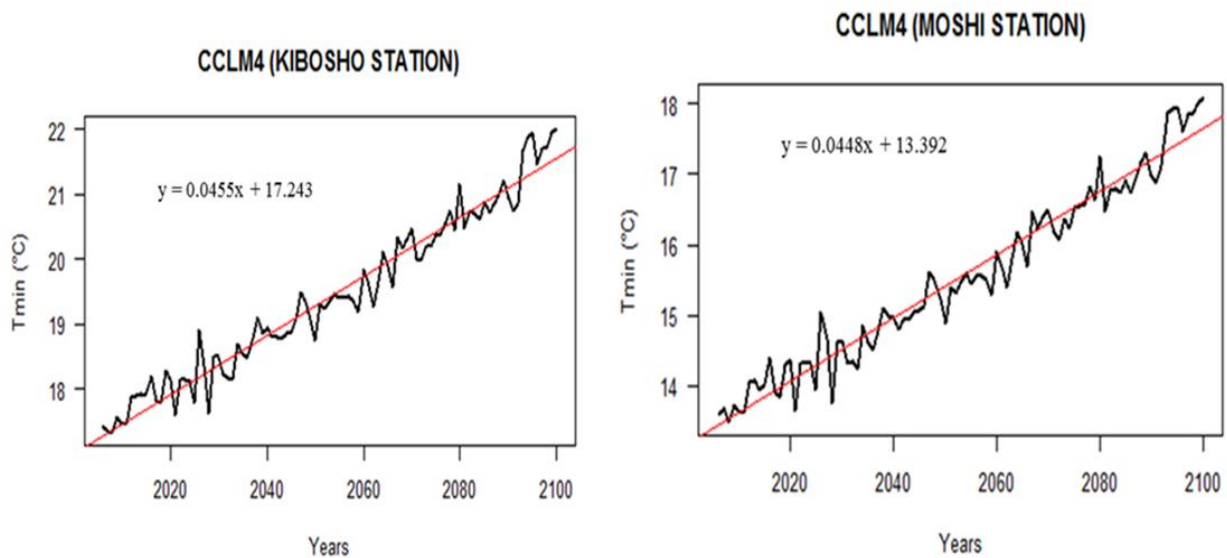


Figure 51: Future average minimum temperature for climate limited area modeling 4 model under representative concentration pathway 8.5

Both minimum and maximum temperatures in the two models show a consistency increase. This observation translates into an increase in the number of hot days and nights and a decrease in the

number of cold days and nights. An increase in the evapotranspiration rates goes along with the increase in temperature; this phenomenon is foreseen to increase the water stress by reducing available soil moisture and will affect the water level in rivers, lakes, and reservoirs. Also, an increase in evaporative demand increases water and moisture demand (Adhikari *et al.*, 2015). Thus, irrigation activities on the foothills of Kilimanjaro need to integrate drought-resistant crops and early maturing plants into their adaptation plans.

The temperatures on the northern foothill of mount Kilimanjaro are reported to increase considerably since 1976 (Altmann *et al.*, 2002). The report further highlights that the average daily maximum temperature increased at about 0.2752°C per decade, and the highest temperature elevation were during February and March. Other studies reported increased temperatures from 1951 and 1960, and 1981 to 1995, and a slight decrease and or stable temperatures in the remaining intervals (Hay *et al.*, 2002).

In other parts of Tanzania, studies also project an increase in Temperatures at varying degrees. For example, the model projections show the highest magnitude increase in temperature by the 2040s along the central regions of Tanzania (Daron, 2014). In other parts of the world, reports show that the global mean temperature rose by about 0.7°C from 1900 (Thompson *et al.*, 2011). Also, the projected rise in average air temperatures from 1990 to 1999 and from 2090 to 2099 show a doubling in warming in the mid to upper troposphere in the tropics (Bradley *et al.*, 2006); although it is worth mentioning that the projections were based on CO₂ levels. Furthermore, studies report warming of about 0.1°C per decade in the last 50 years, taking into account high elevation temperatures and upper-air data (Bradley *et al.*, 2009).

4.4.3 Expected Future Hydrology of the Watershed

The relationship between climate change and water availability in watersheds is assessed using climate and hydrological records (Lalika *et al.*, 2015). Water balance-related fluxes are named important to be monitored because substantial changes in the local hydrological cycle are expected to result in benefits or consequences for the regional ecological system (Mölg *et al.*, 2012). Thus, the average annual values of water balance components for the KWK watershed were simulated by the SWAT model when using climate variables from RACMO22T-ICHEC and CCLM4-CNRM RCM-GCM combinations during the baseline (1979–2005), present century (2006–2040), mid-century (2041–2070) and end century (2071–2100).

The results show that during the historical climate (1971-2000), the highest surface runoff of 297.34 mm is simulated by SWAT forced with RACMO22T-ICHEC (Table 24) and the lowest surface runoff of 39.15 mm is simulated by SWAT forced with CCLM4-CNRM (Table 25). The simulated hydrological parameters differ when different RCMs and GCMs are used. The differences might have emanated from the RCMs construction (Luhunga *et al.*, 2016; Mutayoba *et al.*, 2018). i.e., two or more RCMs can yield different results. For example, the SWAT model simulates WatQ of 698.12 mm and 667.64 mm when forced by RACMO22T-ICHEC and CCLM4-CNRM, respectively. Studies show that even when similar RCMs are using, but with different GCMs, SWAT simulates WatQ differently (Mutayoba *et al.*, 2018).

Table 24: Average annual basin values as simulated by soil and water assessment tool model fed with climate data from regional atmospheric climate model 22T- Irish Centre for High-End Computing for two scenarios representative concentration pathway 4.5 and representative concentration pathway 8.5

Hydrological parameters	Baseline	Present century (2006-2040)		Mid-century (2041-2070)		End Century (2071-2100)	
	1979-2005	RCP 4.5 (%Change)	RCP 8.5 (%Change)	RCP 4.5	RCP 8.5 (%Change)	RCP 4.5	RCP 8.5 (%Change)
PCP	1203.3	1288.3(7.06)	1228.8(2.12)	(%Change)	1213.3(0.83)	(%Change)	1246.7(3.61)
SurfQ	350.23	370.31(5.73)	354.12(1.11)	1236.4(2.75)	421.91(20.47)	1246.4(3.58)	502(43.33)
ET	571.1	572.4(0.23)	573.6(0.43)	388.67(10.98)	571.2(0.02)	391.83(11.88)	602.8(11.5)
WatQ	698.12	691.23(0.23)	676.68(0.43)	570.1(0.18)	671.32(0.02)	606.6(6.22)	636.8(5.55)
GWQ	268.91	256.96(-4.44)	243.98(-9.27)	688.46(-0.17)	258.94(-3.71)	693.29(0.09)	275.73(2.52)

PREC = Precipitation; SurfQ = Surface runoff; ET = Evapotranspiration; WatQ = Water yield; GWQ = Groundwater flow.

The results of this study are inconsistent with other studies that reported a continuous multiyear groundwater level decline with marked episodic recharge events in Tanzania, Namibia and South Africa (Cuthbert *et al.*, 2019). This may be a result of the finer resolution of the dataset used in this study as compared to other similar studies. Furthermore, the detailed analysis carried out for Tanzania where the reports show that groundwater recharge occurs after a continuous rainfall exceeding 70 mm over a 9-day period (Seddon, 2019). Furthermore, the impact assessment on the Ngererengere catchment streamflow shows that the average annual streamflow is projected to decrease by 2.1% in the 2050s; the report further shows the increase in annual streamflow by about 58% in 2080s (Shagega *et al.*, 2020).

Table 25: Average annual basin values as simulated by soil and water assessment tool model fed with climate data from climate limited area modeling 4-CNRM for two scenarios, representative concentration pathway 4.5 and representative concentration pathway 8.5

Hydrological parameters	Baseline	Present century (2006-2040)		Mid-century (2041-2070)		End Century (2071-2100)	
	1979-2005	RCP 4.5 (%Change)	RCP 8.5 (%Change)	RCP 4.5 (%Change)	RCP 8.5 (%Change)	RCP 4.5 (%Change)	RCP 8.5 (%Change)
PCP	1083.9	1109.3(2.34)	1098(1.30)	1067.4(-1.52)	1086.9(-1.01)	1051.2(-3.02)	1080.1(0.57)
SurQ	340.23	447.47(31.52)	555.7(63.33)	538.83(58.37)	546.81(60.72)	652.81(91.87)	797.44(134.38)
ET	574.5	594.34(3.45)	605.2(5.34)	627.7(9.26)	672.4(17.04)	758.8(32.08)	773.4(34.62)
WatQ	667.64	697.35(4.45)	647.7(-2.99)	697.26(4.44)	636.06(-4.73)	708.67(6.15)	662.29(-0.8)
GWQ	203.55	222.86(9.4)	209.8(3.07)	212.35(4.32)	197.02(-3.21)	206.55(1.47)	223.71(-10.73)

PREC = Precipitation; SurfQ = Surface runoff; ET = Evapotranspiration; WatQ = Water yield; GWQ = Groundwater flow

4.4.4 The Impacts of Climate Change on Water Balance Components

The climate model's uncertainties may be associated with the different formulation and parameterization schemes in those models (Mutayoba *et al.*, 2018). Some of the uncertainty may arise from individual Regional Climate Model (RCM), whereas other uncertainty may arise from the driving General Circulation Model (GCM) (Luhunga *et al.*, 2018). The uncertainties resulting from RCM-GCM combinations were accounted for by taking the mean of the four climate model members, as proposed by Mutayoba *et al.* (2018) (Table 26). Finally, the mean of the two climate model members was used to simulate water balance components in the SWAT model.

Table 26: Mean annual basin values as simulated by soil and water assessment tool model fed with climate data from regional climate model ensemble average for two scenarios representative concentration pathway 4.5 and representative concentration pathway 8.5

Hydrological parameters	Baseline	Present century (2006-2040)		Mid-century (2041-2070)		End Century (2071-2100)	
	1979-2005	RCP 4.5 (%Change)	RCP 8.5 (%Change)	RCP 4.5 (%Change)	RCP 8.5 (%Change)	RCP 4.5 (%Change)	RCP 8.5 (%Change)
PREC	1143.6	1198.8(4.83)	1163.4(1.73)	1151.9(0.73)	1143.1(0.04)	1148.8(0.45)	1168.4(2.17)
SurfQ	345.23	408.89 (18.44)	454.91(31.77)	463.75 (34.33)	484.36(40.3)	522.32(48.4)	649.72(88.2)
ET	572.8	583.37(1.85)	589.4(2.9)	598.9(4.56)	621.8(8.55)	682.7(19.19)	787.1(37.41)
WatQ	682.88	694.29 (1.67)	662.19(-3.03)	692.86(1.46)	653.69(-4.27)	700.98(2.65)	672.79(-1.48)
GWQ	236.23	239.91(1.56)	226.89(-3.95)	237.12(0.38)	227.98(-3.49)	242.73(2.75)	228.72(-3.18)

PREC = Precipitation; SurfQ = Surface runoff; ET = Evapotranspiration; WatQ = Water yield; GWQ = Groundwater flow

The water balance components in Table 26 are aimed to minimize uncertainties in the KWK watershed. Thus, the results are envisaged to provide the best estimates of the future climate change in the watershed as they take into account the uncertainties from RCMs and driving GCMs used. The results in Table 26 show an increase in the annual rainfall over the current, mid and end centuries for both RCP 4.5 and RCP 8.5. Furthermore, the results reflect increased temperature projections in the KWK watershed under RCP 4.5 and RCP 8.5. Also, the groundwater and water yield component are projected to decrease under RCP 8.5 during the present (for about 4.27%), mid and end centuries (for about 1.48%). Furthermore, the surface runoff shows increases under RCP 4.5 and RCP 8.5 during the present, mid and end centuries. Generally, surface runoff is expected to increase by 37.96% at a 95% confidence level.

On the other hand, groundwater flow is predicted to decrease under RCP 8.5 during the present, mid and end centuries while the same show a relatively slight increase under RCP 4.5. Also, the surface runoff and evapotranspiration are projected to increase under two emission scenarios during the present, mid and end centuries. The high increase in evapotranspiration and surface runoff (37.41% and 88.2%, respectively) are projected during the end century (1971-2100), reflecting the increased short period storms that may cause environmental problems such as floods and siltation in downstream dams. The high short period storms might result in the destruction of infrastructures, destroy crops, and cause siltation in downstream dams (i.e., Nyumba ya Mungu dam), impacting fishing and hydropower production. The increased flood order may occur with a high degree of uncertainty; thus, communities along the southern slopes of Kilimanjaro and the Pangani basin need to take into account the projected impacts in adaptation measures.

During the mid and end century, the predicted surface runoff may be significantly higher; 48.4% and 88.2% for RCP - 4.5 and RCP-8.5 for the end century, respectively, and 34.33 for RCP-4.5 and 40.3% for RCP-8.5. This increase means mid and end centuries may exhibit a higher degree of uncertainty in the expected runoff volumes in the KWK watershed. Therefore, the fluctuation and severity of the flood events are evident owing to the nature of the topography and land use that it contains. Increased evapotranspiration reflects the projected increased temperatures; generally, evapotranspiration increases as the temperature increases (Mwamila *et al.*, 2008).

4.4.5 The Projected Hydrology and its Implication in Water-Food-Energy (WFE nexus)

Climate change afflicts human wellbeing by posing a substantial impact on the environment, crop and livestock production, and water resources (Araya *et al.*, 2015). Temperature influences water availability through increased/reduced evapotranspiration. Generally, the higher the temperature, the higher the evapotranspiration (Christensen *et al.*, 2004; Mwamila *et al.*, 2008). Decreased precipitation is envisaged to affect both food and livestock production and hydropower plants downstream.

The projected increase in temperature is expected to influence wilting and drying of plants, multiplication of pest, weeds, and diseases that would result in increased costs of crop production and failures in crop yields (URT, 2003). This phenomenon is projected to threaten livelihood by decreasing food security. Also, the availability of raw materials for industries will also be affected; in the long run, impacts in raw materials is viewed to be a stumbling block for the national target towards building the industrialized economy. In addition, warmer temperatures are also likely to cause an eruption of pests, new parasites and diseases that would affect a huge number of animals (IPCC, 2012). An increase in temperatures has been reported to affect maize and bean production in the Hai district (Munishi *et al.*, 2015), and coffee production declined due to an increase in the minimum temperatures (Craparo *et al.*, 2015; Mmbaga *et al.*, 2017). The projected increase in minimum and maximum temperatures is likely to influence further decline in crop production. A similar trend is projected to impact coffee production until the 2060s if the current land-use changes and climate change go unattended (URT, 2012). This phenomenon is envisaged to affect the economic wellbeing of livestock keepers and smallholder farmers that solely depend on farming for their livelihood.

The projected decrease in precipitation from CCLM4 model is likely to decrease discharges in rivers and streams. Other studies already projected 6% and 9% annually (Agrawala *et al.*, 2003). The observation from this study capitalized on the future decrease in available water for various uses; this decrease is likely to strengthen the impacts on the livelihood of the local population relying on streams and springs as major sources for crop production (Lalika *et al.*, 2015), and domestic uses (Mckenzie *et al.*, 2010). However, about 85% of the arable land is dominated by Smallholder farmers and traditional agro-pastoralist; the former mainly rely on rainfed agriculture (Lein, 2004).

The water-related conflicts are already reported and detailed in chapter two. A study by Kishiwa *et al.* (2018) shows that the water demand deficit for irrigation and livestock production is projected to increase by 71.12% and 1.41% (by 2060s). Scholars worldwide have reported water-related conflicts; there is a strong belief that 21st-century wars will be fought over water (Adams *et al.*, 2010; Mbonile, 2005). Tagseth (2008) reported the water crisis in the Kilimanjaro region at alarming levels for decades today. Thus, there is a need to integrate future adaptation responses to future development plans (Kangalawe, 2016).

Hydropower production is the primary power generation means in Tanzania; energy production needs replanning due to the focus of the country to build an industrialized economy. The projected decrease in annual rainfall is likely to affect this area. Reports show that the water efficiency for hydropower production is as low as 35%; thus, this figure is expected to decrease more in future. Contrary to these results, Cole *et al.* (2014) predicted increases in the mean hydropower power production from dams in Tanzania. However, their report contradicts the findings of this study and other studies (Agrawala *et al.*, 2003; Kishiwa *et al.*, 2018; Lalika *et al.*, 2015). Their results still insist on climate variability and anthropogenic pressure as the chief factor to be considered during dam design, which means the analysis did not consider climate variability in its depth.

CHAPTER FIVE

CONCLUSION AND RECOMMENDATIONS

5.1 Conclusion

This study assessed current and future climate and land use/cover changes and the impacts on surface and groundwater resources. Apart from the discussions carried out, the following conclusions can be inferred from the present study.

In the first objective, the LULC changes revealed a rapid increase in built-up area and agricultural land. The future prediction results show that agricultural and urban growth might continue to expand in the future, which will impact land and other resources if the situation goes unattended. However, expansion in agricultural land and production of staple food crops are not a one to one function. Thus, an increase in agricultural land has a flimsy contribution to increasing food production in the KWK watershed.

In the second objective, the findings of this work show that changes in the water balance components are the function of the land-use changes and vegetation distribution within the watershed. The major LULC changes that affected surface runoff and groundwater components in the watershed during the study period were the expansion of agricultural land, built-up area, and shrinking of the grassland. Furthermore, the morphological study revealed that runoff is the most important hydrological flux for managing water resources on the KWK watershed. The watershed is prone to increased surface runoff due to its location on mountain slopes, and hence the reoccurrence of floods; this makes farming in the lowland areas challenging due to increased erosion and damage crops.

In the third objective, small scale irrigation activities were confirmed as important pollution sources to surface water bodies that may pollute groundwater and transfer pollutants in respective aquifers. This mutual dynamic increases pollution, rendering both sources unfit for potable uses, prioritized in any water resource consumption trade-offs. Also, the $\delta^2\text{H}$ and $\delta^{18}\text{O}$ values confirmed that; groundwater in the dry season has similar properties to surface water along watercourses, and recycled water is the major recharge means. Contrary, a ten-year ice core study on Mount Kilimanjaro suggests that as the glacier melts during the dry season on Mount Kilimanjaro, it sustains downstream water availability along the mountain's slope.

Furthermore, the Piper trilinear and Durov diagrams showed HCO_3 enrichment and mixed CaNaHCO_3 water types. Although most water sources were suitable for irrigation use, it is worth noting that some of the water sources have small to medium salinity and sodium hazard. Thus, it is essential to take necessary measures during application before the situation becomes unmanageable.

In the fourth objective, the sensitivity CCLM4 RCM model satisfactorily represented the historical and future climate on the mountainous KWK watershed. This conclusion is reached based on the coefficient of variation between the simulated and observed historical precipitation data. The future minimum and maximum temperatures are projected to increase in the future. This increment may be reflected in evapotranspiration and decreased soil moisture; thus, future agriculture production will necessitate engagement of the early maturity crops for ensuring food security. These observations can be translated as described hereunder.

- (i) The economies and livelihoods of people dwelling on the mountain slopes are highly relying on rain-dependent systems and so are vulnerable to current and future rainfall variability and potential changes in rainfall due to climate change. The projected decrease in long rains and the perceived increased variability of the short rains is determined to affect food crops production, livestock production and energy production. Generally, the livelihood of people dwelling on the mountain slopes will necessitate future replanning.
- (ii) The current population pressure necessitates more water abstraction. However, the KWK watershed and the Pangani basin are already water-stressed, and the projected variation in water balance components is envisaged to increase the water stress on the mountain suburbs, thus, affecting the livelihood of the communities.
- (iii) poor implementation/enforcement of the current water governance structure, including laws, bylaws, procedures, guidelines, policies and strategies, primarily due to resources constraints, does not make it easy for sustainable water resources governance and one can argue that it is disjointed and has major slots that compromise meaningful water resource management,
- (iv) It was concluded that planning for water resources necessitate site-specific information on the impacts of the future climate and anthropogenic pressure on the available resources. However, the combination of the various methodology used in this study

enabled filling that research gap and the information generated herein can help in planning and managing similar watersheds. It is also worth stating that the methodology applied in this study can be applied to other similar watersheds with or without adjustment.

5.2 Recommendations

In addition to the results and discussions, this study proposes recommendations for sustainable management of surface and groundwater resources on the Mount Kilimanjaro slopes. Generally, the recommendations may be separated into policy and catchment recommendations, as well as the recommendations for further study.

- (i) Translating the results of this study into an integrated climate and anthropogenic resilient water management system would have produced impressive output; this component has not been carried out. Thus, future projects could focus on translating the results of this study to a water management framework.
- (ii) Integrating soil and water management strategies and agronomic practices focused on increasing crop production per unit area rather than agricultural land expansion. This is due to the fact that the rapid increase in agricultural land is mainly focused on increasing food production; however, this expansion does not guarantee an increase in crop production.
- (iii) Due to increased pressures on agriculture and built-up areas, most of the activities and settlements fall within the reserved areas for water resources protected by Tanzanian laws and regulations. However, some of the structures (for example residential houses), especially where the rivers crosses the suburbs, existed before enacting these regulations. Thus, future projects could focus on the best strategies to conserve water resources taking into account the current and future development. Some of the strategies includes participatory water resources management programmes, implementation of regulations restricting conduction of the activities close to water resources, as well as proper land use planning.
- (iv) To raise awareness among all stakeholders, farmers, and pastoralists on the impacts of polluting water sources and risks of consuming and irrigating water of unknown quality;

furthermore, water users need to be trained on the risks of developing wells without prior authorization from the Water Board authorities.

- (v) The KWK watershed is located on the southern slopes of Kilimanjaro and part of the northern part of the Pangani Basin. Future projects should consider extending the methodology used in this study to the entire basin to obtain the complete scenario throughout the basin and other similar basins.
- (vi) The results of this study may have been affected by the sparse/absence of the precipitation observation network, especially for the upper slopes of Mount Kilimanjaro. Also, unavailability of good-quality data and data discontinuation have been reported in this and several other studies. Thus, future projects could focus on creating a good observation network, data cleaning and proper storage that is determined to increase the efficiency of future hydrological simulations.
- (vii) While glacier ice and water were included in this model, it is worth noting that the preparation of suitability maps and future simulation accuracy, especially with glacier ice, posed a significant challenge. Although annual rainfall was included in this simulation, adding more variables such as solar radiation and humidity could increase simulation accuracy in the future. However, high quality altitudinal data is scarce or non-existent. As a result, future research should concentrate on the use of cutting-edge techniques to accurately model the future dynamics.
- (viii) Since SWAT is not good at simulating localized recharge, further studies could focus on using the integrated SWAT-MODFLOW in hydrological simulations. SWAT is powerful in simulating distributed recharge, whereas MODFLOW is good in simulating localized recharge; this combination is expected to produce the best results than using these models separately.
- (ix) The PLSR is inefficient in analyzing the spatial relationship between predictors (land use/cover types) and water balance components. Thus, future research could focus on the relationship between spatial land-use patterns and changes in the water balance components.
- (x) Some of the drivers and determinants of land use/cover changes have been difficult to simulate with current land use/cover change models. For example, government policies,

socio-cultural and behavioral changes increase influence changes in land use/cover on the slopes of Kilimanjaro. The political will and environmental due diligence to control the implementation of the current environmental programs are also out of scientific control. Future studies could focus on generating scenarios that integrates drivers due to changes in government policies and behavioral changes in future land cover simulation.

- (xi) Socio-economic drivers of LULC are assumed to remain as per the current situation in future. Thus, simulating different LULC change scenarios with different changes in driving forces can provide alternative future trajectories. Although the variables used were measured over a prolonged time, it is believed that the model accounted for dynamic regular driving forces that were happening in time series and during the prediction. Except for extreme events such as prolonged droughts or civil wars, which future works could focus on.
- (xii) Information about the recharge areas and their stability, which includes the degree to which the changes in land use and climate influence the recharge and thereby the spring's yield of the Kilimanjaro slopes, is scanty or absent. Although this study established a link between hydrological fluxes, land use/cover and climate changes, future studies could focus on the generation of information about recharge areas and their stability.
- (xiii) The KWK being located on mountainous is prone to extreme events such as floods and sedimentation. Thus, future research may be focused on predicting high flows, which include extreme events and flooding events and sedimentation using high resolution datasets.
- (xiv) The details of water demand for each land use plan and representation of each vegetation type in most of the models are approximate and mostly generalized in the process. The local adaptation strategies are mostly site-specific and need to be included in the recent models; hence, future studies could focus on documenting the local mitigation and adaptation strategies and include them in the future decision support systems.
- (xv) Impacts of LULC on water resources regarding the recharge response to the land-use change were not considered in the current work. This could be realized by identifying recharge areas, the contribution of the fog interception zone to the hydrology of the area and substantial protection laws imposed for future water sustainability. This research can

then be used as input to future research focused on determining the impact of land-use changes in localized recharge and conditions against flooding in the research area.

- (xvi) Due to increased surface runoff, future studies should focus on quantification and strategies focused on managing floods. Strategies such as planting vegetation to retain extra water, terracing hillsides to slow flow downhill, and the construction of floodways (man-made channels to divert floodwater) may be used. This is because increased surface runoff is likely to increase sedimentation to the downstream hydropower dams (e.g., Nyumba Ya Mungu Dam), which contributes electricity to the national grid.

REFERENCES

- Abbaspour, K. (2015). *SWAT Calibration and Uncertainty Programs: A User Manual*. https://swat.tamu.edu/media/114860/usermanual_swatcup.pdf
- Abbaspour, K., Vaghefi, S. A., Yang, H., & Srinivasan, R. (2019). Global soil, land use, evapotranspiration, historical and future weather databases for SWAT Applications. *Scientific Data*, 6(1), 1-11. <https://doi.org/10.6084/m9.figshare.10043090>
- Abbaspour, K. C. (2011). *Swat-Cup2: SWAT Calibration and Uncertainty Programs Manual Version 2*. Switzerland: <http://www.utd.edu/~herve>
- Abdi, H. (2007). Partial least square regression. In N. J. Salkind (Ed), *Encyclopedia of Measurement and Statistics* (pp. 1-13). Sage Publications. <http://www.utd.edu/~herve>
- Abdi, H. (2010). Partial least squares regression and projection on latent structure regression. *Wiley Interdisciplinary reviews: Computational Statistics*, 2(1), 97-106. <https://doi.org/10.1002/wics.51>
- Abe, C. A., Lobo, F. D. L., Dibike, Y. B., Costa, M. P. D. F., Dos Santos, V., & Novo, E. M. L. (2018). Modelling the effects of historical and future land cover changes on the hydrology of an Amazonian Basin. *Water*, 10(7), 1-19. <https://doi.org/10.3390/w10070932>
- Abudu, S., Cui, C. l., Saydi, M., & King, J. P. (2012). Application of snowmelt runoff model in mountainous watersheds: A review. *Water Science and Engineering*, 5(2), 123-136. <https://doi.org/10.3882/j.issn.1674-2370.2012.02.001>
- Ackah, M., Agyemang, O., Anim, A., Osei, J., Bentil, N., Kpattah, L., Gyamfi, E., & Hanson, J. (2011). Assessment of groundwater quality for drinking and irrigation: The case study of Teiman-Oyarifa Community, Ga East Municipality, Ghana. *Proceedings of the International Academy of Ecology and Environmental Sciences*, 1(3-4), 186-194.
- Adams, W., Brun, C., & Havnevik, K. (2010). Studies of the waterscape of Kilimanjaro, Tanzania: Water management in hill furrow irrigation. *Norwegian Journal of Geography*, 64(3), 6172-6173. <https://doi.org/10.1080/00291951.2010.502657>

- Adhikari, U., Nejadhashemi, A. P., & Herman, M. R. (2015). A Review of Climate Change Impacts on Water Resources in East Africa. *Transactions of the American Society of Agricultural and Biological Engineers*, 58(6), 1493-1507. <https://doi.org/10.13031/trans.58.10907>
- Adhikari, U., Nejadhashemi, A. P., Herman, M. R., & Messina, J. P. (2017). Multiscale Assessment of the Impacts of Climate Change on Water Resources in Tanzania. *Journal of Hydrologic Engineering*, 22(2), 1-13. [https://doi.org/10.1061/\(ASCE\)HE.1943-5584.0001467](https://doi.org/10.1061/(ASCE)HE.1943-5584.0001467)
- Adimalla, N. (2020). Controlling factors and mechanism of groundwater quality variation in semiarid region of South India: An approach of water quality index and health risk assessment (HRA). *Environmental Geochemistry and Health*, 42(6), 1725-1752. <https://doi.org/10.1007/s10653-019-00374-8>
- Agrawala, S., Moehner, A., Hemp, A., Aalst, M. V., Hitz, S., Smith, J., Meena, H., Mwakifwamba, S. M., Hyera, T., & Mwaipopo, O. U. (2003). *Development and climate change in Tanzania: Focus on Mount Kilimanjaro*. <https://www.oecd.org/env/cc/21058838.pdf>
- Ahmed, B., Ahmed, R., & Zhu, X. (2013). Evaluation of model validation techniques in land cover dynamics. *International Journal of Geo-Information*, 2(3), 577-597. <https://doi.org/10.3390/ijgi2030577>
- Ahmed, R., Hussain, M., Tanwir, R., & Qureshi, S. (2020). Monitoring of fluoride and iodide levels in drinking water using ion selective electrodes. *The Nucleus*, 41(1-4), 51-58.
- Ai, L., Shi, Z., Yin, W., & Huang, X. (2015). Spatial and seasonal patterns in stream water contamination across mountainous watersheds: Linkage with landscape characteristics. *Journal of Hydrology*, 523, 398-408. <https://doi.org/10.1016/j.jhydrol.2015.01.082>
- Al-Bakri, J. T., Duqqah, M., & Brewer, T. R. (2013). Application of remote sensing and GIS for modeling and assessment of land use/cover change in Amman/Jordan. *Journal of Geographic Information System*, 5, 509-519. <https://doi.org/10.4236/jgis.2013.55048>

- Al-Manmi, D. (2008). *Water resources management in Rania area, Sulaimaniyah NE-Iraq*. [Unpublished PhD thesis, University of Baghdad]. <http://thesis.mandumah.com/Record/325332>
- Aleke, C. G., Okogbue, C. O., Aghamelu, O. P., & Nnaji, N. J. (2016). Hydrogeological potential and qualitative assessment of groundwater from the Ajali Sandstone at Ninth mile area, southeastern Nigeria. *Environmental Earth Sciences*, 75(4), 1-16. <https://doi.org/10.1007/s12665-015-4843-3>
- Altmann, J., Alberts, S. C., Altmann, S. A., & Roy, S. B. (2002). Dramatic change in local climate patterns in the Amboseli basin, Kenya. *African Journal of Ecology*, 40(3), 248-251. <https://doi.org/https://doi.org/10.1046/j.1365-2028.2002.00366.x>
- Anand, J., Gosain, A., Khosa, R., & Srinivasan, R. (2018a). Regional scale hydrologic modeling for prediction of water balance, analysis of trends in streamflow and variations in streamflow: The case study of the Ganga River basin. *Journal of Hydrology: Regional Studies*, 16, 32-53. <https://doi.org/10.1016/j.ejrh.2018.02.007>
- Anand, J., Gosain, A. K., & Khosa, R. (2018b). Prediction of land use changes based on Land Change Modeler and attribution of changes in the water balance of Ganga basin to land use change using the SWAT model. *Science of the Total Environment*, 644, 503-519. <https://doi.org/10.1016/j.scitotenv.2018.07.017>
- Andersen, F. H. (2008). *Hydrological modeling in a semi-arid area using remote sensing data* [Ph.D. Thesis, University of Copenhagen]. Copenhagen, Denmark http://www.vinr.ir/sites/default/files/phd_thesis_flemminghaugandersen.pdf
- Anderson, W. (2015). Cultural tourism and poverty alleviation in rural Kilimanjaro, Tanzania. *Journal of Tourism and Cultural Change*, 13(3), 208-224. <https://doi.org/10.1080/14766825.2014.935387>
- Andersson, R., Wanseth, F., Cuellar, M., & Von Mitzlaff, U. (2006). *Pangani falls re-development project in Tanzania Sida Evaluation*. (unpublished.). <http://www.sida.se/publications>

- Andrilli, S., & Hecker, D. (2010). Additional Applications. In S. Andrilli & D. Hecker (Eds.), *Elementary Linear Algebra (Fourth Edition)* (pp. 491-585). Academic Press. <https://doi.org/https://doi.org/10.1016/B978-0-12-374751-8.00019-6>
- Anyah, R. O., & Qiu, W. (2012). Characteristic 20th and 21st century rainfall and temperature patterns and changes over the Greater Horn of Africa. *International Journal of Climatology*, 32, 347-363.
- Appelhans, T., Mwangomo, E., Otte, I., Detsch, F., Nauss, T., & Hemp, A. (2015). Eco-meteorological characteristics of the southern slopes of Kilimanjaro, Tanzania. *International Journal of Climatology*, 36(9), 3245-3258. <https://doi.org/10.1002/joc.4552>
- Araya, A., Girma, A., & Getachew, F. (2015). Exploring impacts of climate change on maize yield in two contrasting agro-ecologies of Ethiopia. *Asian Journal of Applied Science and Engineering*, 4(1), 26-36.
- Araya, Y. H., & Cabral, P. (2010). Analysis and modeling of urban land cover change in Setúbal and Sesimbra, Portugal. *Remote Sensing*, 2(6), 1549-1563. <https://doi.org/10.3390/rs2061549>
- Arnold, J. G., Moriasi, D. N., Gassman, P. W., Abbaspour, K. C., White, M. J., Srinivasan, R., Santhi, C., Harmel, R., Van Griensven, A., & Van Liew, M. W. (2012). Soil and Water Assessment Tool: Model use, calibration, and validation. *Transactions of the American Society of Agricultural and Biological Engineers*, 55(4), 1491-1508.
- Arsanjani, J. J., Helbich, M., Kainz, W., & Boloorani, A. D. (2013). Integration of logistic regression, Markov chain and cellular automata models to simulate urban expansion. *International Journal of Applied Earth Observation and Geoinformation*, 21, 265-275.
- Arsanjani, J. J., Kainz, W., & Mousivand, A. J. (2011). Tracking dynamic land-use change using spatially explicit Markov Chain based on cellular automata: the case of Tehran. *International Journal of Image and Data Fusion*, 2(4), 329-345. <https://doi.org/10.1080/19479832.2011.605397>

- Assessment, M. E. (2005). *Ecosystems and human well-being: Synthesis*. <https://www.millenniumassessment.org/documents/document.356.aspx.pdf>
- Bailey, R. T., Wible, T. C., Arabi, M., Records, R. M., & Ditty, J. (2016). Assessing regional-scale spatio-temporal patterns of groundwater–surface water interactions using a coupled Soil and Water Assessment Tool-Modular-Three-Dimensional Finite Difference Groundwater Flow Model. *Hydrological Processes*, 30(23), 4420-4433. <https://doi.org/10.1002/hyp.10933>
- Baldus, R., Hahn, R., Mpanduji, D., & Siege, L. (2003). *The selous-niassa wildlife corridor*. In *Tanzania Wildlife Discussion Series*. Dar Es Salaam, Tanzania: Wildlife Division Deutsche Gesellschaft für Technische Zusammenarbeit GTZ Wildlife Programme in Tanzania. http://wildlife-baldus.com/download/nr_34.pdf
- Barbieri, M. (2019). Isotopes in Hydrology and Hydrogeology. *Water*, 11(2), 1-6. <https://www.mdpi.com/2073-4441/11/2/291>
- Barredo, J. I., Kasanko, M., McCormick, N., & Lavalley, C. (2003). Modelling dynamic spatial processes: Simulation of urban future scenarios through cellular automata. *Landscape and Urban Planning*, 64(3), 145-160. [https://doi.org/10.1016/S0169-2046\(02\)00218-9](https://doi.org/10.1016/S0169-2046(02)00218-9)
- Bashir, E., Naseem, S., Hanif, H., & Pirzada, T. (2013). Geochemical study of groundwater of Uthal and Bela areas, Balochistan and its appraisal for drinking and irrigation water quality. *International Journal of Agricultural Environment*, 2, 1-13.
- Baysal, G. (2013). *Urban land use and land cover change analysis and modeling a case study area Malatya, Turkey [Masters Thesis, Universität, Münster, Germany]*. Münster, Germany. <https://run.unl.pt/bitstream/10362/9187/1/TGEO0086.pdf>
- Behera, M. D., Borate, S. N., Panda, S. N., Behera, P. R., & Roy, P. S. (2012). Modelling and analyzing the watershed dynamics using Cellular Automata–Markov model–A geo-information based approach. *Journal of Earth System Science*, 121(4), 1011-1024.
- Benettin, P., Fovet, O., & Li, L. (2020). Nitrate removal and young stream water fractions at the catchment scale. *Hydrological Processes*, 34(12), 2725-2738. <https://doi.org/10.1002/hyp.13781>

- Berrang-Ford, L., Ford, J. D., & Paterson, J. (2011). Are we adapting to climate change? *Global Environmental Change*, 21(1), 25-33. [https:// doi.org/https:// doi.org/ 10.1016/j.gloenvcha.2010.09.012](https://doi.org/10.1016/j.gloenvcha.2010.09.012)
- Bhardwaj, V., & Singh, D. S. (2011). Surface and groundwater quality characterization of Deoria District, Ganga plain, India. *Environmental Earth Sciences*, 63(2), 383-395.
- Bishop, K. (1991). *Episodic increases in stream acidity, catchment flow pathways and hydrograph separation*, [Ph.D Thesis, University of Cambridge]. Cambridge, UK. <https://ethos.bl.uk/OrderDetails.do?uin=uk.bl.ethos.239601>
- Bishop, Y., Feinberg, S., & Holland, P. (1975). *Discrete multivariate analysis—theory and practice*. MIT Press. <https://www.jstor.org/stable/2344845?>
- Bodé, S., De Wispelaere, L., Hemp, A., Verschuren, D., & Boeckx, P. (2020). Water-isotope ecohydrology of Mount Kilimanjaro. *Ecohydrology*, 13(1), 1-19. [https:// doi.org/ https:// doi.org/10.1002/eco.2171](https://doi.org/10.1002/eco.2171)
- Bohté, R., Mul, M., Bogaard, T., Savenije, H., Uhlenbrook, S., & Kessler, T. (2010). Hydrograph separation and scale dependency of natural tracers in a semi-arid catchment. *Hydrology & Earth System Sciences Discussions*, 7(1), 1343-1372.
- Bradford, A., Zhang, L., & Hairsine, P. (2001). *Implementation of a mean annual water balance model within a Geographic Information System framework and application to the Murray-Darling Basin*. Cooperative Cesearch Centre for Catchment Hydrology. [https:// ewater.org.au/ archive/ crcch/ archive/ pubs/pdfs/technical200108.pdf](https://ewater.org.au/archive/crcch/archive/pubs/pdfs/technical200108.pdf)
- Bradley, R. S., Keimig, F. T., Diaz, H. F., & Hardy, D. R. (2009). Recent changes in freezing level heights in the Tropics with implications for the deglaciation of high mountain regions. *Geophysical Research Letters*, 36(17), 1-4. [https:// doi. org/ https:// doi. org/ 10. 1029/ 2009 GL03 7712](https://doi.org/10.1029/2009GL037712)
- Bradley, R. S., Vuille, M., Diaz, H. F., & Vergara, W. (2006). Threats to Water Supplies in the Tropical Andes. *Science*, 312(5781), 1755-1756. [https:// doi. org/ 10. 1126/ science. 1128087](https://doi.org/10.1126/science.1128087)

- Brender, J. D. (2020). Human health effects of exposure to nitrate, nitrite, and nitrogen dioxide. In M. A. Sutton, K. E. Mason, A. Bleeker, W. K. Hicks, C. Masso, N. Raghuram, S. Reis, & M. Bekunda (Eds), *Just Enough Nitrogen* (pp. 283-294). Springer. https://doi.org/10.1007/978-3-030-58065-0_18
- Brindha, K., & Kavitha, R. (2015). Hydrochemical assessment of surface water and groundwater quality along Uyyakondan channel, south India. *Environmental Earth Sciences*, 73(9), 5383-5393.
- Briones, R., Ella, V., & Bantayan, N. (2016). Hydrologic impact evaluation of land use and land cover change in Palico Watershed, Batangas, Philippines Using the SWAT model. *Journal of Environmental Science and Management*, 19, 96-107.
- Brown, D. G., Band, L. E., Green, K. O., Irwin, E. G., Jain, A., Lambin, E. F., Pontius, R. G., Seto, K. C., Turner, I. I., & Verburg, P. H. (2013). *Advancing Land Change Modeling: Opportunities and Research Requirements*. [https:// www. nap. edu/ catalog/ 18385/ advancing - land-change-modeling-opportunities-and-research-requirements](https://www.nap.edu/catalog/18385/advancing-land-change-modeling-opportunities-and-research-requirements)
- Bruijnzeel, L. A. (2004). Hydrological functions of tropical forests: Not seeing the soil for the trees? *Agriculture, Ecosystems & Environment*, 104(1), 185-228. [https:// doi.org/ 10.1016/j.agee.2004.01.015](https://doi.org/10.1016/j.agee.2004.01.015)
- Brunsell, N. (2010). A multiscale information theory approach to assess spatial: Temporal variability of daily precipitation. *Journal of Hydrology*, 385(1-4), 165-172. [https://doi.org/ 10.1016/j.jhydrol.2010.02.016](https://doi.org/10.1016/j.jhydrol.2010.02.016)
- Burton, M., & Chiza, C. (1997). Water, conflict and the environment: A case study from Tanzania. CRC Press. [https:// www. routledge. com/ Water- Economics- Management- and-Demand/ Kay- anks-Smith/p/book/9780367447830](https://www.routledge.com/Water-Economics-Management-and-Demand/Kay-anks-Smith/p/book/9780367447830)
- Byerlee, D., Stevenson, J., & Villoria, N. (2014). Does intensification slow crop land expansion or encourage deforestation? *Global Food Security*, 3(2), 92-98. [https:// doi.org/ 10.1016/j.gfs.2014.04.001](https://doi.org/10.1016/j.gfs.2014.04.001)
- Camberlin, P., & Philippon, N. (2002). The East African March–May Rainy Season: Associated Atmospheric Dynamics and Predictability over the 1968–97 Period. *Journal of Climate*,

15(9), 1002-1019. [https://doi.org/10.1175/1520-0442\(2002\)015<1002:Teammr>2.0.Co;2](https://doi.org/10.1175/1520-0442(2002)015<1002:Teammr>2.0.Co;2)

- Cao, M., Huang, M., Xu, R., Lü, G., & Chen, M. (2019a). A grey wolf optimizer–cellular automata integrated model for urban growth simulation and optimization. *Transactions in Geographical Information System*, 23(4), 672-687. <https://doi.org/10.1111/tgis.12517>
- Cao, M., Zhu, Y., Quan, J., Zhou, S., Lü, G., Chen, M., & Huang, M. (2019b). Spatial Sequential Modeling and Predication of Global Land Use and Land Cover Changes by Integrating a Global Change Assessment Model and Cellular Automata. *Earth's Future*, 7(9), 1102-1116. <https://doi.org/10.1029/2019EF001228>
- Carreira, P. M., Marques, J. M., & Nunes, D. (2014). Source of groundwater salinity in coastline aquifers based on environmental isotopes (Portugal): Natural vs. human interference. A review and reinterpretation. *Applied Geochemistry*, 41, 163-175. <https://doi.org/10.1016/j.apgeochem.2013.12.012>
- CEP. (1995). *Country Environmental Profile, Tanzania Environment and social policy working paper series. Working paper No. 26*. African Development Bank. http://www.afdb.org/african_countries/pdf/cep-tz.pdf.
- Chacha, N., Njau, K. N., Lugomela, G. V., & Muzuka, A. N. N. (2018). Hydrogeochemical characteristics and spatial distribution of groundwater quality in Arusha well fields, Northern Tanzania. *Applied Water Science*, 8(4), 1-23. <https://doi.org/10.1007/s13201-018-0760-4>
- Challinor, A. J., Watson, J., Lobell, D. B., Howden, S. M., Smith, D. R., & Chhetri, N. (2014). A meta-analysis of crop yield under climate change and adaptation. *Nature Climate Change*, 4(4), 287-291. <https://doi.org/10.1038/nclimate2153>
- Chan, R., Vuille, M., Hardy, D., & Bradley, R. (2008). Intraseasonal precipitation variability on Kilimanjaro and the East African region and its relationship to the large-scale circulation. *Theoretical and Applied Climatology*, 93(3), 149-165.

- Chanapathi, T., Thatikonda, S., & Raghavan, S. (2018). Analysis of rainfall extremes and water yield of Krishna river basin under future climate scenarios. *Journal of Hydrology: Regional Studies*, 19, 287-306. <https://doi.org/10.1016/j.ejrh.2018.10.004>
- Chegbeleh, L. P., Aklika, D. K., & Akurugu, B. A. (2020). Hydrochemical Characterization and Suitability Assessment of Groundwater Quality in the Saboba and Chereponi Districts, Ghana. *Hydrology*, 7(3), 1-21. <https://doi.org/10.3390/hydrology7030053>
- Chen, Y., & Yu, B. (2013). Impacts of climate and land-use changes on floods in an urban catchment in southeast Queensland, Australia. *Climate and Land-surface Changes in Hydrology*, 1, 23-29.
- Chiwa, R. (2012). *Effects Of Land Use And Land Cover Changes On The Hydrology Of Weruweru-Kiladeda Sub-Catchment In Pangani River Basin, Tanzania* [Kenyatta University]. Nairobi, Kenya. <https://ir-library.ku.ac.ke/bitstream/handle/123456789/6852/Renny%20Chiwa.pdf>
- Christensen, N. S., Wood, A. W., Voisin, N., Lettenmaier, D. P., & Palmer, R. N. (2004). The Effects of Climate Change on the Hydrology and Water Resources of the Colorado River Basin. *Climatic change*, 62(1), 337-363. <https://doi.org/10.1023/B:CLIM.0000013684.13621.1f>
- Clark, I., & Fritz, P. (2000). *Environmental Isotopes in Hydrogeology (Third Edition)*. Lewis Publishers. <https://www.routledge.com/Environmental-Isotopes-in-Hydrogeology/Clark-Fritz/p/book/9781566702492>
- Clark, I. D., & Fritz, P. (1997). *Environmental Isotopes in Hydrogeology (First edition)*. CRC Press. <https://www.routledge.com/Environmental-Isotopes-in-Hydrogeology/Clark-Fritz/p/book/9781566702492>
- Cole, M. A., Elliott, R. J., & Strobl, E. (2014). Climate change, hydro-dependency, and the African Dam boom. *World Development*, 60, 84-98. <https://doi.org/10.1016/j.worlddev.2014.03.016>
- Conway, D., Mittal, N., & Vincent, K. (2017). *Future climate projections for Tanzania*. https://media.africaportal.org/documents/fcfa_tanzania_climatebrief_web.pdf

- Costanza, R. (1989). Model goodness of fit: A multiple resolution procedure. *Ecological Modelling*, 47(3), 199-215. [https://doi.org/10.1016/0304-3800\(89\)90001-X](https://doi.org/10.1016/0304-3800(89)90001-X)
- Coutts, H. (1969). Rainfall of the Kilimanjaro area. *Weather*, 24(2), 66-69.
- Craparo, A. C. W., Van Asten, P. J. A., Läderach, P., Jassogne, L. T. P., & Grab, S. W. (2015). Coffea arabica yields decline in Tanzania due to climate change: Global implications. *Agricultural and Forest Meteorology*, 207, 1-10. <https://doi.org/10.1016/j.agrformet.2015.03.005>
- Cullen, N., Sirguey, P., Mölg, T., Kaser, G., Winkler, M., & Fitzsimons, S. (2013). A century of ice retreat on Kilimanjaro: The mapping reloaded. *The Cryosphere*, 7(2), 419-431. <https://doi.org/10.5194/tc-7-419-2013>
- Cullen, N. J., Mölg, T., Kaser, G., Hussein, K., Steffen, K., & Hardy, D. R. (2006). Kilimanjaro Glaciers: Recent areal extent from satellite data and new interpretation of observed 20th century retreat rates. *Geophysical Research Letters*, 33(L16502), 1-6. <https://doi.org/10.1029/2006GL027084>
- Cuthbert, M. O., Taylor, R. G., Favreau, G., Todd, M. C., Shamsudduha, M., Villholth, K. G., MacDonald, A. M., Scanlon, B. R., Kotchoni, D. O. V., Vouillamoz, J. M., Lawson, F. M. A., Adjomayi, P. A., Kashaigili, J., Seddon, D., Sorensen, J. P. R., Ebrahim, G. Y., Owor, M., Nyenje, P. M., Nazoumou, Y., & ... Kukuric, N. (2019). Observed controls on resilience of groundwater to climate variability in sub-Saharan Africa. *Nature*, 572(7768), 230-234. <https://doi.org/10.1038/s41586-019-1441-7>
- Daluti, L. (1994). *Report on the Agro-Socio-Economic Situation in Pangani River Catchment Conculancy for NORPLAN*. Zonal Irrigation Office, United Republic of Tanzania, Moshi. <https://portals.iucn.org/library/efiles/documents/2003-079.pdf>
- Daniels, A., Morrison, J., Joyce, L., Crookston, N., Chen, S.C., & McNulty, S. (2012). Climate Projections Frequently Asked Questions. *United States Department of Agriculture Forest Service General Technical Report*. https://www.fs.fed.us/rm/pubs/rmrs_gtr277.pdf

- Daron, J. (2014). *Regional climate messages: East Africa. Scientific report from the Adaptation at Scale in Semi-Arid Regions Project*. <https://www.weadapt.org/knowledge-base/assar>
- De Wit, M., & Stankiewicz, J. (2006). Changes in surface water supply across Africa with predicted climate change. *Science*, 311(5769), 1917-1921.
- Defersha, M. B., & Melesse, A. M. (2012). Field-scale investigation of the effect of land use on sediment yield and runoff using runoff plot data and models in the Mara River basin, Kenya. *Catena*, 89(1), 54-64. <https://doi.org/10.1016/j.catena.2011.07.010>
- Deng, Z., Zhang, X., Li, D., & Pan, G. (2015). Simulation of land use/land cover change and its effects on the hydrological characteristics of the upper reaches of the Hanjiang Basin. *Environmental Earth Sciences*, 73(3), 1119-1132. <https://doi.org/10.1016/j.scitotenv.2017.11.191>
- Dietrich, A. M., & Devesa, R. (2019). Characterization and removal of minerals that cause taste. In T. F. Lin, S. Watson, A. M. Dietrich, & I. H. Suffet (Eds), *Taste and Odour in Source and Drinking Water: Causes, Controls, and Consequences* (pp. 245-340). IWA Publishing. https://doi.org/10.2166/9781780406664_0245
- Dobaradaran, S., Mahvi, A. H., Dehdashti, S., Dobaradaran, S., & Shoara, R. (2009). Correlation of fluoride with some inorganic constituents in groundwater of Dashtestan, Iran. *Fluoride*, 42(1), 50-53.
- Dos Santos, V., Laurent, F., Abe, C., & Messner, F. (2018). Hydrologic response to land use change in a large basin in eastern Amazon. *Water*, 10(4), 1-19. <https://doi.org/10.3390/w10040429>
- Dosio, A., Jones, R. G., Jack, C., Lennard, C., Nikulin, G., & Hewitson, B. (2019). What can we know about future precipitation in Africa? Robustness, significance and added value of projections from a large ensemble of regional climate models. *Climate Dynamics*, 53(9), 5833-5858. <https://doi.org/10.1007/s00382-019-04900-3>
- Downie, C., Humphries, D., Wilcockson, W., & Wilkinson, P. (1956). Geology of Kilimanjaro. *Nature*, 178(4538), 828-830.

- Downie, C., & Wilkinson, P. (1972). *The geology of Kilimanjaro*. University of Sheffield, Earth Sciences. <https://catalogue.nla.gov.au/Record/1909453>
- Drever, J. I. (1997). *The Geochemistry of Natural Waters: Surface and Groundwater Environments*. Prentice Hall. <https://access.onlinelibrary.wiley.com/doi/10.2134/jeq1998.00472425002700010037x>
- Du, J., Qian, L., Rui, H., Zuo, T., Zheng, D., Xu, Y., & Xu, C. Y. (2012). Assessing the effects of urbanization on annual runoff and flood events using an integrated hydrological modeling system for Qinhuai River basin, China. *Journal of Hydrology*, 464-465, 127-139. <https://doi.org/https://doi.org/10.1016/j.jhydrol.2012.06.057>
- Duane, W., Pepin, N., Losleben, M., & Hardy, D. (2008). General characteristics of temperature and humidity variability on Kilimanjaro, Tanzania. *Arctic, Antarctic, and Alpine Research*, 40(2), 323-334. [https://doi.org/10.1657/1523-0430\(06-127\)\[DUANE\]2.0.CO;2](https://doi.org/10.1657/1523-0430(06-127)[DUANE]2.0.CO;2)
- Durowoju, O. S., Ekosse, G. I. E., & Odiyo, J. O. (2019). Determination of isotopic composition of rainwater to generate local meteoric water line in Thohoyandou, Limpopo Province, South Africa. *Water South Africa*, 45(2), 183-189. <https://doi.org/doi:10.4314/wsa.v45i2.04>
- Dwarakish, G. S., & Ganasri, B. P. (2015). Impact of land use change on hydrological systems: A review of current modeling approaches. *Cogent Geoscience*, 1(1), 1-18. <https://doi.org/10.1080/23312041.2015.1115691>
- Eastman, J. (2012). *IDRISI Selva: Guide to GIS and Image Processing*. Retrieved from Worcester, MA USA. <https://clarklabs.org/download/tutorial>
- Eastman, J. R. (2009). *IDRISI Taiga Guide to GIS and Image Processing*. <https://www.scirp.org/reference/ReferencesPapers.aspx?ReferenceID=1826143>
- Ehleringer, J. R., & Dawson, T. E. (1992). Water uptake by plants: perspectives from stable isotope composition. *Plant, Cell & Environment*, 15(9), 1073-1082. <https://doi.org/https://doi.org/10.1111/j.1365-3040.1992.tb01657.x>

- El-Hallaq, M. A., & Habboub, M. O. (2014). Using GIS for Time Series Analysis of the Dead Sea from Remotely Sensing Data. *Open Journal of Civil Engineering*, 4, 386-396. <https://doi.org/10.4236/ojce.2014.44033>
- Endris, H. S., Omondi, P., Jain, S., Lennard, C., Hewitson, B., Chang'a, L., Awange, J. L., Dosio, A., Ketiem, P., Nikulin, G., Panitz, H. J., Büchner, M., Stordal, F., & Tazalika, L. (2013). Assessment of the Performance of CORDEX Regional Climate Models in Simulating East African Rainfall. *Journal of Climate*, 26(21), 8453-8475. <https://doi.org/10.1175/jcli-d-12-00708.1>
- Enfors, E., Barron, J., Makurira, H., Rockström, J., & Tumbo, S. (2011). Yield and soil system changes from conservation tillage in dryland farming: A case study from North Eastern Tanzania. *Agricultural Water Management*, 98(11), 1687-1695.
- Epaphra, M., & Mwakalasya, A. H. (2017). Analysis of Foreign Direct Investment, Agricultural Sector and Economic Growth in Tanzania. *Modern Economy*, 8, 111-140. <https://doi.org/http://dx.doi.org/10.4236/me.2017.81008>
- Eriksen, S., Klein, T. R. J., Ulsrud, K., Nass, O. L., & O'Brien, K. (2008). *Climate change adaptation and poverty reduction: Key interactions and critical measures*, Report prepared for the Norwegian Agency for Development Cooperation. <https://citeseerx.ist.psu.edu/viewdoc/download?doi=10.1.1.579.4219&rep=rep1&type=pdf>
- Esmaili, R., Hoseinzadeh, M. M., & Akbari, M. (2013). Hydrogeochemistry and groundwater quality assessment in Nour coastal plain, Mazandaran province, Iran. *Journal of Tethys*, 1(4), 254-265.
- Fairman, J. G., Nair, U. S., Christopher, S. A., & Moelg, T. (2011). Land use change impacts on regional climate over Kilimanjaro. *Journal of Geophysical Research*, 116(D03110), 1-24. <https://doi.org/10.1029/2010JD014712>
- FAO. (2017). *Sustainable Land Management (SLM) in Practice in the Kagera Basin: Lessons Learned for Scaling Up at Landscape Level: Results of the Kagera Transboundary Agro-ecosystem Management Project (Kagera TAMP)*. <https://www.fao.org/downloads>

- Feyen, J., & Vazquez, R. (2011). Modelling the hydrological consequences of climate change and land use: Advances and challenges. *Maskana*, 2(2), 83-100. [https:// doi.org/ https:// doi.org/10.18537/mskn.02.02.07](https://doi.org/10.18537/mskn.02.02.07)
- Fipps, G. (2003). Irrigation water quality standards and salinity management strategies. *Texas Farmer Collection*. [https:// oaktrust.library.tamu.edu/ bitstream/ handle/ 1969.1/ 87829/ pdf_94.pdf?seq](https://oaktrust.library.tamu.edu/bitstream/handle/1969.1/87829/pdf_94.pdf?seq)
- Fischer, S. (2013). *Exploring a water balance method on recharge estimations in the Kilombero Valley, Tanzania* [Ground level degree project, Stockholm University]. Stockholm. <https://www.diva-portal.org/smash/get/diva2:638613/FULLTEXT01.pdf>
- Fisher, B., Kulindwa, K., Mwanyoka, I., Turner, R. K., & Burgess, N. D. (2010). Common pool resource management and PES: lessons and constraints for water PES in Tanzania. *Ecological Economics*, 69(6), 1253-1261. [https:// doi. org/ 10. 1016/j .ecolecon. 2009. 11. 008](https://doi.org/10.1016/j.ecolecon.2009.11.008)
- Fohrer, N., Haverkamp, S., Eckhardt, K., & Frede, H.G. (2001). Hydrologic response to land use changes on the catchment scale. *Physics and Chemistry of the Earth, Part B: Hydrology, Oceans and Atmosphere*, 26(7-8), 577-582. [https:// doi.org/ 10.1016/ S1464-1909 \(01\) 00052-1](https://doi.org/10.1016/S1464-1909(01)00052-1)
- Foley, J. A., DeFries, R., Asner, G. P., Barford, C., Bonan, G., Carpenter, S. R., Chapin, F. S., Coe, M. T., Daily, G. C., & Gibbs, H. K. (2005). Global consequences of land use. *Science*, 309(5734), 570-574. <https://doi.org/10.1126/science.1111772>
- Foody, G. M. (2008). Harshness in image classification accuracy assessment. *International Journal of Remote Sensing*, 29(11), 3137-3158. [https:// doi.org/ 10.1080/ 014311 607 0144 2120](https://doi.org/10.1080/01431160701442120)
- Fu, B. J., Wang, Y. F., Lu, Y. H., He, C. S., Chen, L. D., & Song, C. J. (2009). The effects of land-use combinations on soil erosion: A case study in the Loess Plateau of China. *Progress in Physical Geography*, 33(6), 793-804. [https:// doi. org/ 10. 1177/ 0309133309350264](https://doi.org/10.1177/0309133309350264)

- Funk, C., Dettinger, M. D., Michaelsen, J. C., Verdin, J. P., Brown, M. E., Barlow, M., & Hoell, A. (2008). Warming of the Indian Ocean threatens eastern and southern African food security but could be mitigated by agricultural development. *Proceedings of the National Academy of Sciences*, 105(32), 11081-11086. <https://doi.org/10.1073/pnas.0708196105>
- Gan, T. Y., Ito, M., Hülsmann, S., Qin, X., Lu, X. X., Liong, S. Y., Rutschman, P., Disse, M., & Koivusalo, H. (2016). Possible climate change/variability and human impacts, vulnerability of drought-prone regions, water resources and capacity building for Africa. *Hydrological Sciences Journal*, 61(7), 1209-1226. <https://doi.org/10.1080/02626667.2015.1057143>
- Gao, J., Li, F., Gao, H., Zhou, C., & Zhang, X. (2017). The impact of land-use change on water-related ecosystem services: A study of the Guishui River Basin, Beijing, China. *Journal of Cleaner Production*, 163, 148-155. <https://doi.org/10.1016/j.jclepro.2016.01.049>
- Garcia, M. C., & Alvarez, R. (1994). TM digital processing of a tropical forest region in southeastern Mexico. *International Journal of Remote Sensing*, 15(8), 1611-1632. <https://doi.org/10.1080/01431169408954195>
- Gashaw, T., Tulu, T., Argaw, M., & Worqlul, A. W. (2017). Evaluation and prediction of land use/land cover changes in the Andassa watershed, Blue Nile Basin, Ethiopia. *Environmental Systems Research*, 6(1), 1-15. <https://doi.org/10.1186/s40068-017-0094-5>
- Gashaw, T., Tulu, T., Argaw, M., & Worqlul, A. W. (2018). Modeling the hydrological impacts of land use/land cover changes in the Andassa watershed, Blue Nile Basin, Ethiopia. *Science of the Total Environment*, 619, 1394-1408. <https://doi.org/10.1016/j.scitotenv.2017.11.191>
- Gassman, P. W., Reyes, M. R., Green, C. H., & Arnold, J. G. (2007). The soil and water assessment tool: Historical development, applications, and future research directions. *Transactions of the American Society of Agricultural and Biological Engineers* 50(4), 1211-1250.
- Gautam, S. K., Maharana, C., Sharma, D., Singh, A. K., Tripathi, J. K., & Singh, S. K. (2015). Evaluation of groundwater quality in the Chotanagpur plateau region of the Subarnarekha

- river basin, Jharkhand State, India. *Sustainability of Water Quality and Ecology*, 6, 57-74. <https://doi.org/https://doi.org/10.1016/j.swaqe.2015.06.001>
- Gedney, N., Cox, P. M., Betts, R. A., Boucher, O., Huntingford, C., & Stott, P. A. (2006). Detection of a direct carbon dioxide effect in continental river runoff records. *Nature*, 439(7078), 835-838. <https://doi.org/10.1038/nature04504>
- Geilinger, W. (1936). The retreat of the Kilimanjaro glaciers. *Tanganyika Notes and Records*, 2, 1-7.
- Ghiglieri, G., Pittalis, D., Cerri, G., & Oggiano, G. (2012). Hydrogeology and hydrogeochemistry of an alkaline volcanic area: The North Eastern Mount Meru slope (East African Rift & ndash; Northern Tanzania). *Hydrological Earth System Science*, 16(2), 529-541. <https://doi.org/10.5194/hess-16-529-2012>
- Gibbs, R. J. (1970). Mechanisms Controlling World Water Chemistry. *Science*, 170(3962), 1088-1090. <https://doi.org/10.1126/science.170.3962.1088>
- Gillman, C. (1932). Some geographical controls in East Africa. *The South African Geographical Journal*, 15, 3-14.
- Giorgi, F., Jones, C., & Asrar, G. R. (2009). Addressing climate information needs at the regional level: The Coordinated Regional Climate Downscaling Experiment framework. *World Meteorological Organization Bulletin*, 58(3), 1-9.
- GITEC, W. (2011). *Groundwater assessment of the Pangani Basin, Tanzania*. <https://portals.iucn.org/library/efiles/documents/2011-098.pdf>
- Godoy, J. L., Vega, J. R., & Marchetti, J. L. (2014). Relationships between Principal Component Analysis and Partial Least Square-regression. *Chemometrics and Intelligent Laboratory Systems*, 130, 182-191. <https://doi.org/https://doi.org/10.1016/j.chemolab.2013.11.008>
- Gorski, G., Strong, C., Good, S. P., Bares, R., Ehleringer, J. R., & Bowen, G. J. (2015). Vapor hydrogen and oxygen isotopes reflect water of combustion in the urban atmosphere. *Proceedings of the National Academy of Sciences*, 112(11), 3247-3252. <https://doi.org/10.1073/pnas.1424728112>

- Grossmann, M. (2008). *The Kilimanjaro Aquifer: A case study for the research project Transboundary groundwater management in Africa: Conceptualizing cooperation on Africa's transboundary groundwater resources*. German Development Institute. https://www.die-gdi.de/uploads/media/Studie_32.pdf
- Grove, A. (1993). Water use by the Chagga on Kilimanjaro. *African Affairs*, 92(368), 431-448.
- Grusson, Y., Sun, X., Gascoin, S., Sauvage, S., Raghavan, S., Anctil, F., & Sánchez-Pérez, J. M. (2015). Assessing the capability of the SWAT model to simulate snow, snow melt and streamflow dynamics over an alpine watershed. *Journal of Hydrology*, 531, 574-588. <https://doi.org/10.1016/j.jhydrol.2015.10.070>
- Guan, D., Li, H., Inohae, T., Su, W., Nagaie, T., & Hokao, K. (2011). Modeling urban land use change by the integration of cellular automaton and Markov model. *Ecological Modelling*, 222(20), 3761-3772. <https://doi.org/10.1016/j.ecolmodel.2011.09.009>
- Gupta, S. K., & Gupta, I. (1997). *Management of saline soils and waters*. Scientific Publishers. <https://www.fao.org/3/x5871e/x5871e04.htm>
- Gütlein, A., Gerschlauser, F., Kikoti, I., & Kiese, R. (2017). Impacts of climate and land use on N₂O and CH₄ fluxes from tropical ecosystems in the Mt. Kilimanjaro region, Tanzania. *Global Change Biology*, 24(3), 1239-1255.
- Guzha, A., Rufino, M. C., Okoth, S., Jacobs, S., & Nóbrega, R. (2018). Impacts of land use and land cover change on surface runoff, discharge and low flows: Evidence from East Africa. *Journal of Hydrology: Regional Studies*, 15, 49-67. <https://doi.org/10.1016/j.ejrh.2017.11.005>
- Gyamfi, C., Ndambuki, J. M., & Salim, R. W. (2016). Hydrological responses to land use/cover changes in the Olifants Basin, South Africa. *Water*, 8(12), 1-16. <https://doi.org/10.3390/w8120588>
- Hammer, Ø., Harper, D. A., & Ryan, P. D. (2001). Paleontological statistics software package for education and data analysis. *Palaeontologia electronica*, 4(1), 1-9.

- Hashem, N., & Balakrishnan, P. (2015). Change analysis of land use/land cover and modelling urban growth in Greater Doha, Qatar. *Annals of Geographical Information System*, 21(3), 233-247. <https://doi.org/10.1080/19475683.2014.992369>
- Haslinger, K., Anders, I., & Hofstätter, M. (2013). Regional climate modelling over complex terrain: An evaluation study of COSMO-CLM hindcast model runs for the Greater Alpine Region. *Climate Dynamics*, 40(1), 511-529. <https://doi.org/10.1007/s00382-012-1452-7>
- Hastenrath, S. (2000). Zonal Circulations over the Equatorial Indian Ocean. *Journal of Climate*, 13(15), 2746-2756. [https://doi.org/10.1175/1520-0442\(2000\)013<2746:Zcotei>2.0.Co;2](https://doi.org/10.1175/1520-0442(2000)013<2746:Zcotei>2.0.Co;2)
- Hastenrath, S., & Greischar, L. (1997). Glacier recession on Kilimanjaro, East Africa, 1912–89. *Journal of Glaciology*, 43(145), 455-459.
- Hatibu, N., Lazaro, E., Mahoo, H., Rwehumbiza, F., & Bakari, A. (1999). Soil and water conservation in semi-arid areas of Tanzania: National policies and local practices. *Tanzania Journal of Agricultural Sciences*, 2(2), 51- 170.
- Hay, S. I., Cox, J., Rogers, D. J., Randolph, S. E., Stern, D. I., Shanks, G. D., Myers, M. F., & Snow, R. W. (2002). Climate change and the resurgence of malaria in the East African highlands. *Nature*, 415(6874), 1-5.
- Hchaichi, Z., Abid, K., & Zouari, K. (2014). Use of hydrochemistry and environmental isotopes for assessment of groundwater resources in the intermediate aquifer of the Sfax basin (Southern Tunisia). *Carbonates and Evaporites*, 29(2), 177-192. <https://doi.org/10.1007/s13146-013-0165-2>
- Hemp, A. (2005). Climate change-driven forest fires marginalize the impact of ice cap wasting on Kilimanjaro. *Global Change Biology*, 11(7), 1013-1023. <https://doi.org/10.1111/j.1365-2486.2005.00968.x>
- Hemp, A. (2006a). Continuum or zonation? Altitudinal gradients in the forest vegetation of Mt. Kilimanjaro. *Plant Ecology*, 184(1), 27-42. <https://doi.org/10.1007/s11258-005-9049-4>
- Hemp, A. (2006b). Vegetation of Kilimanjaro: Hidden endemics and missing bamboo. *African Journal of Ecology*, 44(3), 305-328. <https://doi.org/10.1111/j.1365-2028.2006.00679.x>

- Hijioka, Y., Lin, E., Pereira, J., Corlett, R., Cui, X., Insarov, G., Lasco, R., Lindgren, E., & Surjan, A. (2014). *Climate Change 2014: Impacts, Adaptation, and Vulnerability. Part B: Regional Aspects. Contribution of Working Group II to the Fifth Assessment Report of the Intergovernmental Panel on Climate Change. Cambridge University Press, Cambridge, United Kingdom and New York*, 1327-1370. [https:// www. ipcc. ch/ report/ ar5/ wg2/](https://www.ipcc.ch/report/ar5/wg2/)
- Hirsch, R. M., & Slack, J. R. (1984). A Nonparametric Trend Test for Seasonal Data With Serial Dependence. *Water Resources Research*, 20(6), 727-732. [https:// doi.org/ https:// doi.org/ 10.1029/WR020i006p00727](https://doi.org/10.1029/WR020i006p00727)
- Hooper, R. P., & Shoemaker, C. A. (1986). A comparison of chemical and isotopic hydrograph separation. *Water Resources Research*, 22(10), 1444-1454. [https:// doi.org/ 10.1029/ WR0 22i010p01444](https://doi.org/10.1029/WR022i010p01444)
- Hossain, M., & Patra, P. K. (2020). Water pollution index: A new integrated approach to rank water quality. *Ecological Indicators*, 117, 1-9. [https:// doi.org/ https:// doi.org/ 10.1016/ j. ecolind.2020.106668](https://doi.org/10.1016/j.ecolind.2020.106668)
- Hounslow, A. W. (1995). *Water quality data: analysis and interpretation*. CRS press, Boca Raton. [https:// www. routledge. com/ Water- Quality- Data- Analysis- and-Interpretation/ Hounslow/ p /book/9780873716765](https://www.routledge.com/Water-Quality-Data-Analysis-and-Interpretation/Hounslow/p/book/9780873716765)
- Houton, J., Ding, Y., Griggs, D., Nougier, M., Van der hinden, P., Dai, X., Maskell, K., & Johnson, C. (2001). Climate change. The Scientific Basis. Intergovernmental Panel on Climate Change. *Cambridge University Press: Cambridge*.
- Hu, Y., Maskey, S., & Uhlenbrook, S. (2012a). Downscaling daily precipitation over the Yellow River source region in China: A comparison of three statistical downscaling methods. *Theoretical and Applied Climatology*, 112, 1-14.
- Hu, Y., Maskey, S., & Uhlenbrook, S. (2012b). Downscaling daily precipitation over the Yellow River source region in China: A comparison of three statistical downscaling methods. *Theoretical and Applied Climatology*, 112(3), 447-460. <https://doi.org/10.1007/s00704-012-0745-4>

- Huisman, J., Breuer, L., Bormann, H., Bronstert, A., Croke, B., Frede, H.G., Gräff, T., Hubrechts, L., Jakeman, A., & Kite, G. (2009). Assessing the impact of land use change on hydrology by ensemble modeling III: Scenario analysis. *Advances in Water Resources*, 32(2), 159-170. <https://doi.org/10.1016/j.advwatres.2008.06.009>
- Hyandye, C., & Martz, L. W. (2017). A Markovian and cellular automata land-use change predictive model of the Usangu Catchment. *International Journal of Remote Sensing*, 38(1), 64-81. <https://doi.org/10.1080/01431161.2016.1259675>
- Hyandye, C. B., Worqul, A., Martz, L. W., & Muzuka, A. N. (2018). The impact of future climate and land use/cover change on water resources in the Ndembera watershed and their mitigation and adaptation strategies. *Environmental Systems Research*, 7(1), 1-24. <https://doi.org/10.1186/s40068-018-0110-4>
- IPCC. (2007). *Climate Change 2007: The Physical Science Basis, Contribution of Working Group I to the Fourth Assessment Report of the Intergovernmental Panel on Climate Change*, <https://www.ipcc.ch/report/ar4/wg1/>
- IPCC. (2012). Managing the risks of extreme events and disasters to advance climate change adaptation - summary for policy makers. In Field, C. B., V. Barros, T. F. Stocker, D. Qin, D. J. Dokken, K. L. Ebi, M. D. Mastrandrea, K. J. Mach, G. K. Plattner, S. K. Allen, M. Tignor, and P. M. Midgley (Eds), *A Special Report of Working Groups I, and II of the Intergovernmental Panel on Climate Change*. Cambridge University Press. <https://www.ipcc.ch/report/managing-the-risks-of-extreme-events-and-disasters-to-advance-climate-change-adaptation/>
- IPCC. (2014a). *AR5 IPCC Whats in It for Africa*. http://cdkn.org/wp-content/uploads/2014/04/AR5_IPCC_Whats_in_it_for_Africa.pdf.
- IPCC. (2014b). *Climate Change 2014-Impacts, Adaptation and Vulnerability: Regional Aspects*. <https://www.ipcc.ch/report/ar5/wg2/>
- IPCC. (2014c). *Climate Change 2014-Impacts, Adaptation and Vulnerability: Regional Aspects*. Cambridge University Press. <https://www.ipcc.ch/report/ar5/wg2/>

- IPCC. (2014d). *Climate Change 2014: Synthesis Report. Contribution of Working Groups I, II and III to the Fifth Assessment Report of the Intergovernmental Panel on Climate Change*.
https://www.ipcc.ch/site/assets/uploads/2018/05/SYR_AR5_FINAL_full_wcover.pdf
- IPCC. (2014e). *Working Group II Fourth Assessment Report. Climate Change Impacts, Adaptation and Vulnerability*. <https://www.ipcc.ch/report/ar5/wg2/>
- Jafar, A. A., Ananthakrishnan, S., Loganathan, K., & Manikandan, K. (2013). Assessment of groundwater quality for irrigation use in Alathur Block, Perambalur District, Tamilnadu, South India. *Applied Water Science*, 3(4), 763-771. <https://doi.org/10.1007/s13201-013-0124-z>
- Jankowski, J., & Acworth, R. I. (1997). Impact of Debris-Flow Deposits on Hydrogeochemical Processes and the Development of Dryland Salinity in the Yass River Catchment, New South Wales, Australia. *Hydrogeology Journal*, 5(4), 71-88. <https://doi.org/10.1007/s100400050119>
- Jensen, J. R. (2007). *Introductory digital image processing: A remote sensing perspective*. Prentice Hall. <https://dl.acm.org/doi/book/10.5555/2834479>
- Jokar, A. J., & Kainz, W. (2011). *Integration of agent based modeling and Markov model in simulation of urban sprawl*. Proceeding of Association of Geographic Information Laboratories in Europe, Utrecht, The Netherlands. https://agile-online.org/conference_paper/cds/agile_2011/contents/pdf/shortpapers/sp_101.pdf
- Kaka, E., Akiti, T., Nartey, V., Bam, E., & Adomako, D. (2011). Hydrochemistry and evaluation of groundwater suitability for irrigation and drinking purposes in the southeastern Volta River basin: Manya Krobo area, Ghana. *Elixir Agriculture*, 39, 4793-4807.
- Kangalawe, R. Y. (2016). Climate change impacts on water resource management and community livelihoods in the southern highlands of Tanzania. *Climate and Development*, 9(3), 191-201.

- Kangalawe, R. Y. (2017). Climate change impacts on water resource management and community livelihoods in the southern highlands of Tanzania. *Climate and Development*, 9(3), 191-201. <https://doi.org/10.1080/17565529.2016.1139487>
- Karamage, F., Zhang, C., Fang, X., Liu, T., Ndayisaba, F., Nahayo, L., Kayiranga, A., & Nsengiyumva, J. B. (2017). Modeling rainfall-runoff response to land use and land cover change in Rwanda (1990–2016). *Water*, 9(2), 1-24. <https://doi.org/10.3390/w9020147>
- Karar, A., & Henni, A. (2020). *Scale Inhibition in Hard Water System*. Springer, Cham. https://doi.org/10.1007/978-94-007-698-2020_530
- Karimi, H., Jafarnezhad, J., Khaledi, J., & Ahmadi, P. (2018). Monitoring and prediction of land use/land cover changes using CA-Markov model: A case study of Ravansar County in Iran. *Arabian Journal of Geosciences*, 11(19), 1-9. <https://doi.org/10.1007/s12517-018-3940-5>
- Karl, T. R., & Trenberth, K. E. (2003). Modern global climate change. *Science*, 302(5651), 1719-1723.
- Karthikeyan, G., & Shunmugasundarraaj, A. (2000). *Isopleth mapping and in-situ fluoride dependence on water quality in the Krishnagiri block of Tamil Nadu in South India*. Fluoride. <https://citeseerx.ist.psu.edu/viewdoc/download?doi=10.1.1.1089.2542&rep=rep1&type=pdf>
- Kaser, G. (1999). A review of the modern fluctuations of tropical glaciers. *Global and Planetary Change*, 22(1), 93-103. [https://doi.org/10.1016/S0921-8181\(99\)00028-4](https://doi.org/10.1016/S0921-8181(99)00028-4)
- Kaser, G., Hardy, D. R., Mölg, T., Bradley, R. S., & Hyera, T. M. (2004). Modern glacier retreat on Kilimanjaro as evidence of climate change: Observations and facts. *International Journal of Climatology*, 24(3), 329-339. <https://doi.org/10.1002/joc.1008>
- Kaser, G., Mölg, T., Cullen, N. J., Hardy, D. R., & Winkler, M. (2010). Is the decline of ice on Kilimanjaro unprecedented in the Holocene? *The Holocene*, 20(7), 1079-1091. <https://doi.org/10.1177/0959683610369498>

- Kashaigili, J., & Majaliwa, A. (2013). Implications of land use and land cover changes on hydrological regimes of the Malagarasi River, Tanzania. *Journal of Agricultural Science and Applications*, 2(1), 45-50.
- Kashaigili, J. J. (2010). *Assessment of groundwater availability and its current and potential use and impacts in Tanzania*.
<http://www.suaire.sua.ac.tz/bitstream/handle/123456789/1484/Kashaigili21.pdf?sequence=1>
- Katana, S., Uakuwun, E., & Munyao, T. (2013). Detection and prediction of land cover changes in upper Athi River catchment, Kenya: A strategy towards monitoring environmental changes. *Greener Journal of Environmental Management and Public Safety*, 2(4), 146-157. <https://doi.org/10.15580/GJEMPS>.
- Kelley, W. P. (1963). Use of Saline irrigation water. *Soil Science*, 95(6), 385-391.
- Kelly, W. P. (1940). Permissible composition and concentration of irrigated waters. *Proceedings of the American Society of Civil Engineers*, 66, 607-613.
- Kendall, C., & MacDonnell, J. J. (1998). *Isotope tracers in catchment hydrology*. Elsevier. <https://www.sciencedirect.com/book/9780444815460/isotope-tracers-in-catchment-hydrology>
- Kendall, C., & McDonnell, J. J. (2012). *Isotope tracers in catchment hydrology*. www.sciencedirect.com/book/9780444815460/isotope-tracers-in-catchment-hydrology-v2
- Kiesel, J., Gericke, A., Rathjens, H., Wetzig, A., Kakouei, K., Jähnig, S. C., & Fohrer, N. (2019). Climate change impacts on ecologically relevant hydrological indicators in three catchments in three European ecoregions. *Ecological Engineering*, 127, 404-416. <https://doi.org/10.1016/j.ecoleng.2018.12.019>
- King, R. S., Baker, M. E., Whigham, D. F., Weller, D. E., Jordan, T. E., Kazyak, P. F., & Hurd, M. K. (2005). Spatial considerations for linking watershed land cover to ecological indicators in streams. *Ecological Applications*, 15(1), 137-153. <https://doi.org/10.1016/j.jhydrol.2013.01.008>

- Kishiwa, P., Nobert, J., Kongo, V., & Ndomba, P. (2018). Assessment of impacts of climate change on surface water availability using coupled Soil and Water Assessment Tool and Water Evaluation And Planning Models: Case of upper Pangani River Basin, Tanzania. *Proceedings of the International Association of Hydrological Sciences*, 378, 23-27. <https://doi.org/10.5194/piahs-378-23-2018>
- Kitalika, A., Machunda, R. L., Komakech, H. C., & Njau, K. N. (2017). Physicochemical and Microbiological Variations in Rivers on the Foothills of Mount Meru, Tanzania. *International Journal of Scientific & Engineering Research*, 8(9), 1320-1346. <https://doi.org/10.14299/ijser.2017.09.005>
- Kitalika, A. J, Machunda, R. L, Komakech, H. C, & Nicholus, N. K. (2018). Land-Use and Land Cover Changes on the Slopes of Mount Meru-Tanzania. *Current World Environment*, 53(59), 331-352. <https://doi.org/10.12944/cwe.13.3.07>
- Koch, M., & Cherie, N. (2013). *Soil and Water Assessment Tool-modeling of the impact of future climate change on the hydrology and the water resources in the upper blue Nile river basin, Ethiopia. Proceedings of the 6th International Conference on Water Resources and Environment Research, ICWRER, Koblenz, Germany.* <https://www.waterandchange.org/proceedings.html>
- Kotlarski, S., Keuler, K., Christensen, O. B., Colette, A., Déqué, M., Gobiet, A., Goergen, K., Jacob, D., Lüthi, D., Van Meijgaard, E., Nikulin, G., Schär, C., Teichmann, C., Vautard, R., Warrach-Sagi, K., & Wulfmeyer, V. (2014). Regional climate modeling on European scales: A joint standard evaluation of the EURO-CORDEX RCM ensemble. *Geoscience Model Development*, 7(4), 1297-1333. <https://doi.org/10.5194/gmd-7-1297-2014>
- Kumar, A., Tiwari, S. K., Verma, A., & Gupta, A. K. (2018). Tracing isotopic signatures (δD and $\delta^{18}O$) in precipitation and glacier melt over Chorabari Glacier–Hydroclimatic inferences for the Upper Ganga Basin (UGB), Garhwal Himalaya. *Journal of Hydrology: Regional Studies*, 15, 68-89. <https://doi.org/https://doi.org/10.1016/j.ejrh.2017.11.009>
- Kumar, C. (2016). *Impact of climate change on groundwater resources: Handbook of research on climate change impact on health and environmental sustainability*. IGI Global. <https://doi.org/10.4018/978-1-4666-8814-8.ch010>

- Kumar, N., Tischbein, B., Kusche, J., Laux, P., Beg, M. K., & Bogardi, J. J. (2017). Impact of climate change on water resources of upper Kharun catchment in Chhattisgarh, India. *Journal of Hydrology: Regional Studies*, 13, 189-207. <https://doi.org/10.1016/j.ejrh.2017.07.008>
- Kumar, S. K., Rammohan, V., Sahayam, J. D., & Jeevanandam, M. (2009). *Assessment of groundwater quality and hydrogeochemistry of Manimuktha River basin, Tamil Nadu, India*. <https://link.springer.com/article/10.1007/s10661-008-0633-7>
- Kundu, S., Khare, D., & Mondal, A. (2017). Past, present and future land use changes and their impact on water balance. *Journal of Environmental Management*, 197, 582-596. <https://doi.org/https://doi.org/10.1016/j.jenvman.2017.04.018>
- Kundzewicz, Z., Mata, L., Arnell, N., Döll, P., Kabat, P., Jiménez, B., Miller, K., Oki, T., Sen, Z., & Shiklomanov, I. (2007). Freshwater resources and their management. Climate Change 2007: Impacts, Adaptation and Vulnerability. In M. Parry, O. Canziani, J. Palutikof, P. V. d. Linden, & C. Hanson (Eds), *Contribution of Working Group II to the Fourth Assessment Report of the Intergovernmental Panel on Climate Change* (pp. 173-210). Cambridge University Press. www.centaur.reading.ac.uk
- Kundzewicz, Z., Mata, L., Arnell, N., Döll, P., Kabat, P., Jiménez, B., Miller, K., Oki, T., Sen, Z., & Shiklomanov, I. (2009). The implications of projected climate change for freshwater resources and their management. *Hydrological Sciences Journal*, 53(1), 1-9. <https://doi.org/10.1623/hysj.53.1.3>
- Kurukulasuriya, P., & Mendelsohn, R. (2008). A Ricardian analysis of the impact of climate change on African cropland. *African Journal of Agricultural and Resource Economics*, 2(1), 1-23.
- Lalika, M. C., Meire, P., Ngaga, Y. M., & Chang'a, L. (2015). Understanding watershed dynamics and impacts of climate change and variability in the Pangani River Basin, Tanzania. *Ecohydrology & Hydrobiology*, 15(1), 26-38. <https://doi.org/10.1016/j.ecohyd.2014.11.002>
- Lam, Q., Schmalz, B., & Fohrer, N. (2011). The impact of agricultural Best Management Practices on water quality in a North German lowland catchment. *Environmental*

Monitoring and Assessment, 183(1-4), 351-379. <https://doi.org/10.1007/s10661-011-1926-9>

Lambin, E. F., Geist, H. J., & Lepers, E. (2003). Dynamics of land-use and land-cover change in tropical regions. *Annual Review of Environment and Resources*, 28(1), 205-241. <https://doi.org/10.1146/annurev.energy.28.050302.105459>

Lambrechts, C., Hemp, C., Nnyiti, P., Woodley, B., & Hemp, A. (2002). *Aerial survey of the threats to Mt. Kilimanjaro forests*. <https://www.google.com>

Lein, H. (2004). Managing the water of Kilimanjaro: Water, peasants, and hydropower development. *GeoJournal*, 61(2), 155-162. <https://doi.org/10.1007/s10708-004-2870-9>

Leterme, B., & Mallants, D. (2011). Climate and land-use change impacts on groundwater recharge. *Models-Repositories of Knowledge*, 355, 313-319.

Liang, X., Liu, X., Li, X., Chen, Y., Tian, H., & Yao, Y. (2018). Delineating multi-scenario urban growth boundaries with a CA-based FLUS model and morphological method. *Landscape and Urban Planning*, 177, 47-63.

Lin, C., Kou, G., & Ergu, D. (2014). A statistical approach to measure the consistency level of the pairwise comparison matrix. *Journal of the Operational Research Society*, 65(9), 1380-1386. <https://doi.org/10.1057/jors.2013.92>

Liping, C., Yujun, S., & Saeed, S. (2018). Monitoring and predicting land use and land cover changes using remote sensing and GIS techniques: A case study of a hilly area, Jiangle, China. *Plos One*, 13(7), 1-23. <https://doi.org/10.1371/journal.pone.0200493>

Little, M. G., & Lee, C.T. A. (2006). On the formation of an inverted weathering profile on Mount Kilimanjaro, Tanzania: Buried paleosol or groundwater weathering? *Chemical Geology*, 235(3-4), 205-221. <https://doi.org/10.1016/j.chemgeo.2006.06.012>

Liu, J., Chen, Z., Zhang, Y., Li, Z., Zhang, L., & Liu, F. (2016). Stable isotope evidences on sources and mechanisms of groundwater recharge in Hohhot basin, China. *Environmental Earth Sciences*, 75(5), 1-10. <https://doi.org/10.1007/s12665-015-4886-5>

- Lobell, D. B., & Field, C. B. (2007). Global scale climate–crop yield relationships and the impacts of recent warming. *Environmental Research Letters*, 2(1), 1-8. <https://doi.org/https://doi.org/10.1088/1748-9326/2/1/014002>
- Loures, L. C. (2019). Introductory Chapter: Land-Use Planning and Land-Use Change as Catalysts of Sustainable Development, Land Use. In L. C. Loures (Ed.), *Assessing the Past, Envisioning the Future* (pp. 1-58). IntechOpen. <https://doi.org/10.5772/intechopen.84520>
- Lugodisha, I., Komakech, H. C., Nakaya, S., Takada, R., Yoshitani, J., & Yasumoto, J. (2020). Evaluation of recharge areas of Arusha Aquifer, Northern Tanzania: Application of water isotope tracers. *Hydrology Research*, 51(6), 1490-1505. <https://doi.org/10.2166/nh.2020.179>
- Luhunga, P. M., Botai, J. O., & Kahimba, F. (2016). Evaluation of the performance of CORDEX regional climate models in simulating present climate conditions of Tanzania. *Journal of Southern Hemisphere Earth Systems Science*, 66, 32–54.
- Luhunga, P. M., Kijazi, A. L., Chang'a, L., Kondowe, A., Ng'ongolo, H., & Mtongori, H. (2018). Climate Change Projections for Tanzania Based on High-Resolution Regional Climate Models From the Coordinated Regional Climate Downscaling Experiment (CORDEX)-Africa. *Frontiers in Environmental Science*, 6(122), 1-20. <https://doi.org/10.3389/fenvs.2018.00122>
- Lwimbo, Z. D., Komakech, H. C., & Muzuka, A. N. (2019). Impacts of emerging agricultural practices on groundwater quality in Kahe catchment, Tanzania. *Water*, 11(11), 1-25. <https://doi.org/https://doi.org/10.3390/w11112263>
- Lyle, J. T. (1996). *Regenerative design for sustainable development*. John Wiley & Sons. <https://www.wiley.com/en-am/Regenerative+Design+for+Sustainable+Development-p-9780471178439>
- Lyon, B., & DeWitt, D. G. (2012). A recent and abrupt decline in the East African long rains. *Geophysical Research Letters*, 39(2), 1-5. <https://doi.org/https://doi.org/10.1029/2011GL050337>

- Ma, B., Liang, X., Liu, S., Jin, M., Nimmo, J. R., & Li, J. (2017). Evaluation of diffuse and preferential flow pathways of infiltrated precipitation and irrigation using oxygen and hydrogen isotopes. *Hydrogeology Journal*, 25(3), 675-688. <https://doi.org/10.1007/s10040-016-1525-5>
- MacDonald, A. M., Calow, R. C., Macdonald, D. M., Darling, W. G., & Dochartaigh, B. E. (2009a). What impact will climate change have on rural groundwater supplies in Africa? *Hydrological Sciences Journal*, 54, 690-703.
- MacDonald, A. M., Calow, R. C., MacDonald, D. M., Darling, W. G., & Dochartaigh, B. E. (2009b). What impact will climate change have on rural groundwater supplies in Africa? *Hydrological Sciences Journal*, 54(4), 690-703.
- Mächler, L., Peter, S., Brennwald, M. S., & Kipfer, R. (2013). Excess air formation as a mechanism for delivering oxygen to groundwater. *Water Resources Research*, 49(10), 6847-6856. <https://doi.org/https://doi.org/10.1002/wrcr.20547>
- Mahoo, H., Simukanga, L., & Kashaga, R. (2015). Water resources management in Tanzania: Identifying research gaps and needs and recommendations for a research agenda. *Tanzania Journal of Agricultural Sciences*, 14(1), 57-77.
- Maitima, J. M., Mugatha, S. M., Reid, R. S., Gachimbi, L. N., Majule, A., Lyaruu, H., Pomery, D., Mathai, S., & Mugisha, S. (2009). The linkages between land use change, land degradation and biodiversity across East Africa. *African Journal of Environmental Science and Technology*, 3(10), 310-325.
- Makurira, H., Savenije, H., Uhlenbrook, S., Rockström, J., & Senzanje, A. (2011). The effect of system innovations on water productivity in subsistence rainfed agricultural systems in semi-arid Tanzania. *Agricultural Water Management*, 98(11), 1696-1703.
- Malard, F., & Hervant, F. (1999). Oxygen supply and the adaptations of animals in groundwater. *Freshwater Biology*, 41(1), 1-30. <https://doi.org/https://doi.org/10.1046/j.1365-2427.1999.00379.x>
- Marghade, D., Malpe, D. B., Duraisamy, K., Patil, P. D., & Li, P. (2020). Hydrogeochemical evaluation, suitability, and health risk assessment of groundwater in the watershed of

- Godavari basin, Maharashtra, Central India. *Environmental Science and Pollution Research*, 28, 18471–18494. <https://doi.org/10.1007/s11356-020-10032-7>
- Marhaento, H., Booij, M. J., & Hoekstra, A. Y. (2018). Hydrological response to future land-use change and climate change in a tropical catchment. *Hydrological Sciences Journal*, 63(9), 1368-1385. <https://doi.org/10.1080/02626667.2018.1511054>
- Marhaento, H., Booij, M. J., Rientjes, T. H. M., & Hoekstra, A. Y. (2017). Attribution of changes in the water balance of a tropical catchment to land use change using the Soils and Water Assessment Tool Model. *Hydrological Processes*, 31(11), 2029-2040. <https://doi.org/10.1002/hyp.11167>.
- Massmann, G., & Sültenfuß, J. (2008). Identification of processes affecting excess air formation during natural bank filtration and managed aquifer recharge. *Journal of Hydrology*, 359(3), 235-246. <https://doi.org/https://doi.org/10.1016/j.jhydrol.2008.07.004>
- Maurya, J., Pradhan, S. N., Seema, & Ghosh, A. K. (2020). Evaluation of ground water quality and health risk assessment due to nitrate and fluoride in the Middle Indo-Gangetic plains of India. *Human and Ecological Risk Assessment: An International Journal*, 27, 1349-1365. <https://doi.org/10.1080/10807039.2020.1844559>
- Mazvimavi, D. (2003). *Estimation of Flow Characteristic of Ungauged Catchments, Case study in Zimbabwe [PhD Dissertation, Wageningen University]*. The Netherlands. <https://library.wur.nl/WebQuery/wurpubs/fulltext/121502>
- Mbonile, M. J. (2005). Migration and intensification of water conflicts in the Pangani Basin, Tanzania. *Habitat International*, 29(1), 41-67. [https://doi.org/10.1016/S0197-3975\(03\)00061-4](https://doi.org/10.1016/S0197-3975(03)00061-4)
- Mbonile, M. J., Misana, S., & Sokoni, C. (2003). *Land use change patterns and root causes of land use change on the southern slopes of Mount Kilimanjaro, Tanzania*. Land Use Change Impacts and Dynamics Project working paper number 38. www.lucideastafrica.org
- Mckenzie, J. M., Mark, B. G., Thompson, L. G., Schotterer, U., & Lin, P. N. (2010). A hydrogeochemical survey of Kilimanjaro (Tanzania): Implications for water sources and

- Mearns, L., Giorgi, F., McDaniel, L., & Shields, C. (2003). *Climate scenarios for the southeastern US based on GCM and regional model simulations: Issues in the Impacts of Climate Variability and Change on Agriculture*. Springer. [https:// library. wur.nl/ WebQ- uery/ wurpubs/fulltext/121502](https://library.wur.nl/WebQuery/wurpubs/fulltext/121502)
- Meaurio, M., Zabaleta, A., Uriarte, J. A., Srinivasan, R., & Antigüedad, I. (2015). Evaluation of SWAT models performance to simulate streamflow spatial origin. The case of a small forested watershed. *Journal of Hydrology*, 525, 326-334. [https://doi.org/ 10.1016/ j.jhydrol .2015.03.050](https://doi.org/10.1016/j.jhydrol.2015.03.050)
- Meinzer, O. E. (1923). *The occurrence of ground water in the United States with a discussion of principles* [PhD thesis, University of Chicago]. Chicago, USA. <https://pubs.usgs.gov/wsp/0489/report.pdf>
- Mekasha, A., Tesfaye, K., & Duncan, A. J. (2014). Trends in daily observed temperature and precipitation extremes over three Ethiopian eco-environments. *International Journal of Climatology*, 34(6), 1990-1999. [https://doi.org/https://doi.org/10.1002/joc.3816](https://doi.org/10.1002/joc.3816)
- Mekuriaw, A., Cherinet, M., & Tsegaye, L. (2019). Assessing the impact of land cover changes on selected ecosystem services in upper Suha watershed, Gojjam, Ethiopia. *International Journal of River Basin Management*, 1-24. <https://doi.org/10.1080/15715124.2019.1704767>.
- Melsen, L. A., Addor, N., Mizukami, N., Newman, A. J., Torfs, P. J., Clark, M. P., Uijlenhoet, R., & Teuling, A. J. (2018). Mapping (dis) agreement in hydrologic projections. *Hydrology and Earth System Sciences*, 22(3), 1775-1791. <https://doi.org/10.5194/hess-2017-564>
- Memarian, H., Balasundram, S. K., Abbaspour, K. C., Talib, J. B., Boon Sung, C. T., & Sood, A. M. (2014). SWAT-based hydrological modelling of tropical land-use scenarios. *Hydrological Sciences Journal*, 59(10), 1808-1829. <https://doi.org/10.1080/02626667.2014.892598>

- Memarian, H., Balasundram, S. K., Talib, J. B., Sung, C. T. B., Sood, A. M., & Abbaspour, K. (2012). Validation of CA-Markov for simulation of land use and cover change in the Langat Basin, Malaysia. *Journal of Geographic Information System*, 4(6), 542-554. <https://doi.org/10.4236/jgis.2012.46059>
- Mengistu, D., Bewket, W., & Lal, R. (2014). Recent spatiotemporal temperature and rainfall variability and trends over the Upper Blue Nile River Basin, Ethiopia. *International Journal of Climatology*, 34(7), 2278-2292. <https://doi.org/10.1002/joc.3837>
- Merz, R., Parajka, J., & Blöschl, G. (2011). Time stability of catchment model parameters: Implications for climate impact analyses. *Water Resources Research*, 47(2), 1-17. <https://doi.org/10.1029/2010WR009505>
- Middelkoop, H., Daamen, K., Gellens, D., Grabs, W., Kwadijk, J. C., Lang, H., Parmet, B. W., Schädler, B., Schulla, J., & Wilke, K. (2001). Impact of climate change on hydrological regimes and water resources management in the Rhine basin. *Climatic Change*, 49(1-2), 105-128.
- Min, E., Hazeleger, W., van Oldenborgh, G. J., & Sterl, A. (2013). Evaluation of trends in high temperature extremes in north-western Europe in regional climate models. *Environmental Research Letters*, 8(1), 1-6. <https://doi.org/10.1088/1748-9326/8/1/014011>
- Miraj, A., Pal, S., Bhattacharya, S., Chakraborty, K., Miraj, A., Pal, S., & Chakraborty, K. (2017). Observation on the TDS and EC Values of Different Water Bodies at Cooch Behar, West Bengal, India. *International Journal of Theoretical & Applied Sciences*, 9(2), 106-113.
- Miralles-Wilhelm, F., Clarke, L., Hejazi, M., Kim, S., Gustafson, K., Munoz-Castillo, R., & Graham, N. (2017). *Physical Impacts of Climate Change on Water Resources. A Discussion Paper Series*. Washington DC: World Bank. <https://openknowledge.worldbank.org/handle/10986/26028>
- Misana, S. B., Majule, A., & Lyaruu, H. V. (2003). *Linkages between Changes in Land Use, Biodiversity and Land Degradation on the Slopes of Mount Kilimanjaro, Tanzania*. Land

Use Change Impacts and Dynamics (LUCID). Project Working Paper number 38. http://www.lucideastafrica.org/publications/Misana_LUCID_WP38.doc

- Misana, S. B., Sokoni, C., & Mbonile, M. J. (2012). Land-use/cover changes and their drivers on the slopes of Mount Kilimanjaro, Tanzania. *Journal of Geography and Regional Planning*, 5(8), 151-164. <https://doi.org/10.5897/JGRP11.050>
- Mitchell, S. A. (2013). The status of wetlands, threats and the predicted effect of global climate change: the situation in Sub-Saharan Africa. *Aquatic Sciences*, 75(1), 95-112.
- Mmbaga, N. E., Munishi, L. K., & Treydte, A. C. (2017). How dynamics and drivers of land use/land cover change impact elephant conservation and agricultural livelihood development in Rombo, Tanzania. *Journal of Land Use Science*, 12(2-3), 168-181. <https://doi.org/10.1080/1747423X.2017.1313324>
- Mohammed, A. Q., Naser, R. S., Farid, H., Abderrahman, A., Khadija, E., Achaouch, A., & Driss, B. (2018). Hydro-chemical monitoring of Groundwater Quality for Irrigation in Sidi Allal Tazi area, Kenitra, Morocco. *Research Journal of Chemistry and Environment*, 22, 36-44.
- Mölg, T., Cullen, N. J., Hardy, D. R., Kaser, G., & Klok, L. (2008). Mass balance of a slope glacier on Kilimanjaro and its sensitivity to climate. *International Journal of Climatology*, 28(7), 881-892. <https://doi.org/10.1002/joc.1589>
- Mölg, T., Cullen, N. J., Hardy, D. R., Kaser, G., Nicholson, L., Prinz, R., & Winkler, M. (2014). East African glacier loss and climate change: Corrections to the UNEP article Africa without ice and snow. *Environmental Development*(6), 1-6. <https://doi.org/10.1016/j.envdev.2013.02.001>
- Mölg, T., Cullen, N. J., Hardy, D. R., Winkler, M., & Kaser, G. (2009). Quantifying climate change in the tropical midtroposphere over East Africa from glacier shrinkage on Kilimanjaro. *Journal of Climate*, 22(15), 4162-4181. <https://doi.org/10.175/2009JCLI2954.1>

- Mölg, T., Großhauser, M., Hemp, A., Hofer, M., & Marzeion, B. (2012). Limited forcing of glacier loss through land-cover change on Kilimanjaro. *Nature Climate Change*, 2(4), 254-258. <https://doi.org/10.1038/nclimate1390>
- Mölg, T., Hardy, D. R., & Kaser, G. (2003). Solar-radiation-maintained glacier recession on Kilimanjaro drawn from combined ice-radiation geometry modeling. *Journal of Geophysical Research: Atmospheres*, 108(D23), 1-11. <https://doi.org/10.1029/2003JD003546>
- Mondal, M. S. H. (2019). The implications of population growth and climate change on sustainable development in Bangladesh. *Jàmbá: Journal of Disaster Risk Studies*, 11, 1-10.
- Moriasi, D. N. G., Arnold, J., Van Liew, W., Bingner, M. L., Harmel, R. R. D., & Veith, T. L. (2007). Model Evaluation Guidelines for Systematic Quantification of Accuracy in Watershed Simulations. *Transactions of the American Society of Agricultural and Biological Engineers*, 50(3), 885-900. <https://doi.org/10.13031/2013.23153>
- Mote, P. W., & Kaser, G. (2007). The Shrinking Glaciers of Kilimanjaro: Can Global Warming Be Blamed? *American Scientist*, 95(4), 318-325.
- Msoffe, F., Nauss, T., & Zeuss, D. (2020). Use of Current Remote Sensing Methods for Biodiversity Monitoring and Conservation of Mount Kilimanjaro National Park Ecosystems. Proceedings of the 6th International Conference on Geographical Information Systems Theory, Applications and Management, 6, 175-183. <https://www.scitepress.org/Papers/2020/93577/93577.pdf>
- Mtalo, F., Mulungu, D., Mwanuzi, F., Mkhandi, S., Kimaro, T., & Valimba, P. (2005a). *Hydrological analysis of the Eastern Arc Mountain forests*. [http:// 41. 86. 178.5:8080/xmlui/ handle/1234 56789/14000](http://41.86.178.5:8080/xmlui/handle/123456789/14000)
- Mtalo, F., Mkhandi, S., Mwanuzi, F., & Mulungu, D. (2005b). Water: Is the amount of water flowing from the Eastern Arc Mountains decreasing or increasing. *The Arc Journal. Tanzanian Forest Conservation Group* (19), 6-7.

- Muerth, M. J., Gauvin St-Denis, B., Ricard, S., Velázquez, J. A., Schmid, J., Minville, M., Caya, D., Chaumont, D., Ludwig, R., & Turcotte, R. (2013). On the need for bias correction in regional climate scenarios to assess climate change impacts on river runoff. *Hydrological Earth System Science*, 17(3), 1189-1204. <https://doi.org/10.5194/hess-17-1189-2013>
- Mul, M., Mutiibwa, R., Foppen, J., Uhlenbrook, S., & Savenije, H. (2007a). Identification of groundwater flow systems using geological mapping and chemical spring analysis in South Pare Mountains, Tanzania. *Physics and Chemistry of the Earth, Parts A/B/C*, 32(15-18), 1015-1022. <https://doi.org/10.1016/j.pce.2007.07.004>
- Mul, M. L. (2009). *Understanding hydrological processes in an ungauged catchment in sub-Saharan Africa*. <https://www.cabdirect.org/cabdirect/abstract/20113309843>
- Mul, M. L., Mutiibwa, R. K., Uhlenbrook, S., & Savenije, H. H. (2007b). Hydrograph separation using hydrochemical tracers in the Makanya catchment, Tanzania. *Physics and Chemistry of the Earth*, 33(1), 151-156. <https://doi.org/10.1016/j.pce.2007.04.015>
- Mulangu, F., & Kraybill, D. (2013). Climate change and the future of mountain farming on Mt. Kilimanjaro. In S. Mann (Ed.) *The Future of Mountain Agriculture* (pp. 73-88). Springer, Germany. https://doi.org/10.1007/978-3-642-33584-6_6
- Munishi, L. K., Lema, A. A., & Ndakidemi, P. A. (2015). Decline in maize and beans production in the face of climate change at Hai District in Kilimanjaro Region, Tanzania. *International Journal of Climate Change Strategies and Management*, 7(1), 17-26. <https://doi.org/10.1108/IJCCSM-07-2013-0094>
- Munishi, L. K., & Sawere, P. C. (2014). Climate change and decline in water resources in Kikuletwa Catchment, Pangani, Northern Tanzania. *African Journal of Environmental Science and Technology*, 8(1), 58-65. <https://doi.org/10.5897/AJEST2013.1597>
- Munishi, P. K. T., Hermegast, A. M., & Mbilinyi, B. P. (2009). The impacts of changes in vegetation cover on dry season flow in the Kikuletwa River, northern Tanzania. *African Journal of Ecology*, 47(s1), 84-92. <https://doi.org/https://doi.org/10.1111/j.1365-2028.2008.01083.x>

- Musa, S. I., Hashim, M., & Reba, M. N. M. (2018). Geospatial modelling of urban growth for sustainable development in the Niger Delta Region, Nigeria. *International Journal of Remote Sensing*, 40(8), 3076-3104. <https://doi.org/10.1080/01431161.2018.1539271>
- Mustard, J. F., Defries, R. S., Fisher, T., & Moran, E. (2012). Land-use and land-cover change pathways and impacts. In G. Gutman, A. C. Janetos, C. O. Justice, E. F. Moran, J. F. Mustard, R. R. Rindfuss, D. Skole, B. L. T. II, & M. A. Cochrane (Eds), *Land Change Science: Observing, Monitoring, and Understanding Trajectories of Change on Earth's Surface* (pp. 411-429). Springer. <http://citeseerx.ist.psu.edu/viewdoc/download?doi=10.1.1.1039.6320&rep=rep1&type=pdf>
- Mutayoba, E., Kashaigili, J. J., Kahimba, F. C., Mbungu, W., & Chilagane, N. A. (2018). Assessment of the Impacts of Climate Change on Hydrological Characteristics of the Mbarali River Sub Catchment Using High Resolution Climate Simulations from CORDEX Regional Climate Models. *Applied Physics Research*, 10(5), 61-73. <https://doi.org/10.5539/apr.v10n5p61>
- Mwamila, T. B., Kimwaga, R. J., & Mtalio, F. W. (2008). Eco-hydrology of the Pangani River downstream of Nyumba ya Mungu reservoir, Tanzania. *Physics and Chemistry of the Earth, Parts A/B/C*, 33(8), 695-700. <https://doi.org/https://doi.org/10.1016/j.pce.2008.06.054>
- Mwende, E. A. (2009). *Hydro-geological aspects in the Kilimanjaro region for water development and management*. <https://core.ac.uk/download/pdf/71918067.pdf#page=48>.
- Myers, N., Mittermeier, R. A., Mittermeier, C. G., Da Fonseca, G. A. B., & Kent, J. (2000). Biodiversity hotspots for conservation priorities. *Nature*, 403(6772), 853-858. <https://doi.org/10.1038/35002501>
- Nagaraju, A., Sunil Kumar, K., & Thejaswi, A. (2014). Assessment of groundwater quality for irrigation: A case study from Bandalamottu lead mining area, Guntur District, Andhra Pradesh, South India. *Applied Water Science*, 4(4), 385-396. <https://doi.org/10.1007/s13201-014-0154-1>

- Nair, U., Ray, D., Lawton, R., Welch, R., Pielke, R., & Calvo-Alvarado, J. (2011). The impact of deforestation on orographic cloud formation in a complex tropical environment. In L. Bruijnzeel, F. Scatena, & L. Hamilton (Eds), *Tropical Montane Cloud Forests: Science for Conservation and Management: International Hydrology Series*, (pp. 538-548). Cambridge: Cambridge University Press. doi:10.1017/CBO9780511778384.057
- National Bureau of Statistics. (2012). *Population and housing census: population distribution by administrative areas*. Ministry of Finance, Dar es Salaam. [https:// www. nbs. go.tz/ index. php/ en/ census- surveys/ population- and- housing- census/ 168-2002-census- population- distr ibution-as-per-2012-population-census-administrative-units](https://www.nbs.go.tz/index.php/en/census-surveys/population-and-housing-census/168-2002-census-population-distribution-as-per-2012-population-census-administrative-units)
- National Bureau of Statistics. (2018). *Population estimates by districts for the year 2016 and 2017*. National Bureau of Statistics. [https://www.nbs.go.tz/ nbs/takwimu/census2012/ Projection-Report-20132035.pdf](https://www.nbs.go.tz/nbs/takwimu/census2012/Projection-Report-20132035.pdf)
- United Nations. (2019). *The Sustainable Development Goals Report 2019*. <https://unstats.un.org/sdgs/report/2019/>
- Ndomba, P., Mtalo, F., & Killingtveit, A. (2008a). SWAT model application in a data scarce tropical complex catchment in Tanzania. *Physics and Chemistry of the Earth, Parts A/B/C*, 33(8-13), 626-632. <https://doi.org/10.1016/j.pce.2008.06.013>
- Ndomba, P. M., Mtalo, F. W., & Killingtveit, Å. (2008b). A guided SWAT model application on sediment yield modeling in Pangani river basin: Lessons learnt. *Journal of Urban and Environmental Engineering*, 2(2), 53-62. [https:// doi. org/ 10. 4090/ juee. 2008. v2n2. 053062](https://doi.org/10.4090/juee.2008.v2n2.053062)
- Neupane, R. P., & Kumar, S. (2015). Estimating the effects of potential climate and land use changes on hydrologic processes of a large agriculture dominated watershed. *Journal of Hydrology*, 529, 418-429. <https://doi.org/https://doi.org/10.1016/j.jhydrol.2015.07.050>
- Ngugi, K., Ogindo, H., & Ertsen, M. (2015). *Impact of land use changes on hydrology of Mt. Kilimanjaro. The case of Lake Jipe catchment. European Geosciences Union General Assembly Conference Abstracts, Vienna, Austria*. <https://ui.adsabs.harvard.edu/abs/2015EGUGA..17.4526N/abstract>

- Niang, I., Ruppel, O. C., Abdrabo, M. A., Essel, A., Lennard, C., Padgham, J. a., & Urquhart, P. (2014). Africa. In V. R. Barros, C. B. Field, D. J. Dokken, M. D. Mastrandrea, K. J. Mach, T. E. Bilir, M. Chatterjee, K. L. Ebi, Y. O. Estrada, R. C. Genova, B. Girma, E. S. Kissel, A. N. Levy, S. MacCracken, P. R. A. Mastrandrea, & L. L. White (Eds), *Climate Change 2014: Impacts, Adaptation, and Vulnerability. Part B: Regional Aspects. Contribution of Working Group II to the Fifth Assessment Report of the Intergovernmental Panel on Climate Change (pp. 1199–1265)*. Cambridge University Press. [https:// www. pcc. ch/ report/ ar5/wg2/](https://www.pcc.ch/report/ar5/wg2/)
- Nikulin, G., Jones, C., Giorgi, F., Asrar, G., Büchner, M., Cerezo-Mota, R., Christensen, O. B., Déqué, M., Fernandez, J., Hänsler, A., van Meijgaard, E., Samuelsson, P., Sylla, M. B., & Sushama, L. (2012). Precipitation Climatology in an Ensemble of Coordinated Regional Climate Downscaling Experiment-Africa Regional Climate Simulations. *Journal of Climate*, 25(18), 6057-6078. <https://doi.org/10.1175/jcli-d-11-00375.1>
- Nkotagu, H. H., & Mwambo, K. (2000). *Hydrology of selected watersheds along the Lake Tanganyika shoreline: Final report series, Lake Tanganyika Biodiversity Project*. <http://www.ltbp.org/FTP/SSS11.PDF>
- Nkya, K., Mbowe, A., & Makoi, J. (2015). Low-cost irrigation technology, in the context of sustainable land management and adaptation to climate change in the Kilimanjaro Region. *Journal of Environment and Earth Science*, 5(7), 45-56.
- Olson, J. M., Alagarwamy, G., Andresen, J. A., Campbell, D. J., Davis, A. Y., Ge, J., Huebner, M., Lofgren, B. M., Lusch, D. P., & Moore, N. J. (2008). Integrating diverse methods to understand climate–land interactions in East Africa. *Geoforum*, 39(2), 898-911. <https://doi.org/10.1016/j.geoforum.2007.03.011>
- Omambia, A. N., Shemsanga, C., & Hernandez, I. A. S. (2017). *Climate change impacts, vulnerability, and adaptation in East Africa and South America. Handbook of climate change mitigation and adaptation*. Springer International Publishing Switzerland, 749-799. <https://link.springer.com/referencework/10.1007%2F978-1-4614-6431-0>
- Ongoma, V., & Chen, H. (2017). Temporal and spatial variability of temperature and precipitation over East Africa from 1951 to 2010. *Meteorology and Atmospheric Physics*, 129(2), 131-144. <https://doi.org/10.1007/s00703-016-0462-0>

- Osima, S., Indasi, V. S., Zaroug, M., Endris, H. S., Gudoshava, M., Misiani, H. O., Nimusiima, A., Anyah, R. O., Otieno, G., Ogwang, B. A., Jain, S., Kondowe, A. L., Mwangi, E., Lennard, C., Nikulin, G., & Dosio, A. (2018). Projected climate over the Greater Horn of Africa under 1.5 °C and 2 °C global warming. *Environmental Research Letters*, 13(6), 1-11. <https://doi.org/10.1088/1748-9326/aaba1b>
- Otte, I., Detsch, F., Gütlein, A., Scholl, M., Kiese, R., Appelhans, T., & Nauss, T. (2017). Seasonality of stable isotope composition of atmospheric water input at the southern slopes of Mt. Kilimanjaro, Tanzania. *Hydrological Processes*, 31(22), 3932-3947. <https://doi.org/doi.org/10.1002/hyp.11311>
- Otte, I., Detsch, F., Mwangomo, E., Hemp, A., Appelhans, T., & Nauss, T. (2016). Multidecadal trends and interannual variability of rainfall as observed from five lowland stations at Mt. Kilimanjaro, Tanzania. *Journal of Hydrometeorology*, 18(2), 349-361. <https://doi.org/10.1175/JHM-D-16-0062.s1>
- Oyarzún, R., Jofré, E., Morales, P., Maturana, H., Oyarzún, J., Kretschmer, N., Aguirre, E., Gallardo, P., Toro, L. E., Muñoz, J. F., & Aravena, R. (2015). A hydrogeochemistry and isotopic approach for the assessment of surface water–groundwater dynamics in an arid basin: The Limarí watershed, North-Central Chile. *Environmental Earth Sciences*, 73(1), 39-55. <https://doi.org/10.1007/s12665-014-3393-4>
- Pachauri, R. K., Allen, M. R., Barros, V. R., Broome, J., Cramer, W., Christ, R., & Dubash, N. K. (2014a). *Climate change 2014: Synthesis Report. Contribution of Working Groups I, II and III to the fifth assessment report of the Intergovernmental Panel on Climate Change*. [https:// www. ipcc.ch/ site/ assets/ uploads/ 2018/ 05/ SYR_ AR5_ FINAL_ full_ wcover.pdf](https://www.ipcc.ch/site/assets/uploads/2018/05/SYR_AR5_FINAL_full_wcover.pdf)
- Pachauri, R. K., Allen, M. R., Barros, V. R., Broome, J., Cramer, W., Christ, R., & Dubash, N. K. (2014b). *Climate change 2014: Synthesis Report. Contribution of Working Groups I, II and III to the fifth assessment report of the Intergovernmental Panel on Climate Change*. [https:// www. ipcc. ch/ site/ assets/ uploads/ 2018/ 05/ SYR_ AR5_ FINAL_ full_ wcover.pdf](https://www.ipcc.ch/site/assets/uploads/2018/05/SYR_AR5_FINAL_full_wcover.pdf)

- Palamuleni, L. G., Ndomba, P. M., & Annegarn, H. J. (2011). Evaluating land cover change and its impact on hydrological regime in Upper Shire river catchment, Malawi. *Regional Environmental Change*, 11(4), 845-855.
- Paliwal, K. (1972). *Irrigation with saline water, Monogram no. 2 (New series)*. Indian Agriculture Research Institute, New Delhi. <http://www.sciepub.com/reference/82318>
- Pan, X., Li, X., Shi, X., Han, X., Luo, L., & Wang, L. (2012). Dynamic downscaling of near-surface air temperature at the basin scale using WRF-a case study in the Heihe River Basin, China. *Frontiers of Earth Science*, 6(3), 314-323. <https://doi.org/10.1007/s11707-012-0306-2>
- PBWO, & IUCN. (2010). *Climate change modelling for the Pangani Basin to support the Integrated Water Resources Management planning process*. Moshi, Tanzania. <https://www.iucn.org/content/climate-change-modelling-pangani-basin-support-iwrm-planning-process>
- Peel, M. C., & McMahon, T. A. (2006). Continental runoff: A quality-controlled global runoff data set. *Nature*, 444(7120), 1-5. <https://doi.org/10.1038/nature05480>
- Pervez, M. S., & Henebry, G. M. (2015). Assessing the impacts of climate and land use and land cover change on the freshwater availability in the Brahmaputra River basin. *Journal of Hydrology: Regional Studies*, 3, 285-311.
- Piper, A. M. (1944). A graphic procedure in the geochemical interpretation of water-analyses. *Eos, Transactions American Geophysical Union*, 25(6), 914-928. <https://doi.org/10.1029/TR025i006p00914>
- Pontius, R. G., & Millones, M. (2011). Death to Kappa: Birth of quantity disagreement and allocation disagreement for accuracy assessment. *International Journal of Remote Sensing*, 32(15), 4407-4429. <https://doi.org/10.1080/01431161.2011.552923>
- Pontius, R. G., & Schneider, L. C. (2001). Land-cover change model validation by an ROC method for the Ipswich watershed, Massachusetts, USA. *Agriculture, Ecosystems & Environment*, 85(1-3), 239-248. [https://doi.org/10.1016/S0167-8809\(01\)00187-6](https://doi.org/10.1016/S0167-8809(01)00187-6)

- Pontius, R. G., & Schneider, L. C. (2001). Land-cover change model validation by an ROC method for the Ipswich watershed, Massachusetts, USA. *Agriculture, Ecosystems & Environment*, 85(1), 239-248. [https://doi.org/10.1016/S0167-8809\(01\)00187-6](https://doi.org/10.1016/S0167-8809(01)00187-6)
- Prada, S., De Sequeira, M. M., Figueira, C., & Da Silva, M. O. (2009). Fog precipitation and rainfall interception in the natural forests of Madeira Island (Portugal). *Agricultural and Forest Meteorology*, 149(6-7), 1179-1187. <https://doi.org/10.1016/j.agrformet.2009.02.010>
- Prada, S., De Sequeira, M. M., Figueira, C., Prior, V., & Da Silva, M. O. (2010). Response to comment on fog precipitation and rainfall interception in the natural forests of Madeira Island (Portugal). *Agricultural and Forest Meteorology*, 150(7-8), 1154-1157. <https://doi.org/10.1016/j.agrformet.2010.04.009>
- PWBO/IUCN. (2010). *Climate change modelling for the Pangani Basin to support the Integrated Water Resources Management planning process*. Pangani River Basin Flow Assessment. <https://www.iucn.org/content/climate-change-modelling-pangani-basin-support-iwrm-planning-process>
- Qi, J., Li, S., Li, Q., Xing, Z., Bourque, C. P. A., & Meng, F. R. (2016). Assessing an enhanced version of SWAT on water quantity and quality simulation in regions with seasonal snow cover. *Water Resources Management*, 30(14), 5021-5037. <https://doi.org/10.1007/s11269-016-1466-8>
- Ramírez, V. J., & Thornton, P. K. (2015). Climate change impacts on African crop production. *Climate Change, Agriculture and Food Security Working Paper no. 119*. Copenhagen, Denmark: Research Program on Climate Change, Agriculture and Food Security. <https://www.uncclearn.org/wp-content/uploads/library/fao34.pdf>
- Rao, K., Verchot, L. V., & Laarman, J. (2007). Adaptation to Climate Change through Sustainable Management and Development of Agroforestry Systems. *International Crops Research Institute for the Semi-Arid Tropics* 4, 1-30.
- Rastner, P., Prinz, R., Notarnicola, C., Nicholson, L., Sailer, R., Schwaizer, G., & Paul, F. (2019). On the Automated Mapping of Snow Cover on Glaciers and Calculation of Snow Line

- Altitudes from Multi-Temporal Landsat Data. *Remote Sensing*, 11(12), 1-24. <https://doi.org/10.3390/rs11121410>
- Raum, O. F. (1940). *A Description of Indigenous Education in an East African Tribe*. Oxford University Press, London: https://librarysearch.lse.ac.uk/primo-explore/fulldisplay/44LSE_ALMA_DS21113510240002021/44LSE_VU1
- Richards, L. (1968). *Diagnosis and Improvement of Saline and Alkali Soils*, US Dept Agriculture Handbook. https://www.ars.usda.gov/ARSPUserFiles/20360500/hb60_pdf/hb60intro.pdf
- Richards, L. A. (1954). *Diagnosis and improvement of saline and alkaline soils*. US Salinity Laboratory. <https://books.google.co.tz/books?hl>
- Roa-García, M. C., Brown, S., Schreier, H., & Lavkulich, L. M. (2011). The role of land use and soils in regulating water flow in small headwater catchments of the Andes. *Water Resources Research*, 47(5), 1-12. <https://doi.org/10.1029/2010WR009582>
- Rodrigo, F. S., & Trigo, R. M. (2007). Trends in daily rainfall in the Iberian Peninsula from 1951 to 2002. *International Journal of Climatology*, 27(4), 513-529. <https://doi.org/10.1002/joc.1409>
- Røhr, P. C. (2003). *A Hydrological Study Concerning the Southern Slopes of Mt Kilimanjaro, Tanzania* [Doctoral dissertation, Norwegian University of Science and Technology]. Trondheim, Norway. <https://ntnuopen.ntnu.no/ntnu-xmlui/handle/11250/231188>
- Røhr, P. C., & Killingtveit, Å. (2003). Rainfall distribution on the slopes of Mt. Kilimanjaro. *Hydrological Sciences Journal*, 48(1), 65-77. <https://doi.org/10.1623/hysj.48.1.65.43483>
- Roth, V., & Lemann, T. (2016). Comparing CFSR and conventional weather data for discharge and soil loss modelling with SWAT in small catchments in the Ethiopian Highlands. *Hydrology and Earth System Sciences*, 20(2), 921-934. <https://doi.org/10.5194/hess-20-921-2016>
- Rothfuss, Y., Merz, S., Vanderborght, J., Hermes, N., Weuthen, A., Pohlmeier, A., Vereecken, H., & Brüggemann, N. (2015). Long-term and high-frequency non-destructive

- monitoring of water stable isotope profiles in an evaporating soil column. *Hydrological Earth System Science*, 19(10), 4067-4080. <https://doi.org/10.5194/hess-19-4067-2015>
- Roux, B. (2009). *Ultra high-resolution climate simulations over the Stellenbosch wine producing region using a variable-resolution model* [Masters Dissertation, University of Pretoria]. South Africa. <http://hdl.handle.net/2263/29962>
- Rowhani, P., Lobell, D. B., Linderman, M., & Ramankutty, N. (2011). Climate variability and crop production in Tanzania. *Agricultural and Forest Meteorology*, 151(4), 449-460. <https://doi.org/10.1016/j.agrformet.2010.12.002>
- Rwebugisa, R. A. (2008). *Groundwater re-charge assessment in the Makutupora Basin, Dodoma, Tanzania* [Masters Thesis. International Institute for Geo-Information Science and Earth Observation]. Enschede, The Netherlands. https://webapps.itc.utwente.nl/librarywww/papers_2008/msc/wrem/althanael.pdf
- Sadashivaiah, C., Ramakrishnaiah, C. R., & Ranganna, G. (2008). Hydrochemical Analysis and Evaluation of Groundwater Quality in Tumkur Taluk, Karnataka State, India. *International Journal of Environmental Research and Public Health*, 5(3), 158-164. <https://www.mdpi.com/1660-4601/5/3/158>
- Said, M., Hyandye, C., Komakech, H., Mjemah, I., & Munishi, L. (2021). Predicting land use/cover changes and its association to agricultural production on the slopes of Mount Kilimanjaro, Tanzania. *Annals of Geographic Information System*, 27(2), 189-209. <https://doi.org/10.1080/19475683.2020.1871406>
- Said, M., Komakech, H. C., Munishi, L. K., & Muzuka, A. N. N. (2019). Evidence of climate change impacts on water, food and energy resources around Kilimanjaro, Tanzania. *Regional Environmental Change*, 19, 2521–2534. <https://doi.org/10.1007/s10113-019-01568-7>
- Salama, R. B. (1979). *Dodoma capital city water resources study*. Government printers. (Unpublished Government Report). <https://www.google.com>
- Salifu, M., Aidoo, F., Hayford, M. S., Adomako, D., & Asare, E. (2017). Evaluating the suitability of groundwater for irrigational purposes in some selected districts of the Upper

West region of Ghana. *Applied Water Science*, 7(2), 653-662.
<https://doi.org/10.1007/s13201-015-0277-z>

Salve, P. R., Maurya, A., Kumbhare, P. S., Ramteke, D. S., & Wate, S. R. (2008). Assessment of Groundwater Quality with Respect to Fluoride. *Bulletin of Environmental Contamination and Toxicology*, 81(3), 289–293. <https://doi.org/10.1007/s00128-008-9466-x>

Sandström, K. (1995). The recent lake Babati floods in semi-arid Tanzania: A response to changes in land cover? *Geografiska Annaler: Series A, Physical Geography*, 77(1-2), 35-44. <https://doi.org/10.1080/04353676.1995.11880427>

Santhi, C., Arnold, J. G., Williams, J. R., Dugas, W. A., Srinivasan, R., & Hauck, L. M. (2001). Validation of SWAT Model on a large river basin with point and non-point sources. *Journal of the American Water Resources Association*, 37(5), 1169-1188. <https://doi.org/10.1111/j.1752-1688.2001.tb03630.x>

Sarmett, J. D. a., & Faraji, S. A. (1991). The hydrology of Mount Kilimanjaro: An examination of dry season runoff and possible factors leading to its decrease. In W. D. Newmark (Ed.), *The Conservation of Mount Kilimanjaro* (pp. 53-70). The IUCN Tropical Forest Programme. <https://portals.iucn.org/library/sites/library/files/documents/FR-TF-017.pdf>

Schlüter, T. (2006). *Geological atlas of Africa: With Notes on Stratigraphy, Tectonics, Economic Geology, Geohazards, Geosites and Geoscientific Education of Each Country*. Springer. <https://doi.org/10.1007/3-540-29145-8>

Schmidli, J., Frei, C., & Vidale, P. L. (2006). Downscaling from General Circulation Models precipitation: A benchmark for dynamical and statistical downscaling methods. *International Journal of Climatology*, 26, 679-689.

Schmidt, P. R. (1989). Early exploitation and settlement in the Usambara Mountains. In A. Hamilton, & R. Bensted-Smith (Eds), *Forest Conservation in the East Usambara Mountains, Tanzania* (pp. 75-78). Gland and Cambridge. <https://portals.iucn.org/library/sites/library/files/documents/FR-TF-016.pdf>

- Schoeller, H. (1965). Qualitative evaluation of groundwater resources: Methods and techniques of groundwater investigations and development. *Water Resource Series*, 33, 44-52.
- Schulze, R. E. (2000). Modelling hydrological responses to land use and climate change: A southern African perspective. *AMBIO: A Journal of the Human Environment*, 29(1), 12-22. <https://doi.org/10.1579/0044-7447-29.1.12>
- Seddon, D. (2019). *The Climate Controls and Process of Groundwater Recharge in a Semi-Arid Tropical Environment: Evidence from the Makutapora Basin, Tanzania [PhD Thesis, University College London]*. https://discovery.ucl.ac.uk/id/eprint/10078654/1/Seddon_10078654_thesis_redacted.pdf
- Sen, P. K. (1968). Estimates of the Regression Coefficient Based on Kendall's Tau. *Journal of the American Statistical Association*, 63(324), 1379-1389. <https://doi.org/10.1080/01621459.1968.10480934>
- Senarathne, S., Jayawardana, J. M. C. K., Edirisinghe, E. A. N. V., & Chandrajith, R. (2020). Influence of regional climatic on the hydrogeochemistry of a tropical river basin: A study from the Walawe river basin of Sri Lanka. *Environmental Science and Pollution Research*, 28(13), 15701-15715. <https://doi.org/10.1007/s11356-020-11712-0>
- Seneviratne, S. I., Nicholls, N., Easterling, D., Goodess, C. M., Kanae, S., Kossin, J., Luo, Y., Marengo, J., McInnes, K., Rahimi, M., Reichstein, M., Sorteberg, A., Vera, C., & Zhang, X. (2012). *Changes in climate extremes and their impacts on the natural physical environment Managing the Risks of Extreme Events and Disasters to Advance Climate Change Adaptation. A Special Report of Working Groups I and II of the Intergovernmental Panel on Climate Change*. <https://www.ipcc.ch/report/managing-the-risks-of-extreme-events-and-disasters-to-advance-climate-change-adaptation/>
- Serdeczny, O., Adams, S., Baarsch, F., Coumou, D., Robinson, A., Hare, W., Schaeffer, M., Perrette, M., & Reinhardt, J. (2016). Climate change impacts in Sub-Saharan Africa: From physical changes to their social repercussions. *Regional Environmental Change*, 17(6), 1585-1600. <https://doi.org/10.1007/s10113-015-0910-2>
- Setegn, S. G., Srinivasan, R., & Dargahi, B. (2008). Hydrological modelling in the Lake Tana Basin, Ethiopia using SWAT model. *The Open Hydrology Journal*, 2(1), 49-62.

- Shagega, F. P., Munishi, S. E., & Kongo, V. M. (2020). Assessment of potential impacts of climate change on water resources in Ngerengere catchment, Tanzania. *Physics and Chemistry of the Earth, Parts A/B/C*, 116, 1-30. <https://doi.org/10.1016/j.pce.2019.11.001>
- Shaghude, Y. W. (2006). Review of water resource exploitation and landuse pressure in the Pangani river basin. *Western Indian Ocean Journal of Marine Science*, 5(2), 195-208. <https://doi.org/10.4314/wiojms.v5i2.28510>
- Shah, T. (2009). Climate change and groundwater: India's opportunities for mitigation and adaptation. *Environmental Research Letters*, 4(3), 1-13.
- Shawul, A. A., Alamirew, T., & Dinka, M. (2013). Calibration and validation of SWAT model and estimation of water balance components of Shaya mountainous watershed, Southeastern Ethiopia. *Hydrology and Earth System Sciences Discussions*, 10(11), 13955-13978. <https://doi.org/10.5194/hessd-10-13955-2013>
- Shawul, A. A., Chakma, S., & Melesse, A. M. (2019). The response of water balance components to land cover change based on hydrologic modeling and Partial Least Squares regression analysis in the Upper Awash Basin. *Journal of Hydrology: Regional Studies*, 26, 1-19. <https://doi.org/10.1016/j.ejrh.2019.100640>
- Shemsanga, C., Anne, N. O., & Yansheng, G. (2010). The cost of climate change in Tanzania: Impacts and adaptations. *Journal of American Science*, 6(3), 182-196.
- Shi, P., Ma, X., Hou, Y., Li, Q., Zhang, Z., Qu, S., Chen, C., Cai, T., & Fang, X. (2013a). Effects of Land-Use and Climate Change on Hydrological Processes in the Upstream of Huai River, China. *Water Resources Management*, 27(5), 1263-1278. <https://doi.org/10.1007/s11269-012-0237-4>
- Shi, Z., Ai, L., Li, X., Huang, X., Wu, G., & Liao, W. (2013b). Partial least-squares regression for linking land-cover patterns to soil erosion and sediment yield in watersheds. *Journal of Hydrology*, 498, 165-176. <https://doi.org/10.1016/j.jhydrol.2013.06.031>

- Shishira, E., & Yanda, P. Z. (2018). *Forestry conservation and resource utilisation on the southern slopes of Mount Kilimanjaro: trends, conflicts and resolutions*. http://hdl.handle.net/12345_6789/869
- Shongwe, M., Lennard, C., Liebmann, B., Kalognomou, E. A., Ntsangwane, L., & Pinto, I. (2014). An evaluation of CORDEX regional climate models in simulating precipitation over Southern Africa. *Atmospheric Science Letters*, 16, 199–207. <https://doi.org/10.1002/asl2.538>
- Siriwardena, L., Finlayson, B. L., & McMahon, T. A. (2006). The impact of land use change on catchment hydrology in large catchments: The Comet River, Central Queensland, Australia. *Journal of Hydrology*, 326(1), 199–214. <https://doi.org/10.1016/j.jhydrol.2005.10.030>
- Smith, P., House, J. I., Bustamante, M., Sobocká, J., Harper, R., Pan, G., West, P. C., Clark, J. M., Adhya, T., & Rumpel, C. (2016). Global change pressures on soils from land use and management. *Global Change Biology*, 22(3), 1008–1028. <https://doi.org/10.1111/gcb.13068>
- Soini, E. (2005a). Changing livelihoods on the slopes of Mt. Kilimanjaro, Tanzania: Challenges and opportunities in the Chagga homegarden system. *Agroforestry Systems*, 64(2), 157–167. <https://doi.org/10.1007/s10457-004-1023-y>
- Soini, E. (2005b). Land use change patterns and livelihood dynamics on the slopes of Mt. Kilimanjaro, Tanzania. *Agricultural Systems*, 85(3), 306–323. <https://doi.org/10.1016/j.agry.2005.06.013>
- Srivastava, S., & Flora, S. J. S. (2020). Fluoride in Drinking Water and Skeletal Fluorosis: a Review of the Global Impact. *Current Environmental Health Reports*, 7(2), 140–146. <https://doi.org/10.1007/s40572-020-00270-9>
- Stonestrom, D. A., Scanlon, B. R., & Zhang, L. (2009). Introduction to special section on Impacts of Land Use Change on Water Resources. *Water Resources Research*, 45(7), 1–3. <https://doi.org/10.1029/2009WR007937>

- Stump, D., & Tagseth, M. (2009). The history of precolonial and early colonial agriculture on Kilimanjaro: a review. In T. Clack (Ed), *Culture, History and Identity: Landscapes of Inhabitation in the Mount Kilimanjaro Area* (pp. 107-124). Archaeopress. https://www.si.edu/object/siris_sil_1005053
- Sunyer, M. A., Madsen, H., & Yamagata, K. (2010). *On the use of statistical downscaling for assessing climate change impacts on hydrology. International workshop advances in statistical hydrology, Taormina, Italy.* [http:// www.environmetrics.org /Postings/091106. pdf](http://www.environmetrics.org/Postings/091106.pdf)
- Tagseth, M. (2008). The expansion of traditional irrigation in Kilimanjaro, Tanzania. *The International Journal of African Historical Studies*, 41(3), 461-490.
- Tagseth, M. (2010). *Studies of the waterscape of Kilimanjaro, Tanzania Water management in hill furrow irrigation [PhD theis, Norwegian University of Science and Technology].* Trondheim. <https://ntnuopen.ntnu.no/ntnu-xmlui/handle/11250/265336>
- Tattoni, C., Ciolli, M., & Ferretti, F. (2011). The fate of priority areas for conservation in protected areas: A fine-scale Markov chain approach. *Environmental Management*, 47(2), 263-278. <https://doi.org/10.1007/s00267-010-9601-4>
- Tavakoli, M., De Smedt, F., Vansteenkiste, T., & Willems, P. (2014). Impact of climate change and urban development on extreme flows in the Grote Nete watershed, Belgium. *Natural Hazards*, 71(3), 2127-2142. <https://doi.org/10.1007/s11069-013-1001-7>
- Taweasuk, S., & Thammapala, P. (2005). *Expert classification technique for mapping teak plantation areas in Thailand. Sioux Falls, South Dakota.* [http:// www. asprs. org/a/publicati ons/ proceedings/ pecora16/Taweasuk_s.pdf](http://www.asprs.org/a/publications/proceedings/pecora16/Taweasuk_s.pdf)
- Taylor, R. G., Scanlon, B., Döll, P., Rodell, M., Van Beek, R., Wada, Y., Longuevergne, L., Leblanc, M., Famiglietti, J. S., & Edmunds, M. (2012a). Ground water and climate change. *Nature Climate Change*, 54, 655-664.
- Taylor, R. G., Scanlon, B., Döll, P., Rodell, M., Van Beek, R., Wada, Y., Longuevergne, L., Leblanc, M., Famiglietti, J. S., & Edmunds, M. (2013). Ground water and climate change. *Nature Climate Change*, 3(4), 1-27. <https://doi.org/10.1038/nclimate1744>

- Taylor, R. G., Todd, M. C., Kongola, L., Maurice, L., Nahozya, E., Sanga, H., & MacDonald, A. M. (2012b). Evidence of the dependence of groundwater resources on extreme rainfall in East Africa. *Nature Climate Change*, 3, 374-378.
- Teale, E. O., & Gillman, C. (1935). *Report on the Investigation of the Proper Control of Water and the Re-organization of Water Boards in the Northern Province of Tanganyika Territory: November-December 1934*. Government Printer. [https:// www. abeebooks. co.uk/ Report-investigation-proper-control-water-re-organization/21350199114/bd](https://www.abeebooks.co.uk/Report-investigation-proper-control-water-re-organization/21350199114/bd)
- Tenenhaus, M., Pagès, J., Ambroisine, L., & Guinot, C. (2005). PLS methodology to study relationships between hedonic judgements and product characteristics. *Food Quality and Preference*, 16(4), 315-325. [https:// doi. org/ https:// doi. org/ 10. 1016/j. foodqual. 2004. 05. 013](https://doi.org/10.1016/j.foodqual.2004.05.013)
- Tesfaw, A. T., Pfaff, A., Golden Kroner, R. E., Qin, S., Medeiros, R., & Mascia, M. B. (2018). Land-use and land-cover change shape the sustainability and impacts of protected areas. *Proceedings of the National Academy of Sciences*, 115(9), 2084-2089. <https://doi.org/10.1073/pnas.1716462115>
- Thompson, L. G. (2000). Ice core evidence for climate change in the Tropics: Implications for our future. *Quaternary Science Reviews*, 19(1), 19-35. [https://doi.org/10.1016/S0277-3791\(99\)00052-9](https://doi.org/10.1016/S0277-3791(99)00052-9)
- Thompson, L. G., Brecher, H. H., Mosley-Thompson, E., Hardy, D. R., & Mark, B. G. (2009). Glacier loss on Kilimanjaro continues unabated. *Proceedings of the National Academy of Sciences*, 106(47), 19770-19775. <https://doi.org/10.1073/pnas.0906029106>
- Thompson, L. G., Mosley-Thompson, E., Davis, M. E., & Brecher, H. H. (2011). Tropical glaciers, recorders and indicators of climate change, are disappearing globally. *Annals of Glaciology*, 52(59), 23-34. <https://doi.org/10.3189/172756411799096231>
- Thompson, L. G., Mosley-Thompson, E., Davis, M. E., Henderson, K. A., Brecher, H. H., Zagorodnov, V. S., Mashiotto, T. A., Lin, P. N., Mikhaleiko, V. N., Hardy, D. R., & Beer, J. (2002). Kilimanjaro ice core records: Evidence of holocene climate change in tropical Africa. *Science*, 298(5593), 589-593. <https://doi.org/10.1126/science.1073198>

- Tripathi, S., Srinivas, V., & Nanjundiah, R. S. (2006). Downscaling of precipitation for climate change scenarios: A support vector machine approach. *Journal of Hydrology*, 330(3), 621-640.
- Turpie, J., Ngaga, Y., & Karanja, F. (2003). A preliminary Economic Assessment of water Resources of Pangani River Basin, Tanzania. *Economic Value, Incentives for Sustainable Use and Mechanisms for financing management*. International Union for Conservation of Nature–East Africa Region Office and Pangani Basin Water Office. <https://core.ac.uk/download/pdf/6764886.pdf>
- Twisa, S., Kazumba, S., Kurian, M., & Buchroithner, M. F. (2020). Evaluating and Predicting the Effects of Land Use Changes on Hydrology in Wami River Basin, Tanzania. *Hydrology*, 7(1), 1-18. <https://doi.org/10.3390/hydrology7010017>
- Ullrich, A., & Volk, M. (2009). Application of the Soil and Water Assessment Tool to predict the impact of alternative management practices on water quality and quantity. *Agricultural Water Management*, 96(8), 1207-1217. <https://doi.org/10.1016/j.agwat.2009.03.010>
- UNDP. (2014). *Reducing Land Degradation on the Highlands of Kilimanjaro Region*. <https://www.thegef.org/project/sip-reducing-land-degradation-highlands-kilimanjaro>
- UNDP, U., Worldbank & WRI. (2000). *A guide to world resources 2000–2001: People and ecosystems: The fraying web of life*. (Unpublished report)
- Uniyal, B., Jha, M. K., & Verma, A. K. (2015). Assessing Climate Change Impact on Water Balance Components of a River Basin Using SWAT Model. *Water Resources Management*, 29(13), 4767-4785. <https://doi.org/10.1007/s11269-015-1089-5>
- URT. (2002). *Tanzania National Water Policy*. <http://maji.go.tz/uploads/publications/sw1552315386-NAWAPO.pdf>. M. o. Water.
- URT. (2003). *Initial National Communication under the United Nations Framework Convention on Climate Change*. <https://unfccc.int/resource/docs/natc/tannc1.pdf>
- URT. (2012). *Tanzania Coffee Industry Development Strategy 2011/2021*. <http://repository.Businessinsightz.org/handle/20.500.12018/2690>

- URT. (2018). *2016/17 Agriculture Production Report*. [https:// www. nbs. go. tz/ nbs/ takwimu/ Agric ulture/ 2016-17 _AASS%20Report%20_Final.pdf](https://www.nbs.go.tz/nbs/takwimu/Agriculture/2016-17_AASS%20Report%20_Final.pdf)
- Vakhshoori, V., & Zare, M. (2018). Is the ROC curve a reliable tool to compare the validity of landslide susceptibility maps? *Geomatics, Natural Hazards and Risk*, 9(1), 249-266. <https://doi.org/10.1080/19475705.2018.1424043>
- Valimba, P. (2007). *Spatial variation of hydrological floods during the short rains in Northeast Tanzania*. <https://helda.helsinki.fi/publications>
- Van-Camp, M., Mjemah, I. C., Al-Farrah, N., & Walraevens, K. (2013). Modeling approaches and strategies for data-scarce aquifers: Example of the Dar es Salaam aquifer in Tanzania. *Hydrogeology Journal*, 21, 341-356.
- Van Liew, M. W., Arnold, J. G., & Garbrecht, J. D. (2003). Hydrologic Simulation on agricultural watersheds: Choosing between two models. *Transactions of the American Society of Agricultural Engineers*, 46(6), 1539-1551. [https:// doi. org/ https:// doi. org/ 10. 13031/2013 .15643](https://doi.org/10.13031/2013.15643)
- Vasu, D., Singh, S. K., Tiwary, P., Sahu, N., Ray, S. K., Butte, P., & Duraisami, V. P. (2017). Influence of geochemical processes on hydrochemistry and irrigation suitability of groundwater in part of semi-arid Deccan Plateau, India. *Applied Water Science*, 7(7), 3803-3815. <https://doi.org/10.1007/s13201-017-0528-2>
- Verburg, P. H., van Eck, J. R. R., de Nijs, T. C., Dijst, M. J., & Schot, P. (2004). Determinants of land-use change patterns in the Netherlands. *Environment and Planning B: Planning and Design*, 31(1), 125-150. <https://doi.org/10.1029/2006WR005653>
- Viteri-García, A., Parise-Vasco, J. M., Cabrera-Dávila, M. J., Zambrano-Bonilla, M. C., Ordonez-Romero, I., Maridueña-León, M. G., Caiza-Rennella, A., Zambrano-Mendoza, A., Ponce-Faula, C., & Pérez-Granja, M. (2020). Prevalence and incidence of dental caries associated with the effect of tooth brushing and fluoride varnishing in schoolchildren at Galapagos Islands, Ecuador: Protocol of the EESO-Gal study. *Medwave*, 20(06), 1-7.

- Viviroli, D., Dürr, H. H., Messerli, B., Meybeck, M., & Weingartner, R. (2007). Mountains of the world, water towers for humanity: Typology, mapping, and global significance. *Water Resources Research*, 43(W07447), 1-13. <https://doi.org/10.1029/2006WR005653>
- Wagner, P. D., Kumar, S., & Schneider, K. (2013). An assessment of land use change impacts on the water resources of the Mula and Mutha Rivers catchment upstream of Pune, India. *Hydrological Earth System Science*, 17(6), 2233-2246. <https://doi.org/10.5194/hess-17-2233-2013>
- Walter, H., Harnickell E., & Mueller-Dombois D. (1975). *Climate Diagram Maps of the Individual Continents and the Ecological Climatic Regions of the Earth*. <https://agris.fao.org/agris-search/search.do?recordID=US201300690288>
- Wang, G., Yang, H., Wang, L., Xu, Z., & Xue, B. (2014). Using the SWAT model to assess impacts of land use changes on runoff generation in headwaters. *Hydrological Processes*, 28(3), 1032-1042. <https://doi.org/10.1002/hyp.9645>
- Wang, L., Wang, S., Zhou, Y., Zhu, J., Zhang, J., Hou, Y., & Liu, W. (2020). Landscape pattern variation, protection measures, and land use/land cover changes in drinking water source protection areas: A case study in Danjiangkou Reservoir, China. *Global Ecology and Conservation*, 21, 1-14. <https://doi.org/https://doi.org/10.1016/j.gecco.2019.e00827>
- Wilby, R. L., Charles, S., Zorita, E., Timbal, B., Whetton, P., & Mearns, L. (2004). *Guidelines for use of climate scenarios developed from statistical downscaling methods. Supporting material of the Intergovernmental Panel on Climate Change*. https://www.ipcc-data.org/guidelines/dgm_no2_v1_09_2004.pdf
- Wilby, R. L., & Wigley, T. (1997). Downscaling general circulation model output: A review of methods and limitations. *Progress in Physical Geography*, 21(4), 530-548.
- Wilcox, L. V. (1958). *Determining the quality of irrigation water*. https://link.springer.com/content/pdf/10.1007%2F978-3-319-96190-3_5.pdf
- Williams, A. P., & Funk, C. (2011). A westward extension of the warm pool leads to a westward extension of the Walker circulation, drying eastern Africa. *Climate Dynamics*, 37(11), 2417-2435. <https://doi.org/10.1007/s00382-010-0984-y>

- Williams, M. D., & Oostrom, M. (2000). Oxygenation of anoxic water in a fluctuating water table system: an experimental and numerical study. *Journal of Hydrology*, 230(1), 70-85. [https://doi.org/https://doi.org/10.1016/S0022-1694\(00\)00172-4](https://doi.org/https://doi.org/10.1016/S0022-1694(00)00172-4)
- Wold, S. (1995). *Partial Least Squares for multivariate linear modeling*. <https://ci.nii.ac.jp/naid/10031086076/>
- Wold, S., Sjöström, M., & Eriksson, L. (2001). Partial Least Square Regression: A basic tool of chemometrics. *Chemometrics and Intelligent Laboratory Systems*, 58(2), 109-130. [https://doi.org/https://doi.org/10.1016/S0169-7439\(01\)00155-1](https://doi.org/https://doi.org/10.1016/S0169-7439(01)00155-1)
- Woldesenbet, T. A., Elagib, N. A., Ribbe, L., & Heinrich, J. (2017). Hydrological responses to land use/cover changes in the source region of the Upper Blue Nile Basin, Ethiopia. *Science of the Total Environment*, 575, 724-741. <https://doi.org/10.1016/j.scitotenv.2016.09.124>
- Worqlul, A. W., Yen, H., Collick, A. S., Tilahun, S. A., Langan, S., & Steenhuis, T. S. (2017). Evaluation of CFSR, TMPA 3B42 and ground-based rainfall data as input for hydrological models, in data-scarce regions: The upper Blue Nile Basin, Ethiopia. *Catena*, 152, 242-251. <https://doi.org/10.1016/j.catena.2017.01.019>
- Wu, Y., Du, T., Li, F., Li, S., Ding, R., & Tong, L. (2016). Quantification of maize water uptake from different layers and root zones under alternate furrow irrigation using stable oxygen isotope. *Agricultural Water Management*, 168, 35-44. <https://doi.org/https://doi.org/10.1016/j.agwat.2016.01.013>
- Xia, J., Duan, Q. Y., Luo, Y., Xie, Z. H., Liu, Z. Y., & Mo, X. G. (2017). Climate change and water resources: Case study of Eastern Monsoon Region of China. *Advances in Climate Change Research*, 8(2), 63-67. <https://doi.org/10.1016/j.accre.2017.03.007>
- Yanda, P., & Munishi, P. (2007). *Hydrologic and land use/cover change analysis for the Ruvu River (Uluguru) and Sigi River (East Usambara) watersheds*. <http://hdl.handle.net/123456789/834>

- Yanda, P., & Shishira, E. (2001). *Forestry Conservation and Resource Utilization on Southern Slopes of Mount Kilimanjaro: Trends, Conflicts and Resolutions. Conflicts in Water Management in Pangani River Basin*. <http://hdl.handle.net/123456789/869>
- Yang, D., Kanae, S., Oki, T., Koike, T., & Musiake, K. (2003). Global potential soil erosion with reference to land use and climate changes. *Hydrological Processes*, 17(14), 2913-2928.
- Yang, W., Seager, R., Cane, M. A., & Lyon, B. (2014). The East African Long Rains in Observations and Models. *Journal of Climate*, 27(19), 7185-7202. <https://doi.org/10.1175/jcli-d-13-00447.1>
- Yehia, A., & Ezzat, K. (2009). Fluoride Ion Uptake by Synthetic Apatites. *Adsorption Science & Technology*, 27(3), 337-347. <https://doi.org/10.1260/026361709789868910>
- Yevenes, M. A., & Mannaerts, C. M. (2011). Seasonal and land use impacts on the nitrate budget and export of a mesoscale catchment in Southern Portugal. *Agricultural Water Management*, 102(1), 54-65. <https://doi.org/10.1016/j.agwat.2011.10.006>
- Yidana, S. M., Ophori, D., & Banoeng-Yakubo, B. (2008). A multivariate statistical analysis of surface water chemistry data: The Ankobra Basin, Ghana. *Journal of Environmental Management*, 86(1), 80-87. <https://doi.org/10.1016/j.jenvman.2006.11.023>
- Yin, Z., Feng, Q., Yang, L., Wen, X., Si, J., & Zou, S. (2017). Long Term Quantification of Climate and Land Cover Change Impacts on Streamflow in an Alpine River Catchment, Northwestern China. *Sustainability*, 9(7), 1-17. <https://doi.org/10.3390/su9071278>
- Yu, G., Wang, J., Liu, L., Li, Y., Zhang, Y., & Wang, S. (2020). The analysis of groundwater nitrate pollution and health risk assessment in rural areas of Yantai, China. *BioMedical Central Public Health*, 20(1), 1-6. <https://doi.org/10.1186/s12889-020-08583-y>
- Zawierucha, K., & Shain, D. H. (2019). Disappearing Kilimanjaro snow: Are we the last generation to explore equatorial glacier biodiversity? *Ecology and Evolution*, 9(15), 8911-8918. <https://doi.org/10.1002/ece3.5327>

- Zhai, R., Zhang, C., Allen, J. M., Li, W., Boyer, M. A., Segerson, K., & Foote, K. E. (2018). Predicting land use/cover change in Long Island Sound Watersheds and its effect on invasive species: a case study for glossy buckthorn. *Annals of Geographic Information System*, 24(2), 83-97. <https://doi.org/10.1080/19475683.2018.1450786>
- Zhan, L., Chen, J., Zhang, S., Li, L., Huang, D., & Wang, T. (2016). Isotopic signatures of precipitation, surface water, and groundwater interactions, Poyang Lake Basin, China. *Environmental Earth Sciences*, 75(19), 1-14. <https://doi.org/10.1007/s12665-016-6081-8>
- Zhang, L., Karthikeyan, R., Bai, Z., & Srinivasan, R. (2017). Analysis of streamflow responses to climate variability and land use change in the Loess Plateau region of China. *Catena*, 154, 1-11. <https://doi.org/10.1016/j.catena.2017.02.012>
- Zhang, L., Nan, Z., Xu, Y., & Li, S. (2016). Hydrological impacts of land use change and climate variability in the headwater region of the Heihe River Basin, Northwest China. *Plos One*, 11(6), 1-25.
- Zhou, Y. (2011). *Smallholder Mapping II: Trends in demographics and driving forces*. Basel: Syngenta Foundation for Sustainable Agriculture. <https://www.cinfo.ch/en/syngenta-foundation-sustainable-agriculture>.
- Zhou, Y., Xu, Y. J., Xiao, W., Wang, J., Huang, Y., & Yang, H. (2017). Climate change impacts on flow and suspended sediment yield in headwaters of high-latitude regions: A case study in China's far northeast. *Water*, 9(12), 1-17.
- Zomlot, Z., Verbeiren, B., Huysmans, M., & Batelaan, O. (2015). Spatial distribution of groundwater recharge and base flow: Assessment of controlling factors. *Journal of Hydrology: Regional Studies*, 4, 349-368. <https://doi.org/10.1016/j.ejrh.2015.07.005>
- Zongolo, S., Kiluvia, S., & Mghase, G. (2000). *Traditional irrigation assessment report, Moshi rural district*. <https://zenodo.org>

APPENDICES

Appendix 1: Historical and scenario simulation for October-November-December (OND) and March-April-May (MAM) for regional atmospheric climate mode (RACMO22T) under representative concentration pathways (RCPs) 4.5 and 8.5

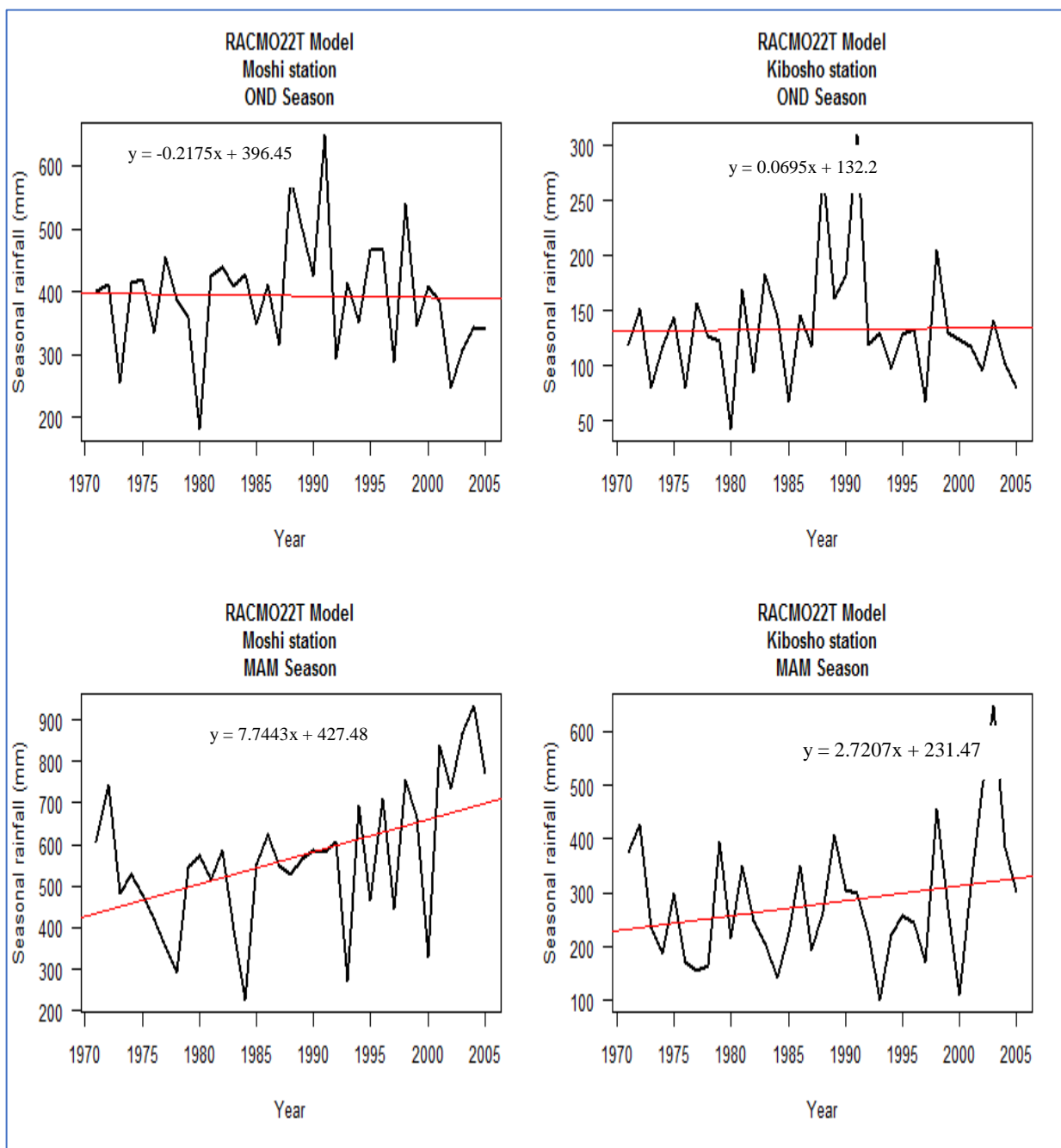


Figure A: Regional atmospheric climate mode 22T model indicating historical precipitation (i.e. Rainfall) projections in October-November-December and March-April-May seasons

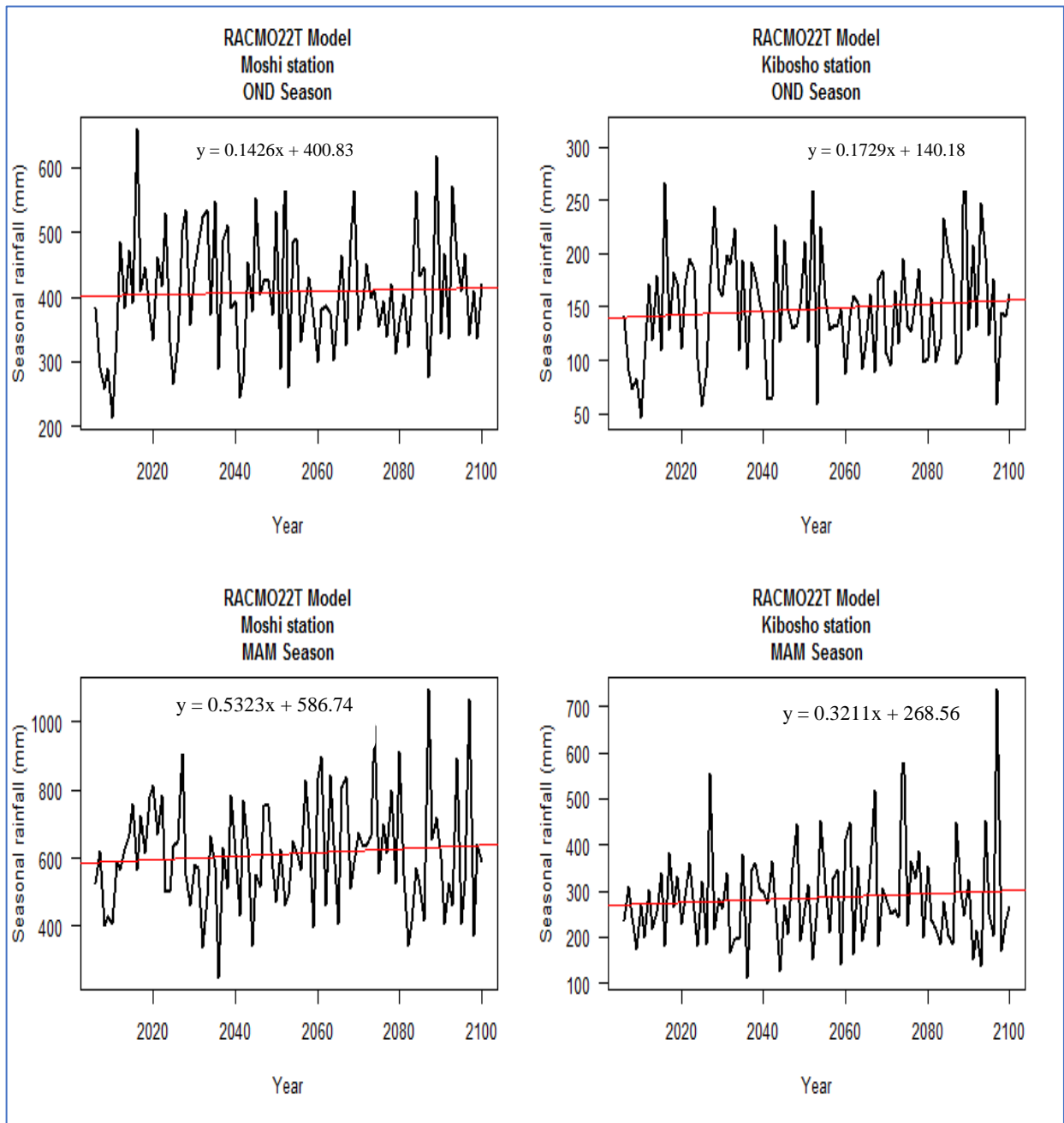


Figure B: Regional atmospheric climate mode 22T model indicating future precipitation (i.e. Rainfall) projections in October-November-December and March-April-May seasons under representative concentration pathway 4.5

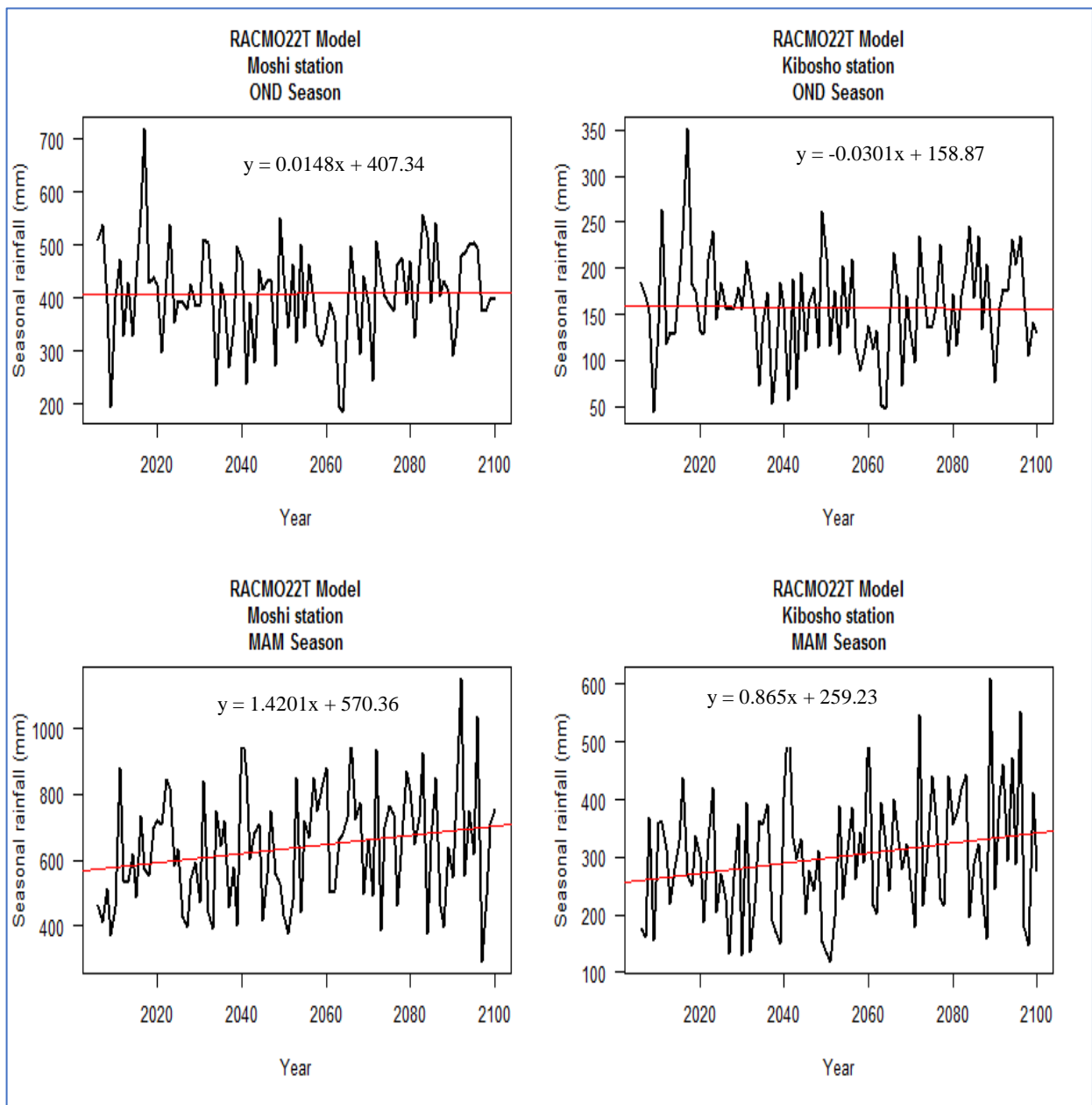


Figure C: Regional atmospheric climate mode 22T model indicating future precipitation (i.e. Rainfall) projections in October-November-December and March-April-May seasons under representative concentration pathway 8.5

Appendix 2: Historical and scenario simulation for October-November-December (OND) and March-April-May (MAM) for climate limited area modeling 4 (CCLM4) under representative concentration pathways (RCPs) 4.5 and 8.5.

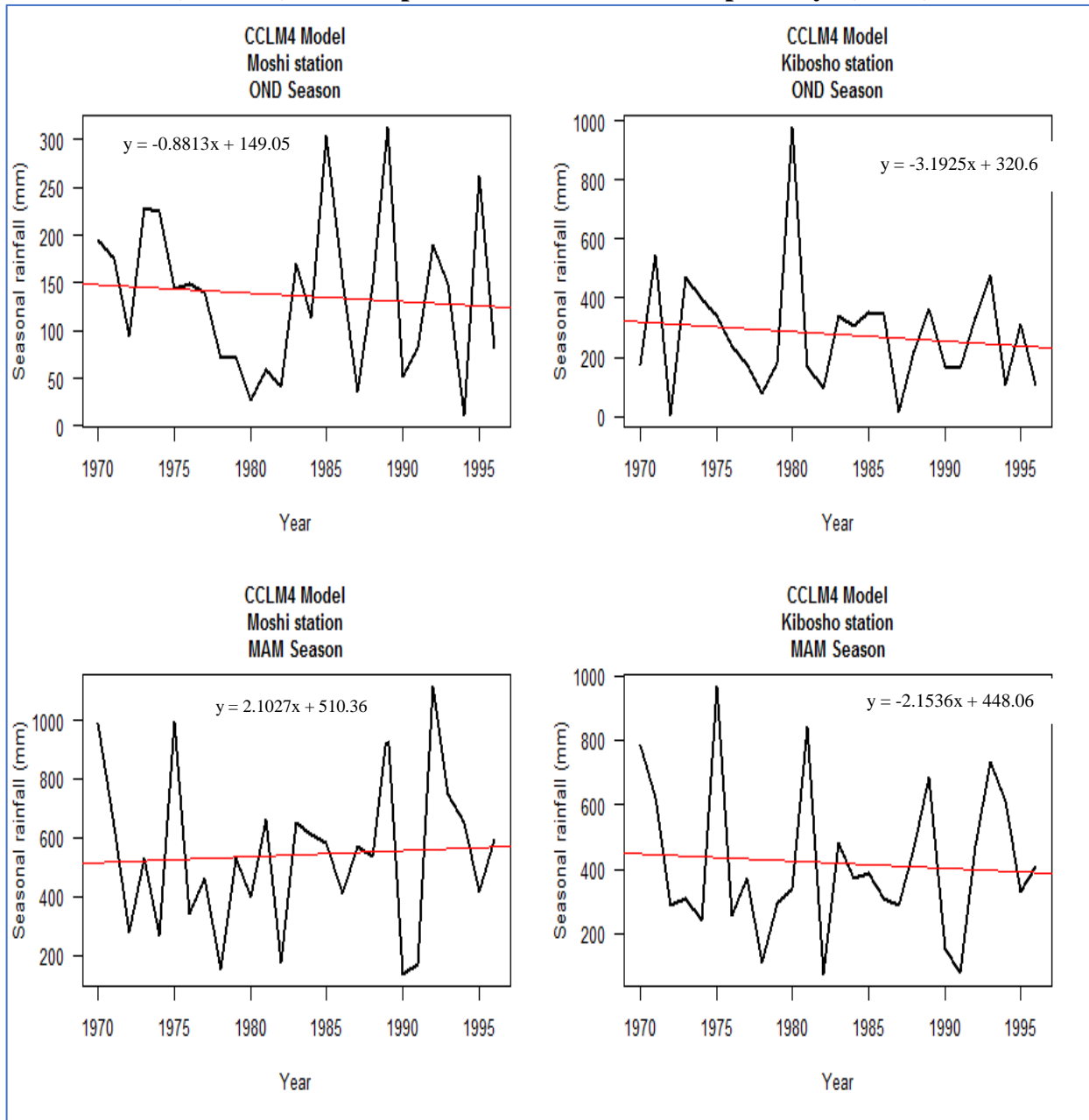


Figure D: Climate limited area modeling 4 model precipitation projections in historical period for October-November-December and March-April-May seasons

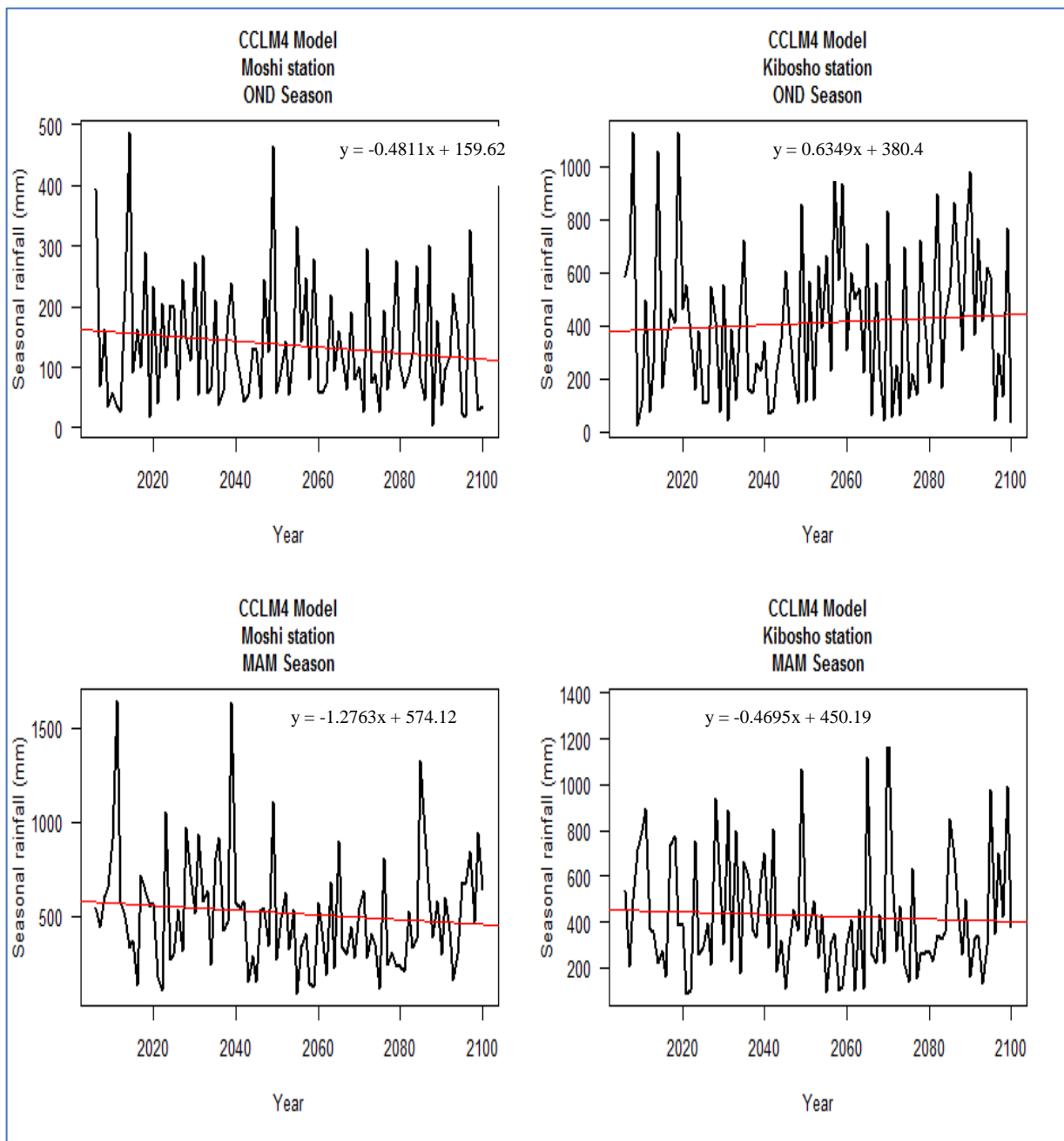


Figure E: Climate limited area modeling 4 future precipitation projections under representative concentration pathway 4.5 for October-November-December and March-April-May seasons

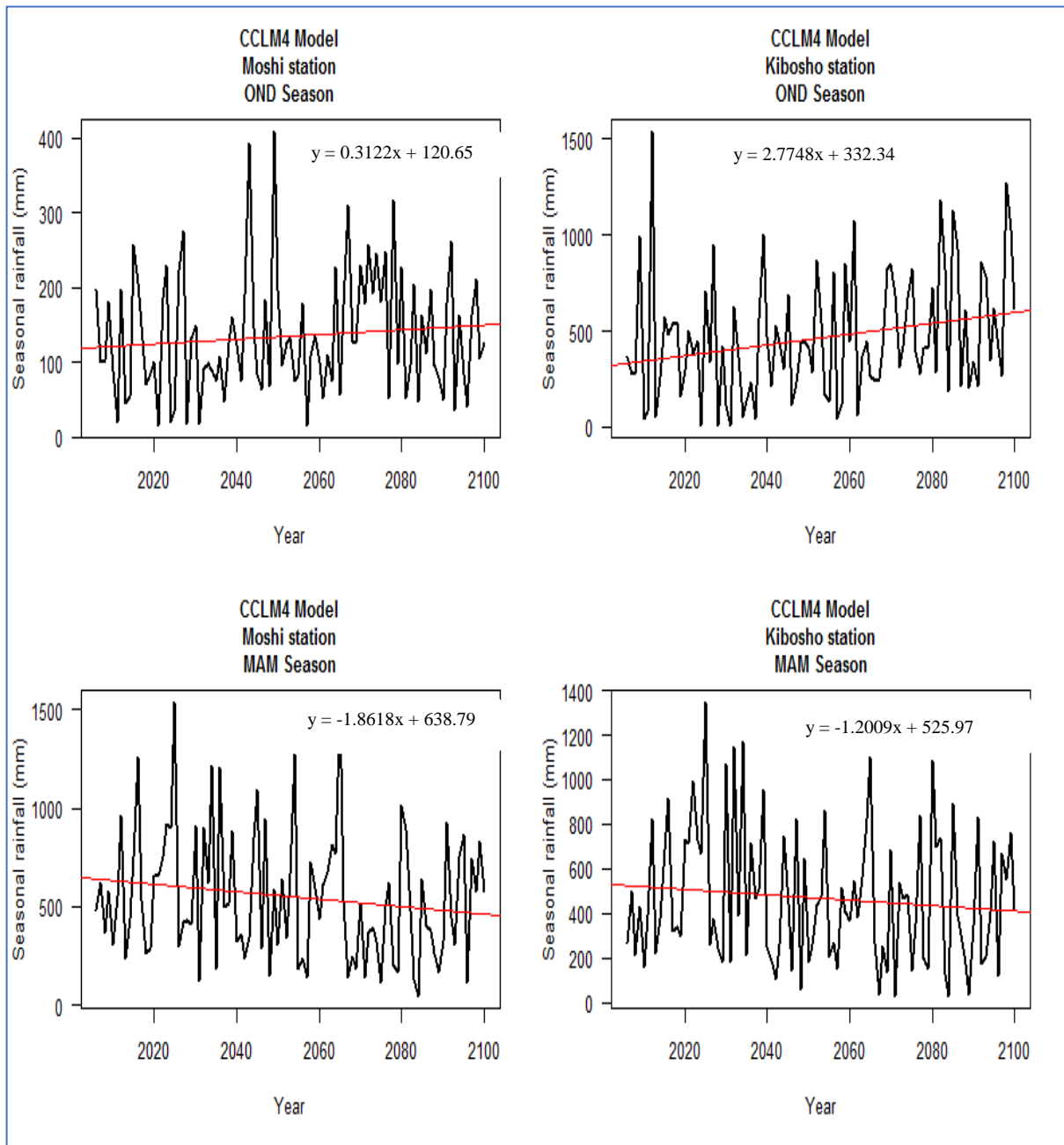
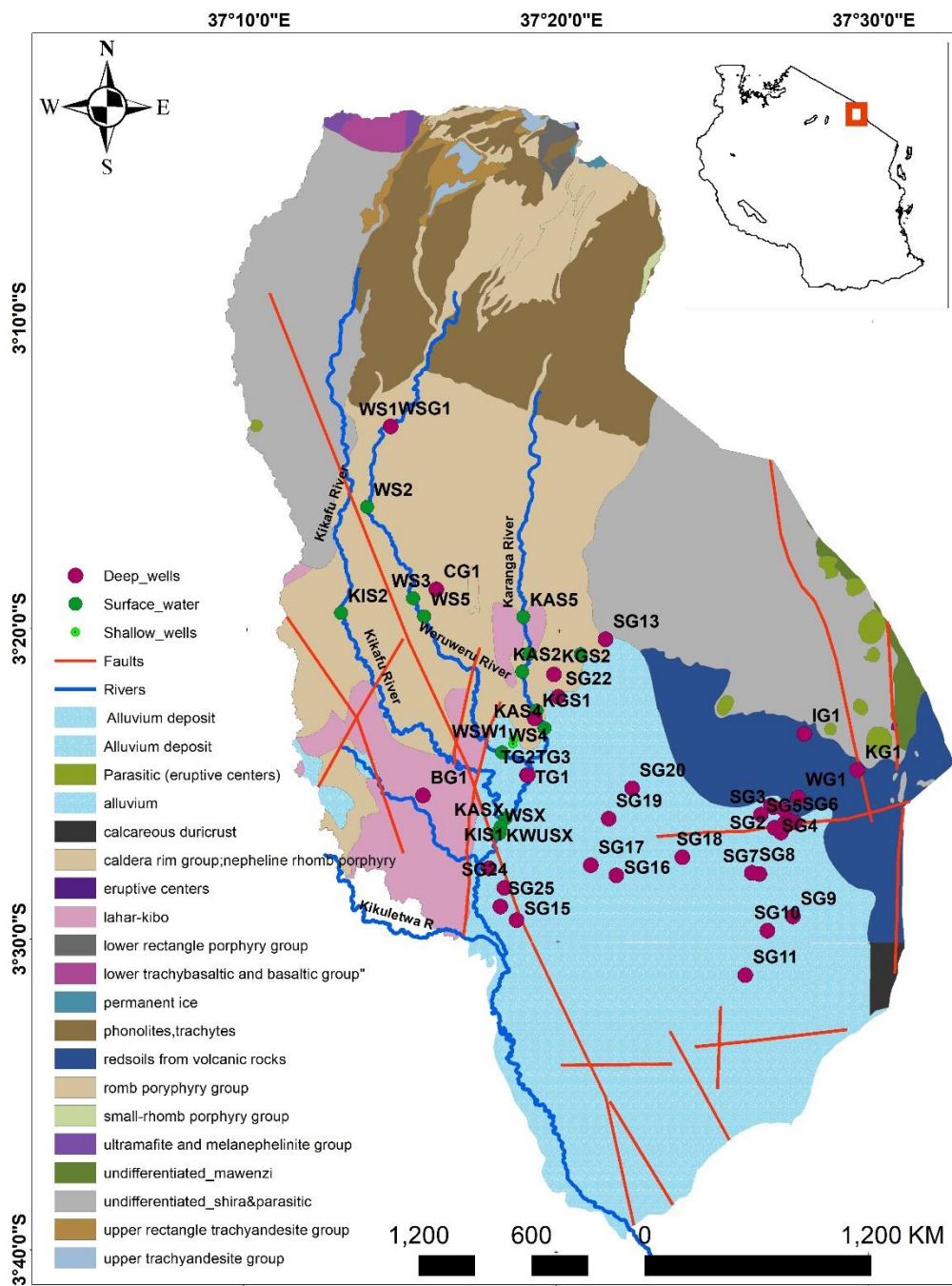


Figure F: Climate limited area modeling 4 future precipitation projections under representative concentration pathway 8.5 for October-November-December and March-April-May seasons

Appendix 3: Geological map and sampling locations for surface and extended groundwater



RESEARCH OUTPUTS

(i) Publications

Mateso, S., Hans, C. K., Linus, K. M., & Alfred, N. N. M. (2019). Evidence of climate change impacts on water, food and energy resources around Kilimanjaro, Tanzania. *Regional Environmental Change*, 19, 2521–2534.

Mateso, S., Canute, H., Hans, C. K., Ibrahimu, C. M., & Linus, K. M. (2021) Predicting land use/cover changes and its association to agricultural production on the slopes of Mount Kilimanjaro, Tanzania. *Annals of GIS*, 27(2), 189-209.

Said, M., Hyandye, C., Mjemah, I. C., Komakech, H. C., & Munishi, L. K. (2021). Evaluation and Prediction of the Impacts of Land Cover Changes on Hydrological Processes in Data Constrained Southern Slopes of Kilimanjaro, Tanzania. *Earth*, 2, 225–247.

(ii) Poster Presentation